



Integrating Experimental and Omics Approaches for Investigation of Novel Combination Therapies to Overcome Therapeutic Resistance in Triple-Negative Breast Cancer

Ву

Yasir Mohammed Farhan

A thesis presented in fulfilment of the requirements for the degree of Doctor of Philosophy

Strathclyde Institute of Pharmacy and Biomedical Sciences
University of Strathclyde, Glasgow, UK

Declaration and Author's Rights

This thesis is the result of the author's original research. It has been composed by

the author and has not been previously submitted for examination that has led to the

award of a degree.

The copyright of this thesis belongs to the author under the terms of the United

Kingdom Copyright Acts as qualified by the University of Strathclyde Regulation 3.50.

The due acknowledgement must always be made of the use of any material contained

in, or derived from, this thesis.

Signed: Wasir

Date: 28/5/2025

1

COVID impact statement

I commenced my PhD in January 2021, amid COVID-19 pandemic. At that time, Scotland was under national lockdown, and there were strict restrictions for student's entry to the labs, particularly for new students. Consequently, I was unable to access the lab or doing on campus work and I had to return my country (IRAQ) and working from home, focusing on literature review and experimental plans. When I re-joint the university in August 2021, some restrictions were still in place including limited building access and reduced occupancy in laboratories. Essential inductions and mandatory training such as health and safety and radiation machine were delayed, as well as restricted access of the staff, together slowing my progression toward independent laboratory work. Furthermore, disturbances in supply chains affected on the availability of essential cell cultures, reagents and consumables which contributed to further delays in conducting experimental works. The opportunities for networking, attending the in-person workshops and other post graduate related activities and incorporation into wider research community were significantly restricted. Consequently, my first year encompassed few laboratories work, however, I exploited this time for preparing the protocols and planning for experimental work which enabled me to lay the groundwork for later stages of the PhD project.

Acknowledgment

First and foremost, I am deeply grateful to Almighty Allah for giving me the health, strength, and perseverance to complete my PhD journey.

I am sincerely grateful to my supervisor, Dr. Marie Boyd, for her exceptional guidance, continuous support, and generous encouragement throughout my PhD journey. Her insightful advice and thoughtful support, both academically and personally, have been truly inspiring. I especially appreciate her genuine care for my well-being, always asking about my family, and offering comfort during challenging times. I am truly thankful for the chance to be part of her research group, which not only enriched my scientific training but also provided me with valuable opportunities to share my work at national and international events.

I would also like to thank my second supervisor, Professor Alexander Mullen, for his support, encouragement, and helpful feedback throughout this project.

I want to sincerely thank Dr. Nicholas Rattray for his generous support and guidance throughout the metabolomics part of this project. I truly appreciate the time he dedicated to assisting me in the lab and his expert advice during the data analysis. I am also thankful to his group members, Layla, Abdullah, and Jillian, for their helpful cooperation and technical support during this phase of the study.

I would also like to express my gratitude to The Boyd Group, both past and present, for creating a supportive and friendly research environment throughout my PhD journey. Special thanks to Calum, Rosh, Olena, Manal, Sara, Wedad, Amy, Hannah, Samantha, and Reem for their companionship, helpful discussions, and encouragement along the journey. Your kindness and collaboration made this experience truly memorable.

I would also like to thank all the students, postdoctoral researchers, and technical staff in the shared office and lab spaces for creating a pleasant and supportive working environment. Your everyday kindness, friendly conversations, and words of encouragement contributed greatly to a positive atmosphere that helped me stay motivated throughout my PhD. A special thanks to my colleagues, Saddam, and Mohammed, for their constant support and shared journey along the way.

I also want to thank my family, father, mother, sisters, and brothers, for their endless love, encouragement, and prayers throughout this journey. This achievement would not have been possible without their belief in me.

I am sincerely grateful to my beloved wife, Asmaa Majid, whose strength, patience, and unwavering support have been the backbone of this journey. She endured my absence gracefully, shouldering responsibilities at home with steadfast dedication and love. I am truly grateful for her sacrifices and encouragement every step of the way. To my wonderful children, Rawan, Rand, and Ammar, thank you for being my source of joy and motivation, even from a distance. This achievement is as much yours as it is mine.

Abstract

Triple-negative breast cancer (TNBC) is a highly aggressive subtype of breast cancer characterised by negative expression of typical receptors including oestrogen (ER). progesterone (PR), and human epidermal growth factor receptor 2 (HER2). The current therapeutic strategies of TNBC primarily rely on chemotherapeutics, such as Anthracyclines, Taxanes, and Platinum-based agents, as well as radiotherapy for regionally located tumours. However, therapy resistance and tumour reoccurrence remain the major challenges, highlighting that the development of novel targeted and combination therapy is urgently needed. This project aimed to investigate targeted therapeutic approaches for TNBC by assessing the effectiveness of gedatolisib, a dual PI3K/mTOR inhibitor, combined with conventional treatments such as doxorubicin and radiotherapy. A radioresistant TNBC cell line was established in our lab alongside its parental counterpart to further investigate the potential of these gedatolisib-based combination therapies in overcoming therapy resistance. A metabolomics approach was also employed to investigate the metabolic adaptations associated with radioresistance in TNBC, aiming to identify key resistance pathways and potential therapeutic targets.

The therapeutic efficacy of single and combination treatments in both parent and radioresistant MDA-MB-231 cell lines was assessed utilising two-dimensional clonogenic assays and three-dimensional tumour spheroids. To determine the mode of action of any promising combinations, mechanistic assays, including Annexin V (for apoptosis), COMET assay (for DNA damage), cell cycle analysis, and autophagy assay, were conducted to provide molecular insights into the mechanisms of therapy-induced cytotoxicity. Furthermore, the liquid chromatography-mass spectrometry (LC/MS) technique was employed to identify the metabolites and their intensities

altered in the parent and radioresistant MDA-MB-231 cells to determine the pathways potentially utilised in inducing radioresistance.

The data demonstrated that combining gedatolisib with gold standard treatments such as radiation or doxorubicin was effective in the wild-type and resistant MDA-MB-231 cell lines. In both cell lines, cell survival and tumour spheroid growth were significantly reduced following treatment with combination therapy compared to monotherapy (P<0.05). These results were further supported by mechanistic assays, which demonstrated increased apoptosis induction, enhanced DNA damage, and altered cell cycle patterns in response to a combination of 0.1µM gedatolisib with either 2 Gy radiation or 0.01µM doxorubicin. The metabolomics data analysis identified alterations in crucial metabolic pathways, including arginine biosynthesis, alanine-aspartate-glutamate metabolism, and the TCA cycle. Although these metabolic pathways are vital for cancer cells, their dysregulation may contribute to inducing radioresistance in MDA-MB-231 cells. The collective results propose that targeting metabolic reprogramming alongside inhibiting the PI3K/Akt/mTOR pathway may offer a novel therapeutic approach for overcoming radioresistance in TNBC. Overall, the current project highlights the potential of gedatolisib in combination therapy to improve treatment outcomes in TNBC patients and identifies metabolic pathways that may serve as future therapeutic targets.

Professional Society membership

European Association of Cancer research (EACR) March-2022-Present

Training and professional Development: PG Cert classes, Courses, and conferences

A new potential combination therapy for triple negative breast cancer. University of Strathclyde, UK. SIPBS research day, Poster Presentation, 1st of June 2023

The use of gedatolisib for combination therapy of triple negative breast cancer.

Annual Congress of European Association of Cancer Research, Poster Presentation

Turin, Italy, 12th -15th of June 2023

Investigating metabolism in biological systems applying metabolomics – from cells to whole organisms. University of Liverpool Training Centre for Metabolomics, Liverpool, UK, 4th -8th of September 2023.

Generic Biomedical and Pharmaceutical Research Skills. PG certified class (20 credits), University of Strathclyde, Glasgow, UK, 27th April 2022

Post Graduate certificate in research professional development, University of Strathclyde, Glasgow, UK, November 2024

Abbreviations

ANOVA - A non-repeated one-way analysis of variance

AR – Androgen receptor

ATM - Ataxia Telangiectasia Mutant gene

AUC - Area under the curve

BC - Breast cancer

BRCA - BReast CAncer gene

DMSO - Dimethyl sulfoxide

DNA - Deoxyribose nucleic acid

DSB - Double strand breaks

DOX - Doxorubicin

EGFR – Endothelial growth factor receptor

ER – Oestrogen receptor.

FACS - Fluorescence-activated cell sorting

FBS - Foetal bovine serum

FC - Fold change

FDA – Food and drugs administration

FDR - False discovery rate

GED - Gedatolisib

Gy - Gray (radiation unit)

HER2 - human epidermal growth factor receptor 2

HIF – Hypoxia inducing factor.

HMDB - Human Metabolome Database

HR – Homologous recombination

HPLC – High-performance liquid chromatography

IC50 – Half maximal inhibitory concentration

IHC - Immunohistochemistry

KEGG - Kyoto Encyclopaedia of Genes and Genomes

KRAS - Kirsten rat sarcoma viral oncogene homolog

LC-MS - Liquid chromatography-mass spectrometry

mRNA - messenger ribonucleic acid

MS – Mass spectrometry

MSEA – Metabolite set enrichment analysis

mTOR - Mammalian target of the rapamycin

MTS – Multicellular tumour spheroids

NADPH – Nicotinamide adenine dinucleotide phosphate

NMR – Nuclear magnetic resonance spectroscopy

OPLS-DA - Orthogonal partial least squares-discriminant analysis

OS - Oxidative stress

OXPHOS - Oxidative phosphorylation

PARP - Poly-ADP ribose polymerase

PBS – Phosphate-buffered saline

PCA - Principal component analysis

pCR - Complete pathological response

PI3K – Phosphatidylinositol-4,5-bisphosphate 3-kinase

PLS-DA – Partial least squares discriminant analysis

PPP - Pentose phosphate pathway

PR – Progesterone receptor

PS - Phosphatidylserine

QC – Quality control

RNase A - Ribonuclease A

ROS – Reactive oxygen species

RT – Retention Time

SD – Standard Deviation

SSB – Single strand breaks

TCA – Citric acid cycle

TNBC - Triple negative breast cancer

UK – United Kingdom

WHO - World health organisation

WT - Wild type

VIP – Variable importance in the projection

Table of contents

1 Ir	ntroduction	. 23
1.1	Cancer statistics	. 24
1.2	Breast Cancer	. 28
1.3	Classification of breast cancer	. 29
1.4	Current treatment of breast cancer	. 31
1	.4.1 Surgery	. 31
1	.4.2 Radiotherapy	. 31
1	.4.3 Chemotherapy	. 33
1	.4.4 The targeted treatments	. 33
1.5	Triple negative breast cancer	. 36
1	.5.1 Classification of TNBC	. 40
1	.5.2 Current treatment of TNBC	. 42
1	.5.3 New approved therapies for TNBC	. 44
1	.5.4 Therapeutic resistance of TNBC	. 46
1.6	The mechanisms of therapeutic resistance	. 47
1	.6.1 The potent antioxidant activity	. 48
1	.6.2 Promoted DNA Repair	. 50
1	.6.3 Metabolic adaptation	. 51
1.7	Role of PI3K/mTOR pathway in TNBC	. 54
1.8	Combination therapy and repurposing drugs strategy for the treatment of TN	IBC
	55	

1.9	Metabolomics	59
1.	9.1 Metabolomics of TNBC	62
1.10	Aims of the project	65
1.	10.1Hypothesis	66
2 M	aterials and Methods	67
2.1	Cell line and routine passage	68
2.2	Establishing of MDA-MB-231 cultures from frozen stocks	69
2.3	Mycoplasma test	70
2.4	Freezing of cells	70
2.5	Cell Doubling Time	71
2.6	Plating efficiency	72
2.7	Drug preparations	73
2.8	Clonogenic assay	74
2.9	Tumour spheroids	76
2.10	Establishment of resistant cell line	77
2.11	Combination index analysis	79
2.12	Cell Cycle analysis	80
2.13	Annexin V assay	81
2.14	DNA damage assay (Comet assay)	82
2.15	Western blot	84
2.16	Autophagy Assay	86
2.17	Statistical Analysis	87

2.18	Cell lines maintenance and treatment for metabolomics	87
2.19	Chemicals	88
2.20	Cell sample preparation and metabolites extraction	88
2.21	Cell sample preparation and metabolites extraction	89
2.22	Processing of mass spectrometry data	91
2.23	Pathway and Statistical Analysis	92
	vitro evaluation of gedatolisib in combination with doxorubicin or radiation	
3.1	Introduction	95
3.2	Aims96	
3.2	2.1 Hypothesis	96
3.3	Results	97
3.3	3.1 MDA-MB-231 cells doubling time	97
3.3	3.2 Clonogenic survival of MDA-MB-231 following exposure to single can agents	
3.4	Utilising spheroids model to evaluate the effectiveness of single agents in MDA-MB-231 cell line	
3.4	4.1 The assessment of gedatolisib effect on the growth of MDA-MB-2 spheroids	
3.4	4.2 The assessment of doxorubicin effect on the growth of MDA-MB-2 spheroids	
3.4	4.3 The assessment of radiation effect on the growth of MDA-MB-231 sphero	
3 5	Combination therapy	109

3.5.1 Assessment of the clonogenic survival of MDA-MB-231 cells after treatment
with a combination therapy of gedatolisib and radiation
3.5.2 Assessment of the clonogenic survival of MDA-MB-231 cells after treatment
with a combination therapy of gedatolisib and doxorubicin
3.6 Combination index analysis for combination therapy
3.6.1 Assessment of synergy of the various combinations of gedatolisib and
radiation in MDA-MB-231 cell line utilising combination Index analysis 117
3.6.2 Assessment of synergy of the various combinations of gedatolisib and
doxorubicin in MDA-MB-231 cell line utilising combination Index analysis
119
3.7 Evaluation of the effect of gedatolisib, doxorubicin, and radiation treatments
alone and in combination using MDA spheroids
3.7.1 Evaluation of the effect of gedatolisib and radiation treatments alone and in
combination using MDA spheroids121
3.7.2 Evaluation of the effect of gedatolisib and radiation treatments alone and in
combination using MDA spheroids126
3.8 Evaluation of the mechanistic effect of single and combination treatment in
MDA-MB-231 cell line
3.8.1 Assessment of MDA-MB-231 cell cycle progression following exposure to
single and combination treatments
3.8.2 Assessment of apoptosis in MDA-MB-231 cells induced by single and
combination treatment using Annexin V assay
3.8.3 Assessment of DNA damage induction in the MDA-MB-231 cell line utilising
COMET assay147

3.8.4 Assessment of the effect of gedatolisib on autophagy in the MDA-MB-23
cell line
3.8.5 Evaluation the effect of gedatolisib on the expression of PI3K/Akt/mTOF
pathway using western blot analysis162
3.9 Discussion
4 Establishment of an MDA-MB-231 radioresistant cell line and assessment of the response of the therapy resistant cell line to single and combination therapy of gedatolisib, doxorubicin and radiation
4.1 Introduction
4.2 Aims180
4.2.1 Hypothesis
4.3 Results
4.3.1 Establishment of Radioresistant MDA-MB-231 cells
4.3.2 Clonogenic assay for radioresistant (RR)-MDA-MB-231 cell line following
exposure to single therapy183
4.3.3 Assessment of combination therapy effectiveness in the radioresistant (RR)
MDA-MB-231 cell line
4.3.4 Evaluation of the effect of gedatolisib, doxorubicin, and radiation treatment
alone and in combination using (RR)- MDA-MB-231 spheroids 203
4.3.5 Evaluation of the mechanistic effect of single and combination treatments in
RR-MDA-MB-231 Cells
4.4 Discussion
5 Metabolomics profiling of radiotherapy resistance MDA-MB-231 cell line 239
E. 1. Introduction

	5.2.	1 Hypothesis
5.3	3 F	Results
	5.3.	1 Cellular metabolome of an established radioresistant and wild type triple
		negative breast cancer cell lines at 1hr following exposure to 2Gy radiation
		244
	5.3.	2 Cellular metabolome of an established radioresistant and wild type triple
		negative breast cancer cell lines at 4hr following exposure to 2 Gy radiation
		259
	5.3.	3 Cellular metabolome of an established radioresistant and wild type triple
		negative breast cancer cell lines at 24hr following exposure to 2Gy radiation
		274
5.4	4 C	Discussion
	5.4.	1 Early Response of Resistant and Wild type MDA-MB-231 cells to radiation
		290
	5.4.	2 Intermediate Response of Resistant and Wild type MDA-MB-231 Cells to
		Radiation
	5.4.3	Late Response (24 hr post irradiation) of Resistant and Wild type MDA-MB-
		231 Cells to Radiation
	5.4.4	Metabolic Pathways Potentially Driving Overall Resistance to Radiotherapy
		302
6	Gen	eral discussion, Conclusion and Future Works

5.2 Aims242

6.	1.1 Therapeutic effectiveness of combining gedatolisib with doxorubicing	or
	radiation in MDA-MB-231 cell line	309
6.	1.2 Metabolic reprograming as driver of radioresistance	311
6.2	Conclusions	313
6.3	Future works	314
7 R	eferences	317
8 A _l	ppendix	350

List of Figures

Figure 1-1 Incidence and mortality rate of cancers
Figure 1-2: Molecular targets for the prevention and treatment of breast cancer 36
Figure 1-3 Schematic illustration for key molecular pathways in TNBC
Figure 1-4 Common metabolic adaptations in breast cancer (Garg et al., 2025) 53
Figure 1-5 Scheme of general cell metabolomics workflow (Adapted from León et al.,
2013)60
Figure 2-1 Flow chart for the development of MDA-MB-231 resistant cell line 78
Figure 3-1 MDA-MB-231 cells doubling time
Figure 3-2 Survival fraction of MDA-MB-231 cells exposed to gedatolisib99
Figure 3-3 Survival fraction of MDA-MB-231 cells exposed to doxorubicin 101
Figure 3-4 Linear quadratic survival curve of MDA-MB-231 cells exposed to radiation
Figure 3-5 Growth curve of MDA-MB-231 tumour spheroid exposed to gedatolisib
Figure 3-6 Growth curve of MDA-MB-231 tumour spheroid exposed to doxorubicing
Figure 3-7 Growth curve of MDA-MB-231 tumour spheroid exposed to radiation. 108
Figure 3-8 Survival fraction of MDA-MB-231 cells exposed to combination of
gedatolisib and radiation112
Figure 3-9 Survival fraction of MDA-MB-231 cells exposed to combination of
gedatolisib and doxorubicin115
Figure 3-10 Combination index analysis for the simultaneous combination of
gedatolisib and radiation in MDA-MB-231 cell line
Figure 3-11 Combination index analysis for the simultaneous combination of
gedatolisib and doxorubicin in MDA-MB-231 cell line

Figure 3-12 Growth curve for MDA-MB-231 spheroid exposed to a simultaneous
combination of gedatolisib and radiation
Figure 3-13 MDA-MB-231 tumour spheroids growth dynamics following exposure to
single and simultaneously given combination of gedatolisib and radiation 125
Figure 3-14 Growth curve for MDA-MB-231 tumour spheroid exposed to a
combination therapy of gedatolisib and doxorubicin
Figure 3-15 MDA-MB-231 tumour spheroids growth following exposure to single and
simultaneous combination of gedatolisib and doxorubicin
Figure 3-16 Cell cycle phases distribution over time following exposure to gedatolisib
Figure 3-17 Cell cycle phases distribution over time following exposure to doxorubicin
Figure 3-18 Cell cycle phases distribution over time following exposure to radiation
Figure 3-19 Cell cycle phases distribution following exposure to simultaneous
combination of gedatolisib and radiation
Figure 3-20 Cell cycle phases distribution following exposure to a simultaneous
combination of gedatolisib and doxorubicin
Figure 3-21 Apoptosis of MDA-MB-231 cells following treatment with single
gedatolisib, doxoubcin and radiation assessed by the Annexin V assay 141
Figure 3-22 Apoptosis of MDA-MB-231 cells following treatment with simultaneous
combination of gedatolisib and radiation assessed by the Annexin V assay 144
Figure 3-23 Apoptosis of MDA-MB-231 cells following treatment with simultaneous
combination of gedatolisib and doxorubicin assessed by the Annexin V assay 146

Figure 3-24 DNA damage in MDA-MB-231 cells following exposure to single agents
of gedatolisib, doxorubicin or radiation assessed by COMET assay 149
Figure 3-25-A DNA damage in MDA-MB-231 cells following treatment with a
simultaneous combination of gedatolisib with radiation assessed by COMET assay
Figure 3-26-B DNA damage in MDA-MB-231 cells following treatment with a
simultaneous combination of gedatolisib with radiation assessed by COMET assay
Figure 3-27-A DNA damage in MDA-MB-231 cells following treatment with a
simultaneous combination of gedatolisib with doxorubicin assessed by COMET assay
Figure 3-28-B DNA damage in MDA-MB-231 cells following treatment with a
simultaneous combination of gedatolisib with doxorubicin assessed by COMET assay
Figure 3-27 MDA-MB-231 Representative images for COMET assay 158
Figure 3-29-A Assessment of autophagy induction by gedatolisib
Figure 3-29-B Autophagic vacuoles following treatment with gedatolisib
Figure 3-30 Evaluation of the effect of gedatolisib on the expression of Akt protein in
MDA-MB-231 cells using western blot analysis
Figure 4-1 Characteristics of radioresistant and parent MDA-MB-231 cells 182
Figure 4-2 Survival fraction curves of the resistant and wild type MDA-MB-231 cell
lines following treatment with gedatolisib
Figure 4-3 Survival fraction curves of the resistant and wild type MDA-MB-231 cell
lines following treatment with doxorubicin
lines following treatment with doxorubicin

Figure 4-5 Survival of RR-MDA-MB-231 cells following combination treatment with
gedatolisib and radiation191
Figure 4-7 Survival fraction of RR-MDA-MB-231 cells exposed to gedatolisib -
radiation scheduled combination therapy
Figure 4-8 Survival fraction of RR-MDA-MB-231 cells exposed to gedatolisib-
doxorubicin scheduled combinations
Figure 4-9 Growth curve of RR-MDA-MB-231 spheroids following exposure to a
combination of gedatolisib and radiation
Figure 4-10 RR-MDA-MB-231 representative spheroids images treated with
gedatolisib and radiation combination
Figure 4-11 Growth curve of RR-MDA-MB-231 spheroids treated with single and
combination of gedatolisib and doxorubicin
Figure 4-12 RR-MDA-MB-231 spheroids images across different time points following
treatment with Gedatolisib-Doxorubicin combination therapy
Figure 4-14 Apoptosis of MDA-MB-231 cells following treatment with simultaneous
combination of gedatolisib with radiation or doxorubicin assessed by the Annexin V
assay
Figure 4-15 DNA damage in RR-MDA-MB-231 cells following treatment with a
simultaneous combination of gedatolisib with radiation or doxorubicin assessed by
COMET assay
Figure 4-16 Assessment of induction of autophagy by gedatolisib in RR-MDA-MB-
231 cells utilising an autophagy assay
Figure 4-17 Evaluation of the effect of gedatolisib on the expression of Akt protein in
RR-MDA-MB-231 cells using western blot analysis
Figure 5-1 Metabolite abundance distribution after normalisation across samples in
response to radiation 245

Figure 5-2 Multivariate analysis of extracted MDA-MB-231 cell samples at	1hr
following exposure to radiation	247
Figure 5-3 Univariate analysis of extracted MDA-MB-231 cell samples	250
Figure 5-4 Metabolites clustering analysis	252
Figure 5-5 Variable importance in projection (VIP) for top 15 metabolites	254
Figure 5-6 Metabolic pathway analysis and MSEA	255
	256
Figure 5-7 Metabolites identification utilising ROC	258
Figure 5-8 Metabolites abundances distribution across samples in respons	e to
radiation	260
	262
Figure 5-9 Multivariate analysis of extracted MDA-MB-231 cell samples at	4hr
following exposure to radiation	262
Figure 5-10 Univariate analysis of extracted MDA-MB-231 cell samples	264
Figure 5-11 Metabolites clustering analysis	266
Figure 5-12 Variable importance in projection (VIP) for top 15 metabolites	268
	271
Figure 5-14 Biomarkers identification utilising ROC	273
Figure 5-15 Metabolites abundances distribution across samples in respons	e to
radiation	275
	279
Figure 5-17 Univariate analysis of extracted MDA-MB-231 cell samples	279
Figure 5-18 Metabolites clustering analysis	281
Figure 5-19 Variable importance in projection (VIP) for top 15 metabolites	283
Figure 5-20 Metabolic pathway analysis and MSEA	285
Figure 5-21 Metabolites identification utilising ROC	288

Chapter 1

1 Introduction

1.1 Cancer statistics

Cancer is a cluster of diseases characterised by genetic and epigenetic alterations which disrupt the normal cell growth mechanisms, causing uncontrolled proliferation, tissue invasion and metastasis (World Health Organization, 2022). It is important to differentiate between premalignancy and the evolution of malignant disease or cancer. Premalignant alterations denote an intermediate stage in the entire process of cancer development, where abnormal cells undergo genetic changes and continuous proliferation but remain within their original tissue boundaries (Curtius, Wright, & Graham, 2017). However, if these premalignant cells acquired some characteristics such as basement membrane penetration, stromal infiltration and spreading via lymphatic or haematologic pathways, it will result in what is called invasive cancer.

A cohesive framework for the comprehension of cancer biology was provided by Hanahan and Weinberg, where they proposed that majority of malignancies acquire common functional capabilities termed as -hallmarks of cancer- despite the diversity of tumour types (Hanahan & Weinberg, 2000). They described six hallmarks in their first published model: self-sufficiency in growth signals, insensitivity to antigrowth signals, tissue invasion and metastasis, limitless replicative potential, persistent angiogenesis, and evading apoptosis (Hanahan & Weinberg, 2000). The reprogramming of energy metabolism and evading immune destruction were the two emerging hallmarks that were incorporated into the first list (Hanahan & Weinberg, 2011). A further update was introduced by Hanahan (2022), proposing a discrete hallmark capability represented by phenotypic plasticity and disrupted differentiation. Furthermore, the functional contributions of senescent cells of varying origin within

the tumour microenvironment and their role in promoting malignancy was highlighted (Hanahan, 2022).

According to the World Health Organization (WHO), cancer is one of the leading causes of death, where 1 in 6 deaths is due to cancer worldwide, and is associated with substantial socioeconomic costs (Chen et al., 2023; Bray et al., 2024). The International Agency for Research on Cancer (IARC) estimated the incidence and mortality of cancer in 2022 globally, with 20 million new cancer cases and 9.7 million cancer deaths (Bray et al., 2024). Female breast cancer and lung cancer were the most frequent new diagnoses globally, while the mortality rate was the highest in patients with lung cancer, as shown in (Figure 1.1). The most common types of cancer in males are lung, prostate, and colorectal cancer with an estimated incidence rate of 15.3%, 14.2% and 10.4%, respectively. In females, the most common types of cancer are breast, lung and colorectal cancer with an estimated incidence rate of 23.8%, 9.4% and 8.9%, respectively (Bray et al., 2024). The variability in the incidence and mortality rates across cancer types and populations may be attributed to several epidemiological and clinical factors such as exposure to risk factors including tobacco use, infections, and environmental carcinogens as well as obesity, diet, and demographic population shifts (Sung et al. 2021). Furthermore, mortality rates are not only affected by the biological behaviour, but also the accessibility and the efficiency of early detection and screening programs, the aggressiveness of some tumours and the variation in the availability and timely access to the effective treatment, together contributes to the variation in the cancer incidence. For instance, breast and prostate cancers frequently show relatively high incidence but lower mortality, potentially due to advances in screening and treatment strategies, however, lung cancers still display comparatively higher mortality, suggesting late-stage diagnoses and poorer prognosis (Sung et al., 2021; Bray et al., 2024).

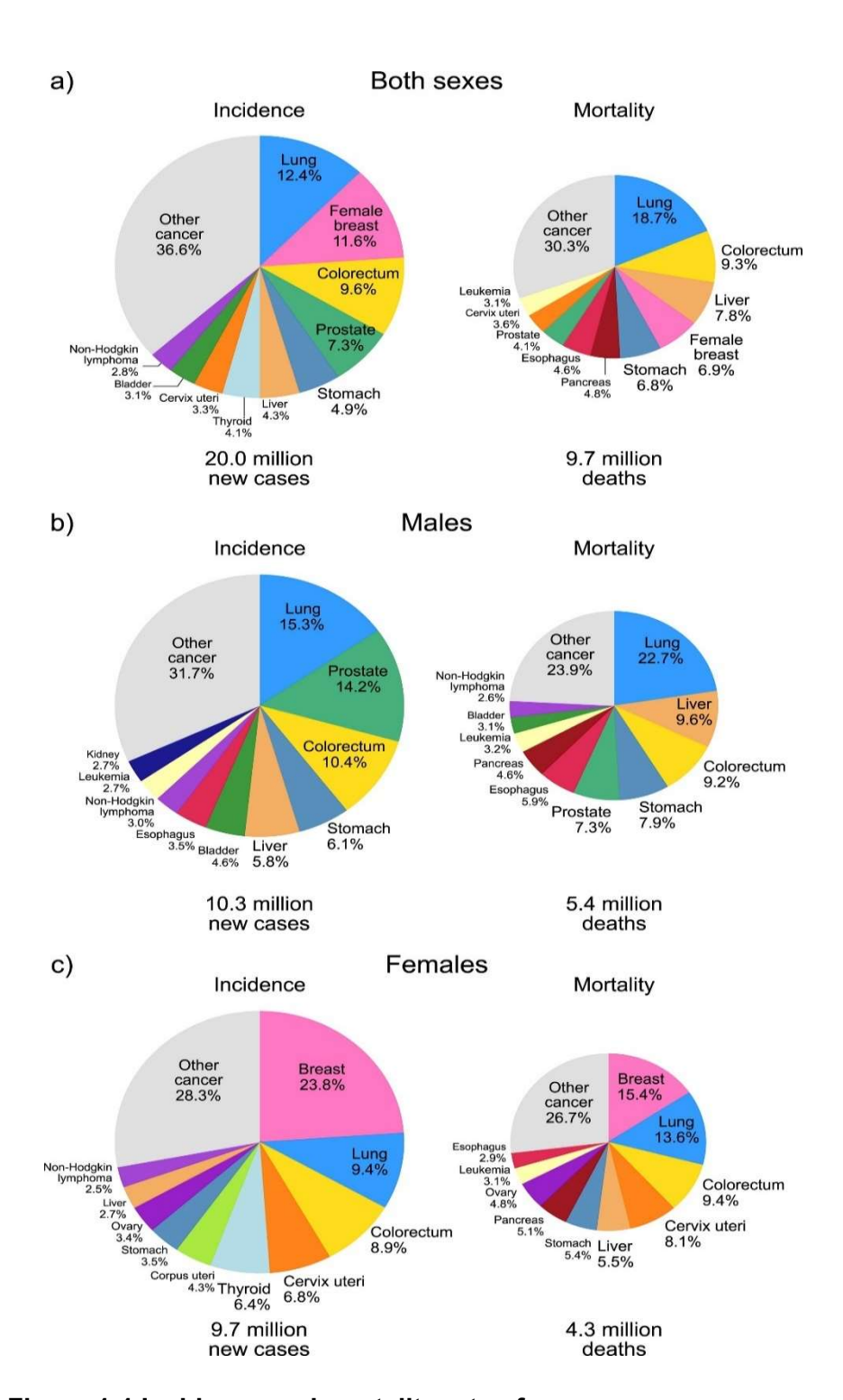


Figure 1-1 Incidence and mortality rate of cancers.

Distribution of new Cases and Deaths for the Most Common Cancers in 2022 for (A) both sexes, (B) Males and (C) Females. Source: GLOBOCAN 2022

In the UK, the incidence rate of breast, lung, prostate, and bowel cancers collectively accounted for 53% of all new cases of cancer in 2017-2019, where there were more than 385000 new cases every year between 2017-2019, which is more than 1000 new case each day (Cancer Research UK, 2025).

Cancer survival rates, which mean the percentage of people who stay alive for a specific period after the diagnosis of cancer, are variable among different types of cancers. In cancer statistics, an overall five-year survival rate is commonly used (Mariotto *et al.*, 2014). In addition, the ten-year survival rate was standardized for different types of cancer, where a substantial variable survival rate range was demonstrated from 98% for testicular cancer to 1% for pancreatic cancer (Quaresma et al., 2015). However, some types of cancer such as stomach, brain and lung cancers have very low survival rates (less than 20%) which may be due in part to their late diagnosis and treatment resistant phenotype (Quaresma, Coleman and Rachet, 2015).

1.2 Breast Cancer

Breast cancer is a heterogenous malignant tumour that originates primarily in the epithelial lining of the breast ducts or lobules (World Health Organization, 2022). In 2022, 2.3 million cases of breast cancer were newly diagnosed globally and the estimated number of deaths was 670000 worldwide (Kim et al., 2025). The incidence rate of breast cancer is positively correlated with age where people older than 50 years have a higher incidence rate than younger women (Li et al., 2022). The incidence rate of breast cancer in males is very low, in the UK only about 1% of total cancer cases occur in males (Cancer Research UK, 2025). Factors such as ethnicity and race show variation in the incidence rate of breast cancer. For example, black women have lower incidence rate than white women, however, the incidence is reversed for white women older than 40 years (Ren et al., 2019). The mortality rate also differs by race and ethnicity, where the rate of deaths caused by breast cancer is higher in black than white patients (Whitaker et al., 2022). The diverse incidence and mortality rates of breast cancers, particularly across ethnic groups, may arise from biological factors, such as the prevalence of BRCA1 and BRCA2 mutations, and other factors, including socioeconomic disparities, access to screening as well as treatment inequalities, all of which may contribute to the observed differences in incidence and mortality rates (Whitaker et al., 2022, Ren et al., 2019)

The future numbers of breast cancer cases have been predicted by the International Agency for Research on Cancer, where an incremental increase in the incidence of breast cancer is expected in the next 20 years. By 2050, the incidence and mortality rate of breast cancer will have increased by 38% and 68, respectively, with 3.2 million estimated new cases and 1.1 million deaths (Kim *et al.*, 2025).

1.3 Classification of breast cancer

Breast cancer is a heterogeneous disease, where different subtypes have been categorised based on histological and molecular features. The histopathological phenotyping may reflect the site of tumour origin and whether the tumour is restricted within the epithelial lining or invading other parts such as the surrounding stroma, and if the cancer appeared in the lobules or ducts of the mammary glands (Henry & Cannon-Albright, 2019). Two distinct types of breast cancer were identified based on histological features, one of them is called the *in situ* type which mean that the cancer cells originated in a certain sites of the breast such as ductal carcinoma in situ (DCIS) and the lobular carcinoma in situ (LCIS), while the other type infiltrates other areas of breast or the body so is named invasive breast cancer which may cause secondary tumours in different organs (Nascimento & Otoni, 2020; Tsang & Tse, 2020).

Molecular profiling of breast cancer has further suggested four distinct subtypes of breast cancer which are luminal A and luminal B, human epidermal receptor 2 and triple negative breast cancer (Perou *et al.*, 2000). Classically, these subtypes are defined by expression or absence of the receptors biomarkers oestrogen receptor (ER), progesterone receptor (PR) and HER2 receptors (Perou *et al.*, 2000). Expression of oestrogen receptors is the hallmark of luminal breast cancer, which comprises 60 % all of breast cancer cases, while progesterone receptor expression can also be found in both luminal A and luminal B subtypes (Roy *et al.*, 2023; Zhang *et al.*, 2023). The HER2 subtype is an invasive breast cancer which has high protein and gene expression of HER2, and this subtype accounts for around 15% of all breast cancer cases (Zhang *et al.*, 2023). Most of HER2 breast cancer cases do not have oestrogen and progesterone receptors (von Minckwitz *et al.*, 2017). These molecular characteristics may arise from the reliance of HER2 positive subtype on signalling

pathways rather than the hormonal receptors, suggesting the suppression of the activities and expression of these hormonal receptors (Belli *et al.*, 2024; Liu *et al.*, 2025). The negative expression of ER, PR and HER2 is the hallmark of an aggressive subtype of breast cancer called triple negative breast cancer (TNBC).

Breast cancer staging is essential for diagnosis and therapeutic planning. The tumour node metastasis (TNM) system, developed by the American joint committee on cancer (AJCC), is widely used for staging of breast cancer. This system categorises breast cancer stages based on the size of the primary tumour (T), the lymph node involvement (N), and the presence of spreading cells into other organs referred to as distant metastases (M) (Olawaiye *et al.*, 2021; Giuliano *et al.*, 2017). Within the TNM staging system, the primary tumour (T) category is determined by measuring the greatest dimension of the lesion, rounded to the nearest millimetre. Tumours ≤20 mm are classified as T1, those >20–50 mm as T2, and those >50 mm as T3, while T4 indicates tumours of any size with direct extension to the chest wall or skin. These categories are associated with survival outcomes, and this staging has an influence on the selection of systemic and local treatments (Amin *et al.*, 2017; Giuliano *et al.*, 2017).

Clinically, breast cancers are categorised into; early-stage invasive, locally advanced primary, and metastatic breast cancer, based on clinical presentation and pathological features such as tumour size, histopathological grade, and lymphatic infiltration (Sun *et al.*, 2024 Edge & Compton, 2010; Franceschini *et al.*, 2007). In patients with early breast cancer, the tumour cells infiltrate to areas beyond the ducts and lobules but remain within the boundaries of breast and regional tissues, and this represent stages I and II of the disease. The locally advanced primary tumour denotes stage III of the disease, where these tumours have not metastasised, involve the chest wall or skin and have a large size (>5 cm) (Aebi *et al.*, 2021; Garg & Prakash,

2015). Finally, metastatic breast cancer refers to stage IV that is characterised by spreading of the breast cancer cells out of their original breast tissue boundaries into distant vital organs such as the lung, liver, and brain (Park *et al.*, 2022).

1.4 Current treatment of breast cancer

The expression or lack of expression of hormonal receptors including ER, PR, and HER2 plays an important role in the management of breast cancers, and receptor expression was correlated positively with the prognosis of the disease (Masoud and Pagès, 2017; Wang and Wu, 2023). Breast cancer treatment strategies rely on several factors such as the tumour subtype, patient's age and personal preference regarding treatment options, and patient overall health.

1.4.1 Surgery

Surgery remains the first line management for most patients with early-stage breast cancer (Loibl *et al.*, 2024). Surgical interventions include lumpectomy, a breast-conserving surgery, followed by adjuvant radiotherapy, or mastectomy that may be accompanied by immediate surgical reconstruction, which depends on tumour size and patient choice (Loibl *et al.*, 2024). Alongside the surgery, the treatment strategies for breast cancer employs neoadjuvant and adjuvant therapy. Neoadjuvant therapy is given preoperatively to decrease the tumour size and improve surgical outcomes, whereas adjuvant treatment is administered postoperatively to eliminate residual disease and minimize the risk of recurrence (Asselain *et al.*, 2018; Nagpal *et al.*, 2023; Xiong *et al.*, 2025).

1.4.2 Radiotherapy

Radiotherapy is a vital component of breast cancer treatment strategies, particularly in treatment of microscopic residual cells, which helps in reducing locoregional recurrence and improving overall survival following surgery. Whole-breast radiotherapy (WBRT) after breast conserving surgery in early invasive breast cancer,

demonstrated an absolute reduction in the 10-year risk of recurrence and improved long-term breast cancer-related mortality (Loibl *et al.*, 2024). Postmastectomy radiotherapy (PMRT) induced a significant reduction in the recurrence and breast cancer related mortality in patients with node-positive disease (McGale, P. 2014).

In the recent years, the treatment protocols have shifted towards shorter regimens. The evidence-based guidelines recommend a hypofractionation of whole breast irradiation regimen, such as delivering of 40–42.5 Gy in 15–16 fractions (Smith *et al.*, 2018). Additionally, recent evidences support using ultra-hypofractionated regimens, for instance, delivering of 26 Gy in 5 fractions over one week as suggested by the FAST-Forward trial which demonstrated the non-inferior outcomes compared to the current standard whole breast irradiation (Brunt *et al.*, 2023; Yadav *et al.*, 2024).

1.4.2.1 Radiobiological requirements for fractionated radiotherapy

The biological rational for fractionated radiotherapy is represented by the 5Rs of radiobiology (Pajonk, Vlashi & McBride, 2010).

- Repair: Normal tissues can repair the sublethal damage between fractions, suggesting reduced cytotoxicity compared to tumour tissue.
- Redistribution: Cancer cells redistribute through cell cycle among fractions, increasing the opportunities for the radiation to hit in the radiosensitive G2/M phase.
- Repopulation: The surviving subclones have the capability to proliferate under treatment condition, prolonged treatment by fractionation can compromise the tumour proliferative capacity.
- Reoxygenation: Radioresistance is associated with tumour hypoxia, hence, progressed treatment may give the chance for reoxygenation of hypoxic region, thereby improving radiosensitivity.

5. Radiosensitivity: The intrinsic radiosensitivity varies between tumours, impacting the clinical response to radiotherapy.

1.4.3 Chemotherapy

Chemotherapy remains the cornerstone of systemic therapy, particularly for high-risk breast cancer subtypes. Standard chemotherapies including anthracyclines, taxanes, and platinum-based agents which are frequently used as neoadjuvant and adjuvant treatments. Despite its efficacy in tumour size reduction and survival improvement, chemotherapy frequently produces systemic toxicity and may be associated with acquired drug resistance. The capability of standard chemotherapy to differentiate between normal and malignant cells is challenging, resulting in drug-related side effects negatively influencing the patients' quality of life (Dagogo-Jack and Shaw, 2018; Correia, Gärtner and Vale, 2021a). To improve the therapeutic outcomes, combination therapy has been widely utilised. This approach enables the potential dose reduction of individual therapies, potentially decreasing toxicity and lowering the probability of resistance (Ji et al., 2019a; Iweala et al., 2024). For instance, combining chemotherapy with HER2-targeted therapies has demonstrated improved outcomes in HER2-positive breast cancer patients, both in neoadjuvant and adjuvant contexts (Gianni et al., 2016; von Minckwitz et al., 2017). Synergistic combinations targeting multiple pathways may also suppress metastasis and delay the emergence of resistance (Wang et al., 2023; Alés-Martínez et al., 2024)

1.4.4 The targeted treatments

The long-term treatment of breast cancer may include molecular targeted treatment, particularly for subtypes with positive expression of hormone receptor and HER2. The most commonly targeted agents currently utilised for breast cancer are endocrine and HER2 targeting agents (Correia, Gärtner and Vale, 2021a; Nagpal *et al.*, 2023). Luminal A and luminal B breast cancers are rich in oestrogen receptors that are the

target for endocrine agents. There are two major classes of hormonal therapies used for the treatment of ER positive hormone receptor breast cancer, namely selective oestrogen receptor modulators and aromatase inhibitors (Peddi, 2018; Cucciniello et al., 2023). Tamoxifen, a class of ER modulators, is an important endocrine agent that selectively modulates the ER. It binds competitively with oestrogen receptors, thereby blocking the binding of endogenous oestrogen, leading to a decrease in the cancer cells proliferation that is driven by oestrogen (Caciolla et al., 2021; Howell and Howell, 2023). Aromatase inhibitors such as letrozole, anastrozole and exemestane are another class of hormonal therapies for breast cancer, particularly in postmenopausal women, that decreases the production of oestrogen by blocking aromatase, a key enzyme involved in the biosynthesis of oestrogen (Ferreira Almeida et al., 2020; Hoppe et al., 2025). Several side effects of hormonal therapy may affect the patient's adherence to the treatment, where some patients experienced fatigue, hot flashes, alopecia, musculoskeletal pain, weight gain, depression, anxiety and cognitive side effects (Peddie et al., 2021). Furthermore, drug induced menopause is one of the major issues related to adjuvant hormonal therapy, and menopause related symptoms including hot flashes, anxiety and sleep disturbances have been reported to impair the quality of life and treatment adherence significantly (Ibrar et al., 2022; Eliassen et al., 2023). As a therapeutic option, endocrine therapies are considered the gold standard regimen for ER+ breast cancer. However, acquired resistance to these treatments may arise due to variable changes mainly concerned with structural modifications of oestrogen receptor itself, activation of pathways such as PI3/Akt/mTOR and MAPK, and the function of the oestrogen receptors(Brett et al. 2021; Hao et al. 2025; Mills, Rutkovsky, and Giordano 2018; Skolariki et al. 2022). Mutations in gene expression that encode the oestrogen receptors, modifications in the binding sites on the cellular membrane and the tumour microenvironment are common mechanisms that can contribute to endocrine therapy resistance (Fribbens

et al., 2016; Brett et al., 2021). Furthermore, low levels of ESR1 was associated with poor prognosis of postmenopausal women treated with aromatase inhibitors (Schuster et al., 2023). The heterogeneity of breast tumour highlights the need for identification of new pathways required for tumour cell survival and using these as therapeutic targets with appropriate therapeutic combinations.

The other target for breast cancer therapy is HER2 protein expression that can be blocked by targeted therapies such as Herceptin (trastuzumab) and pertuzumab, resulting in inhibiting the activating pathways of cell proliferation and tumour growth (Swain, Shastry and Hamilton, 2022; Zhu et al., 2024). Approximately 50% of HER2-positive breast cancer patients also have hormonal receptor (ER/PR) expression(Peleg Hasson et al., 2021). Hence, oestrogen receptor modulators such as tamoxifen and aromatase inhibitors such as letrozole may be added to the therapeutic regimen in combination with anti HER2 therapy depending on the patient's protein expression pattern (Schettini et al., 2016; Vici et al., 2016; Peleg Hasson et al., 2021). Nonetheless, HER2-targeted drugs were also associated with specific toxicities, including cardiotoxicity, which requires consistent monitoring of cardiac function, mainly left ventricular ejection fraction (Koulaouzidis et al., 2021). The molecular targets for the therapies utilised in the prevention and treatment of breast cancer are illustrated in Figure 1.2 (adapted from Hollander et al. 2013)

Triple negative breast cancer (TNBC) remains the most aggressive breast cancer subtype due to the negative expression of the typical receptors including oestrogen receptor, progesterone receptor and human epidermal growth receptor (Agelidis *et al.*, 2025; Asleh and Polyak, 2022). These characteristics make the treatment of this subtype challenging, leading to therapy resistance and a lower survival rate. The following section will discuss the biological characteristics of TNBC, current treatment, and challenges with potential therapeutic strategies.

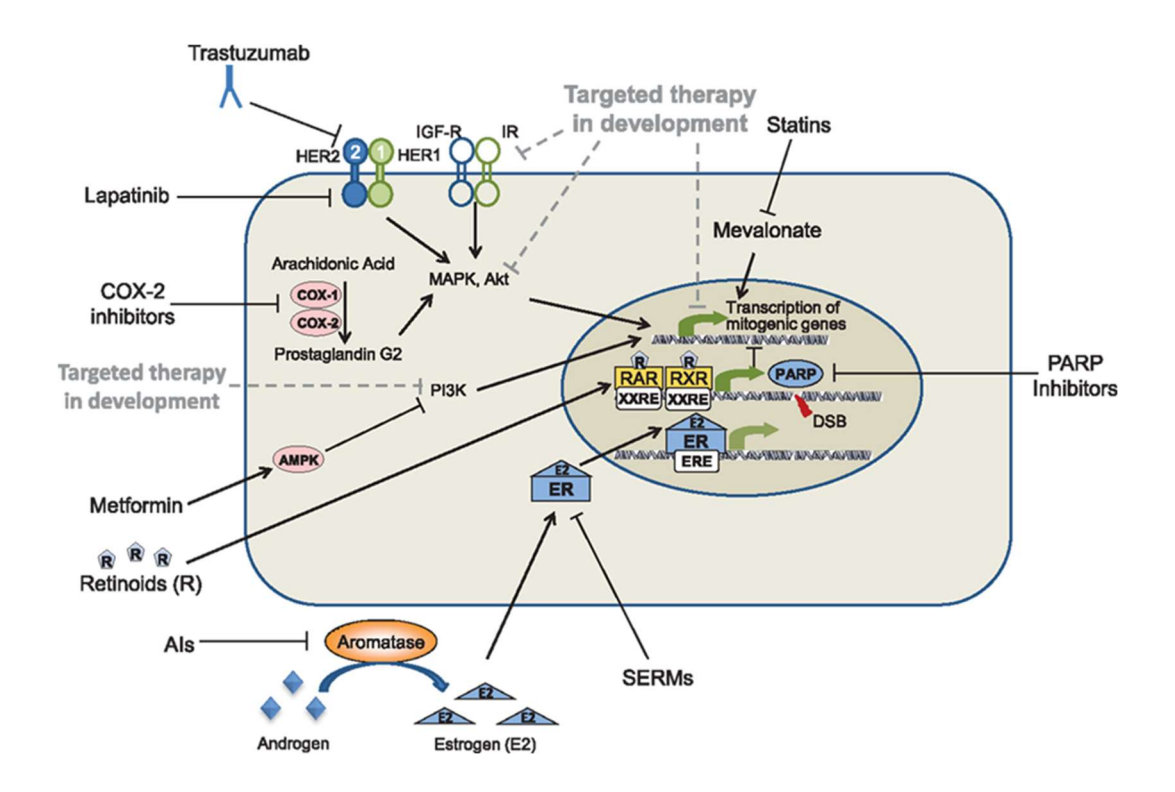


Figure 1-2: Molecular targets for the prevention and treatment of breast cancer

The common molecular targets for therapeutic agents utilised in the prevention and treatment of breast cancer (adapted from Hollander *et al.* 2013)

1.5 Triple negative breast cancer

TNBC is a type of breast cancer that represents 15-20% of breast cancer cases globally and is commonly observed in young women under 40 years of age (Al-Saraireh *et al.*, 2021; Chen *et al.*, 2025). From its name, this subtype has negative expression of oestrogen receptors (ER), progesterone receptors (PR), and also has no overexpression of human epidermal growth factor receptor 2 (HER2) (Hammershoi Madsen *et al.*, 2024). The incidence rate is high in young black, African-American, Indian and Hispanic women as compared with other ethnic groups of young ages (Ren *et al.*, 2019). Furthermore, premenopausal African – American women have high risk of TNBC in comparison with postmenopausal women of the

same ethnicity(Chen *et al.*, 2025). Due to the heterogeneity of TNBC, it is considered as a biologically aggressive subtype, and the identification of molecular targets could help in the development of effective treatments (Lehmann *et al.*, 2011).

The breast cancer genes 1 and 2 (BRCA 1/2) are genes that encode proteins responsible for the repair of damaged DNA, and mutations of these genes have a role in the development of breast cancer, particularly familial breast cancer (Hatano *et al.*, 2020). Triple negative breast cancer is often associated with BRCA1 and BRCA2 mutations. For instance, Mavaddat *et al.* (2012) conducted a large cohort analysis for the data from 3,797 BRCA1 and 2,392 BRCA2 mutation carriers diagnosed with invasive breast cancer, revealing that 68% of tumour arising in BRCA1 carriers were triple negative. However, only 16% of BRCA2 carriers displayed a triple-negative phenotype tumour. These findings underscore the significant association between BRCA1 mutations and triple-negative breast cancer (TNBC).

Clinically, the recurrence of TNBC is high, with a substantial risk of metastasis and poor prognosis compared to other subtypes of breast cancer (Hammershoi Madsen *et al.*, 2024; Xu *et al.*, 2025). For instance, Hennigs *et al.* (2016) demonstrated that 69.1% of TNBC patients have a five-year disease-free survival rate which is significantly lower than the 92.1% five survival rate reported in patients with the luminal A subtype. Likewise, the five-year overall survival rate for luminal A was 95.1%, significantly higher than 78.5% for TNBC, indicating the aggressive nature and poorer prognosis of TNBC.

The biological complexity of TNBC has been revealed by several molecular studies, highlighting key molecular pathways contributing to its biological aggressiveness (Agelidis *et al.*, 2025; Asleh and Polyak, 2022). Aberrations in DNA damage repair, particularly in patients with BRCA1/2 mutations, underpins the sensitivity to poly (ADP-ribose) polymerase (PARP) inhibitors (ter Brugge et al., 2023; Du et al., 2025).

Dysregulation of the PI3K/AKT/mTOR pathway has also been frequently demonstrated to enhance TNBC tumour growth, suggesting a promising target for novel inhibitors (Zhang *et al.*, 2024; Hassan *et al.*, 2025). TNBC cells, particularly basal-like subtypes, have shown overexpression of EGFR and the downstream MAPK, that further contribute to tumour growth (Jiang *et al.* 2020). Furthermore, the activation of STAT3 via the JAK-STAT signalling pathway has been associated with TNBC progression, immune evasion, and therapy resistance, highlighting it also as an emerging therapeutic target (Qin *et al.* 2019). Additionally, the immunogenicity of TNBC characterised by PD-1/PD-L1 checkpoint activation has been implicated in the immune evasion, rationalising the development of targeted immunotherapeutic agents such as pembrolizumab (Syrnioti *et al.*, 2024). Collectively, these pathways provide a comprehension for TNBC heterogeneity and underscore the targets for development of novel drugs. The key pathways involved in TNBC proliferation and survival, and promising therapies are shown in Figure 1.3 (adapted from Ryu and Sohn, 2021)

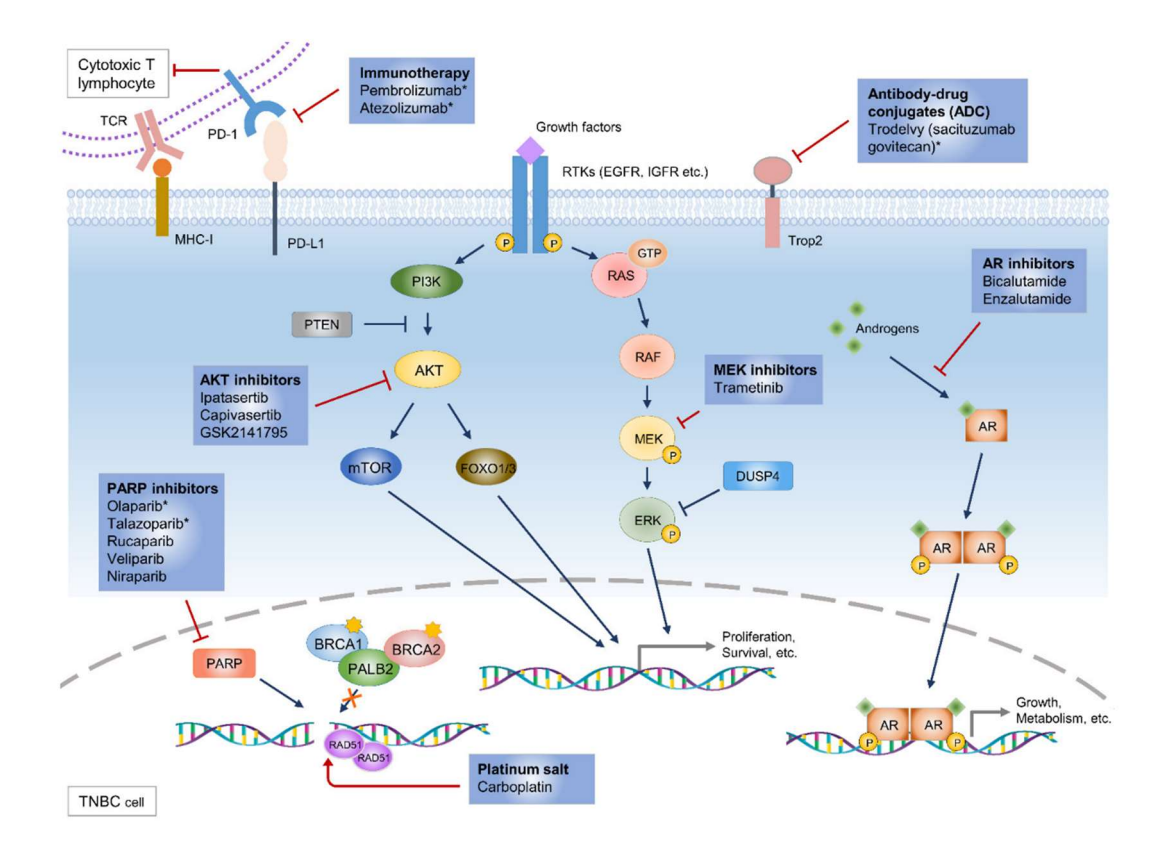


Figure 1-3 Schematic illustration for key molecular pathways in TNBC

The intracellular and extracellular pathways involved in TNBC pathogenesis with current targeting drugs (adapted from Ryu and Sohn, 2021)

1.5.1 Classification of TNBC

TNBC is a heterogeneous tumour which has no targeted receptor such as ER, PR, and HER2 and this has encouraged researchers to investigate the phenotypes of TNBC relative to the molecular characteristics. Previous histopathological studies categorised the disease into different subtypes groups, where (Lehmann, Pietenpol and Tan, 2015) identified six molecular subtypes of TNBC, basal like 1 (BL1), Basal like 2(BL2), mesenchymal (M), immunomodulatory (IM), mesenchymal stem-like (MSL) and luminal androgen receptor (LAR). In a previous study on 465 Chinese patients with TNBC, (Jiang *et al.* 2019) categorised them into four subtypes, basal like immune- suppressed, immunomodulatory, mesenchymal- like and luminal androgen receptor. Combining the results of these studies leads to four major subtypes being identified which are basal like (BL), mesenchymal like (MEL), immunomodulatory (IM) and luminal androgen receptor (LAR).

The basal-like subtype is characterised by higher mutation rates of the tumour suppressor breast cancer gene (BRCA1/2) and overexpression of cell cycle and DNA damage response genes (Lehmann *et al.*, 2016). Furthermore, this subtype showed increased expression of Ki-67, a nuclear protein that is involved in ribosomal RNA synthesis and it is considered as a biomarker for cellular proliferation (Balko *et al.*, 2014; Abramson *et al.*, 2015). The basal like subtype may display downregulation of cytokine and immune regulating pathways, reflected by low expression of molecules controlling immune cell differentiation, antigen presentation and adaptive immune cell communication, resulting in low disease free survival (Burstein *et al.*, 2016). Additionally, this molecular subtype was also associated with the upregulation of genes controlling immune cell functions such as B cells, T cells and natural killer cells,

and therefore it may be called a basal like immune activated subtype which has good prognosis (Burstein *et al.*, 2016).

The mesenchymal-like subtype is characterised by upregulation of pathways that are commonly aberrant in breast cancer. This may include signalling pathways regulating cell motility and differentiation such as mismatch repair and DNA damage networks, overexpression of growth factors such as insulin like growth factor (IGF1) and higher expression of genes involved in epithelial mesenchymal transition (EMT) (Burstein et al., 2016; Lehmann et al., 2016). Mesenchymal-like subtype, often associated with claudin- low phenotype, is characterised by decreased expression of key cell-cell adhesion molecules including claudins and E-cadherin, enhancing the motility and invasiveness of the cells, thereby increasing the aggressiveness and metastasis of TNBC tumours (Dias et al. 2017; Tang et al. 2022; Zhang et al. 2021). The immunomodulatory (IM) subtype is characterised by higher expression of genes involved in immune mediating pathways, including T cell signalling, natural killer cell functions, cytokine signalling and antigen presentation. This immune-related profile reflects the active involvement of immune signalling pathways and potential immune cell infiltration (Lehmann et al. 2016; Tang et al. 2022; Zhang et al. 2021). The luminal androgen receptor (LAR) is the subtype group that has the most differential gene expression among other subtypes of TNBC (Jiang et al., 2019). This subtype is characterised by altered hormonal regulated pathways, and the tumours are enriched in expression of genes that are involved in oestrogen/androgen metabolism and steroid synthesis (Abramson et al., 2015; Lehmann et al., 2016). Overall, the TNBC subtypes are characterised by alterations in many signalling pathways and have overexpression of genes that could be considered as targets for different types of treatments.

1.5.2 Current treatment of TNBC

The absence of primary receptors in TNBC makes the treatment of this type of breast cancer challenging. Therefore, patients with TNBC have limited clinical options, with cytotoxic drug combination, surgery and radiotherapy being the current therapeutic strategies (Chen *et al.* 2025; Gupta *et al.* 2020; Won and Spruck 2020).

Neoadjuvant chemotherapies (NAC) including doxorubicin, docetaxel and cyclophosphamide have been shown beneficial effects in patients with TNBC by decreasing the tumour size (Omarini *et al.*, 2018). NAC has also been reported to induce a complete pathological response (pCR) reflected by disappearance of residual cancer, and thus better long-term outcomes (Amos *et al.*, 2012). The initial response rate of TNBC to NAC is better than other types of breast cancer, where the pCR rates for TNBC and luminal tumour patients have been demonstrated to be 45% and 6% respectively (Rouzier *et al.*, 2005). Additionally, some patients with TNBC achieved a higher pCR rate (22%) compared to 11% of non-TNBC, and those TNBC patients had the same survival rate as other types of BC (Liedtke *et al.*, 2008). However, more than 50% of patients with TNBC could not achieve a pCR, and presented with residual cancer and poorer survival rate compared to non-TNBC patients (68% vs 88%), suggesting the resistance of TNBC patients to chemotherapies (Liedtke *et al.*, 2008; Cortazar *et al.*, 2014).

Chemotherapy is the gold standard option in the treatment of TNBC (Huang *et al.*, 2025). Previous studies have reported that while TNBC patients show a better initial response to chemotherapy than other breast cancer types, and yet there is still a poor prognosis (Caswell-Jin *et al.*, 2018; Plevritis *et al.*, 2018; Xu *et al.*, 2025). In clinical practice, anthracycline- and taxane-based regimens, frequently combined with cyclophosphamide remain the cornerstone of systemic therapy (Lee *et al.*, 2020; Han *et al.*, 2023). These regimens are often administered as sequential combinations, for

instance, doxorubicin and cyclophosphamide followed by paclitaxel or docetaxel (AC→T), or triple combination therapy including docetaxel, doxorubicin, and cyclophosphamide (TAC). Alternative anthracycline-free regimens, such as docetaxel or paclitaxel combined with carboplatin offer comparable efficacy in patients unable to tolerate anthracyclines side effects (Girardi et al., 2025; Du and Huang, 2025). Anthracyclines (e.g., doxorubicin and epirubicin) are cell proliferation inhibitors which prevent cell replication by inhibiting DNA synthesis and topoisomerase enzyme activity (Abrahams, Gerber and Hiss, 2024; Huang et al., 2025). Taxanes (e.g., paclitaxel and docetaxel) are antimicrotubular agents that are commonly used in the treatment of breast cancer, working via preventing depolymerization of microtubules and subsequent separation of chromosomes in mitosis (Sarno et al., 2023; Huang et al., 2025). The alkylating agents (e.g., cyclophosphamide) act by addition of an alkyl group to the nitrogenous base of DNA, thereby forming cross links among quanine bases which prevents DNA replication (Wahba and El-Haddad, 2015; Ge et al., 2022). Due to the variation in tumour microenvironments and molecular characteristic of cancer cells, TNBC treatment with single therapies is challenging and can lead to the development of drug resistance resulting in rapid tumour relapse (Gupta et al., 2020). Therefore, targeting the significant pathways involved in progression of cancer by combination therapy may enhance the efficacy, minimising the chemoresistance and improving disease free survival in TNBC (Leon-Ferre and Goetz, 2023; Sofianidi et al., 2024; Sriramulu et al., 2024)

Despite the common use of combination chemotherapy for TNBC, the response to chemotherapy is not of long term and may be followed by refractory or rapid relapses of the disease with rapid metastasis, mainly to the brain and visceral organs such as liver and lung (Bai *et al.*, 2021; Nedeljković and Damjanović, 2019). Unfortunately, the standard chemotherapeutic regimens are not available for relapsed TNBC (Won

and Spruck, 2020). Due to a high rate of recurrence and poor prognosis, new treatments and targeted therapies are required to be tailored to the clinical need for TNBC management. Furthermore, identifying novel predictive biomarkers that differentiate responders to cancer therapy is important in selecting the appropriate therapeutic regimen. Currently, several predictive biomarkers are clinically valuable, for instance, pathological complete response (pCR) following neoadjuvant chemotherapy is one of the prognostic indicators of long-term survival in TNBC (Cortazar et al., 2014). Furthermore, BRCA1/2 mutations have been implicated to predict the sensitivity to platinum treatment and PARP inhibitors as well as denoting to the risk of tumour progression (Valenza et al. (2023)). Additionally, PD-L1 expression has been demonstrated as a predictive biomarker for the response of TNBC to pembrolizumab, an immune checkpoint inhibitor (Schmid et al., 2020).

1.5.3 New approved therapies for TNBC

In recent years, the FDA has approved new therapeutic agents with various molecular targets for the treatment regimen of TNBC. Immune cell signalling pathways have been investigated for TNBC where programmed cell death ligands (PD-L1) expression was found to be elevated in this subtype of breast cancer (Andrieu *et al.*, 2019). PDL-1 ligands have the ability to bind with PD-1 receptors that are expressed on the surfaces of tumour infiltrating cells (TILs), especially T cells, to deactivate T cell functions and evade the immune checkpoints (Beckers *et al.*, 2016; Candas-Green *et al.*, 2020; Zhou *et al.*, 2021; Ge *et al.*, 2022). The molecules that target these ligands have shown improved anti-tumour immunity leading to tumour cell killing as well as having an additive effective in combination therapy (Andrieu *et al.*, 2019; Huang *et al.*, 2025). The availability of TILs clusters or overexpression of PD-1 may predict a good outcome for patients receiving immunotherapy which induce

increasing of cancer immunity (Tomioka et al., 2018; Sarno et al., 2023). The infiltrating immune cells in tumour stromal of nearly 40% of TNBC patients have PD-L1 overexpression, therefore, targeting of these ligands seem to be promising in treatment of TNBC (Mittendorf et al., 2014; Tomioka et al., 2018; Zhou et al., 2021). Atezolizumab, an FDA approved anti-PD-L1 antibody, has been reported in a recent clinical trial (NCT02425891), to have potential benefits in the treatment of local and metastatic PD-L1 positive TNBC patients when used concurrently used with nabpaclitaxel (Adams et al., 2020). However, some of Anti PD-L1 treatments such as Nivolumab and Ipilimumab have shown adverse effects in patients such as diarrhoea, fatigue and pruritus which are attributed to activation of the immune system and this may lead to discontinuation of treatment (Larkin et al., 2015; Boutros et al., 2016). In the United States, 69-72 % of women who are carrying BRCA 1 and BRCA 2 mutations have developed breast cancer (Safra et al. 2021), and harbouring of BRCA 1&2 mutations is common in TNBC with a prevalence rate of around 10-20 % (Yadav et al., 2018). Poly-ADP ribose polymerase (PARP) proteins have a significant role in repairing DNA strand breaks through the induction of enzymes responsible for DNA repair (Hatano et al., 2020). It has been shown that the inhibition of PARP prevent DNA repair, producing an accumulation of single and double strands DNA breaks and subsequently tumour cell deaths (Caron et al., 2019). This mechanism offers an opportunity for targeted therapy in TNBC as TNBC carriers for BRCA1 and BRCA2 mutations have been demonstrated to benefit from anti PARP therapy (Beniey, Hague and Hassan, 2019; Hammershoi Madsen et al., 2024; Pont, Marqués and Sorolla, 2024). Olaparib, a PARP inhibitor, has shown a promising results in the treatment of breast cancer with HER2 negative and germline BRCA1/2 mutation-carrying breast cancer tumours (Robson et al., 2017). The data demonstrated a significantly improved response rate to Olaparib in comparison with standard therapy (59.9% vs

28.8%) with elevated disease progression free survival from 4.2 months to 7 months in the treatment group.

It has been demonstrated that the growth and invasion of cancer cells could be regulated by a glycoprotein named trophoblast cell-surface antigen (Trop-2), which was found to be overexpressed in many solid cancers in comparison with normal tissues (Goldenberg, Stein and Sharkey, 2018). The targeting of this protein may contribute to the prevention of tumour growth, particularly if conjugated with an antibody. For example, the conjugation of anti-Trop-2 drugs such as Sacituzumab with the active metabolite of the topoisomerase inhibitor, irinotecan, has been shown to inhibit the activity of the topoisomerase enzyme and prevent the repair of DNA damage, thereby increasing cancer cell death (Ocean *et al.*, 2017). This antibody-conjugated drug has shown a promising role in treating TNBC by increasing the response rate and progression survival compared to standard chemotherapy (33% and 5.5 months vs. 10-15% and 2-3 months, respectively) (Bardia *et al.*, 2019).

1.5.4 Therapeutic resistance of TNBC

TNBC is often initially sensitive to chemotherapy administered in an adjuvant or neoadjuvant regimen. However, this biologically aggressive subtype may undergo relapse and the recurrent tumours are highly resistant to chemotherapy, surgery and radiotherapy resulting in low survival rates in comparison with other breast cancer subtypes (Sarno et al., 2023; Huang et al., 2025). Additionally, the invasiveness and therapeutic resistance of TNBC tumours cause challenges in the treatment of relapsed and recurrent TNBC. The mechanisms of resistance will be discussed in the following section.

1.6 The mechanisms of therapeutic resistance

The multifactorial process of TNBC resistance to therapy involves diverse molecular and cellular mechanisms. Enhanced drug efflux has been demonstrated to induce resistance to therapies, where the involvement of P-glycoprotein (P-gp), multidrugresistant protein-1 (MRP1), and breast cancer resistance protein (BCRP) in decreasing the intracellular drug accumulations were demonstrated, resulting in TNBC chemoresistance (Bai et al., 2021). Evasion of cell death via modulating apoptotic pathways contribute to induction of resistance, for instance, the antiapoptotic components such as B-cell lymphoma 2 (Bcl-2) and myeloid leukaemia cell differentiation protein 1 (Mcl-1) were shown to induce TNBC chemoresistance (Balko et al., 2014). One of the increasingly recognised crucial factors mediating resistance to cancer therapies is the tumour microenvironment (TME). In TNBC, the TME including cancer-associated fibroblasts (CAFs), tumour-associated macrophages (TAMs), and infiltrating immune cells are implicated in therapeutic resistance by enhancing stemness, metastasis, and immunosuppression (Singh et al. 2024). Hypoxia, originating from enhanced tumour growth and abnormal vasculature, is a key mediator of resistance, which can promote cancer cell stemness, immune evasion and metastasis by activating the hypoxia inducing factor-1 alpha (HIF-1α) (Han et al. 2024). Moreover, HIF-1α could be involved in reducing DNA damage fixation and modulating drug metabolism, thereby decreasing the effectiveness of both radiotherapy and chemotherapy. In TNBC, hypoxia was shown to mediate docetaxel resistance by decreasing the levels of miR-494, contributing to decreased drug response (Li et al., 2022).

Although each one of the mentioned mechanisms contributes to resistance development, attention has been directed to three crucial and interrelated

mechanisms that are particularly relevant to TNBC and response to radiation: oxidative stress regulation, DNA damage repair capability, and metabolic reprogramming. These mechanisms are discussed in more detail below.

1.6.1 The potent antioxidant activity

The main mechanism of action of radiation to kill the cancer cells is induction of damage to the cell's DNA and macromolecules. This effect can be induced by direct energy deposition of radiation in the DNA strands or by generation of reactive oxygen species (ROS) by interaction of the radiation with water molecules in the cells. Following radiation exposure, ROS is predominantly produced via water hydrolysis, causing damage to the DNA and other critical cellular structure such as the membrane of mitochondria, resulting in releasing of cytochrome C and subsequently enzyme dependent apoptosis (Beatty *et al.*, 2018; Bai *et al.*, 2021). Interestingly, morphological changes in the mitochondria of TNBC following exposure to ROS-inducing agent have been identified, suggesting that mitochondria may be the primary source of ROS in the TNBC cell line, and this ROS level was high in TNBC compared to other subtypes of breast cancer (Sarmiento-Salinas *et al.*, 2019).

To mitigate ROS accumulation, normal and malignant cells rely on antioxidant mechanisms, such as glutathione, which contribute to maintaining redox homeostasis. However, TNBC cells were found to overexpress nuclear factor erythroid 2–related factor 2 (Nrf2), a main protein used in the synthesis of glutathione. Higher levels of Nrf2 and its related proteins were associated with decreased capacity for ROS production in resistant TNBC cells compared to non-resistant cells (Carlisi *et al.*, 2017; Xue, Zhou and Qiu, 2020).

The thioredoxin (Trx) system, including Trx, thioredoxin reductase (TrxR), and NADPH, represent another pivotal antioxidant system that contributes to cancer

progression and resistance to therapies (Jovanović *et al.*, 2022). Alongside its effectiveness regulating ROS detoxification by direct reduction of oxidized proteins, the thioredoxin system also supports cancer cell stemness and angiogenesis. Notably, overexpression of Trx1 and TrxR1 has been demonstrated to enhance TNBC cells migration and invasion, suggesting its involvement in metastasis (Bhatia et al., 2016). Interestingly, inhibition of thioredoxin reductase (TrxR), a critical enzyme that controls intracellular redox homeostasis, by antirheumatic drug-auranofin, results in increased intracellular ROS, disrupted redox buffering system, and suppressed breast cancer cell growth, suggesting the mechanisms of auranofin anticancer activity (Seo *et al.* 2023). Importantly, thioredoxin-interacting protein (TXNIP), an antitumour protein, is the counterbalance of thioredoxin system that directly binds and negatively regulates Trx (Singh *et al.*, 2025). In TNBC, overexpression of TXNIP has been shown to augment ROS accumulation, enhance DNA damage, and improve the sensitivity to doxorubicin, reflecting its crucial role in suppression of the activity of the Trx system (Chen *et al.*, 2022).

Following treatment with radiation, radioresistant TNBC cells have shown lower intracellular accumulation of ROS compared with those sensitive to the therapy, hypothesised to result from induction of \(\chi\)-glutamylcysteine synthase, an antioxidant gene, reflected by upregulation of Nrf2 protein (Lu *et al.*, 2018). Interestingly, ROS or oxidative stress related factors have been highlighted as potential biomarkers for TNBC tumour progression. Moreover, targeting mitochondrial ROS has decreased tumour growth and increased cancer cell death (De Sá Junior *et al.*, 2017; Kubli *et al.*, 2019; Sarmiento-Salinas *et al.*, 2019). This controversy in effects of antioxidants in TNBC needs further work to determine the effective pathways and suggest the best therapeutic interventions.

1.6.2 Promoted DNA Repair

One of the mechanisms that cancer cells utilise to overcome therapy induced cell death is enhanced DNA damage repair. Although DNA repair is upregulated in cancer cells, it is aberrant and thus cancer cells can repair but they do so in a way that does not maintain genome integrity, making repaired cells even more mutated and thus more aggressive. The alkylating agents such cyclophosphamide and carmustine exert cytotoxic effect by adding alkyl groups to the amino acid base of DNA strand breaks producing O⁶- methylguanine or O⁴- methylamine and thereby preventing DNA repair (Alnahhas et al., 2020). However, resistance to alkylating agents may be induced by an enzyme called methylguanine-DNA methyltransferase (MGMT), which can remove the alkyl group from the DNA by transferring it to the amino acid residue of MGMT providing an opportunity for restoring DNA integrity (Raguz et al., 2013; Alnahhas et al., 2020; Xing and Stea, 2024). MGMT methylation status has been found to be correlated with disease progression and response to treatment in different types of tumour, where MGMT gene promoter methylation has been reported to be a prognostic and response-predictive biomarker in glioblastoma patients receiving temozolomide therapy (Alnahhas et al., 2020). Additionally, methylation of MGMT has a role in sensitizing the cells to treatment with alkylating agents. For instance, TNBC patients pre-operatively treated with alkylating agents demonstrated enhanced MGMT methylation and improved clinical response (Fumagalli et al., 2014). The aberration in mismatch repair (MMR), a mechanism responsible for correcting erroneous DNA bases and restoring DNA integrity, contributes to chemoresistance. Defects in this repair machinery have been demonstrated to promote insertion of large

numbers of mismatched bases during DNA replication, making TNBCs resistant to

alkylating agents and antimetabolites (Bai et al., 2021). In a previous study, Staaf et

al. (2019) conducted a whole-genome sequence of 254 TNBC patients in Sweden

50

and found that around 4.7% of TNBC patients had MMR deficiency. Additionally, MMR deficiency has been demonstrated as a predictive biomarker for the response to pembrolizumab, a programmed cell death 1 (PD-1) immune checkpoint inhibitor, in patients with colorectal cancer (Marcus *et al.*, 2019). The partial loss of MMR in patients with TNBC was also significantly correlated with overexpression of PDL-1, suggesting the susceptibility of MMR-deficient TNBC patients to immunotherapy (Mills *et al.*, 2018; Hou *et al.*, 2019).

Overall, detection and targeting of DNA repair pathways in TNBCs seems valuable and promising. Identification of genes relevant to DNA repair may help predict therapeutic sensitivity and contribute to personalized medicine.

1.6.3 Metabolic adaptation

Under physiological conditions, the energy required for normal cellular functions is mainly produced via mitochondrial oxidative phosphorylation. However, cancer cells shift to other energy sources to meet their needs for their proliferation and survival. For instance, the increased cell reliance on glycolysis, even in the presence of oxygen, is a biological process called aerobic glycolysis or the Warburg effect (Stine et al., 2022; Saheed et al., 2024). The key protein in aerobic glycolysis is pyruvate kinase isoenzyme M2 (PKM2), which is responsible for the production of pyruvate that subsequently converts to lactate in the glycolysis pathway. The activity of this enzyme is regulated in response to cellular demands via intracellular signalling pathways and metabolic regulators (Wang, Jiang and Dong, 2020; Mitaishvili et al., 2024). Metabolic reprogramming is crucial for breast cancer cells to adapt to the stress induced by chemotherapy or radiotherapy thereby enhancing therapy resistance (Liu et al. 2024). Moreover, doxorubicin resistant breast cancer cells were

associated with enhanced aerobic glycolysis induction via metabolic reprogramming (Xu et al., 2018).

The upregulation of lactate dehydrogenase enzyme (LDH), a key enzyme for lactate production has been associated with oestrogen positive breast cancer patients resistance to PI3K inhibitors (Ros *et al.*, 2020). Furthermore, lactate released from breast cancer cells has been demonstrated to activate tumour-associated macrophages, leading to HIF-α release, which in turn increases glycolysis in tumour cells and enhances chemotherapeutic resistance (Chen *et al.* 2019). In TNBC cells, higher expression of several proteins including lactate dehydrogenase, pyruvate dehydrogenase -1 and epidermal growth factor-like 9 has been demonstrated, suggesting the cells reliance on aerobic glycolysis to maintain their survive and metastases (Bai *et al.* 2021; Dupuy *et al.* 2015; Meng *et al.* 2019). Targeting of aerobic glycolysis may help in preventing the metastasis of TNBC, but it is not sufficient to reverse the resistance and control the disease due to the presence of other metabolic pathways, therefore using combination therapy to target multiple pathways seem to be a promising strategy (Tseng *et al.*, 2018; Jia *et al.*, 2019).

Amino acid metabolism also represents an essential metabolic boost for cancer cells to converge their increased energy requirements. Glutamine is a primarily amino acid utilised by cancer cells, which acts as a ready bioenergetic and biosynthetic source as well as its role in maintaining cellular homeostasis required for tumour growth (Altman, Stine and Dang, 2016; Halama and Suhre, 2022; Jin *et al.*, 2023; B. Wang *et al.*, 2024). Glutamine enters the cells via specific amino acids transporters, and intracellularly the enzyme glutaminase convert it to glutamate which is further catabolized to α-ketoglutarate, a tricarboxylic acid cycle element, via glutamate dehydrogenase (Pranzini *et al.*, 2021). The altered pattern of glutamine metabolism has been shown to be associated with endocrine therapy resistance (Ananieva and

Wilkinson, 2018; Bacci et al., 2019). Previous studies have revealed a relationship between altered glutamine metabolism and TNBCs suggesting that metabolic reprogramming may be critical in disease progression and can be suggested as a potential target for new therapeutic development (Won and Spruck, 2020; Gong et al., 2021). Promising results for treating TNBC with glutamine metabolism inhibitors have been reported, where TNBCs demonstrated a higher sensitivity for CB-839, a glutaminase inhibitor, in TNBC xenograft models (Dos Reis et al., 2019). However, activating other metabolic drivers may lead to CB-839 resistant TNBC, suggesting that combination therapy may reverse the resistance and improve the outcomes. The metabolic adaptations that potentially contribute to therapy resistance in breast cancer are illustrated in Figure 1.4 (adopted from Garg et.al, 2025)

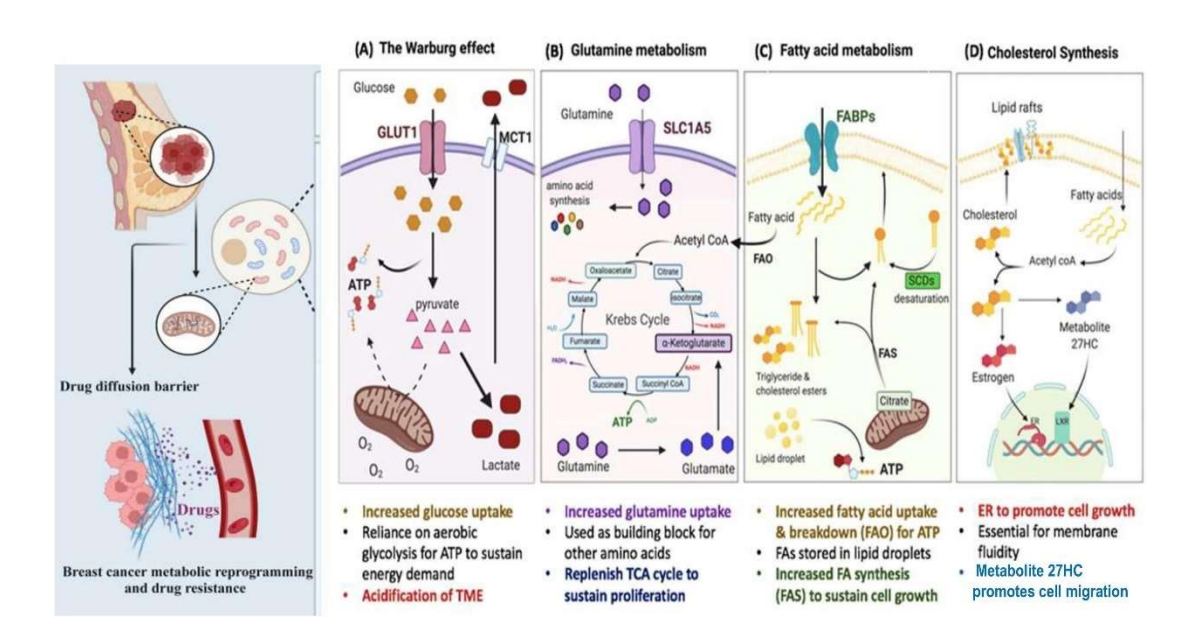


Figure 1-4 Common metabolic adaptations in breast cancer (Garg et al., 2025)

1.7 Role of PI3K/mTOR pathway in TNBC

Identifying pathways involved in promoting cancer cell proliferation and tumour growth has an important impact on developing appropriate therapies for managing cancers. Phosphoinositide 3-kinase (PI3K)/protein kinase B (AKT)/ mammalian target of rapamycin (mTOR) pathway is an important intracellular signalling pathway used in regulation of several physiological and cellular breast cancer processes including cell proliferation, metabolism and stress response (Costa, Sook and William, 2018; Yu, Wei and Liu, 2021). The upregulation of the PI3K/AKT/mTOR pathway may contribute to multidrug resistance of cancer through diverse mechanisms including but not limited to antagonising apoptosis, cross-talk with hormone receptors mediating endocrine therapy resistance, modulating receptors tyrosine kinase activities, reactivation of the same pathway via releasing of negative feedback loops signals, upregulation of drug resistance protein and drug metabolism (Mukohara, 2015; Z. Liu et al., 2015; Hasanovic and Mus-Veteau, 2018; Post et al., 2021; Leon-Ferre and Goetz, 2023). The PI3K/AKT/mTOR pathway has been demonstrated to play a significant role in TNBC, where activating any component of this pathway leads to increased cell proliferation, invasiveness, chemoresistance and tumour survival. Therefore, this pathway has been considered a potential molecular target for designing therapeutic molecules to treat TNBC (Khan et al., 2019a; Medina et al., 2020). Notwithstanding these advancements, the intrinsic plasticity of TNBC allows tumour cells to activate alternate signalling pathways, enhancing treatment resistance and survival. Hence, developing combination therapies with multiple intracellular targets, including the PI3K/AKT/mTOR pathway, represents a potential approach to treating TNBC (Khan et al., 2019; Yu et al., 2021).

1.8 Combination therapy and repurposing drugs strategy for the treatment of TNBC

Due to the absence of receptors on its cellular membranes, TNBC demonstrates unresponsiveness to targeted endocrine or HER2-directed therapies, making chemotherapy the primary treatment approach (Bianchini *et al.*, 2016). However, single chemotherapeutic agents often result in temporary responses, accompanied by higher relapse rates and the development of drug resistance, leading to treatment failure and tumour recurrence (Denkert *et al.*, 2017).

To overcome the acquired drug resistance, combination therapy has emerged as a potential approach for the treatment of this aggressive breast cancer subtype. This approach employs a combination of two or more therapeutic agents to target different molecular pathways, aiming to enhance efficacy, decrease drug resistance development, and potentially minimise the toxicity of monotherapy. The PI3K/AKT/mTOR signalling pathway is frequently overexpressed in TNBC, associated with cancer proliferation and survival as well as contribution to inducing of therapy resistance (Mayer and Arteaga, 2016). Targeted inhibition of this pathway may have the potential to enhance the therapeutic effects of cytotoxic agents and radiation.

Several inhibitors for the PI3K/AKT/mTOR pathway were developed and clinical trials have been undertaken to evaluate the efficacy and safety of these inhibitors as a monotherapy or combination therapy for TNBC. Promising results were highlighted in the PACT trial conducted by Schmid *et al.* (2020), assessing the efficacy of combining capivasertib (an AKT inhibitor) with paclitaxel as a first-line therapy for metastatic TNBC. The data have demonstrated that this combination resulted in significantly longer progression-free and overall survival compared to standard therapy.

Gedatolisib (PF-05212384) was developed by Pfizer as a dual node inhibitor of PI3K and mTOR, disrupting the PI3/Akt/mTOR signalling pathway involved in cancer cell metabolism, proliferation, and survival. This drug has been shown to have a promising role in improving the tumour response to chemotherapy (Wainberg et al., 2017; Colombo et al., 2021; He et al., 2021). The inhibition of the PI3K/AKT/mTOR pathway may increase the cytotoxicity of radiotherapy, where enhanced G2-M arrest, the most radiosensitive cell cycle phase, has been reported (De Vera and Reznik, 2019a; Noorolyai et al., 2019). In vivo, the antitumour effects of combined gedatolisib with radiation in nasopharyngeal cancer xenografts demonstrated >50% reduction in xenograft volume and tumour regrowth delay compared with radiation alone (Liu et al. 2015). The NCT03911973 is an ongoing clinical trial evaluating the efficacy of combining Gedatolisib (dual PI3K/mTOR inhibitor) with talazoparib (PARP inhibitor) for advanced triple negative breast cancer. The safety profile study of gedatolisib revealed manageable adverse effects, where stomatitis and nausea have been demonstrated as the most common adverse effects associated with maximum tolerable dose estimated to be 158 mg once weekly by intravenous administration (Colombo et al., 2021; Layman et al., 2024).

Alongside combination therapy, drug repurposing has emerged as an important strategy in oncology, particularly for cancers with therapeutic challenges. Drug repurposing or repositioning is concerned with finding new therapeutic uses for existing drugs that have already been approved for the treatment of other diseases (Jakhmola-Mani *et al.*, 2024). This approach represents a substantially faster strategy with low cost and higher safety compared to the conventional development way of new medications, as repurposed drugs have well-established pharmacokinetic and safety profiles (Pushpakom *et al.*, 2019; Correia, Gärtner and Vale, 2021b). For instance, while *de novo* drug discovery typically spans 13–17 years with costs \$1.5–

2.5 billion, repurposed agents may reach the market within 3–12 years at a fraction of the cost (~\$300 million) (Nishimura *et al.*, 2017; Weth *et al.*, 2024).

Several repurposed drugs have revealed anticancer activity across different tumour types. For instance, Metformin, initially utilised for type 2 diabetes, has shown anticancer effects by modulating cellular metabolism and enhancing energy homeostasis in cancer cells (Pushpakom et al., 2019). Additionally, Lin et al. (2022) identified repurposing of the antipsychotic Imipramine as a potential therapy for glioblastoma, demonstrating greater efficacy than temozolomide, the current standard chemotherapy. In TNBC models, several agents including statins, propranolol and chloroquine have shown promising preclinical effects, demonstrating anti-proliferative, pro-apoptotic, and anti-metastatic effects (Wolfe et al., 2015; Bouchard et al., 2016; Spini et al., 2019). The repurposed drug for TNBC undertaken in preclinical studies are listed in table 1.1.

Drugs	Main indication	Mechanism of action	References
Acetylsalicylic acid	Analgesia, prophylaxis of further heart attacks or strokes	Cyclooxygenase inhibitor	Maity <i>et al.</i> , 2019 Zhou <i>et al.</i> , 2019 Bhardwaj <i>et al.</i> , 2018
Atorvastatin	Coronary heart disease, acute coronary syndrome	HMGCR inhibitor	Heikal <i>et al.</i> , 2024; Rachner <i>et al.</i> , 2014
Auranofin	Rheumatic Arthritis	NFkB pathway inhibitor	Raninga <i>et al.</i> , 2020, Hatem <i>et al</i> . 2018
Calcitriol	Vitamin D deficiency	Vitamin D receptor agonist	Martínez <i>et al.</i> , 2019 Zheng <i>et al.</i> , 2019
Chloroquine	Malaria, Extraintestinal Amebiasis	Antimalarial agent	Wenzel et al., 2025 Liang et al., 2019 Bouchard et al., 2016
Metformin	Diabetes	Insulin sensitizer	Sahu et al., 2024 Han et al. 2019 Strekalova et al. 2019
Propranolol	Hypertension	Adrenergic receptor antagonist	Spini <i>et al.</i> , 2019 Xie et al. 2019 Choy et al. 2016
Simvastatin	Hyperlipidaemia	HMGCR inhibitor	Tripathi et al. 2023 Yadav et al. 2023 Wolfe et al. 2015

Table 1.1 Repurposed drug for TNBC in pre-clinical studies

Repurposed drugs can be particularly beneficial when concurrently used with standard or targeted therapies. For instance, combining the conventional treatments with drugs that suppress key cell growth pathways, including the PI3K/AKT/mTOR pathway, may enhance the therapeutic effect and reduce drug resistance (Garg *et al.*, 2024). Key clinical trials for repurposed drugs in the management of breast cancers are shown in table 1.2. Overall, utilising repurposed drugs in combination with the standard therapies could improve treatment outcomes for TNBC and offer new therapeutic options for patients.

Drug	Main	BC subtype included in the	Clinical Trial ID
	indication	study	
Metformin	Diabetes	Early-stage breast cancer TNBC	NCT01101438 NCT04248998
Hydroxychloroquine	Malaria, Rheumatoid arthritis	Breast cancer with bone metastasis	NCT03032406
Propranolol	Hypertension	TNBC	NCT05741164
Quadruple Therapy- Quercetin, Zinc, Metformin, and EGCG	Diabetes and dietary supplements	Early Metastatic Breast Cancer and TNBC	NCT05680662

Table 1.2 Key clinical trials for repurposed drugs in breast cancer

1.9 Metabolomics

Metabolomics is an emerging analytical approach in the interrogation of biological systems, which can reflect the metabolic alterations that occur due to pathological, genetic, and environmental changes in cells. While it is described as a recent concept in systems biology, in fact, it has been developing for nearly 30 years, and the metabolomics term was formally introduced 1998 (Schmidt et al., 2021). This emerging field was consolidated by the initiation of the Human Metabolome Project in 2007, which was designed to systematically catalogue the human metabolites and provide methodological and analytical standards (Wishart et al., 2007). Since that time, the metabolomics field has evolved as a mature discipline of the omics group that encompasses genomics, proteomics, and transcriptomics (Díaz-Beltrán et al., 2021; Fan et al., 2016). Metabolomics focuses on the identification and quantification of metabolites such as amino acids, lipids, organic acids, and nucleotides precursors which make the metabolome of living organisms, so the name (metabolomics) was originated (Oliver et al., 1998). The identification of metabolic biomarkers is divided into two analytical sets, either targeted biomarkers analysis which means measurement of specific metabolites known to be associated with pathways of interest, or the untargeted metabolites which means investigating large numbers of metabolites and making statistical comparisons among them without any bias to demonstrate the significant metabolic alterations (McCartney et al., 2018; Reçber et al., 2020).

The specific group of metabolites that are determined by metabolomics techniques could differentiate subclasses of cancers including breast cancer and each class can be defined by the expressed metabolites. The types and numbers of metabolites that are identified in metabolomics studies depend on the required experimental design and aspects such as sample preparation, suitable instrumentation and the data

analysis programs that are utilised as illustrated in figure 1-3 which represents the procedures of metabolomics study (León *et al.*, 2013)

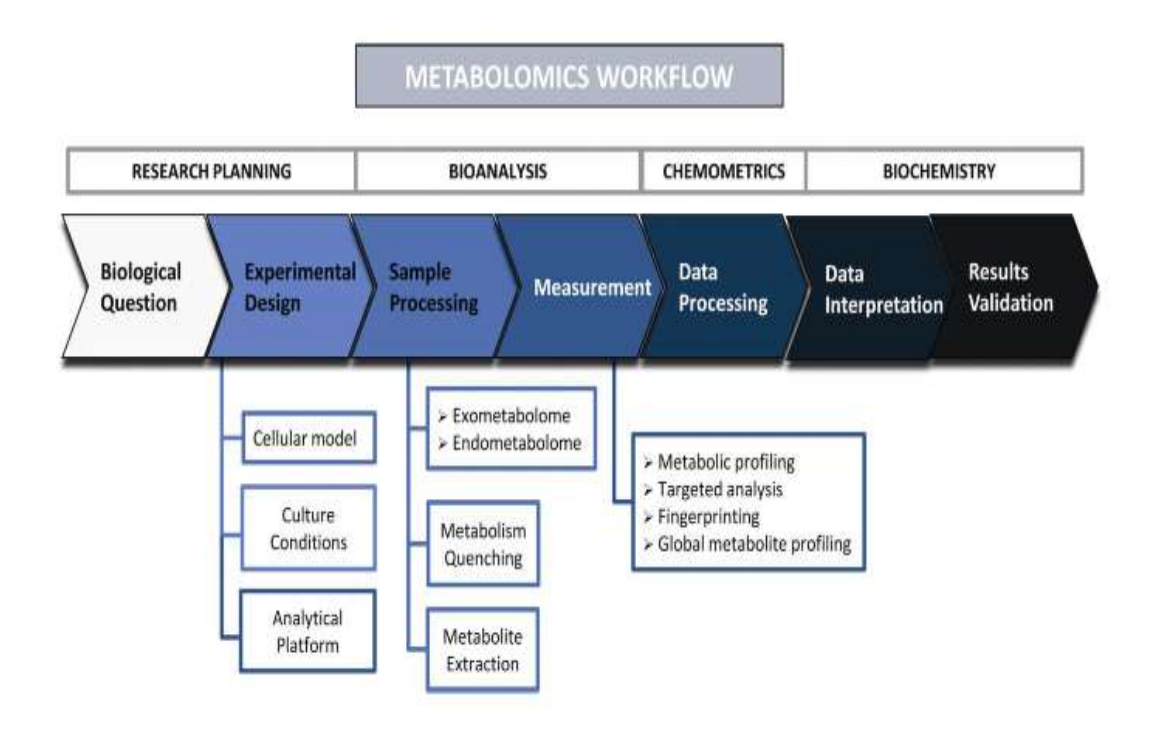


Figure 1-5 Scheme of general cell metabolomics workflow (Adapted from León *et al.*, 2013)

Figure 1.5 outlines the key steps in a cultured cell metabolomics study, commencing with the biological question and experimental framework, proceeding through sample preparation and metabolite quantification, and ending with data analysis, interpretation, and validation. It underlines the essential elements such as cellular model selection, quenching and extraction methods, as well as several analytical approaches including metabolic phenotyping and targeted analysis.

Different analytical techniques have been employed in identifying and quantifying the metabolites in breast cancer, and the highlighted biomarkers have been suggested to be used in different aspects such as diagnosis, progression of the disease and monitoring of the chemotherapies (Díaz-Beltrán *et al.*, 2021; McCartney *et al.*, 2018).

The most important analytical technologies that have been utilised in metabolomics studies are nuclear magnetic resonance (NMR), liquid chromatography and gas chromatography coupled to mass spectrometry (LC-MS, GC-MS), and each technique has limitations and strengths, therefore, there is no superiority for a single technology (Claudino *et al.*, 2007; McCartney *et al.*, 2018). The comparison among several analytical techniques utilised in metabolomics investigations are shown table 1.2 (adapted from Ren *et al.* 2022)

Method	Advantages	Disadvantages	
Great range of detectable molecular species; Simple sample preparation; Excellent reproducibility; High automation		Low sensitivity; Quantification of relatively high concentrations of metabolites/extensiv	
LC-MS	High sensitivity; Small sample volumes; Relatively low costs; Superior resolution	Matrix effects and ion suppression by co-eluting compounds; Limitation of detectable metabolites	
GC-MS	High chromatographic resolution; Large databases of identified peaks; High sensitive; High throughput	A large number of unidentified peaks; Require additional analytical steps; Separate and identify low molecular weight	
HPLC	Robustness; Convenience; Good selectivity; High sensitivity	Low throughput; Inability to observe non-electrochemically active species; Difficulties of metabolite identification; Lack of high efficiency	
UPLC	Short analysis time; Improved peak efficiency; Better resolution; Decreased use of solvents	Less time life of columns	
MALDI-MS	Suitability for solid samples; High sensitivity; Easy sample handling; Salt tolerance; High speed	Limitation of detectable metabolites	

Table 1.2 Advantages and disadvantages of metabolomics techniques (Ren et al. 2022)

1.9.1 Metabolomics of TNBC

The heterogeneity of TNBC makes this type of breast cancer highly aggressive and invasive. A fundamental comprehension of its biology may enable the identification of novel therapeutic targets. Different omics techniques such as genomics and proteomics have been employed to investigate the biological characteristics of TNBC, and recently metabolomics approach have explored a promising analytical technique that can be used in phenotyping of TNBC patients and identification of diagnostic and therapeutic monitoring biomarkers (Brown et al., 2017; Staaf et al., 2019; Tayyari et al., 2018). One of the most important characteristics that provide the opportunities for the diagnosis and treatments of cancer, is metabolic reprogramming described above which mean that cancer cells make an adaptation to different intracellular or extracellular changes that result in metabolic alterations to produce the energy required for replication and growth (Martinez-Outschoorn et al., 2017; Pavlova & Thompson, 2016), previous studies on different breast cancer cell lines revealed metabolic pathways perturbations of TNBC including the tricarboxylic acid cycle (TCA cycle), fatty acid and glutamine metabolism pathways, where they found that TNBC cells viability relies on variable metabolic alterations such as glycolytic and mitochondrial oxidative phosphorylation, lipid metabolism and glutaminolysis (Lanning et al., 2017; Timmerman et al., 2013; Trilla-Fuertes et al., 2020). By comparing the metabolic features of TNBC MDA-MB-231 with ER+ cell lines, TNBC cell lines have manifested with increased glucose uptake, overproduction of lactate and impaired mitochondrial respiration. From this experiment it has been hypothesized that lower oxidative phosphorylation activity may reflect the higher dependency of TNBC on glycolysis (Pelicano et al., 2014).

A recent study reported three subtypes of TNBC based on metabolic pathways with distinctive molecular features using a multi-omics database (Gong *et al.*, 2021). The

first metabolic pathway subtype (MPS1) is characterised by dysregulation of lipids metabolism and was designated the lipogenic subtype. The second subtype, MPS2 is the glycolytic pathway, where the upregulation of nucleotide and carbohydrate metabolism is the main characteristic of this subtype. Finally, the MPS3 subtype is the mixed subtype with partial dysregulation of both metabolic pathways. Furthermore, the sensitivity of these pathways to a metabolic inhibitor was demonstrated, where MPS1 was sensitive to the lipid biosynthesis inhibitors such as cerulenin while MPS2 was more sensitive to glycolytic inhibitors such as oxamate (Gong et al., 2021). Previous study also investigated the metabolic alterations in African- American women with TNBC and significant changes in metabolites were highlighted, such as decreased signals of lipids and glucose which indicated activation of the glycolytic pathway. Higher levels of glutathione, choline and lactate were demonstrated which reflect the metabolic alterations that me be involved in therapeutic resistance (Tayyari et al., 2018). Glutamine dependent pathway is crucial for the synthesis of pyrimidines bases, essential DNA and RNA components that support cell proliferation and growth (Trilla-Fuertes et al., 2020). Studies utilising different TNBC cell lines have demonstrated that adaptive reprogramming of pyrimidine synthesis was triggered following exposure to chemotherapy (Brown et al., 2017). Consequently, higher levels of pyrimidine nucleotides in TNBC may contribute to therapeutic resistance. The de novo pyrimidine synthesis pathway has therefore been identified as a metabolic vulnerability in TNBC, and targeting of this pathway with specific inhibitors may enhance the sensitivity of the cancer cells to chemotherapies (Brown et al., 2017). Supporting its importance in TNBC, low levels of glutamine have been reported in TNBC tissues, suggesting increased glutamine uptake and consumption by TNBC and reflecting the upregulation of glutaminolysis to meet metabolic demands (Timmerman et al., 2013; Trilla-Fuertes et al., 2020). However, in a further study by Tayyari et al. (2018), the TNBC tissues of African

American women demonstrated higher levels of glutamine compared to Caucasian women, which implies that the patient's race may influence metabolite expression. In order to identify potential pathways which could be therapeutic targets based on the tumour metabolome, Beatty et al. (2018) investigated twelve TNBC cell lines in a metabolomics study using mass spectrometry techniques and they identified upregulation of the glutathione biosynthesis pathway in TNBC which may result in suppression of reactive oxygen species and increasing tumour cell survival and thus suggest that inhibition of this pathway could help in management of TNBC. In a further study, the metabolic alterations in TNBC during specific cellular conditions such as hypoxia were investigated using the MDA-MB-231 cell line via a gas chromatography mass spectrometry based untargeted metabolomics technique (Yang et al., 2018). The research demonstrated increased glutaminolysis and glycolysis during hypoxia compared to normoxia whereas the tricarboxylic cycle, pentose phosphate and pyruvate carboxylase pathways were inhibited. These finding imply that TNBC may utilise several pathways such as glycolysis, to adapt to the environmental changes and meet their requirements for growth.

Overall, metabolomics has emerged as a promising approach in cancer research, offering particular insights into tumour heterogeneity and the tendency to develop resistance to standard therapies. In TNBC, where acquired resistance to conventional therapies is common, metabolomics provides a distinctive opportunity to identify the metabolic shifts that drive tumour survival and development of drug resistance. These insights not only provide a comprehension of TNBC biology but also facilitate the identification of metabolic biomarkers and therapeutic targets. Interestingly, metabolomics may significantly inform the effective therapeutic strategies, including drug repurposing utilisation and rational combination therapies tailored to the metabolic profile of resistant cancer cells.

1.10 Aims of the project

Triple-negative breast cancer (TNBC) still represents a clinically challenging subtype of breast cancer due to its aggressive behaviour, lack of targeted therapies, and high incidence of therapeutic resistance. Despite the initial response of TNBC to standard anticancer agents, the emergence of treatment resistance and then tumour reoccurrence make the management of this disease challenging and clinically unmet. Hence, utilising targeted therapies that inhibit the common deregulated molecular pathways as well as the standard cancer treatments may improve the therapeutic outcomes. This project aimed to develop therapeutic strategies for TNBC by evaluation of novel combination therapies encompassing molecularly targeted inhibitors using biological assessments *in vitro*. Additionally, the metabolic pathways associated with radiation resistance were identified through metabolomics study utilising LC-MS analytical platform. Collectively, the current project aimed to provide a comprehensive framework for the identification and mitigation of resistance pathways utilising the integration of pharmacological assessment, establishment of resistant cell models, and cell-based metabolomics.

The specific objectives of this research are:

- Due to the potential of PI3k/AKT/mTOR inhibitors for TNBC, we firstly aimed
 to assess the efficacy of gedatolisib, a dual PI3K/mTOR inhibitor, in
 combination with radiation and doxorubicin in the TNBC cell line (MDA-MB
 231) with the goal of development novel combination therapies.
- The second aim was to develop a radiotherapy-resistant cell line from the parent MDA-MB-231 cell line and subsequently assess their response to the potential novel combination therapies.

 The final aim was to utilise a metabolomics approach to identify the most common metabolic pathways that contributed to the development of radiotherapy resistance in MDA-MB 231 cells.

1.10.1 Hypothesis

In this project, we hypothesised that:

- Combining gedatolisib, a targeted dual inhibitor of PI3K/Akt/mTOR signalling pathway, with either doxorubicin or radiation will enhance the cytotoxicity of the combination in the MDA-MB-231 cell line compared to each single-agent treatment.
- 2. This lab developed combination therapies will retain efficacy in the derived radioresistant MDA-MB-231 cell line.
- 3. Metabolic reprograming, identified by metabolomics study, is one of the driven mechanisms of acquired radioresistance in the MDA-MB-231 cell line.

Chapter 2

2 Materials and Methods

2.1 Cell line and routine passage

The triple negative breast cancer cell line used in all experiments was MDA-MB-231 (ATCC HTB-26), a cell line with an epithelial cell morphology derived from a pleural effusion of a 51-year-old white female with a metastatic mammary adenocarcinoma which was purchased from ATCC. We selected this cell line due to its biological characteristics represented by its high invasiveness, mesenchymal-like phenotype of triple-negative breast cancer and its relevance as a model for studying the mechanisms related to epithelial-to-mesenchymal transition and metastasis potential. At project inception 1 TNBC cell line was chosen for initial analysis- MDA- 231 and 1 HER2 + cell line MDA-453 as a comparison. Initial experiments were undertaken to assess whether each cell line was able to be utilised in all assays – clonogenic assay and spheroid assays. Unfortunately, the MDA- 453 cell line was not amenable to clonogenic assay and did not form spheroids. Thus, it was decided that rather than using 2 different cell lines we decided to generate therapy resistant cell lines derived from MDA-231 with the parental cell line acting as the comparator/control. Overall, this involved full analysis of 4 cell lines and as this was an extensive number of cell lines to put through the full assay cascade, it was not possible to include further cell line due to time constraints. However, another PhD student in the laboratory is assessing this therapy using other techniques recently acquired in the laboratory on a second TNBC cell line as a separate PhD project. The parental cell line was purchased fresh from ATCC and 40 vials frozen down immediately after purchase and growth of cells from the frozen stock. The parental cell lines were not further validated in the project as fresh stocks were utilised every 3 months.

MDA-MB-231 cells were cultured in Dulbecco's Modified Eagle's Medium, high glucose (DMEM, 4.5 g/L glucose, with L-glutamine and sodium pyruvate, Thermo

Fisher Scientific, Perth, UK), supplemented with 10% (v/v) foetal bovine serum (FBS, Thermo Fisher Scientific, Perth, UK), 100 U/mL penicillin and 100 μg/mL streptomycin (Thermo Fisher Scientific, Perth, UK), and 2.5 μg/mL amphotericin B (Sigma-Aldrich, Irvine, UK). Complete medium was filter-sterilized, tested for sterility, and stored at 2–8 °C for further use. Cells were maintained in vented T75 cm² flasks (Fisher Scientific, Renfrew, UK) at 37 °C in a humidified atmosphere containing 5% CO₂ and routinely passaged at 70–80% confluence.

To maintain viable cells ready for different future experiments, the cells were split when approximately 70% confluent. T75 flasks were washed with PBS (Thermo Fisher Scientific, Perth, UK), and 4 ml of trypsin (0.05%) (Sigma Aldrich, Irvine, UK) added for cell detachment. Fresh medium (4 mL) was then added to make the cell suspension. Different volumes of cell suspension representing various cell numbers were then taken depending on the required experiments and added to 2-3 new T75 flasks with 20 ml of fresh media for each to keep stocks of viable cells.

2.2 Establishing of MDA-MB-231 cultures from frozen stocks

Frozen stocks of MDA-MB-231 cells were taken from liquid nitrogen or -80 freezer and cryovials of frozen cells were defrosted at room temperature, and cells transferred to T25 flask (Fisher Scientific UK) containing 5 mL of complete media and incubated at 37 °C at an atmosphere of 5% CO2 for 5-7 days to reach 70% cell confluence. During the incubation period, once the cells had stuck down, the media was changed twice to remove dead cells and refreshed with fresh media to provide the nutrients for the cells.

2.3 Mycoplasma test

The MDA-MB-231 cell line utilised in the experiments of this project was regularly (each 4-8 weeks) tested for mycoplasma contamination by our group using the MycoStrip® mycoplasma detection kit (InvivoGen, France) to ensure the cellular integrity and the validity of the lab work. Based on the kit protocol, 1 mL of MDA-MB-231 cell culture supernatant was collected, centrifuged at 16,000 × g for 5 minutes, and the pellet resuspended in 500 µL sterile phosphate buffer saline. A small volume (5 µl) of the prepared sample was combined with 15 µl Reaction Mix and 5 µl of Reaction Buffer, the already supplied components in the kit, then the mixture was incubated at 65 °C for 40 minutes. Following that, 200 µl of migration Buffer was added to the processed sample and mixed well before transferring 100 µl from the mixture into MycoStrip® detection cassette. The results were demonstrated after 5 minutes, where a single control band indicated a negative result, whereas both control and test bands indicated contamination. Only mycoplasma negative cell lines were utilised for all experiments.

2.4 Freezing of cells

To secure a stock of MDA-MB-231 cells at the initiation of experimental work, stocks of cells were prepared and frozen for future use. Cells were seeded into T75 flasks and grown to 70% confluence. Cells were then washed with 3mL of sterile PBS, detached by addition of 4 mL of 5% trypsin and incubated at 37 °C until the cells had detached. 4 mL of complete medium was then added to neutralize the trypsin and a single cell suspension prepared by passage of the mixture through a sterile 21-gauge needle (BD, Plymouth, UK). Thereafter, cells were centrifuged at 1000 rpm for 5 minutes to form cell pellets. The supernatant was decanted, and the pellets resuspended in 1mL of freezing buffer solution which was prepared by mixing of 8

mL fresh media (80%), 1mL of foetal bovine serum (10%) and 1mL of DMSO (10%). The resuspended solutions were transferred to cryovials at a concentration of 1x106 cells/mL (Fisher Scientific, UK) and kept in – 80 °C freezer for 2 weeks and then moved to storage in liquid nitrogen. The cell cultures were frozen at low passage (less than 5), while the passage number for the cell lines utilised int the experiments was below 15.

2.5 Cell Doubling Time

Doubling time refers to the time required for the seeded cells to be double in number after a complete cell cycle. As per all experiments in our laboratory, doubling times are firstly characterised as doubling times in different laboratories of the same cell lines vary with lab conditions, serum batches and growth conditions. As our project often involve comparison of the efficacy of combinations between cell lines with different doubling times we have to ensure consistency with incubation time.

From stock flasks which were approximately 70% confluent, cell suspensions were prepared as described above and cells counted using a haemocytometer to determine the number of cells per unit volume (μL). 1x10⁵ cells were seeded into 12 x T25 vented flasks (Fisher Scientific, Renfrew, UK) containing 5mL of complete medium and the flasks were incubated at 37°C - 5% CO₂ for four days. On each day, 3 flasks were taken, media was removed, flasks were washed with PBS, and 2 mL of trypsin was added, and the flasks were placed in an incubator for 10 minutes before the addition of 2 mL fresh media to make a cell suspension. The suspension then was passed through a sterile 25 mm needle to make a single cell suspension. The number of cells in the suspension was counted using a haemocytometer (Neubauer improved, Marienfeld, Germany) at 24hour intervals and the counting was done in triplicate. The

number of cells in each flask were counted and the doubling time estimated by the following equation:

Doubling time (DT) = $(t2-t1) \times \ln (2)/\ln(N2/N1)$ Equation 1 where: N1 and N2 represent the number of viable cells that counted at initial time t1 and final time t2, respectively.

2.6 Plating efficiency

This experiment was carried out to determine the number of cells that could be efficiently used in clonogenic assay to evaluate the cell survival after exposure to therapy. A T75 flask with cells approximately 70 % confluence was washed with PBS. 4 mL of 0.05% trypsin was added to detach the cells which then was neutralize by addition of 4 ml of complete medium to make a cell suspension. A Haemocytometer was used to count the cells in the suspension and single cell suspension made by passing through a sterile 21-gauge needle. Thereafter, several volumes containing different numbers of cells (250, 300, 400, 500, 600, 700) were seeded in triplicate in 60 mm Petri dishes (Fisher Scientific, UK) with 5 mL of complete medium and incubated at 37 °C for 14-21 days until the cell colonies were seen by the naked eye. The media was then removed and the dishes washed with PBS. The colonies were fixed by addition of 100% methanol (Thermo Fisher Scientific, Perth, UK) for 10 minutes. The fixed colonies were then stained with 5% Giemsa solution (VWR, Leicestershire, UK) which was left for 30-60 minutes before removal of the stain and washing of the plates under a cold, gently flowing tap. The counting of the colonies was done manually by eye and the plating efficiency was calculated as follows: Plating efficiency = (number of colonies/number of the input cells) X100 Equation-2

2.7 Drug preparations

In this project, drugs and radiotherapy have been utilised to treat the MDA-MB-231 cell line. Gedatolisib (M.Wt. = 615.73) was purchased from (Pfizer, USA) and the stock solution was prepared by dissolving 5 mg of the drug in 8.1mL of DMSO (Sigma-Aldrich, UK) to get a 1mM stock solution. Serial aliquots (100 µL) were made and transferred into 0.5 mL Eppendorf tubes (Fisher Scientific, UK) and stored at -80 °C for future experiments according to manufacturer recommendations and to avoid freeze- thaw cycles. Dilutions with PBS were undertaken to prepare a series of working solutions based on experimental requirements and therapeutic plans.

Doxorubicin (M. Wt. = 579.98) was purchased from (Pfizer, USA), and 500 μ M stock solution was prepared by dissolving 10 mg of the drug in 3.4 mL of DMSO (Sigma-Aldrich, UK) and stored 2-8 °C according to manufacturer recommendations. Serial working solutions were prepared by dilutions of stock solution with autoclaved deionized water depending on experimental requirements.

Radiotherapy is one of the key treatments in this project. The exposure of MA-MB-231 cells to different radiation doses was done utilising a Precision X-RAD 225 machine (North Branford, CT USA). Cells were irradiated at a dose rate of 2.2Gy/min, with single fractions delivered between 0- 10 Gy. Irradiation was carried out at a tube potential of 225 kVp and tube current of 13 mA, with a 0.3 mm Cu filtration and the focus-to-surface distance (FSD) was maintained at 30 cm. The machine output was calibrated according to standards of manufacturer, and the dosimetry was verified biannually by RPS services (Byfleet, Surry, UK). Cells were irradiated in vented T25 flasks containing 5 mL of complete medium to ensure uniform dose distribution.

2.8 Clonogenic assay

The effect of each treatment in the MDA-MB-231 cell line was evaluated by clonogenic assay. 200000 MDA-MB-231 cells were plated in vented T25 flasks (Fisher Scientific, Renfrew, UK) and incubated for 48 hrs. The 48h incubation time was chosen to permit sufficient cell attachment and drug exposure covered at least one full cell cycle (a doubling time). This aligns with the long-term clonogenic survival assay previously assessed, where cells incubated with treatment for 24hr -48hr to investigate the immediate and residual toxicities affecting the proliferative capacity (Forgie et al., 2024). Furthermore, 48hr incubation time allows for the assessment of mitotic catastrophe, a delayed cell death characterised by multinucleation and loss of the capability for colony formation compared to short time treatments (Morse et al. 2005). Hence, a 48h incubation time was selected to ensure all cells in the flask in all stages of the cell cycle were exposed to the treatment and to better reveal residual toxicity and mitosis-related clonogenic weakness. After incubation, media was removed and 1.5 mL of complete medium containing the required drug concentration was added to the flasks. Subsequently, the treatment was removed after 48 hrs and cells were washed with PBS to remove any remaining treatment. 2mL of trypsin was added to detach cells and its activity was ended by addition of 5mL of complete fresh media to generate a cell suspension as described. After counting the cells using a haemocytometer, the volume needed to seed 700 cells per petri dish in triplicate (the number was selected according to the plating efficiency test) was calculated and added to 60 mm petri dishes (Thermo Fisher Scientific, Perth, UK) containing 5mls complete medium. The petri dishes were then incubated for about two weeks to allow for the appearance of cell colonies of 50 cells or more. After incubation, the media was removed, and petri dishes rinsed with PBS. The petri dishes were covered with 100% methanol at room temperature for 10 minutes to fix cell colonies. Giemsa's solution (VWR, Leicestershire, UK), concentration 5% (v/v), was then added to the

petri dishes for 30 minutes to stain the colonies. The survival fraction was determined following counting of the colonies by eye using the following equation (Franken et al., 2006; Brix *et al.* 2020)

Survival Fraction = (number of treated colonies / numbers of the input cells x plating efficiency of control)

Equation-3

This SF formula is the established way to normalise colony counts (Franken *et al.*, 2006) and was applied identically to single agents and their combinations as we want to recruit survival fraction of combination with single-agent SFs to calculate and interpret combination analysis approaches using Chou-Talaly model (Chou, 2010)

Linear quadratic model

To evaluate the radiosensitivity of the MDA-MB-231 cell line, the linear-quadratic (LQ) model was utilised. This model is widely used to identify the relationship between radiation exposure and cell survival, both *in vitro* and *in vivo*, by fitting survival fraction (SF) data across a range of delivered radiation doses (McMahon, 2019). The LQ is a mathematical model assuming that the decrease in SF with increasing radiation dose can be rationalised by two components of lethal damage, identified by the α and β parameters (Bodgi *et al.*, 2016). The α term denotes to cell killing induced by a single ionising hit. The β parameter refers to the damage caused by the interaction of two independent hits, reflecting the accumulation of sub-lethal events that scale with the square of the dose. The α -mediated damage is significant at low radiation doses, while higher doses damage induced by significant β -mediated events, and both (α and β) characterize the cell survival curve. Mathematically, the LQ model equation is expressed as:

SF=e-
$$(\alpha D+\beta D2)$$
 Equation-4

2.9 Tumour spheroids

A cell suspension was created as described above and cells were counted by haemocytometer and the volume containing 2-3 million cells was added to a spheroid spinner flask (Thermo Fisher Scientific, Perth, UK) with 75mL of complete fresh media. A sufficient quantity (around 5%) of gas was added to spinner flask from gas cylinder (BOC limited, England, UK) that contained 5% Carbon dioxide, 20% Oxygen and balanced nitrogen. Thereafter, the spinner flask was incubated on a magnetic platform (Techne, UK) to enable stirring for 4-6 days until growth of visible spheroids was observed, and 25mL of complete fresh media was added every 48 hrs. Once spheroids had formed to a diameter of ~250-350µm they were transferred and treated with drugs or radiation in 7mL bijou tubes (Fisher Scientific, UK), where 3mL of medium containing the required drug concentrations were added to the tubes and complete media was added to the irradiated tubes. The bijous were placed on a roller to prevent clumping of spheroids and incubated for 48 hrs. in the meantime 24 well plates (TPP, Switzerland) were coated with 3% agarose (BioReagent, USA) to prevent spheroid attachment and left to set. Following the end of treatment, the spheroids were picked up by eye using a micropipette and 1 spheroid transferred into each well of 24 well plates that had 1mL of complete fresh media in each well. The media was then subsequently refreshed every 3 – 4 days with fresh media for a total of 21 days. Spheroids were imaged every 3-4 days by the EVOS FL auto system (Life Technologies, UK). The images were processed using ImageJ software (Schindelin et al., 2012), where the maximum and minimum diameters were measured to determine the volume of spheroids via the following equation (Jensen et al., 2008):

Volume= 1/2 (Dmax × (Dmin)^2)

Equation-5

The spheroids growth at different time points were monitored by determining the volume change (V/V_0) which mean the volume (V) at each time point dividing by the initial volume.

2.10 Establishment of resistant cell line

To establish a radioresistant cell line, its name will be (RR-MDA-MB-231). Approximately 2 × 10⁵ cells were plated in a T25 cm³ flask (Thermo Fisher Scientific, Perth, UK) and allowed to reach 70% confluence before being exposed to 2 Gy radiation and incubated at 37°C for 48 hrs. Thereafter, cells were harvested, counted using a haemocytometer and 700 cells were seeded in 60 mm petri dishes (Thermo Fisher Scientific, Perth, UK) for 15-17 days until clear visible colonies formed.

The culture media was removed from the petri dishes, and the colonies were maintained hydrated by PBS washing. The visible colonies were individually isolated utilising sterile Perspex cloning plastic rings sealed with sterile petroleum jelly. The selected isolated colonies were detached with 50 µL trypsin and expanded in 96-well plates. From the 96-well plates, the 24 most rapidly proliferating colony-derived cultures were moved and subcultured in 24-well plates. When they reached more than 70% confluence, the six fastest-growing cultures were transferred to 6-well plates. Of these, three top-performing cultures were sequentially expanded to T25 flasks and then to T75 flasks.

Upon reaching confluence in T75 flasks, the cultures underwent three passages to ensure viability and stable growth. After that, the single culture showing the most robust proliferation capacity was advanced to the next irradiation cycle, repeating the same colony-selection procedure. The remaining two cultures were cryopreserved as

frozen stocks and labelled as the "Cycle 1" stock. This stepwise selection and irradiation process was repeated for three independent cycles (Cycle 1, Cycle 2, and Cycle 3) to produce a more stable radioresistant RR-MDA-MB-231 cell line.

The growing cycle for new resistant clones performed in each treatment repeat is shown in Figure 3.1.

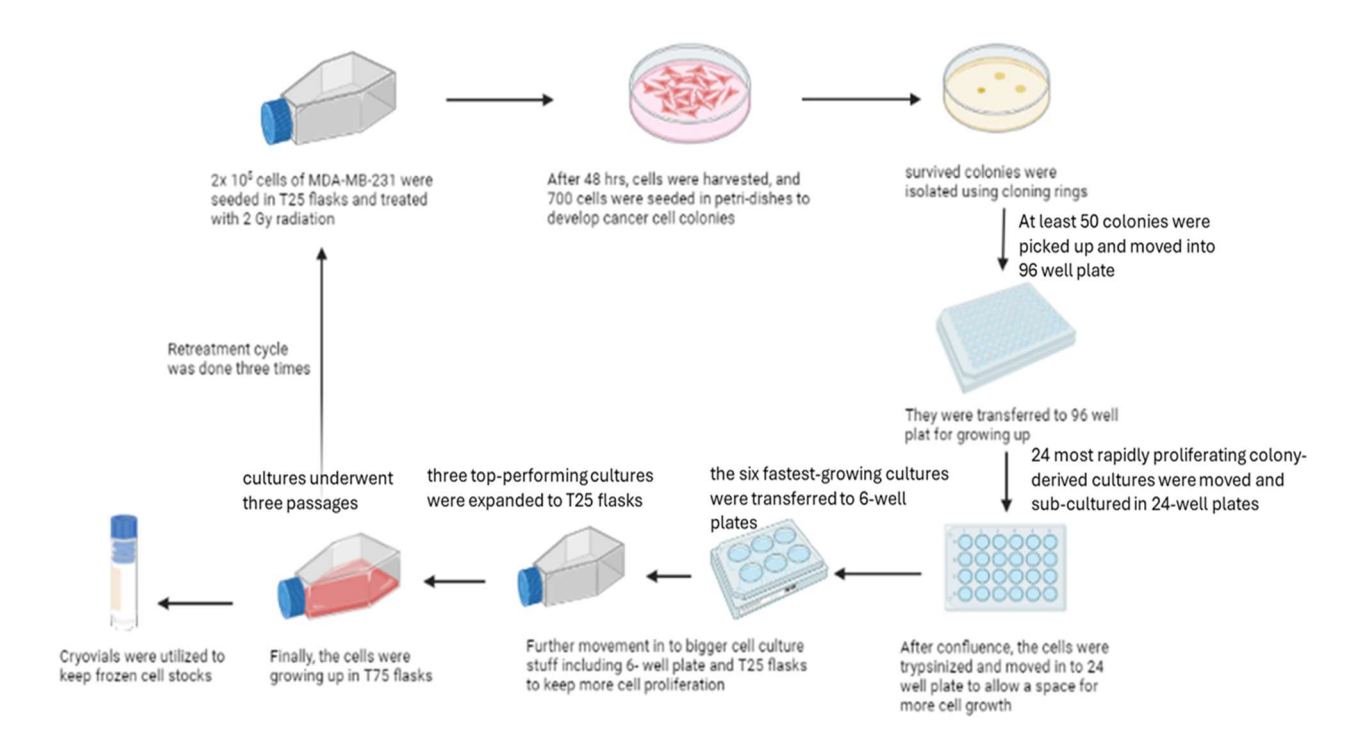


Figure 2-1 Flow chart for the development of MDA-MB-231 resistant cell line

2.11 Combination index analysis

The cytotoxicity relationship between two treatments used in combination therapy was investigated utilising combination index analysis (CIA)(Chou, 2010). This mathematical approach was performed by CompuSyn®, a software that developed by Chou and Martin (Chou T and Martin N, 2005). Clonogenic assays were undertaken as described in section 2.5 and the survival rates were determined post treatment with each therapy. The concentration or dose of single treatment that killed 50% of the cells (IC50) or ED50 for radiation was estimated via Graph Pad prism 10.3.1. The determination of the combination index (CI) value is used to characterize the biological relationship in combination therapy as to whether this was supra-additive (synergistic effect), additive (not synergistic, not antagonistic), or infra-additive (antagonistic). The equation that was performed using CompuSyn software to calculate the combination index (CI) was as follow (Chou, 2005):

$$CI = (D)1/(Dx)1 + (D)2/(Dx)2$$
 Equation-6

Where the treatment dose (D) that kill x percent of cells was dividing by the single agent dose (Dx) that used in combination therapy, and CI is the combination index. The relationship between therapeutic agents would be supra-additive if the CI value was below 0.9, additives if the value between 0.9-1.1, and infra-additive if greater than 1.1 (Chou, 2005)

2.12 Cell Cycle analysis

The distribution of MDA-MB-231 cells in the various phases of cycle following exposure to different therapies was assessed by cell cycle analysis (Darzynkiewicz et al., 2017). 1x10⁵ MDA-MB-231 cells were seeded into 6-well plates and incubated at 37°C with 5% CO2 for 48 hrs in complete media. Cells were then incubated with a range of drug concentrations including gedatolisib (0.05µM, 0.1µM and 0.02µM), doxorubicin (0.005 μ M, 0.01 μ M and 0.02 μ M) that represent The IC₁₀, IC₂₅, and IC₅₀ of each drug respectively, as well as X-radiation doses (1Gy and 2Gy) that were around ED₅₀ as a single treatment. Furthermore, MDA-MB-231 cells were exposure to the combinations that were assessed in clonogenic assay and spheroids, (0.05µM, 0.1μM) gedatolisib with (0.005μM, 0.01μM) doxorubicin and (1 Gy and 2 Gy) radiation doses. In all our studies both published extensively and underway, we actively choose not to undertake cell cycle synchronisation as this project is not a molecular signalling project but translational cancer research, thus we deliberately chose to not synchronise the cells as this is not the case in a tumour in vivo or in spheroids. In these scenarios the cell population is heterogeneous with cells in all phases of the cell cycle. This approach is therefore less artificial and assesses the promise of the treatments in a "real world scenario." We chose to always incubate all cells for a cell doubling time therefore, as this ensured all cells in all phases of the cell cycle get exposed to the combination as each component of these combinations will have varying effects on different phases of the cell cycle- a shorter incubation time would not represent exposure of all cell states- that would be present in the patient being exposed to the treatment.

Following treatment and incubation with the mentioned treatments, cells were harvested at different time points, 4 hrs, 24 hrs and 48 hrs. Media was removed and cells washed with PBS, and 0.05% trypsin was utilised to detach cells. Thereafter,

3mL of fresh medium was added to create a cell suspension which was centrifuged at 1000 RPM for 5 minutes. The resulting cell pellets were fixed by the addition of 70% ice cold ethanol and stored at -20°C for no longer than 3 months. Analysis was performed by washing cell pellets with PBS and centrifuging again at 1000 RPM for 3 minutes before removal of the supernatant layer. The staining of the pellets was done by adding the staining mixture which included 50 µg/mL ribonuclease A (Sigma-Aldrich, UK) and propidium Iodide 10 µg/mL (Sigma Aldrich, UK) to stain DNA content and 1x staining buffer (Sigma-Aldrich, UK). After staining, the samples were incubated on ice in the dark for 1 hr. The cell cycle distribution was determined via an AttuneTM NxT Flow Cytometer (Thermo Fisher Scientific, USA). 10,000 events per sample were measured through the flow cytometry analysis. During analysis, cells were first selected by size and granularity to exclude debris using forward and side scatter (FSC/SSC) gating. Cell clumps and cell doublets were excluded by gating on single cells based on pulse measurements. The DNA content data were processed using the flow cytometer's software (Attune NxT Software), which calculated the percentages of cells in the different cell cycle phases (G0/G1, S, and G2/M).

2.13 Annexin V assay

The apoptosis in MDA-MB-231 cells following exposure to the relevant drugs and combination treatments was carried out utilising an anti-annexin V FITC conjugate antibody assay (BD Biosciences, UK). MDA-MB-231 cells were seeded in 6-well plates at 1x10⁵ cells per well and incubated at 37°C with 5% CO₂ for 48 hrs in complete DMEM media. Cells were then treated as described for cell cycle analysis in section 2.11 above. Following incubation with the relevant drugs and treatment combinations, cells were harvested at different time points, 4 hr, 24 hrs and 48 hrs.

The media was removed and washed with PBS before using 0.05% trypsin to detach the cells from the wells. Fresh media (3mL) was added to create the cell suspension which was then centrifuged at 1000 RPM for 5 minutes to get cell pellets. The pellets were then washed with PBS and recentrifuged to get rid of the remaining of media or trypsin. After disposing the supernatant, pellets were resuspended with Annexin V staining buffer at a concentration of 1x10⁶ cells/mL, the10x staining buffer (25 mM CaCL2, 1.4 M NaCl, and 0.1 M Hepes/NaOH, BD Bioscience) at pH 7.4 provided within the kit was diluted to 1x buffer by adding 1mL of 10x buffer to 9mL distilled water. For staining, 100 µL of the cell suspension was then transferred into Eppendorf tubes, and 5 µL of Annexin V antibody conjugate (BD Bioscience, UK) and 5 µL of propodeum iodide (BD Bioscience, UK) were added to each sample. The samples then gently vortexed and incubated for 15 minutes at room temperature. After incubation, 400 µL of 1× Annexin assay buffer was added to each tube prior to running in the flow cytometric machine. The samples were then run on a flow cytometry machine (AttuneTM NxT, Thermo Fisher Scientific, USA), which measured 10,000 events per sample to determine. During analysis, cells were gated to exclude debris and doublets, and apoptosis stages were identified as viable (Annexin V-/PI-), early apoptotic (Annexin V+/PI-), late apoptotic (Annexin V+/PI+), and necrotic (Annexin V-/PI+) populations. The combined percentage of early and late apoptotic cells was used for statistical comparison among the assessed samples. All experiments were independently conducted in triplicate, and the data were presented as (mean ± SD) for each cell stage.

2.14 DNA damage assay (Comet assay)

The investigation of DNA damage induced by treatment in MDA-MB-231 cells following exposure to the relevant drugs and therapeutic regimen was done by Comet

assay using a single cell gel electrophoresis (SCGE assay) kit, (ENZO, UK). The gel (1%) was prepared by dissolving 1 g of low melting point agarose (Thermo, UK) in 100 ml PBS. MDA-MB-231 cells were seeded in 6-well plates at 1x10⁵ cells per well and incubated at 37 °C with 5% CO2 for 48 hrs in complete DEMEM media. Cells were then treated as described for cell cycle analysis in section 2.11 above. Following treatment and incubation with the relevant drugs and therapeutic regimen, cells were harvested at different time points, 4 hr, 24 hrs and 48 hrs. DEMEM media was removed and washed with PBS. 0.05% trypsin was utilised to detach the cells from the wells. 3 ml of fresh media was added to terminate the trypsin action and create the cell suspension. The single cell suspension was created by passaging the suspension through 23-gauge needle (BD Microlance UK) and then counted by haemocytometer (Fisher scientific, UK) to make a suspension density of 5x105 cells/ml. The cell suspension was mixed with 1% low melting point gel at 37 °C in 1:10 ratio ((10 μL cell suspension: 90 μL gel). 75 μL of the mixture (cells/agarose) was then pipetted onto a Comet slide (included in SCGE kit, ENZO, UK). The slides were incubated on the bench for 5 minutes to let the gel set and then covered with lysis buffer (included in SCGE kit, ENZO, UK), (10 mM tris base, 25 M NaOH, 100 mM EDTA pH10, 1% Triton X-100, 1% sodium lauryl sarcosinate) and kept in the fridge (4 -8 °C) for 2 hours. The slides were then placed for 1 hr in an alkaline solution (300 mM NaOH, 1 mM EDTA) (included in SCGE kit, ENZO, UK). Slides were then washed with TBE buffer (Sigma Aldrich, UK) and moved into a gel tank filled with TBE buffer and run for 10 minutes at 42 V. The slides then stained with 1X SYBR green (included in SCGE kit, ENZO, UK) and left to dry in the dark. EVOS FL auto system (Life Technologies, UK) was used to image the slides, and the images were analysed utilising ImageJ with plug in Open Comet (Gyori et al., 2014). An average of 100 Comets was analysed in each treatment group at each time of the three independent experiments.

2.15 Western blot

The effect of gedatolisib on PI3K and mTORC proteins expression in MDA-MB-231 cell line was evaluated by Western blot analysis. MDA-MB-231 cells were seeded in 12-well plates at a density of 5x10⁴ cells per well and incubated at 37°C with 5% CO₂ for 48 hrs in complete DMEM media until cells became 80% confluent. Cells were then treated with gedatolisib ($0.05\mu M$ and $0.1\mu M$). Following treatment and incubation with the drug, harvesting of cells was initiated at different time points, 1 hr, 4 hr, 24 hrs and 48 hrs post treatment. The plates were kept on ice to stop protein expression, and the media was removed by aspiration. 750µL cold PBS was utilised for cell wash and 200µL of lysis buffer (2mM Na-4P2O7, 63mM Tris-HCl, (pH 6.8), 50mM DTT, 5Mm EDTA, 2% (w/v) SDS, 10% (v/v) glycerol, 0.007% (w/v) bromophenol blue) was added to each well. Cells were collected by scraping using a 21-gauge needle attached to a 1 mL syringe. The resulting cell lysate was transferred into Eppendorf tubes and denatured by heating at 95°C for 3 minutes. The cell lysate samples were then stored at -20°C for future experiments. The cell lysate samples were loaded into 10% SDS-Polyacrylamide Gel Electrophoresis (SDS-PAGE) (Sigma-Aldrich, UK). 12% resolving gels made of (30% (v/v) acrylamide solution, 2.5Ml buffer 1, 3.3 mL dH2O2,10% (w/v) ammonium persulfate (APS) and 0.01% (v/v) N, N, N', N'-Tetramethyl ethylenediamine (TEMED) (Thermo Fisher Scientific, USA) were utilised to resolve the target proteins. Then, gels were transferred into gel chambers of 1.5mm wall thickness. 4% stacking gels made of 30 % (v/v) acrylamide solution, 0.95 ml buffer 2, 10% (w/v) APS and 0.01% (v/v) TEMED were poured on the top of the

resolving gel once it set. 15 well combs were inserted gently between the plates, and the gel then was stored at the cold room to polymerise.

Cell samples were injected utilising microsyringe into the resolving gel wells to separate the sample proteins depending on the molecular weight of the protein, looking for the target protein in this experiment (AKT) as well as protein marker of known molecular weight. Gel electrophoreses was then run at 130 volts for 90 minutes. Following separation, sample proteins were electro-transferred utilising nitrocellulose membrane (Fisher Scientific, UK) at 300 milliamps for 150 minutes. Blocking the nonspecific proteins in membrane was done utilising 2% bovine serum (BSA) for 120 minutes at room temperature. The primary antibodies of rabbit anti-AKT (Cell signalling, UK) diluted 1:2000 in tris-buffered saline (TBS) containing 3% BSA were added into the corresponding membrane of the targeted protein and incubated overnight at room temperature. The following day, the membranes were washed three times with TBS, and the secondary anti-rabbit HRP-conjugated antibody (Proteintech, UK) diluted 1:2000 in TBS containing 3% BSA was added and incubated for 90 minutes at room temperature. The protein bands were identified utilising enhanced chemiluminescence (ECL) substrate (Thermo Fisher Scientific, USA) and the signals were captured on Kodak autoradiography film.

Stripping of nitrocellulose membrane was undertaken to re-probe it for additional proteins. 15mL of stripping buffer (2% (v/v) sodium dodecyl sulphate, 0.1M β-mercaptoethanol, 0.05M Tris-HCl, pH 6.7) (Merckmillipore, UK) was added to each membrane and incubated at 60°C for 60 minutes. Following that, membranes were washed 3 times in TBS buffer.

Lastly, the immunological detection of housekeeping protein GAPDH (Glyceraldehyde-3-phosphate dehydrogenase) was performed to ensure equal protein loading across the gel.

The protein band density on the exposed X-ray film was measured utilising the ImageJ software.

2.16 Autophagy Assay

An autophagy assay was utilised to assess the potential mode of gedatolisib induced MDA-MB-231 cells death following treatment. MDA-MB-231 cells were grown on coverslips (VWR, UK) in 6-well plates at a density of 5000 cells per each coverslip and incubated at 37°C with 5% CO_2 for 48 hrs in complete DMEM media until cells become 80% confluent. Cells were then treated with gedatolisib at a concentration of 0.05 μ M and 0.1 μ M that were utilised in combination with doxorubicin and radiation and assessed by clonogenic assay and spheroids.

1X of assay buffer was prepared by diluting 1 ml of 10X assay buffer (Abcam UK ab139484) with 9 ml deionized water. The staining solution was prepared by adding 2 μl of 2μL of green detection reagent and 1μL of nuclear stain (Abcam UK, ab139484) to 1 ml of 1X assay buffer. 5% FBS was added to the staining solution to preserve the cells and prevent the dislodging of autophagic cells via washing. Following incubation of the cells with the relevant drug, the drug was removed, and the cells were washed with 1X buffer assay. 100 μL of staining solution was added to cover each coverslip and the samples were incubated for 30 minutes at 37°C in the dark. Cells were then washed with 1X assay buffer and fixed with 4% paraformaldehyde (Fisher Scientific, UK) for 30 minutes and then washed three times with 1X buffer assay. The coverslips were transferred to microscope slides (Fisher Scientific, UK) and imaged using Leica Microsystems SP8 confocal microscope with a Leica 63× HC PL APO CS2 1.40 oil objective lens. The images were processed by FIJI image software according to the recommendations of Autophagy Assay Kit (ab139484), Abcam, UK. The autophagic vacuoles quantification was conducted

utilising FIJI software, where, fluorescence channels were separated, and discrete green signal of autophagic vacuoles was identified. The particle analysis, with predefined size range of $0.2–2~\mu\text{m}^2$ and circularity threshold of 0.3–1.0, was used for detection. Autophagic vacuoles were automated counted across minimum of 100 cells per sample and performed in three independent experiments.

2.17 Statistical Analysis

All statistical analysis was carried out using GraphPad Prism version 10.3.1. Prior to performing any data analysis, the normal distribution of the samples was tested by a Shapiro-Wilk normality test. If the data that did not pass the normality test, nonparametric data was analysed by a statistical analysis set including a Kruskal-Wallis with Dunn's post hoc test. If the data was parametric, a one-way or two-way ANOVA with Tukey's post hoc test was used. For statistical comparisons, the significance was assigned at an alpha (α) or P value \leq 0.05. The following labelling was used to reflect significance: ns = not significant; * = P \leq 0.05; ** = P \leq 0.01, *** = P \leq 0.001; and **** = P \leq 0.000

2.18 Cell lines maintenance and treatment for metabolomics

Triple negative breast cancer cell lines used in this study were the radioresistant MDA-MB-231 cell line established in our lab, derived from the wild-type MDA-MB-231 that was purchased from the American Type Culture Collection (ATCC HTB-26, USA). Both types of TNBC cells were cultured in vented flasks of different sizes depending on the experiment (T75 cm³ and T25 cm³) (Thermo Fisher Scientific, Perth, UK) and incubated at 37 °C in an atmosphere of 5% CO2. The media used for culturing was prepared by adding 5 ml (1%) of penicillin/streptomycin (Thermo Fisher Scientific, Perth, UK), 5 ml (1%) of amphotericin B (Sigma Aldrich, Irvine, UK) and 50

mL (10%) of foetal bovine serum (Thermo Fisher Scientific, Perth, UK) to Dulbecco's modified eagle medium (DMEM) (Thermo Fisher Scientific, Perth, UK). The prepared media was kept in the refrigerator at 2-8 °C for further experiments.

To maintain viable cells for different experiments, the cells were subcultured when approximately 70% confluent. T75 flasks were washed with PBS, and 4 mL of trypsin (0.05%) (Sigma Aldrich, Irvine, UK) was added to detach the adhered cells. To create a cell suspension, 4 ml of fresh media was added to the trypsinised cells. After detachment, different volumes of cell suspension were taken depending on the required experiments and added to 2-3 new T75 flasks with 20 mL of fresh media for each to keep stocks of viable cells. The irradiation of cell lines was done utilising a Precision X-RAD machine (North Branford, CT, USA) at a dose rate of 2.2Gy/min.

2.19 Chemicals

HPLC grade acetonitrile, methanol, and formic acid (98%) were purchased from Fisher Scientific, UK. HPLC grade water was produced from Ultrapure Water System (Millipore, UK). Sodium carbonate, ammonium hydroxide and ammonium acetate were purchased from Sigma Aldrich, UK.

2.20 Cell sample preparation and metabolites extraction

MDA-MB-231 cells were seeded in 6-well plates at a density of 2 million cells per well and incubated at 37 °C for 24 hr. Cells were irradiated with 2 Gy of X-radiation and harvested at 1hr, 4hr and 24hr following exposure to radiation. The well plates were kept on ice to stop any further biological reactions from taking place and media was aspirated from each well and the plate washed with cold PBS. Extraction buffer was prepared from methanol (Fisher Scientific, Leicestershire, UK) and ultrapure water at a ratio of 80:20 methanol to water. Once pre-chilled, 0.5 mL of extraction buffer was added to dissolve the cell constituents and facilitate cell scraping. This step was

repeated to collect all the cells in the wells, and a final volume of 2 mL quenched metabolites and cell extract was moved into a 2 mL Eppendorf tube. The tubes were then submerged in liquid nitrogen for 1 min, vortexed, and then sonicated for 3 minutes to enable the cell breakdown, and this cycle was repeated three times. The cell extract was then centrifuged at 13000 x g at 4 °C for 10 minutes. The supernatant layers containing the metabolites were dried utilising a speed vacuum dryer (Savant-SPD121P). The dried metabolites pellets were kept at – 80 °C for further analysis by liquid chromatography-mass spectrometry (LC-MS), whereas the sample pellets were used to quantify the protein content using Bradford assay (Pierce BSA kit, Thermo Scientific, USA).

In this assay, the sample pellet was lysed with 100 µl of lysis buffer constituted from Radio-Immunoprecipitation Assay (RIPA) buffer (Thermo Fisher, UK), Protease Inhibitor 100X (Cell signalling, USA) and PBS. A needle syringe was utilised for homogenization of sample pellets with lysis buffer, and the mixture was incubated on ice for 5 minutes. The samples were then centrifuged at 12000 x g by a cooled centrifuge (4 °C) for 20 minutes, and the supernatants were transferred to new Eppendorf tubes. The sample supernatants as well as standard BSA concentrations were moved into 96 96-well plate, and Coomassie reagent (Pierce BSA kit, Thermo Scientific, USA) was added to stain the wells, and absorbance was measured at 600nm using GM3500 Glomax® plate reader (Promega).

2.21 Cell sample preparation and metabolites extraction

The dried metabolite pellets were reconstituted with a sample buffer containing acetonitrile: water (50:50 v/v) at volumes relevant to protein contents as measured by the Bradford assay. The quality control pool (QC) was prepared by pooling all the samples (treated and untreated control) that were ready to be run in LC-MS machine.

10 μ I of each reconstituted sample was transferred into a glass vial (Chromacol, Thermo Scientific, Germany), and these vials were moved to the LC-MS machine. The QC sample was injected into several glasses, and one QC glass was placed after every five samples to assess the performance and stability of the analytical system. The separation of sample metabolites was performed utilising an Ultra-High Performance Liquid Chromatography (UHPLC) system (Thermo Fisher Scientific, Waltham, MA, USA), where the sample volume was injected into a ZIC-pHILIC column (Thermo Fisher Scientific, USA) with 100 mm x 2.1 mm dimensions and a 2.6 μ m particle size. The column temperature was set and maintained at 50°C and the autosampler temperature was set at 5°C. The mobile phase was run for chromatographic separation at a consistent flow rate of 400 μ I/min in binary heated electrospray ionisation mode (positive and negative).

In positive ionisation mode, the mobile phase was composed of buffer A (10 mM ammonium formate in 95% acetonitrile and 5% water with 0.1% formic acid) (Sigma Aldrich, UK) and buffer B (10 mM ammonium formate in 50% acetonitrile and 50% water with 0.1% formic acid) (Sigma Aldrich, UK).

In negative ionisation mode, the mobile phase was composed of buffer A (10 mM ammonium acetate in 95% acetonitrile and 5% water with 0.1% formic acid) and buffer B (10 mM ammonium acetate in 50% acetonitrile and 50% water with 0.1% formic acid) (Sigma Aldrich, UK).

The binary gradient mode elution utilised for the metabolites chromatographic separation is shown in Table 2.1

Time (min.)	Mobile phase A%	Mobile phase B%	Flow rate (ml/min)
0.00	99	1	0.4
0.50	99	1	0.4
2.00	50	50	0.4
10.50	1	99	0.4
11.00	1	99	0.4
11.50	99	1	0.4
14.90	99	1	0.4
15.00	99	1	0.4

Table 2.1 HPLC gradient mode of the mobile phase

The full scan and fragmentation analysis was performed utilising high resolution 240-Exploris mass spectrometer (Orbitrap) (Thermo Fisher Scientific, USA) with an ESI spray voltage of 3900 V in positive ionisation mode and 3000 V in negative mode. The transfer line temperature was set at 320°C, and the resolution for MS1 and MS2 were 60000 and 15000, respectively.

2.22 Processing of mass spectrometry data

The raw data generated from the LC-MS machine were imported into compound discoverer software (Thermo Fisher, San Jose, CA, USA) to perform the untargeted metabolomics. The workflow analysis included the alignment of retention time, detection of unknown compounds, prediction of compound's elemental composition and elimination of chemical backgrounds (utilising blank samples).

For the detection of compounds, the mass deviation was set to be less than 3 parts per million (ppm) and the retention time was 0.3 minutes. The library search of

compound detection was conducted against three databases, a Human Metabolome Database, Chemical Entities of Biological Interest and MzCloud. A list of compounds was generated in a table with putative known and unknown metabolites (MSI level 2). The known metabolites that matched at least two of the annotated sources were selected. The pathway identification and statistical analysis were then performed for the selected metabolites using the MetaboAnalyst web server v6.0.

2.23 Pathway and Statistical Analysis

Multivariate statistical analysis, including Principal Component Analysis (PCA), was performed to evaluate the analytical accuracy and reproducibility of quality control (QC) samples and to explore the overall metabolic profile across all experimental groups. PCA provides an unsupervised overview of sample distribution, enabling the assessment of clustering patterns and potential outliers. To further examine the statistical differences between the radioresistant and wild-type cell lines, as well as across different time points following radiation exposure, volcano plots were generated. These plots integrate both fold change (FC) and p-value thresholds, allowing for the identification of significantly dysregulated metabolites. The p-values were calculated using a student's t-test.

Metabolic pathway analysis was performed utilising MetaboAnalyst v6.0 webserver (https://www.metaboanalyst.ca/). The metabolites were annotated manually using the human metabolome database (HMDB), and the data were then uploaded to MetaboAnalyst for analysis. Only the statistically significant metabolites determined by P value (P<0.05) and fold change threshold (FC>2 or log2≥ ±1) were selected to be uploaded for the pathway analysis. Metabolites were aligned with corresponding metabolic pathways, and the identified pathways were ranked according to the pathway impact and the enrichment p-value. The experimental details of the

metabolomics study are shown in table 2.2, and in adherence to the standards of Zhang *et al.* 2016.

Cell line	Cell type	Passage number/s	Samples	Quenching	Extraction	No. of biological replicate	Sample normalisation	Analysis	Application
MDA- MB- 231 and RR- MDA- MB- 231	Triple negative breast cancer	Within 10	Cells	Ice-Cold PBS	MeOH: Water (80:20), followed by freezing – thawing cycles to the lysate	3	Protein concentration	LC-MS	Metabolic profiling of resistance to radiation

Table 2.2 Metabolomics experimental details

Chapter 3

3 In vitro evaluation of gedatolisib in combination with doxorubicin or radiation in triple negative breast cancer

3.1 Introduction

Triple negative breast cancer is an aggressive and heterogenous subtype of breast cancer, characterised by the absence of therapeutic receptors expression including, ER, PR and HER2. Due to the lack of targeted therapy, the main treatment strategies rely on chemotherapy and radiotherapy. However, the developing of treatment resistance that causes therapeutic failure and tumour reoccurrence make the management of this breast cancer subtype challenging (Mustafa *et al.*, 2024). Hence, identifying novel potential combination therapies is crucial for the management of triple negative breast cancer.

Anthracyclines, including doxorubicin, remains one of standard chemotherapeutic agents utilised for treatment of breast cancer, particularly TNBC (Guo *et al.*, 2023). Doxorubicin works as a topoisomerase II inhibitor and DNA intercalating agent, resulting in double-strand breaks and apoptosis. However, its efficacy is hindered by the development of resistance and side effects such as cardiotoxicity (Guo et al., 2023).

Radiotherapy is commonly recommended for loco-regional treatment of breast cancer, including TNBC (Ortega *et al.*, 2020). Despite the initial response of TNBC cells to radiation, treatment failure frequently arises due to the emergence of radioresistant subclones, driven by enhanced DNA repair capacity and activation of pro-survival signalling pathways (Ortega *et al.*, 2020). To overcome this challenge, therapeutic strategies combining radiotherapy with molecularly targeted agents that inhibit survival signalling have been proposed, aiming to increase radiosensitivity and improve clinical outcomes.

Gedatolisib, is a dual mode inhibitor of PI3K and mTOR signalling, a common dysregulated pathway in cancer cells, including, TNBC and strongly implicated in tumour progression, therapy resistance, and poor prognosis (Wainberg *et al.*, 2017; Colombo *et al.*, 2021; He *et al.*, 2021).Preclinical studies have shown that gedatolisib

can reduce tumour growth and enhance the effect of cytotoxic agents, suggesting the advantages of its involvement in combination strategies (Broege *et al.* 2024). Knowing that the DNA damage inducing cancer cell death is the main mechanism of action for both of doxorubicin and radiation, and that PI3K/Akt/mTOR signalling supports cell survival by enhancing DNA repair, combining gedatolisib with either doxorubicin or radiation is proposed to promote the cytotoxicity and improve the therapeutic outcomes.

3.2 Aims

The aims of the lab experiments for this chapter were, firstly, to evaluate the cytotoxicity of gedatolisib, a dual PI3K-mTOR inhibitor, doxorubicin, and radiation as a single therapy in the MDA-MB-231 cell line utilising a clonogenic assay. Secondly, we evaluated the cytotoxicity of combination therapies that designed depending on the results of single therapy.

Finally, we aimed to investigate the mechanistic effects of single and combination therapy to understand why any promising therapies which reduced clonogenic survival achieved their effects.

3.2.1 Hypothesis

We hypothesised that combining gedatolisib, a targeted dual inhibitor of PI3K/Akt/mTOR signalling pathway, with either doxorubicin or radiation will enhance the cytotoxicity of the combination in the MDA-MB-231 cell line compared to each single-agent treatment.

3.3 Results

3.3.1 MDA-MB-231 cells doubling time

The time required for the cells to complete one full cell cycle is defined as the doubling time. Following section 2.6, the results of the number of cells counted on daily basis by harvesting at 24 hr intervals are shown in Figure 3.4, which represents the growth curve for these cells.

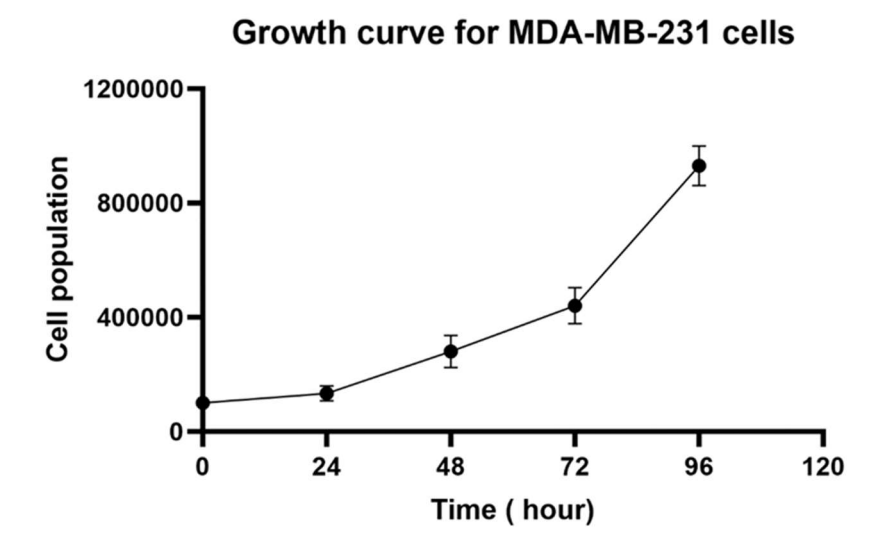


Figure 3-1 MDA-MB-231 cells doubling time.

The growth curve for MDA-MB-231 cells shows the cell population harvested at different time points following cell seeding (time 0). Three T25 flasks for each of five time points (0, 24hr, 48hr, 72hr, and 96hr) were seeded with 100000 MDA-MB-231 cells per flask, and the cells were harvested at 24 hr time interval following seeding and counted using haemocytometer. Data are presented as mean ± standard deviation for 3 independent experiments. The doubling time was calculated from the growth curve utilising the exponential growth equation in Excel 2016. The growth curve figure was plotted using GraphPad Prism 10.3.1.

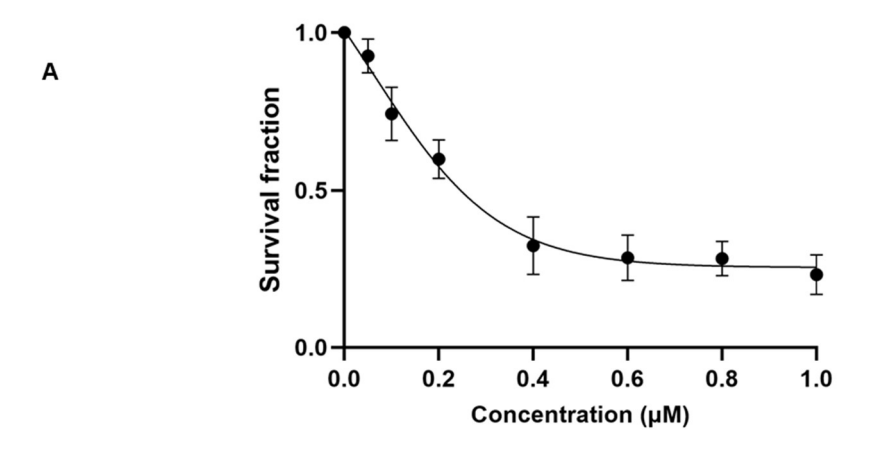
From the growth curve of MDA-MB-231 cells, the calculated doubling time for MDA-MB-231 cells in this experiment was 34 hr ±1.7.

3.3.2 Clonogenic survival of MDA-MB-231 following exposure to single cancer agents

Clonogenic assay was performed to investigate the cytotoxicity of chemotherapies (gedatolisib and doxorubicin) and radiotherapy as a single treatment in the MDA-MB-231 cell line. The assessment of effectiveness of each therapy in term of cell colonies formation was the main goal of this assay, in which the loss of cell ability to form cell colonies following exposure to a treatment is an indicator of toxicity of that treatment. Furthermore, the IC₅₀ values for the mentioned therapies were determined via this assay which were required to inform the concentrations to be used in combination therapy. Importantly, in the current experiments, gedatolisib was dissolved in DMSO as a vehicle. Although a vehicle-only control was not directly included in these experiments, the early experiment conducted in our lab by Gardiner *et al.* (2022) demonstrated that DMSO at the concentration utilised for dissolving of gedatolisib (<0.1%) had no significant impact on MDA-MB-231 cell viability or proliferation. Consequently, the effects of the vehicle were not considered an influential confounding factor in the present study.

3.3.2.1 Clonogenic survival of MDA-MB-231 following exposure to Gedatolisib alone

The cytotoxicity of gedatolisib in MDA-MB-231 cell line was evaluated utilising clonogenic assay. A range of gedatolisib concentrations were assessed where MDA-MB-231 cells were incubated with escalating concentrations of gedatolisib 0.05 -1 μ M (0.05, 0.2, 0.4, 0.6, 0.8, 1 μ M) as described in section 2.7. The data are shown in Figure 3.2



Б	IC _{s0} (μM)	IC ₂₅ (μM)	IC ₁₀ (μM)
В	0.249 ± 0.06	0.124 rounded to 0.1	0.0498 rounded to 0.05

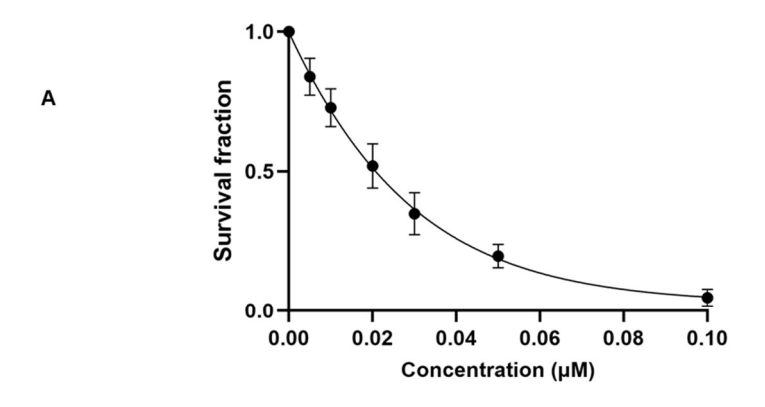
Figure 3-2 Survival fraction of MDA-MB-231 cells exposed to gedatolisib.

A: Clonogenic survival fractions of MDA-MB-231 cells following exposure to a range of gedatolisib concentrations (0.05, 0.1, 0.2, 0.4, 0.6, 0.8, 1 μ M). Data represents the mean \pm standard deviation of 3 independent experiments performed in triplicate. Statistical analysis was performed using GraphPad Prism 10.3.1 B: The inhibitory concentrations (ICs) of gedatolisib in MDA-MB-231 cell line. The PE for the MDA-MB-231 cell line was 45 \pm 4%.

The data demonstrated a concentration dependent reduction in clonogenic survival following exposure of the MDA-MB-231 cells to gedatolisib (Figure 3.2), where the lowest clonogenicity of 15% \pm 1.75 resulted from exposure to the highest utilised concentration of 1 μ M. The inhibitory concentrations (ICs) of gedatolisib are shown in Figure 3.2. B

3.3.2.2 Clonogenic survival of MDA-MB-231 following exposure to doxorubicin alone

The cytotoxicity of doxorubicin was assessed via clonogenic assay. In the initial experiments, the MDA-MB-231 cells were exposed to a concentration range of doxorubicin of 0.1-2.5 μ M (0.1, 0.5, 1, 1.5, 2, 2.5 μ M) as the IC₅₀ of doxorubicin in this cell line was found in the literature to be variable and mostly around 1 μ M. However, in pilot experiments, the clonogenic assay results of the assessed concentration range performed in our lab have demonstrated high cell killing and no colonies were observed for cells exposed to concentration higher than 0.1 μ M. Therefore, the concentration range was modified to be 0.005 - 0.1 μ M (0.005, 0.01, 0.02, 0.03, and 0.1 μ M) and the data are shown in Figure 3.3



	IC ₅₀ (μM)	IC ₂₅ (μM)	IC ₁₀ (μM)
В	0.023 ± 0.003	0.011 rounded to 0.01	0.0046 rounded to 0.005

Figure 3-3 Survival fraction of MDA-MB-231 cells exposed to doxorubicin.

A: Clonogenic survival of MDA-MB-231 cells following exposure to a range of doxorubicin concentrations (0.005, 0.01, 0.02, 0.03 and 0.05 and 0.1 μ M). Data represents the mean \pm SD of 3 independent experiments performed in triplicate. Statistical analysis was performed using GraphPad Prism 10.3.1 B: The inhibitory concentrations (ICs) of gedatolisib in MDA-MB-231 cell line. The PE for the MDA-MB-231 cell line was 45 \pm 4%.

The survival fraction curve in Figure 3.3 showed that doxorubicin induced a dose dependent reduction in survival fraction. The highest concentration utilised in this experiment (0.1 μ M) resulted in a clonogenic survival of 2.8 % ± 0.1. The inhibitory concentrations of doxorubicin are listed in Figure 3.3.B

3.3.2.3 Clonogenic survival assay for MDA-MB-231 following exposure to single radiotherapy

The cytotoxic effect of radiation in MDA-MB-231 cell line was also assessed via clonogenic assay. Cells were exposed to increasing doses of X-irradiation (1, 2, 4, 6, 8, 10 Gy). The survival fractions were fitted by linear quadratic model, and the curve is shown in Figure 3.4.

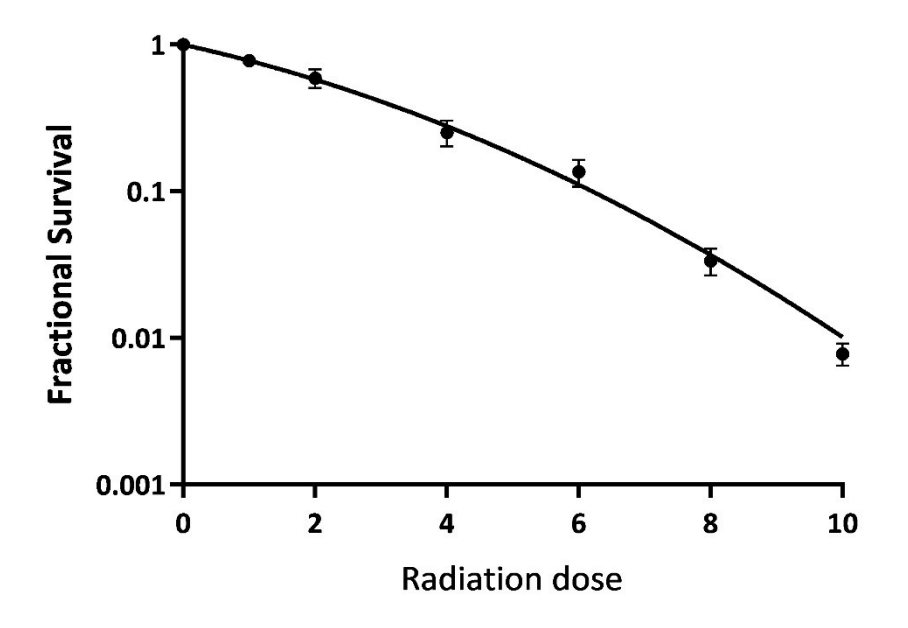


Figure 3-4 Linear quadratic survival curve of MDA-MB-231 cells exposed to radiation.

Clonogenic survival of MDA-MB-231 cells following exposure to a range of radiation doses (1, 2, 4, 6, 8, 10 Gy). The survival curve was fitted by applying the linear quadratic model. Data represents the mean ± SD of 3 independent experiments with each experiment performed in triplicate. Statistical analysis was performed using GraphPad Prism 10.3.1. PE of MDA-MB-231 cells for this experiment was 49±4%

The survival curve in Figure 3.4 showed a consistent decline in the survival of MDA-MB-231 cells as the radiation doses increased, where higher cell killing was demonstrated in the samples exposed to 10Gy dose. The linear quadratic model parameters were α (0.227), β (0.023) and α/β ratio (9.79).

3.4 Utilising spheroids model to evaluate the effectiveness of single agents in the MDA-MB-231 cell line.

Following the clonogenic survival assay, which represents a two-dimensional model, the effectiveness of single anticancer agents, gedatolisib, doxorubicin and radiation was further evaluated by use of three-dimensional tumour spheroids models. Unlike monolayers, spheroids develop gradients of nutrients, oxygen, and pH, leading to physiologically distinct regions, such as a proliferative outer rim and a hypoxic or necrotic core. These characteristics recapitulate certain aspects of the tumour microenvironment giving rise to a more predictive platform for assessing therapeutic response. While it is still an *in vitro* model, spheroids bridge the gap between traditional cell culture and *in vivo* models, offering a valuable translational tool for preclinical evaluation. Tumour spheroids formation from cell culture and the way of treatment were described in section 2.8.

3.4.1 The assessment of gedatolisib effect on the growth of MDA-MB-231 spheroids

MDA-MB-231 spheroids growth over time was assessed following exposure to a range of gedatolisib concentrations 0.05-1 μ M (0.05, 0.1, 0.2, 0.4, 0.6, 0.8, and 1 μ M). The growth of spheroids was determined by dividing the spheroid volume (V) measured at specific time point following incubation with treatment on the initial spheroid volume (V₀) at time 0 hr. The average of V/V₀ for spheroids following

treatment with each gedatolisib concentration at different time points was determined. Spheroids were imaged every 3-4 days for 3 consecutive weeks to measure the volumes at different time points. The growth curves for spheroids treated with different concentrations are shown in Figure 3.5

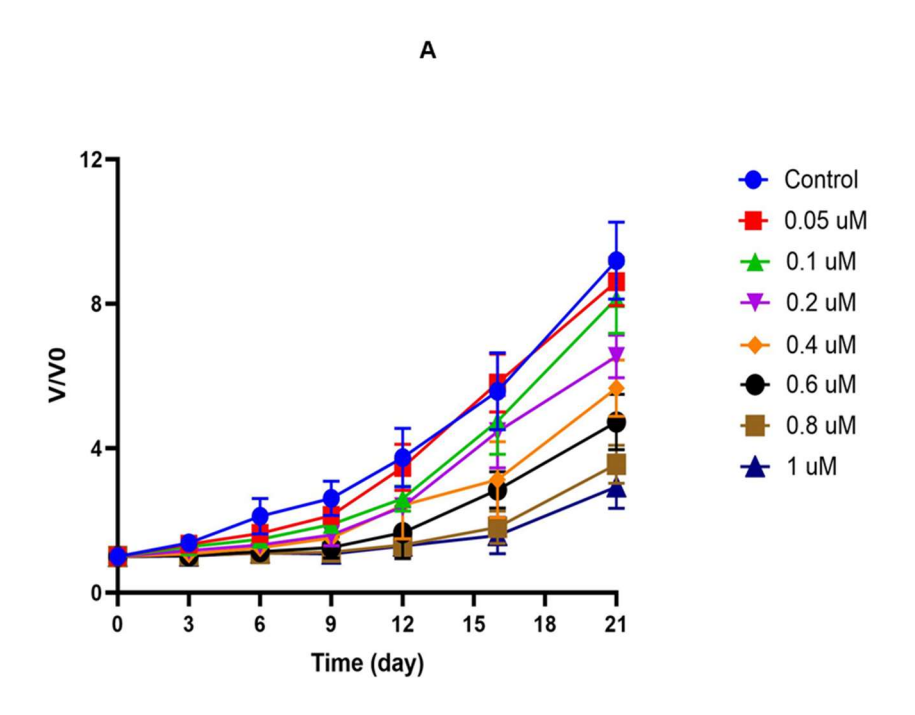


Figure 3-5 Growth curve of MDA-MB-231 tumour spheroid exposed to gedatolisib.

A: tumour spheroids growth curves following exposure to a range of Gedatolisib concentrations. Spheroids were imaged every 3-4 days, and their growth was assessed by measuring the volume (V) at different times, and V/V_0 represent the change in the volume at each time point relative to the initial volume (time 0hr). Data represents an average of $V/V_0 \pm SD$ at different time points. 24 spheroids were assessed for each treatment group, and 3 independent experiments were performed in triplicate. Statistical analysis was performed using GraphPad Prism 10.3.1 with two-way ANOVA. B: The Tukey's multiple comparisons test and the difference was considered significant when P value < 0.05 where na= non-significant, *P < 0.05, **P < 0.01, ***P < 0.001 and ****P < 0.0001

В

Tukey's multiple comparisons test	P (*)	Significant	P-value
Control vs. 0.05 μM	ns	No	>0.9999
Control vs. 0.1 μM	ns	No	0.1995
Control vs. 0.2 μM	**	Yes	0.0032
Control vs. 0.4 μM	****	Yes	<0.0001
Control vs. 0.6 μM	****	Yes	<0.0001
Control vs. 0.8 μM	****	Yes	<0.0001
Control vs. 1 µM	****	Yes	<0.0001

From Figure 3.5, comparison of the spheroid growth curves (V/V_0) over the full monitoring period demonstrated that the V/V_0 of spheroids treated with $0.05\mu M$ and $0.1\mu M$ of gedatolisib was not statistically significantly different compared to the untreated control (P>0.05). Administration of gedatolisib concentration greater than $0.1~\mu M$ induced a statistically significant reduction in spheroid growth relative to the untreated control (p < 0.05). The spheroids growth reduction was correlated with an increase in drug concentrations where spheroids treated with higher gedatolisib concentrations utilised in this experiment $(1\mu M)$ showed a statistically significant reduction in spheroid volume (V/V_0) compared to the untreated control (P<0.0001)

3.4.2 The assessment of doxorubicin effect on the growth of MDA-MB-231 spheroids

Tumour spheroids derived from MDA-MB-231 cells were also utilised to assess the effect of doxorubicin on the growth of MDA-MB-231 spheroids. Tumour spheroids were incubated with a range of doxorubicin concentrations (0.05 μ M – 0.1 μ M) and the spheroids were imaged every 3-4 days for 3 consecutive weeks to measure the volumes at different time points. The growth curves for spheroids treated with different concentrations are shown in Figure 3.6

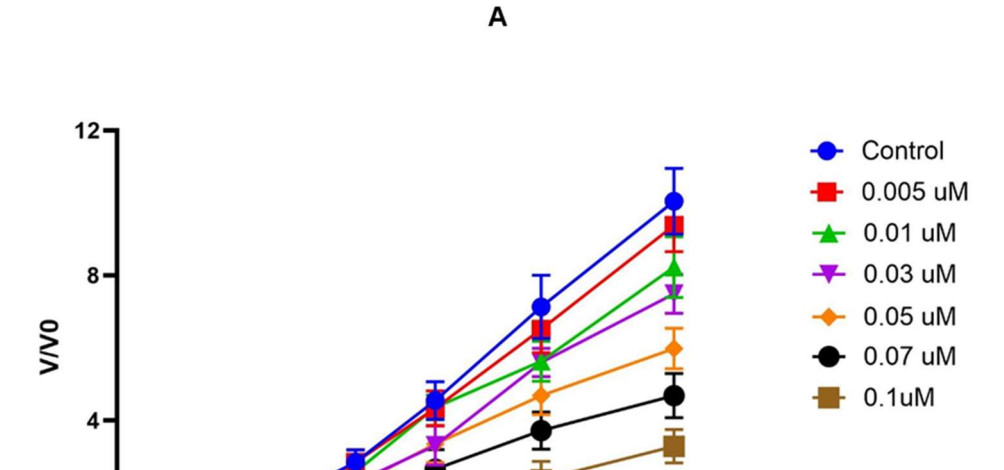


Figure 3-6 Growth curve of MDA-MB-231 tumour spheroid exposed to doxorubicin.

Time (day)

A: Tumour spheroids growth curves following exposure to a range of doxorubicin concentrations. Spheroids were imaged every 3-4 days, and their growth was assessed by measuring the volume (V) at different times, and V/V0 represent the change in the volume at each time point relative to the initial volume (time 0hr). Data represents an average of V/V0 ± SD at different time points. 24 spheroids were assessed for each treatment group, and 3 independent experiments were performed in triplicate. Statistical analysis was performed using GraphPad Prism 10.3.1 with two-way ANOVA. B: The Tukey's multiple comparisons test and the difference was considered significant when P value < 0.05 where na= non-significant, *P < 0.05, **P < 0.01, ***P < 0.001 and ****P < 0.0001

Tukey's multiple comparisons test	P (*)	Significant	P-value
Control vs. 0.005 µM	ns	No	>0.9999
Control vs. 0.01 μM	ns	No	0.062
Control vs. 0.03 μM	**	Yes	0.0035
Control vs. 0.05 μM	****	Yes	<0.0001
Control vs. 0.07 μM	****	Yes	<0.0001
Control vs. 0.1 μM	****	Yes	<0.0001

The growth curve for tumour spheroids treated with increasing concentrations of doxorubicin demonstrated that $0.05\mu M$ drug concentration did not influence V/V₀ when compared to the untreated control (P<0.05). Furthermore, doxorubicin concentrations larger than $0.05\mu M$ resulted in a statistically significant spheroid growth delay compared to the untreated control (p <0.05). The growth delay of spheroids increased with escalating doxorubicin concentrations, where higher growth delay was in response to higher drug concentration (P<0.0001) (Figure 3.6).

3.4.3 The assessment of radiation effect on the growth of MDA-MB-231 spheroids MDA-MB-231 spheroids

The assessment of radiation alone efficacy in reducing tumour growth was performed utilising MDA-MB-231 spheroids. The spheroids were irradiated with several radiation dose ranges (1, 2, 3, and 6 Gy). The average spheroid volume changes (V/V₀) at different time points following X-irradiation are shown in Figure 3.7.



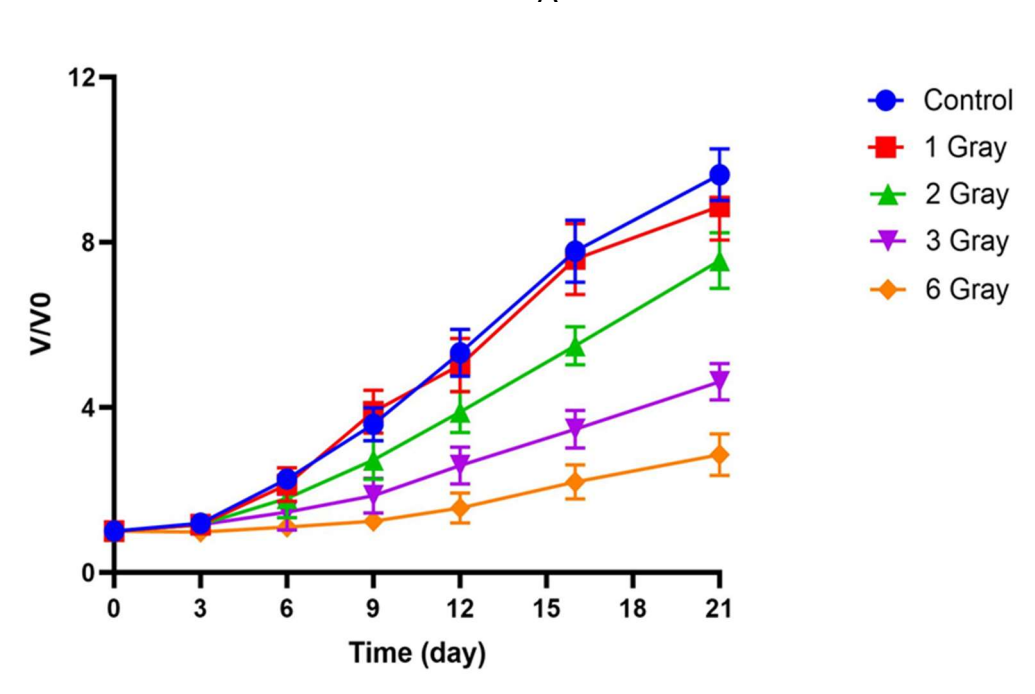


Figure 3-7 Growth curve of MDA-MB-231 tumour spheroid exposed to radiation.

A: tumour spheroids growth curves following exposure to a range of X-radiation doses. Spheroids were imaged every 3-4 days, and their growth was assessed by measuring the volume (V) at different times, and V/V $_0$ represent the change in the volume at each time point relative to the initial volume (time 0hr). Data represents an average of V/V $_0$ ± SD at different time points. 24 spheroids were assessed for each treatment group, and 3 independent experiments were performed in triplicate. Statistical analysis was performed using GraphPad Prism 10.3.1 with two-way ANOVA. B: The Tukey's multiple comparisons test and the difference was considered significant when P value < 0.05 where na= non-significant, *P < 0.05, **P < 0.01, ***P < 0.001 and *****P < 0.0001

Tukey's multiple comparisons test	P (*)	Significant	P-value
Control vs. 1 Gy	ns	No	>0.9999
Control vs. 2 Gy	*	Yes	0.034
Control vs. 3 Gy	****	Yes	<0.0001
Control vs. 6 Gy	****	Yes	<0.0001

Data in Figure 3.7 explored the growth pattern for the spheroids at different time points for several radiation doses as well as the untreated control group. The spheroids irradiated with 1 Gy showed the same growth pattern as compared to non-irradiated control group with no significant difference in growth between 1 Gy radiation and control (P> 0.05). Those spheroids irradiated with 2 Gy, 3Gy and 6 Gy had a statistically significant reduction in V/V₀ compared to the untreated control spheroids (P<0.001), and this significant difference was dose dependent where the higher dose resulted in higher growth delay (P<0.0001) as shown in Figure 3.7

3.5 Combination therapy

The previous experiments with single agents demonstrated the ranges of concentrations of the drugs and the radiation doses that induce dose dependent reductions in clonogenic survival in the MDA-MB-231 cell line. These preliminary results demonstrated that treatment of MDA-MB-231 cells with low concentrations of gedatolisib and doxorubicin, as well as low radiation doses, resulted in relatively low

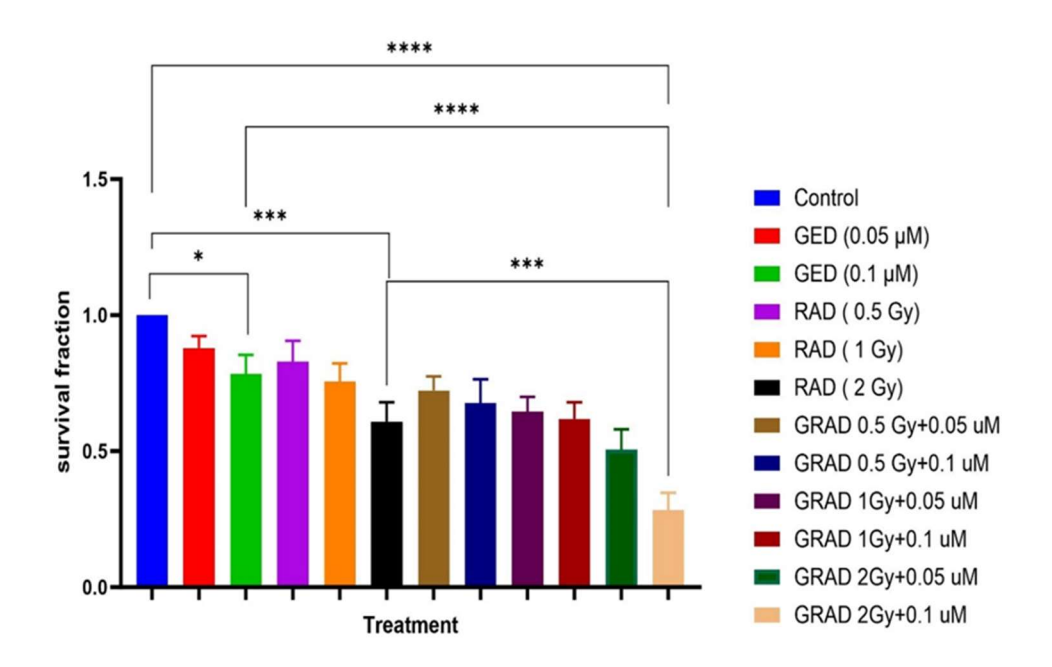
cytotoxic effects when administered alone. However, combining these agents may have a substantial biological rationale. Inhibition of the PI3K/AKT/mTOR pathway has been shown to impair DNA repair mechanisms and promote apoptosis, thus enhancing cancer cell response to DNA-damaging agents, including chemotherapy and radiation (De Vera and Reznik, 2019b; Wanigasooriya et al., 2020). Radiation induces cell death primarily by causing double-strand DNA breaks, a crucial cytotoxic mechanism, and doxorubicin causes DNA intercalation with oxidative stress. Both treatments can overwhelm the DNA repair system of the cancer cells. When these DNA damaging agents are combined with PI3K/Akt/mTOR inhibitors, the ability of cancer cells to repair the DNA damage is further weakened, resulting in accumulation of DNA breaks and enhancing cell death. Based on our preliminary results, we hypothesised that combining gedatolisib, a dual PI3K/mTOR inhibitor, with either radiation or doxorubicin would result in enhanced cytotoxic effects against MDA-MB-231 cells compared to treatment alone. The potential combining of these therapeutic agents may produce synergistic effects, consequently augmenting cytotoxicity and promoting treatment success in TNBC cells.

3.5.1 Assessment of the clonogenic survival of MDA-MB-231 cells after treatment with a combination therapy of gedatolisib and radiation

Radiotherapy causes DNA double-strand breaks, resulting in cancer cell death mainly by the accumulation of unrepaired DNA damage. However, radioresistance remains a significant therapeutic challenge, frequently induced by activation of key survival pathways, including PI3K/AKT/mTOR signalling. Inhibition of this pathway has been shown to impair DNA repair mechanisms, disrupt cell survival signalling, and enhance apoptosis, thus increasing the radiosensitivity of cancer cells (Wanigasooriya *et al.*, 2020; Deng *et al.*, 2023a). A recent study by McGowan *et al.* (2019) demonstrated

that buparlisib, a PI3K inhibitor, could be safely combined with radiotherapy and enhanced the effect of radiation in patients with NSCLC. Based on this rationale, we hypothesised that combining gedatolisib with radiation in MDA-MB-231 cells could enhance the cytotoxicity compared to either treatment alone. Concomitant administration of low radiation doses and small gedatolisib concentrations was proposed as a potential combination therapy for the MDA-MB-231 cell line. A clonogenic survival assay was utilised to evaluate the cytotoxicity of the proposed combination therapy in the MDA-MB-231 cell line in comparison to single agents and the untreated control. Based on our preliminary results, gedatolisib concentrations and radiation doses that produced low to moderate reductions in cell survival were selected. Gedatolisib concentrations of 0.05µM and 0.1µM, corresponding to approximately IC₁₀ and IC₂₅, respectively, were combined with of 0.5, 1 and 2 Gy radiation doses. The results are shown in Figure 3.8

Α



В

Tukey's multiple comparisons test	P (*)	Significance	Adjusted P Value
Control vs. 0.05 GED	ns	No	>0.9999
Control vs. 0.1 GED	*	Yes	0.0358
Control vs. 2 Gy	***	Yes	0.0006
0.1 GED vs. 2 Gy + 0.1 GED	****	Yes	<0.0001
2 Gy vs. 2 Gy + 0.1 GED	***	Yes	0.0001

Figure 3-8 Survival fraction of MDA-MB-231 cells exposed to combination of gedatolisib and radiation.

A: MDA-MB-231 cell survival fraction following exposure to combination of 0.05 and 0.1 μ M gedatolisib with 0.5, 1 and 2 Gy radiation. Data represents the mean \pm SD of the survival fraction of the treated cells that were normalized to the untreated control for 3 independent experiments performed in triplicate. PE of the control in this experiment was 48 \pm 6%. Statistical analysis was performed using GraphPad Prism 10.3.1 with one-way ANOVA. B: Tukey's multiple comparisons test to determine significance, which was undertaken using GraphPad Prism 10.3.1 and the difference considered significant when P value < 0.05 where na= non-significant, *P < 0.05, **P < 0.01, ***P < 0.001 and *****P < 0.0001

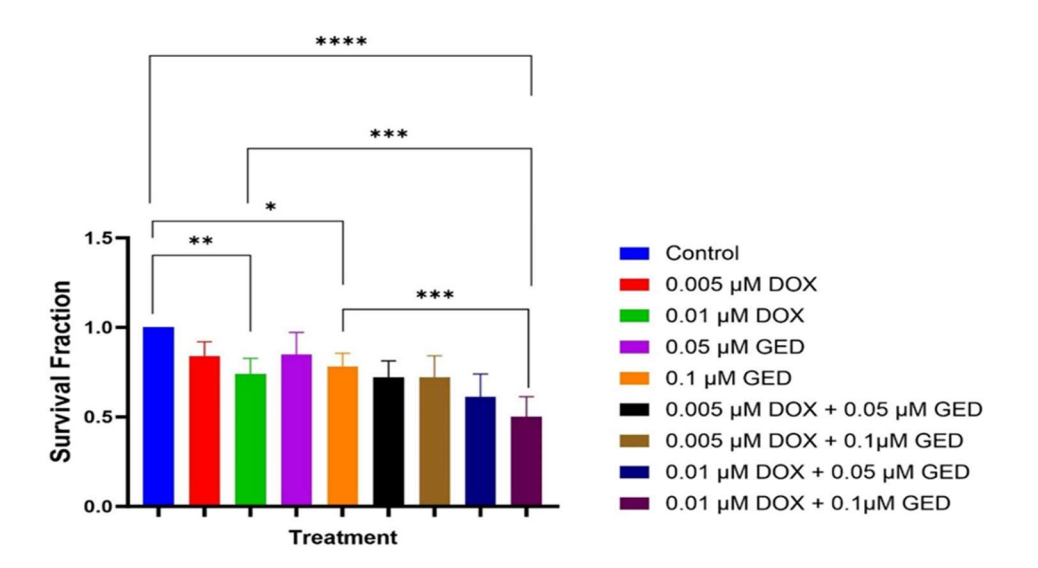
From Figure 3.8, cells treated with 0.1 µM gedatolisib or 1Gy radiation dose showed a statistically significant reduction in cell survival compared to the untreated control (P < 0.05). Moreover, X-irradiation of MDA-MB-231 cells with a single 2Gy dose resulted in significant cell survival reduction when compared to the untreated control (P<0.001) (Figure 3.7). The combination of gedatolisib and radiation induced variable effects on the clonogenic survival of MDA-MB-231 cells in comparison with treatment alone. The combination of 0.1 µM of gedatolisib and 1 Gy of radiation induced a statistically significant reduction of clonogenic survival compared to the untreated control (P<0.001) and the drug its own (P<0.05). However, this combination did not induce a statistically significant reduction in cell survival when compared to treatment with a 1 Gy single radiation dose (P>0.05). The results of this experiment revealed that the combination of 0.1 µM gedatolisib with 2 Gy radiation resulted in a significant survival reduction when compared to the untreated control (P<0.0001), alone 0.1 µM gedatolisib (P<0.0001), and individual 2 Gy radiation dose (P<0.001) (Figure 3.8). The full statistical comparison table for the investigated doses and concentrations of monotreatment and their combinations in the MDA-MB-231 cell line are shown in the Appendix.

3.5.2 Assessment of the clonogenic survival of MDA-MB-231 cells after treatment with a combination therapy of gedatolisib and doxorubicin

Doxorubicin is the gold standard chemotherapy commonly utilised in the treatment of different cancers, including triple-negative breast cancer (TNBC). It primarily promotes cancer cell death by inducing DNA damage via intercalation and inhibition of topoisomerase II. However, the effectiveness of doxorubicin is frequently restricted by the emergence of acquired drug resistance and dose-dependent toxicity. The PI3K/AKT/mTOR pathway is essential for improving cell survival, proliferation, and

DNA repair in cancer cells, and activation of this pathway may contribute to the development of doxorubicin resistance. Preclinical studies have shown that inhibiting the PI3K/AKT/mTOR pathway might enhance the cancer cell response to doxorubicin by disrupting DNA repair mechanisms and promoting apoptosis (Bhatti *et al.*, 2018; Fabi *et al.*, 2021). Based on this biological rationale, we hypothesised that the combination of gedatolisib, a dual PI3K/mTOR inhibitor, with doxorubicin would result in increased cytotoxic effects in the MDA-MB-231 cells compared to treatment alone. To assess the effects of combination of gedatolisib and doxorubicin, clonogenic assay was undertaken utilising the concentrations of each drug that showed low to moderate cytotoxicity in the single agent experiments. Two concentrations of gedatolisib (0.05μM and 0.1μM) were combined with two concentrations of doxorubicin (0.005μM and 0.01μM) that corresponding to approximately the IC₁₀ and IC₂₅ of each drug, respectively. Clonogenic survival after exposure to different combination regimens are shown in Figure 3.9





В

Tukey's multiple comparisons test	Р	Significant	Adjusted P
	(*)	Value	
Control vs. DOX (0.1µM)	**	Yes	0.004
Control vs. GED (0.1µM)	*	Yes	0.0308
GED (0.1μM) vs. DOX (0.1μM) + GED (0.1μM)	***	Yes	0.0002
DOX (0.1μM) vs. DOX (0.1μM) + GED (0.1μM)	***	Yes	0.0002

Figure 3-9 Survival fraction of MDA-MB-231 cells exposed to combination of gedatolisib and doxorubicin.

A: MDA-MB-231 cell survival fraction following exposure to combination of 0.05 and 0.1 μ M gedatolisib with 0.005 and 0.01 μ M doxorubicin. Data represents the mean \pm SD of the survival fraction of the treated cells that were normalized to the untreated control for 3 independent experiments performed in triplicate. PE of the control in this experiment was 48 \pm 6%. Statistical analysis was performed using GraphPad Prism 10.3.1 with one-way ANOVA. B: Tukey's multiple comparisons test to determine significance, which was undertaken using GraphPad Prism 10.3.1 and the difference considered significant when P value < 0.05 where na= non-significant, *P < 0.05, **P < 0.01, ***P < 0.001 and ****P < 0.0001

From Figure 3.9, the treatment with the IC₁₀ of gedatolisib (0.05 μ M), the IC₁₀ of doxorubicin (0.005 μ M), did not induce a statistically significant reduction in clonogenic survival when used alone compared to the untreated control (P>0.05). Furthermore, the combination of these low concentrations (0.05 μ M gedatolisib and 0.005 μ M doxorubicin) also did not induce a statistically significant clonogenic survival reduction when compared to the drug alone (Figure 3.9). However, utilisation of a therapeutic regimen combining 0.1 μ M gedatolisib and 0.01 μ M doxorubicin induced a significant reduction in clonogenic survival of MDA-MB-231 cells when compared to the untreated control (P<0.001). Additionally, a statistically significant reduction in clonogenic survival was produced following treatment of MDA-MB-231 cells with the combination of 0.1 μ M gedatolisib and 0.01 μ M doxorubicin compared to treatment with each drug alone (P<0.001) (Figure 3.9).

3.6 Combination index analysis for combination therapy

The cytotoxic relationship between two or more treatments utilised as a combination treatment for cancer cells can be investigated by using combination index analysis (CI). This mathematical model was derived from the mass action law, enabling a quantitative comparison between the actual cytotoxic effect of a combined treatment and the theoretical expected effect if the agents worked independently. The values of cell survival fractions and cell killed fractions were calculated from the data of the clonogenic survival assay and recruited to the CA analysis model. CompuSyn® is a software developed by Chou and Martin (Chou T and Martin N, 2005) utilised to process the combination index analysis. CI value will inform the type of the relationship either infra-additive (antagonistic), additive (not synergistic or antagonistic), or supra-additive (synergistic) as described in section 2.10.

3.6.1 Assessment of synergy of the various combinations of gedatolisib and radiation in MDA-MB-231 cell line utilising combination Index analysis

Based on the results of the clonogenic assay using combinations of gedatolisib with radiation, the combination index analysis was performed. CI was used to assess whether the combining of both therapeutic agents produces a synergistic response. The synergism of treatments possibly allows for using combinations of low doses of each treatment, which could be beneficial by increasing the effectiveness of treatments and minimising the adverse effects, thus improving the therapeutic outcomes. The cell survival fractions derived from the clonogenic assay of the simultaneous combining of gedatolisib with radiation were recruited to the CompuSyn® software, calculating the CI values for different combinations, to determine the therapeutic relationship between these dose variant combinations. The results are shown in Figure 3.10.

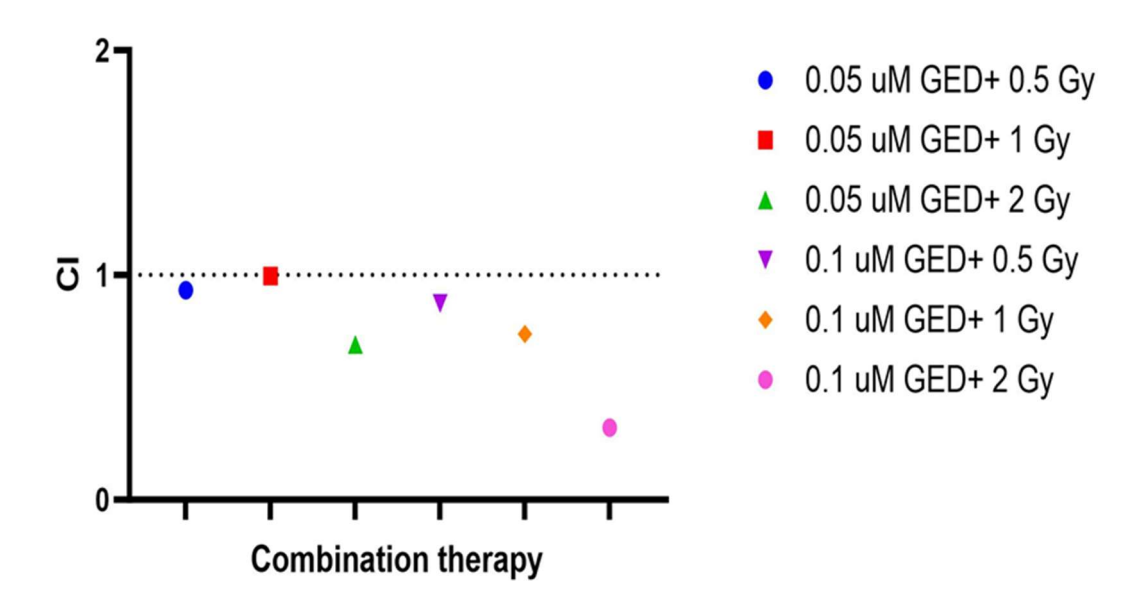


Figure 3-10 Combination index analysis for the simultaneous combination of gedatolisib and radiation in MDA-MB-231 cell line.

Combination index analysis of Gedatolisib-radiation combination therapy in MDA-MB-231 cell line. Two concentrations of gedatolisib (0.05 and 0.1 µM) of gedatolisib were simultaneously combined with (0.5 Gy,1 Gy and 2 Gy) of radiation. The combination index (CI) values were determined by CompuSyn® software. The CI values were plotted using GraphPad Prism 10.3.1. CI values are Chou-Talalay model derived from an algorithm and thus error bars are not conventionally provided or displayed. The points in the plot represent different combination levels. CI <0.9 is synergistic, CI (0.9-1.1) is additives and CI> 1.1 (infra-additive)

Figure 3.10 showed that the combination of low concentration of gedatolisib (0.05 μ M) with 0.5 or 1 Gy radiation, when given simultaneously, resulted in additive cell kill. Conversely, when low concentrations of gedatolisib were combined with 2 Gy, this induced supra-additive (synergistic) reduction in clonogenic survival in the MDA-MB-231 cell line. Furthermore, combination of 0.1 μ M gedatolisib with all radiation doses tested (0.5, 1 and 2 Gy) resulted in supra-additive (synergistic) effects (Figure 3.12). These data suggest that low administered combinations of gedatolisib when

combined with higher doses of radiation (2Gy), induced supra-additive cell kill in MDA-MB-231 cells, but that all combinations induced at least additive effects.

3.6.2 Assessment of synergy of the various combinations of gedatolisib and doxorubicin in MDA-MB-231 cell line utilising combination Index analysis

To assess the therapeutic relationship when combining gedatolisib with doxorubicin, CI analysis was performed. The cell survival fractions, and cell killed fractions derived from the clonogenic assay of the combination of gedatolisib with doxorubicin were recruited into the CompuSyn® software to calculate the CI values. The results are shown in Figure 3.11.

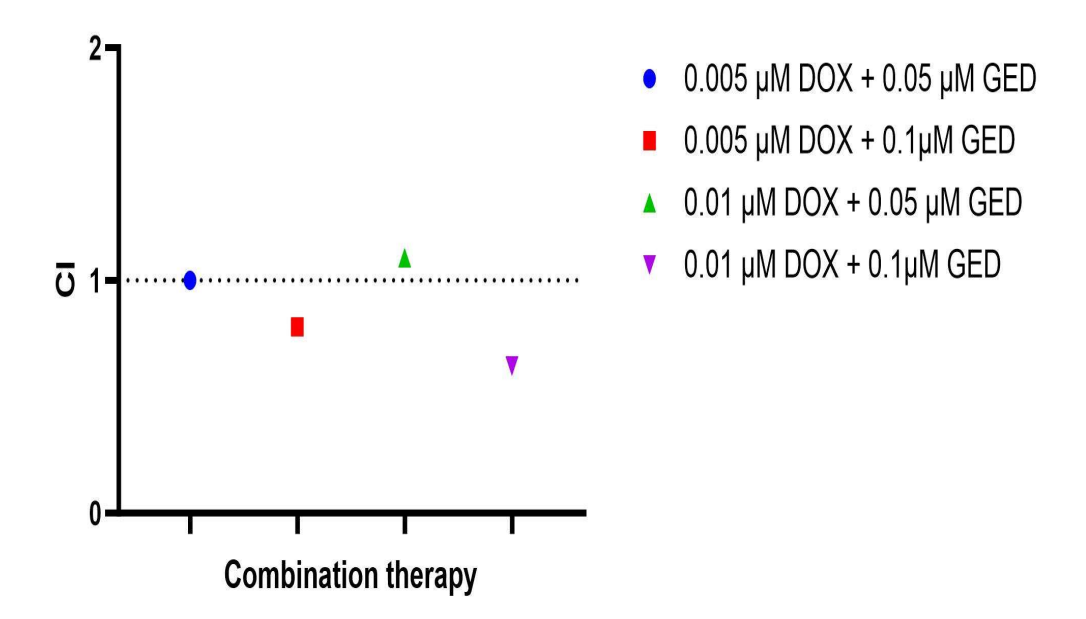


Figure 3-11 Combination index analysis for the simultaneous combination of gedatolisib and doxorubicin in MDA-MB-231 cell line.

Combination index analysis of Gedatolisib-radiation combination therapy in MDA-MB-231 cell line. Two concentrations of gedatolisib (0.05 and 0.1 μ M) were simultaneously administered with (0.005 and 0.01 μ M) of doxorubicin. The combination index (CI) values were determined by CompuSyn® software. The CI values were plotted using GraphPad Prism 10.3.1. CI values are Chou-Talalay model derived from an algorithm and thus error bars are not conventionally provided or displayed. The points in the plot represent different combination levels. CI <0.9 is synergistic, CI (0.9-1.1) is additives and CI> 1.1 (infra-additive)

Figure 3.11 showed that the combination of low gedatolisib concentration (0.05 μ M) with the two doxorubicin concentrations (0.05 and 0.1 μ M) had an additive effect on the cell kill relationship. However, a combination of higher gedatolisib concentration (0.1 μ M) with the two doxorubicin concentrations (0.05 and 0.1 μ M) induced supraadditive (synergistic) effect on cell kill in the MDA-MB-231 cell line. These data suggest that combinations of low gedatolisib concentrations with doxorubicin

produced additive effects, while increasing the gedatolisib concentration in combination with doxorubicin resulted in supra-additive cell kill in MDA-MB-231 cells.

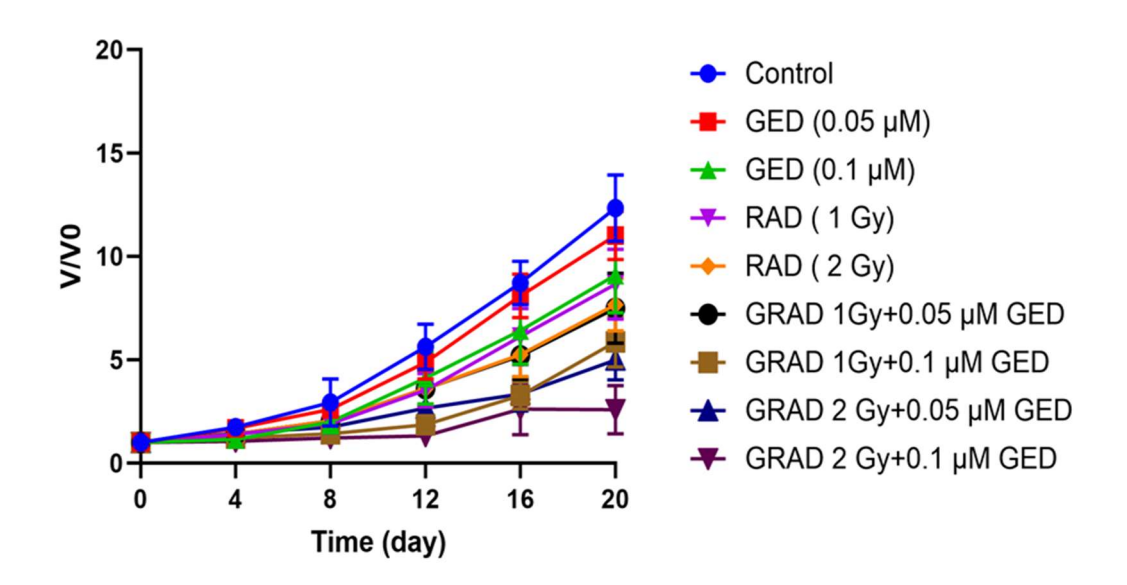
3.7 Evaluation of the effect of gedatolisib, doxorubicin, and radiation treatments alone and in combination using MDA spheroids.

Following the assessment of cytotoxicity for combinations of chemotherapy and radiotherapy via clonogenic assay and CI analysis, tumour spheroids were utilised to evaluate the efficacy of these combinations in spheroid growth. The combination therapy was designed according to the tumour spheroids data for single chemotherapy and radiotherapy as well as clonogenic survival data for each treatment. Low concentrations of gedatolisib and doxorubicin and low doses of radiation were selected for the setting of different combination treatments because they showed minor to moderate cytotoxicity when administered alone in clonogenic assay of MDA-MB-231 cell line. However, combining these gedatolisib concentrations with either radiation or doxorubicin resulted in enhanced cytotoxicity compared to each treatment alone. Additionally, CI analysis demonstrated synergism among these investigated combinations. Therefore, MDA-MB-231 multicellular spheroids were utilised to assess the effects of these combinations in more complex and closer physiological model. Following treatment, spheroid growth was monitored every 3-4 days for three consecutive weeks.

3.7.1 Evaluation of the effect of gedatolisib and radiation treatments alone and in combination using MDA spheroids.

To assess the effect of combining gedatolisib with radiation in MDA-MB-231 spheroids, low concentrations of gedatolisib (0.05 and 0.1 μ M) were combined with

low doses of radiation (1 and 2 Gy) to treat the MDA-MB-231 spheroids. Most of these combinations resulted in clonogenic survival reductions in MDA-MB-231 cells compared to the untreated control. Hence, evaluating their effect in MDA-MB-231 spheroids may reinforce their potential as new therapeutic strategies in TNBC. Following treatment, spheroids were imaged every 3-4 days, and the changes in spheroid volumes at each time point relative to the initial volume (time 0) presented as VIV₀ were measured. The growth curves of MDA-MB-231 spheroids exposed to different combinations of gedatolisib and radiation are shown in Figure 3.12.



В

Tukey's multiple comparisons test	Р	Significance	Adjusted P Value
	(*)		
Control vs. 0.1 GED	ns	No	0.074
Control vs. 2 Gy	**	Yes	0.0046
Control vs. 2 Gy + 0.1 GED	****	Yes	<0.0001
0.1 GED vs. 2 Gy + 0.1 GED	***	Yes	0.0001
2 Gy vs. 2 Gy + 0.1 GED	**	Yes	0.0032

Figure 3-12 Growth curve for MDA-MB-231 spheroid exposed to a simultaneous combination of gedatolisib and radiation.

A: MDA-MB-231 spheroids growth curves following exposure to a combination of 0.05 and 0.1 μ M of gedatolisib with 1 Gy and 2 Gy of radiation. Spheroids were imaged every 3-4 days to measure their volume (V), and V/V₀ represents the change in the volume at each time point (day X) over the initial volume (day 0). Data represents an average of V/V₀ \pm SD at different time points. 24 spheroids were assessed for each treatment group, and 3 independent experiments were performed. The Statistical analysis was performed using GraphPad Prism 10.3.1 with two-way ANOVA. B: Tukey's multiple comparisons test, and the difference

was considered significant when P value < 0.05 where *P < 0.05, **P < 0.01, ***P < 0.001 and ****P < 0.0001

In spheroids treated with single gedatolisib (0.05 or 0.1 µM) or irradiated with 1 Gy radiation as single agents, there was no significant changes in spheroids growth relative to untreated controls (P<0.05). The combination of 0.05 or 0.1 µM gedatolisib with 1 Gy radiation dose, however, resulted in a statistically significant reduction in V/V₀ in comparison to the untreated spheroids. However, no significant differences in spheroid growth were found post-treatment with a combination of 0.05 or 0.1 µM gedatolisib with 1 Gy radiation as compared to each agent alone (P>0.05) (Figure 3.12). Irradiation of the MDA-MB-231 spheroids with 2 Gy radiation resulted in a statistically significant reduction in V/V₀ in comparison with the untreated spheroids (P<0.01). Figure (3.12) also demonstrated a significant reduction in tumour volume for the spheroids exposed to a combination of 0.05 µM gedatolisib with 2 Gy radiation relative to the untreated spheroids and gedatolisib alone, but not to the 2 Gy dose of radiation alone (P>0.05). The combination of 2 Gy radiation with 0.1 µM gedatolisib showed the superior effect on inhibition of spheroid growth, with the greatest statistically significant reduction in V/V₀ as compared to the control and each treatment alone (P<0.001). The full statistical comparison table for the investigated doses and concentrations of monotreatment and their combinations in the MDA-MB-231 cell line are shown in the Appendix.

To visualize the tumour spheroid growth, representative images of spheroids at different time points for different groups are shown in Figure 3.13

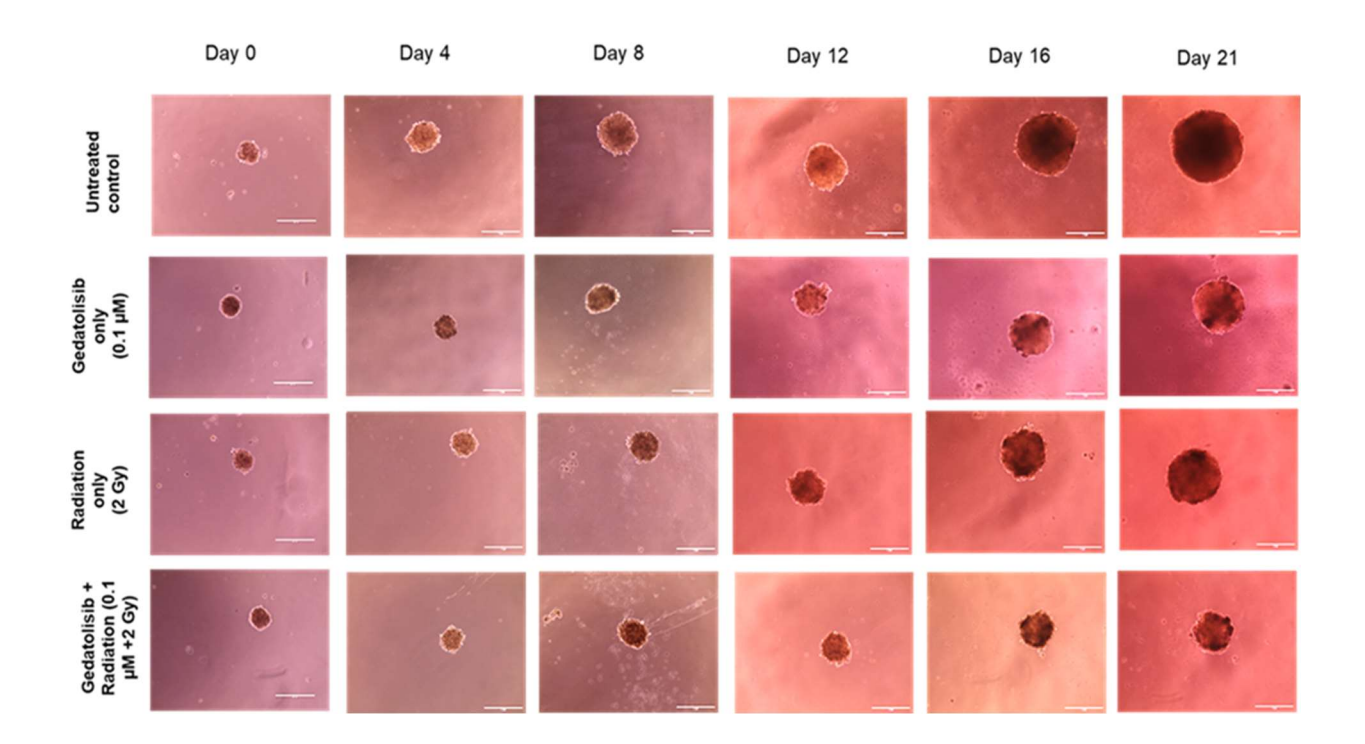


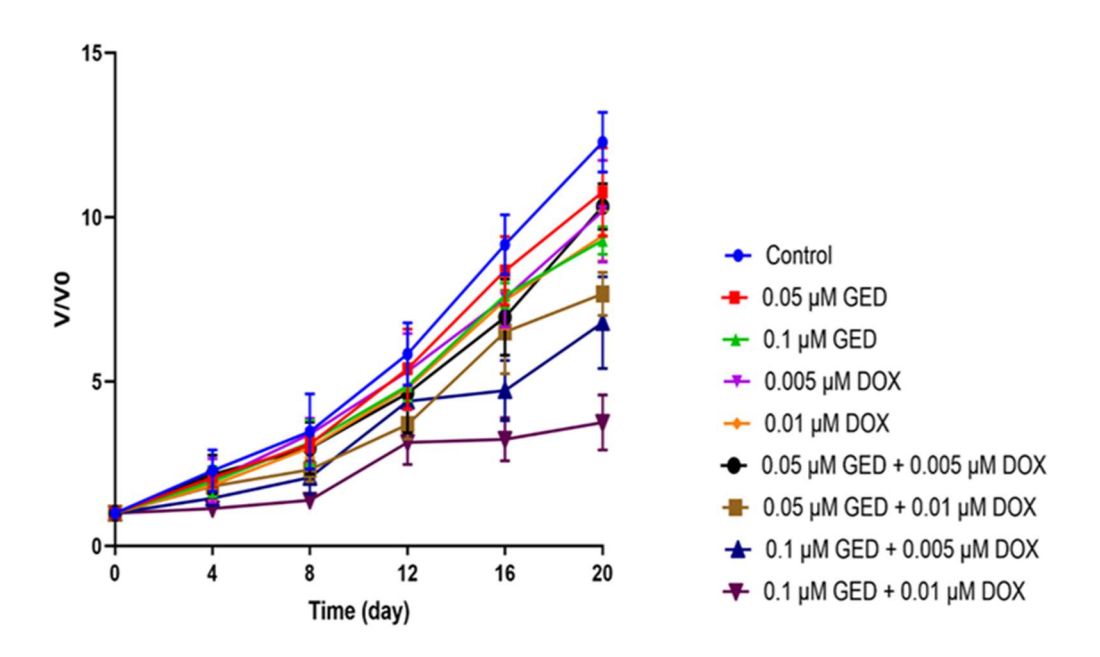
Figure 3-13 MDA-MB-231 tumour spheroids growth dynamics following exposure to single and simultaneously given combination of gedatolisib and radiation

Growth of MDA-MB-231 tumour spheroids following exposure to single and combined treatments with gedatolisib and radiation. Representative bright-field images of MDA-MB-231 spheroids were acquired using an EVOS microscope at 10° magnification. The images are corresponding to spheroids showing the best response to combination therapy among other assessed treatments. They represent spheroids treated with either 0.1 μ M gedatolisib alone, 2 Gy ionising radiation alone, or their combinations, and the images illustrate spheroids morphology and relative growth patterns over time.

3.7.2 Evaluation of the effect of gedatolisib and radiation treatments alone and in combination using MDA spheroids

To evaluate the effectiveness of the combination of gedatolisib and doxorubicin, low concentrations of both drugs were combined to treat the MDA-MB-231 spheroids. Most of these combinations have shown significant reductions in clonogenic survival in MDA-MB-231 cells compared to the untreated control. Therefore, evaluating their effect in MDA-MB-231 spheroids may support their promising role in treatment approaches for TNBC. Following treatment, spheroids were imaged every 3-4 days, and the changes in spheroid volumes at each time point relative to the initial volume (time 0) presented as V/V₀ were measured. The growth curves of MDA-MB-231 spheroids exposed to various combinations of gedatolisib and doxorubicin are shown in Figure 3.14.





В

Tukey's multiple comparisons test		Significance	Adjusted P Value
Control vs. 0.1 µM GED	ns	No	0.1995
Control vs. 0.01 µM DOX	ns	No	0.062
Control vs. 0.1 µM GED + 0.01 µM DOX	****	Yes	<0.0001
0.1 μM GED vs. 0.1 μM GED + 0.01 μM DOX	****	Yes	<0.0001
0.01 μM DOX vs. 0.1 μM GED + 0.01 μM DOX	****	Yes	<0.0001

Figure 3-14 Growth curve for MDA-MB-231 tumour spheroid exposed to a combination therapy of gedatolisib and doxorubicin.

A: MDA-MB-231 spheroids growth curves following exposure to a combination of (0.05 and 0.1 μ M) of gedatolisib with (0.005 and 0.01 μ M) of doxorubicin. Spheroid growth was assessed by measuring the volume (V), and V/V0 represent the change in the volume at different time points over the initial volume. Data represents an average of V/V0 \pm SD at different time points. 24 spheroids were assessed for each treatment group, and 3 independent experiments were performed. The Statistical analysis was performed using GraphPad Prism 10.3.1 with two-way ANOVA. B: Tukey's multiple comparisons test, and the difference was considered significant when P value < 0.05 where *P < 0.05, **P < 0.01, ***P < 0.001 and ****P < 0.0001

The data in Figure 3.14 showed that in spheroids treated with single and combination of low concentrations of gedatolisib and doxorubicin (0.05 μ M and 0.005 μ M, respectively), there was no statistically significant effect on spheroid growth compared to the untreated spheroids (P>0.05). Conversely, the combination of 0.1 μ M gedatolisib with 0.005 μ M doxorubicin resulted in a statistically significant reduction in V/V₀ compared to the untreated controls (P<0.05), but not with each single agent (P>0.05) (Figure 3.14). The higher reduction in V/V₀ was demonstrated in spheroids exposed to a combination of 0.1 μ M gedatolisib and 0.01 μ M doxorubicin compared to the untreated spheroids (p<0.0001), and each drug alone (p<0.0001) (Figure 3.14). These data suggest that a combination of moderate to higher concentrations of gedatolisib and doxorubicin may have a superior effect on the inhibition of spheroid growth. The full statistical comparison table for the investigated doses and concentrations of monotreatment and their combinations in the MDA-MB-231 cell line are shown in the Appendix.

To visualise the tumour spheroid growth, representative images of spheroids at different time points for different combination therapies of gedatolisib plus doxorubicin are shown in Figure 3.15

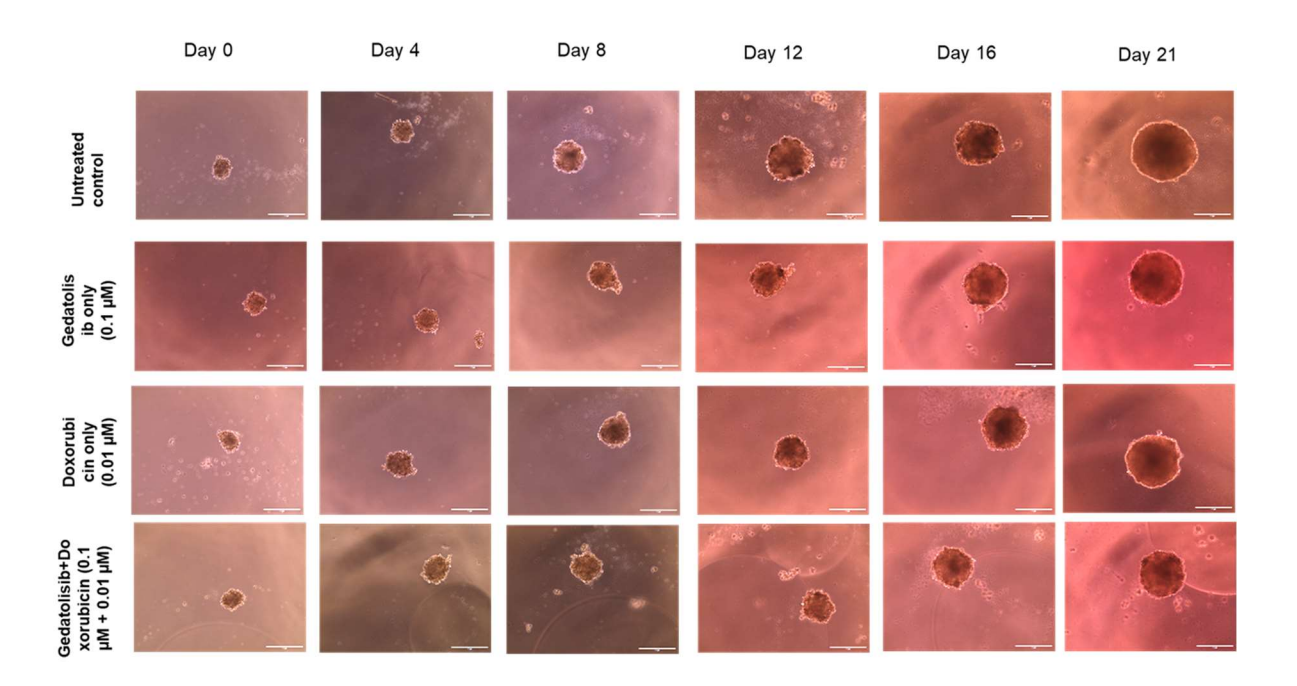


Figure 3-15 MDA-MB-231 tumour spheroids growth following exposure to single and simultaneous combination of gedatolisib and doxorubicin.

Growth of MDA-MB-231 tumour spheroids following exposure to single and combined treatments with gedatolisib and radiation. Representative bright-field images of MDA-MB-231 spheroids were acquired using an EVOS microscope at 10° magnification. The images are corresponding to spheroids showing the best response to combination therapy among other assessed treatments. They represent spheroids treated with either 0.1 μ M gedatolisib alone, 0.01 μ M doxorubicin alone, or their combinations, and the images illustrate spheroids morphology and relative growth patterns over time.

3.8 Evaluation of the mechanistic effect of single and combination treatment in MDA-MB-231 cell line

The earlier experiments demonstrated the cytotoxicity of gedatolisib, doxorubicin and radiation in the MDA-MB-231 cell line when given alone and in combination. However, the underlying mechanisms for these effects remain to be elucidated. Outlining the mechanisms for the effect of alone and combination treatment is essential to validate the therapeutic potential of these combinations and to comprehend the biological basis for their demonstrated synergy. Several mechanistic tests were performed to investigate the effects of these combinations on essential cellular bioprocesses. Cell cycle analysis, DNA damage response, and apoptosis were the specific tests performed to provide the molecular insights underlying enhanced cell death following combination treatment.

3.8.1 Assessment of MDA-MB-231 cell cycle progression following exposure to single and combination treatments

The cell cycle consists of two phases: interphase and mitosis. Most of the period during which the cell prepares for division belongs to interphase, encompassing three phases: G1 (cellular preparation for division), S (DNA replication), and G2 (organisation of genetic material before cell division). After that, the cells proceed to the mitosis (M) phase, during which they undergo full division into two daughter cells. Numerous apoptotic detection tests utilise subG1 (sG1) to assess the amount of fragmented DNA.

Anticancer agents may impair cell growth by alleviation of cell cycle phases. This experiment investigated the cell cycle phase distribution of MDA-MB-231 cells after

treatment alone and in combination. The cells were harvested at different time points following exposure to treatment to demonstrate the cell population at each phase as described in section 2.11.

3.8.1.1 Assessment of MDA-MB-231 cell cycle progression following alone treatment with gedatolisib, doxorubicin and radiation

To evaluate the mechanisms by which these single agents induced their cytotoxicity, cell cycle analysis was performed. This assay was undertaken on the MDA-MB-231 cells treated with low concentrations (IC_{10} and IC_{25}) of gedatolisib and doxorubicin, which were subsequently utilised in combination treatment, as well as their respective IC_{50} values. Additionally, two radiation doses (1 Gy and 2 Gy) that were also involved in combination experiments were assessed in parallel. Following treatment, the cells were harvested at 0 hr, 1 hr, 4 hr, 24 hr and 48 hr and proceeded to the analysis in the flow cytometry machine as described in section 2.1. The distributions of cell population in G1, S, G2/M phases in response to different gedatolisib, doxorubicin concentrations and radiation doses are shown in Figures 3.16, 3.17 and 3.18, respectively.

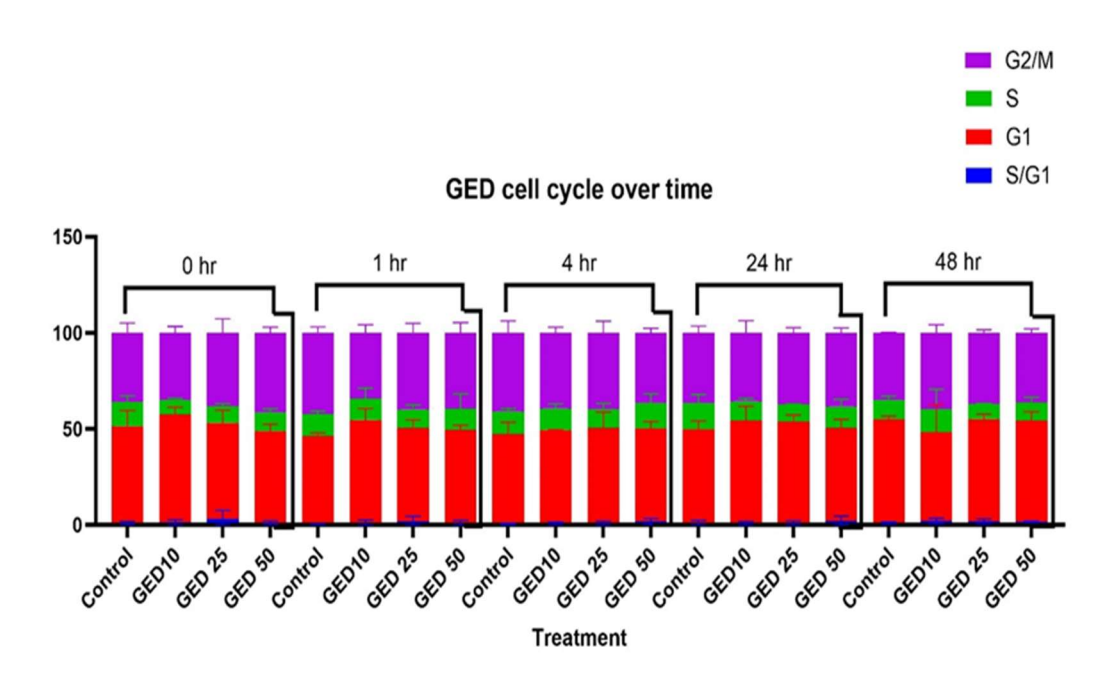


Figure 3-16 Cell cycle phases distribution over time following exposure to gedatolisib.

MDA-MB-231 Cell cycle phases distribution over time following exposure to different concentrations of gedatolisib (IC₁₀, IC₂₅ and IC₅₀). Data represents the mean ± SD of the cell proportion in each phase of the treated cells that are normalized to control for 3 independent experiments performed in triplicate. Statistical analysis was undertaken using one-way ANOVA with Tukey's multiple comparisons test, which was performed using GraphPad Prism 10.3.1.

The data in Figure 3.16 showed no statistically significant changes in cell cycle distribution at any time point following treatment with gedatolisib at IC10, IC25, or IC50 compared to untreated controls (P>0.05). These results indicate that gedatolisib did not induce significant alterations in the cell cycle profile of MDA-MB-231 cells under the experimental conditions employed.

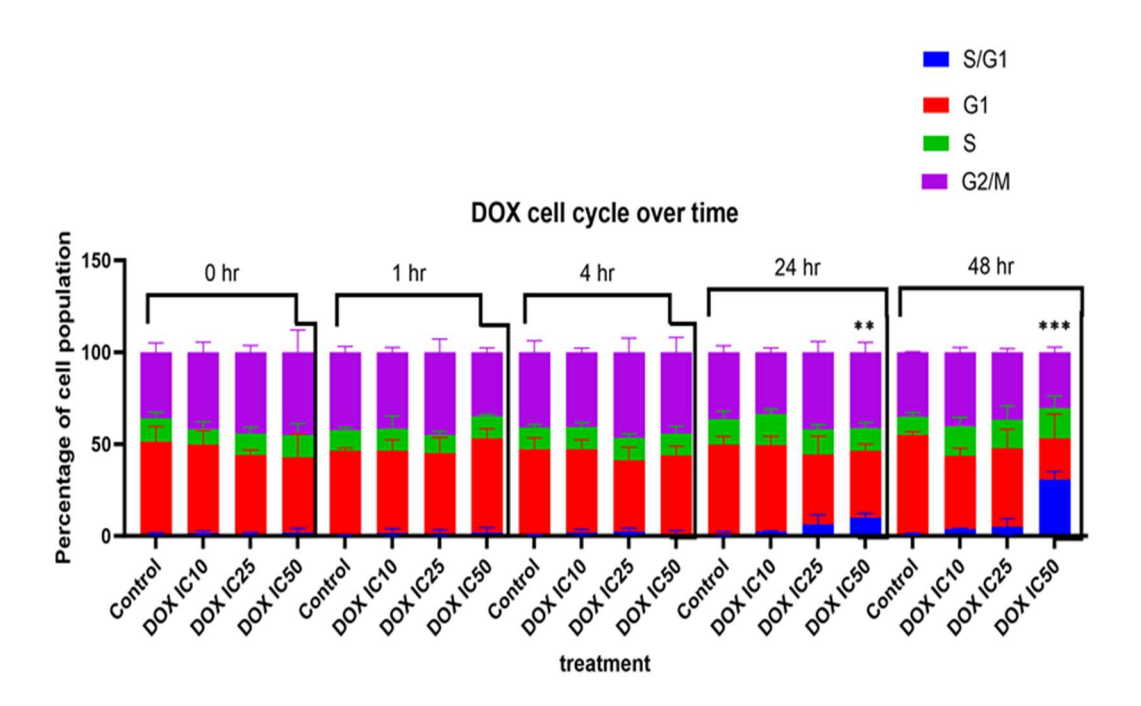


Figure 3-17 Cell cycle phases distribution over time following exposure to doxorubicin.

MDA-MB-231 Cell cycle phases distribution over time following exposure to different doxorubicin concentrations (IC₁₀, IC₂₅ and IC₅₀). Data represents the mean \pm SD of the cell proportion in each phase of the treated cells that are normalized to control for 3 independent experiments performed in triplicate. Statistical analysis was undertaken using one-way ANOVA with Tukey's multiple comparisons test, which was performed using GraphPad Prism 10.3.1. The difference considered significant when P value < 0.05 where *P < 0.05, **P < 0.01, ***P < 0.001 and ****P < 0.0001.

The data in Figure 3.17 demonstrated that treatment with doxorubicin at IC₅₀ resulted in a significant increase in the proportion of cells in the Sub/G1 population at 24 hr and 48 hr post-treatment compared with untreated controls (P < 0.05). At lower concentrations (IC₁₀ and IC₂₅), and for other phases of the cell cycle, no statistically significant changes were observed (P > 0.05).

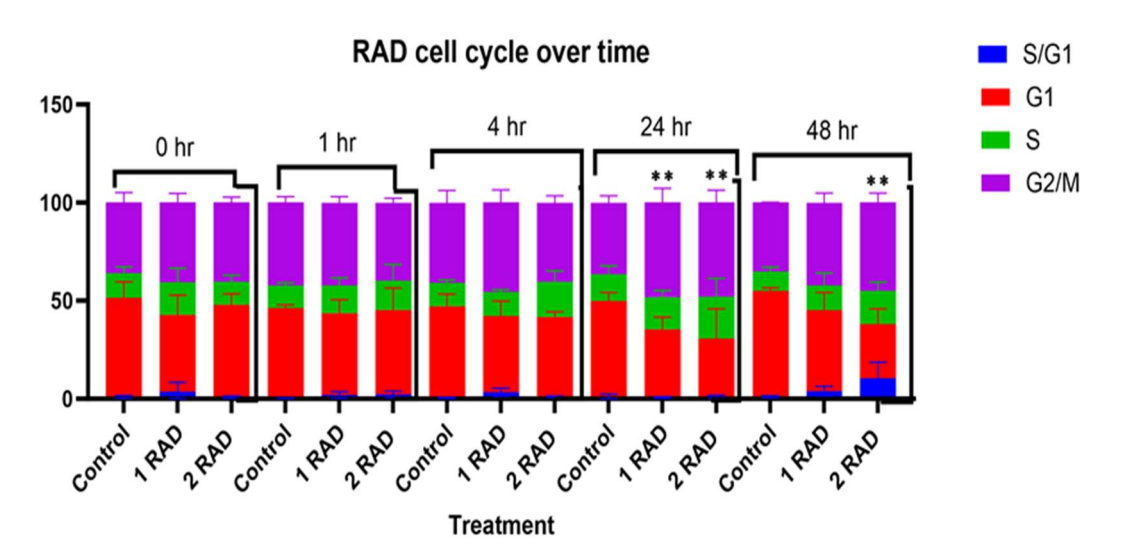


Figure 3-18 Cell cycle phases distribution over time following exposure to radiation.

MDA-MB-231 Cell cycle phases distribution over time following exposure to different doses of radiation. Data represents the mean \pm SD of the cell proportion in each phase of the treated cells that are normalized to control for 3 independent experiments performed in triplicate. Statistical analysis was undertaken using one-way ANOVA with Tukey's multiple comparisons test, which was performed using GraphPad Prism 10.3.1. The difference considered significant when P value < 0.05 where *P < 0.05, **P < 0.01, ***P < 0.001 and ****P < 0.0001.

Frome the data shown in Figure 3.18, a significant accumulation of cells in the G2/M phase was observed 24 hr following exposure to both radiation doses when compared with the untreated control (P < 0.05). Furthermore, treatment with 2 Gy radiation resulted in a significant increase in the Sub/G1 population at 48 h post-irradiation (P < 0.05). At earlier time points (1 h and 4 h), the differences in cell cycle profile were not statistically significant relative to the untreated control (P > 0.05). Together, these findings indicate that radiation induced a G2/M cell cycle arrest, with evidence of a dose-dependent effect.

3.8.1.2 Assessment of MDA-MB-231 cell cycle progression following treatment with a simultaneous combination of gedatolisib with radiation and doxorubicin

The combinations of gedatolisib with either radiation or doxorubicin showed significant cytotoxicity, as evaluated by clonogenic assay and spheroids. Their synergy was reflected by the combination index analysis. These combinations involved low concentrations of gedatolisib and doxorubicin, and low radiation doses. To evaluate the mechanisms by which the investigated combinations induced their effects, cell cycle analysis was performed.

Following assessment of the effect of single agents on the proportion of cells in the various stages of the cell cycle, the effect of combinations on cell cycle distribution of MDA-MB-231 cells was next following treatment with a combination of gedatolisib with either doxorubicin or radiation. Based on the data of single agents, there were no significant changes at 1 hr and 4 hr following exposure to therapy. Therefore, three time points after treatment with combinations (4 hr, 24 hr and 48 hr) were selected to assess cell cycle distribution.

Simultaneous combining two gedatolisib concentrations (0.05 μ M and 0.1 μ M) with either two radiation doses (1 Gy and 2 Gy) or two doxorubicin concentrations (0.005 μ M and 0.01 μ M) was evaluated utilising the cell cycle assay. The distributions of cell populations at 4 hr,24 hr, and 48 hr following exposure of MDA-MB-231 cells to these combinations were assessed, and the results are shown in Figures 3.19 and 3.20.

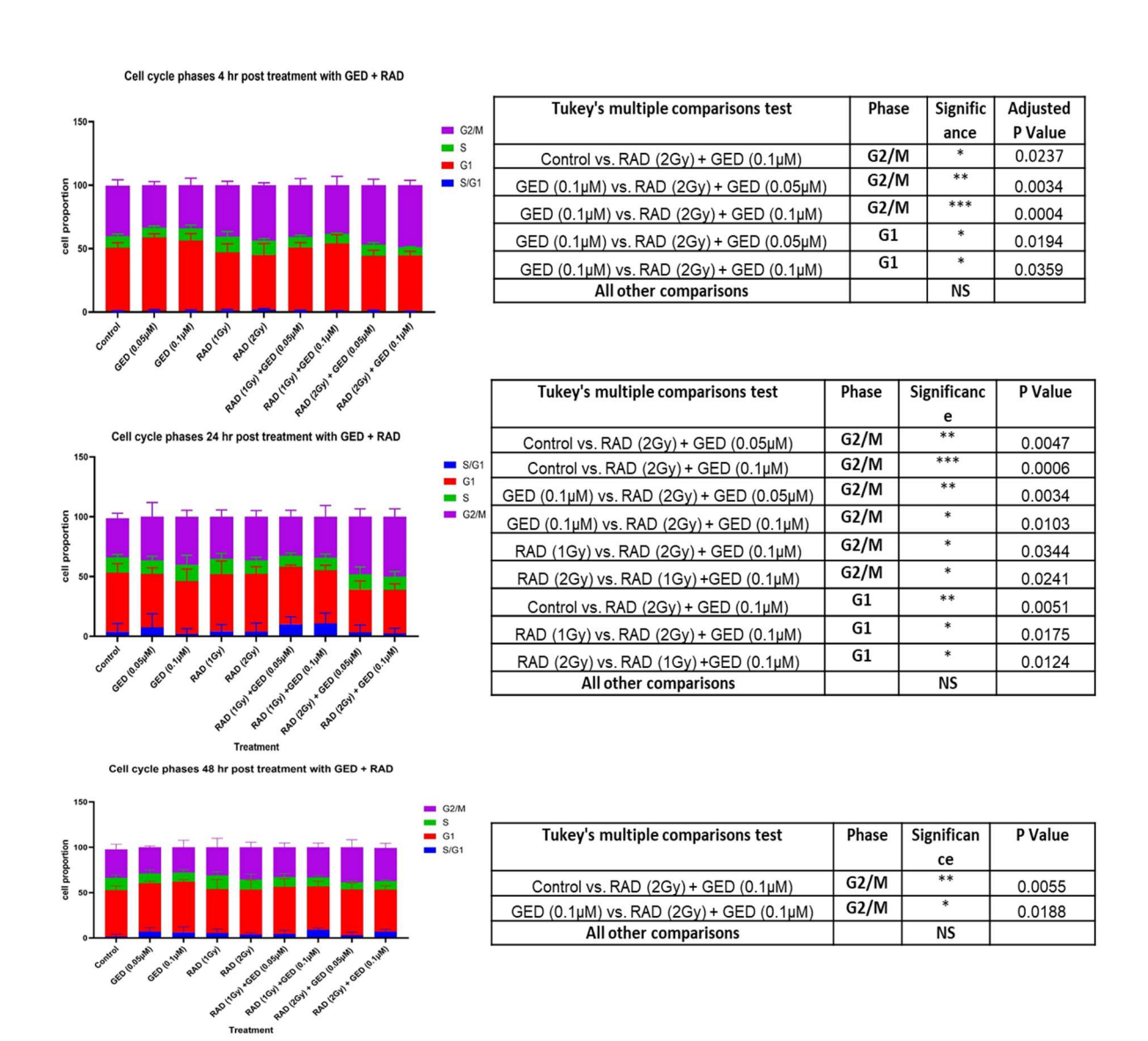


Figure 3-19 Cell cycle phases distribution following exposure to simultaneous combination of gedatolisib and radiation.

MDA-MB-231 Cell cycle phase distribution over time following exposure to different concentrations (0.05 μ M and 0.1 μ M) of gedatolisib and different radiation doses (1 Gy and 2 Gy) alone and in combinations. Data represents the mean \pm SD of the cell population in each phase of the cell cycle of the treated cells that were normalised to control from 3 independent experiments with each experiment performed in triplicate. Statistical analysis was done using one-way ANOVA with Tukey's multiple comparisons test and it was performed using GraphPad Prism 10.3.1. The difference considered significant when P value < 0.05 where *P < 0.05, **P < 0.01, ***P < 0.001 and *****P < 0.0001.

From Figure 3.19, we observed that treatment of cells with gedatolisib and radiation alone induced no significant change in cell cycle distribution compared to the untreated control (P>0.05) at the 4-hr time point. In contrast, the combination of 0.1 µM gedatolisib with 2 Gy radiation dose resulted in a significant increase in the G2/M phase compared to the untreated controls (P< 0.05) (Figure 3.19). Furthermore, this combination induced a reduction in the percentage of cells at G1 phase in comparison to gedatolisib alone therapy (P<0.05), but not to the radiation alone (P>0.05). At 24 hr following treatment, a combination of 0.1 µM gedatolisib with 2 Gy radiation induced a statistically significant cell cycle arrest at G2/M phase compared to the untreated control (P<0.001), gedatolisib alone (P<0.05) and radiation alone (P<0.05). Additionally, G2/M arrest wea demonstrated at 48 hr after treatment with this combination compared to the untreated control (P<0.01), gedatolisib alone (P<0.05), but not with the radiation alone (P>0.05).

These data suggested that combining gedatolisib with radiation resulted in an augmented effect of radiation on the cell cycle distribution of MDA-MB-231 cells.

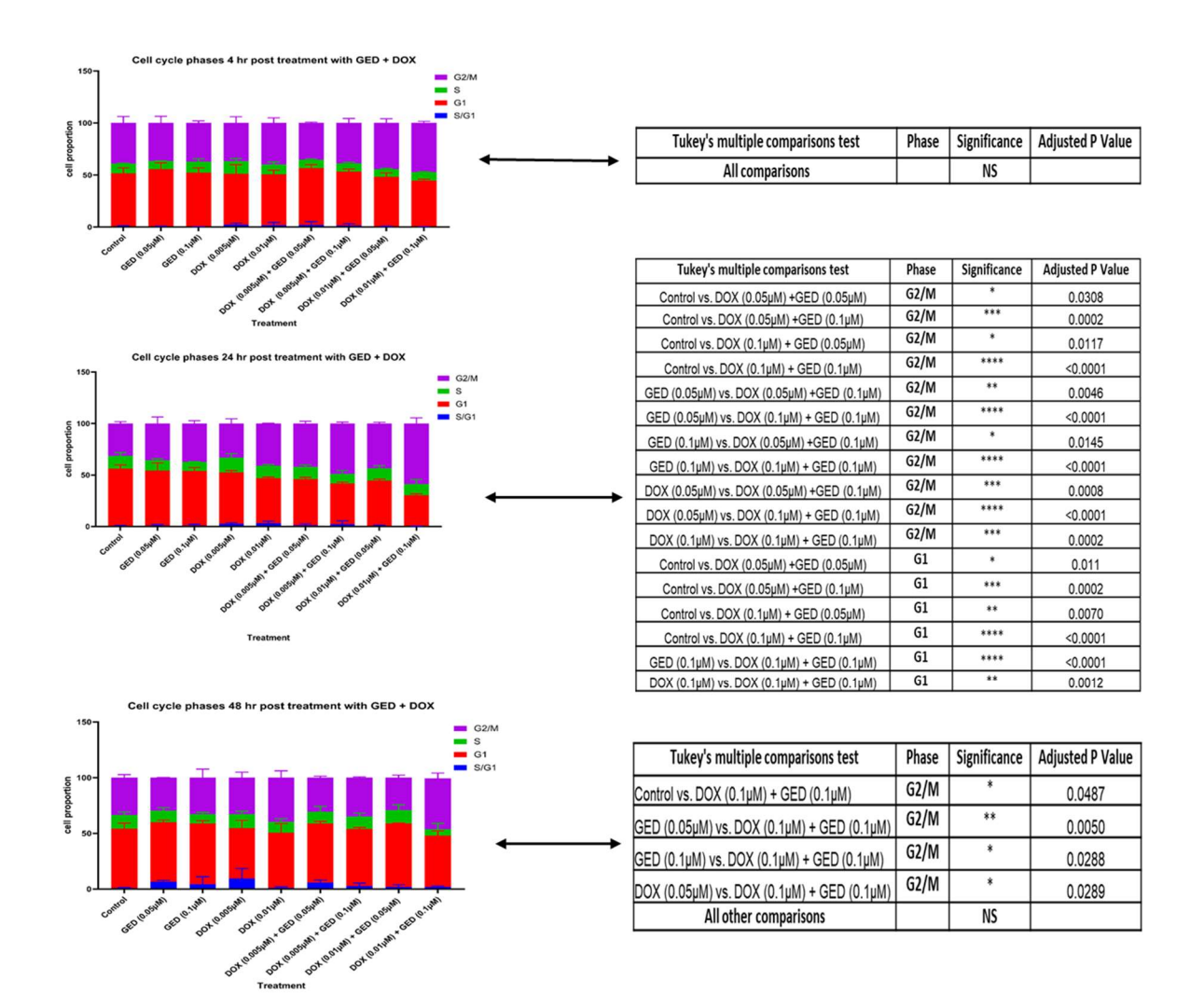


Figure 3-20 Cell cycle phases distribution following exposure to a simultaneous combination of gedatolisib and doxorubicin.

MDA-MB-231 Cell cycle phases distribution over time following exposure to different concentrations (0.05 μ M and 0.1 μ M) of gedatolisib and with 0.005 μ M and 0.01 μ M of doxorubicin alone and in simultaneous combinations. Data represents the mean \pm SD of the cell population in each phase of the cell cycle of the treated cells that were normalised to control from 3 independent experiments with each experiment performed in triplicate. Statistical analysis was done using one-way ANOVA with Tukey's multiple comparisons test and it was performed using GraphPad Prism 10.3.1. The difference considered significant when P value < 0.05 where *P < 0.05, **P < 0.01, ***P < 0.001 and *****P < 0.0001.

The data in Figure 3.20 displayed no significant changes in the distribution of MDA-MB-231 cells across cell cycle phases in early response (4 hr) following treatment with alone and a combination of gedatolisib and doxorubicin compared to the untreated (P>0.05). At 24 hr following treatment, a combination of 0.1 µM gedatolisib and 0.1 µM doxorubicin induced a statistically significant G2/M arrest compared to the untreated control (P<0.0001), gedatolisib alone (P<0.0001) and doxorubicin alone (P< 0.001). Additionally, this combination maintains the statistically significant G2/M arrest at 48 hr after treatment compared to the untreated control (P<0.05), single gedatolisib (P<0.05), but not with the doxorubicin alone (P>0.05), as shown in Figure 3.20. These results indicate that the G2/M cell cycle arrest induced by doxorubicin was enhanced when gedatolisib was concomitantly added with doxorubicin.

3.8.2 Assessment of apoptosis in MDA-MB-231 cells induced by single and combination treatment using Annexin V assay.

To further understand the mechanisms underlying the cytotoxic effects demonstrated with single and combination treatments, apoptosis induction was investigated using Annexin V staining and subsequent analysis by flow cytometry. This assay determines the cellular apoptotic events (early and late) by targeting externally localised phosphatidylserine, a key marker of apoptotic cell death. This assay was performed on MDA-MB-231 cells treated with the same concentrations and combinations of gedatolisib, doxorubicin, and radiation utilised earlier in clonogenic, spheroids, and cell cycle assays, including low concentrations (IC₁₀ and IC₂₅) of the drugs and tow radiation doses (1 Gy, and 2 Gy). Following treatment, the cells were harvested at 4 hr, 24 hr and 48 hr, and apoptotic cell populations were quantified as described in section 2.12.

3.8.2.1 Assessment of apoptosis in MDA-MB-231 cells induced by single gedatolisib, doxorubicin and radiation

To evaluate the apoptotic events in MDA-MB-231 cells induced by alone treatment with gedatolisib, doxorubicin and radiation, annexin V assay was performed. This assay was undertaken on the cells treated with low concentrations (IC₁₀ and IC₂₅) of gedatolisib and doxorubicin that were subsequently utilised in combination treatment, as well as their respective IC₅₀ values. Additionally, two radiation doses (1 Gy and 2 Gy) that were also utilised in combination experiments were investigated in parallel. Following treatment, the cells were harvested at different time points (4 hr, 24 hr and 48 hr) to assess the early and late cell response these single agents. The percentages of healthy, apoptotic, and necrotic cells following exposure to each of gedatolisib, doxorubicin and radiation are shown in Figures 3.21A-C.

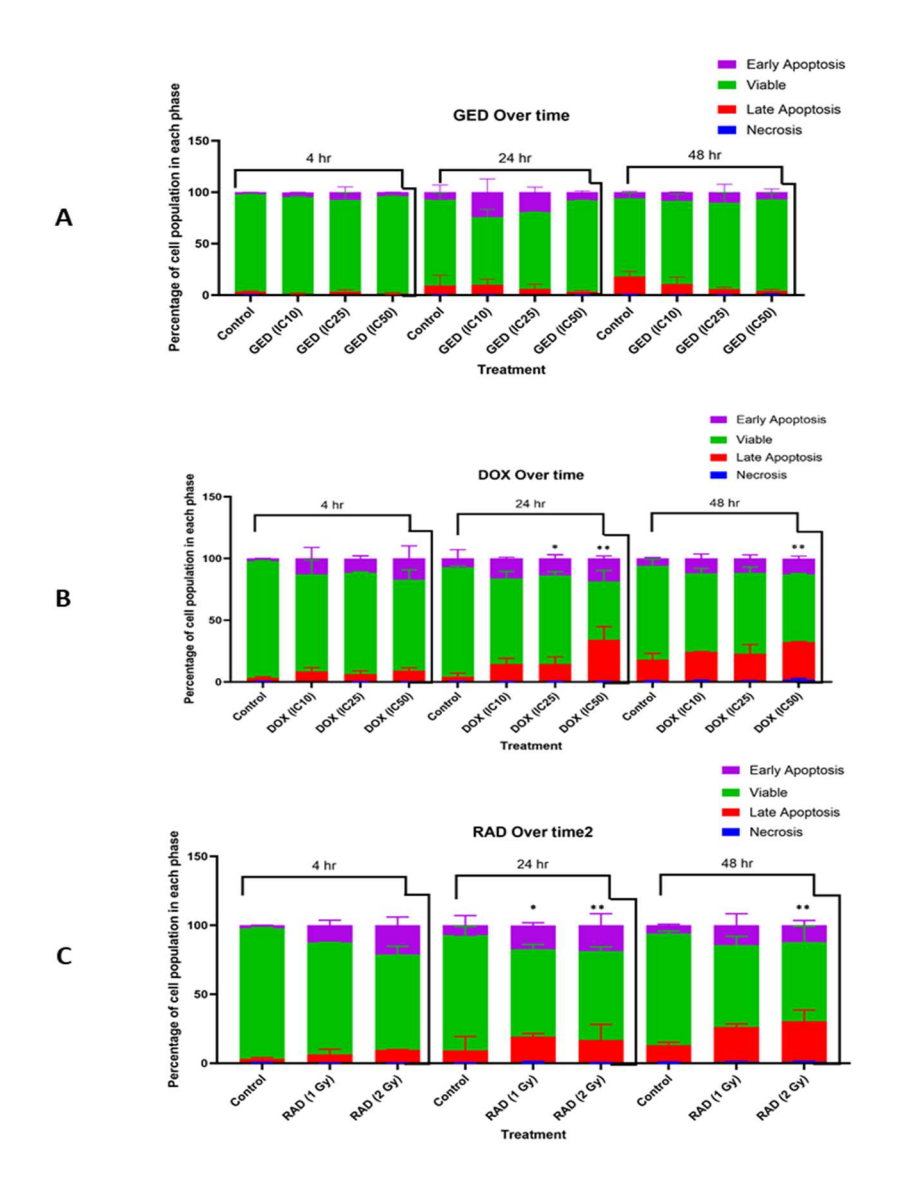


Figure 3-21 Apoptosis of MDA-MB-231 cells following treatment with single gedatolisib, doxorubicin and radiation assessed by the Annexin V assay

The distribution of viable, early apoptotic, late apoptotic, and necrotic cell populations over time after exposure to gedatolisib, doxorubicin, or radiation. Cells were harvested at 4-, 24-, and 48-hours post-treatment and stained with Annexin V and propidium iodide. Data represents the mean \pm SD for 3 independent experiments with each performed in triplicate. Statistical analysis was employed using one-way ANOVA followed by Tukey's multiple comparisons test using GraphPad Prism 10.3.1. (A) Gedatolisib (IC₁₀, IC₂₅ and IC₅₀), (B) Doxorubicin (IC₁₀, IC₂₅ and IC₅₀) and (C) Radiation (1Gy and 2 Gy) were administered alone. The difference considered statistically significant when P value < 0.05 where *P < 0.05, **P < 0.01, ***P < .001 and ****P < 0.0001.

As shown in Figure 3.21A, gedatolisib did not induce a statistically significant apoptosis in MDA-MB-231 cells at 4hr, 24hr and 48 hr following treatment with IC_{10} , IC_{25} and IC_{50} compared to the untreated control (P>0.05). This suggests that the cytotoxicity of this drug in the MDA-MB-231 cell line does not rely on inducing apoptosis and further mechanistic investigation is required.

In contrast, Figure 3.21B showed a statistically significant apoptosis at 24 hr after treatment of the MDA-MB-231 cells with the IC_{25} and IC_{50} of doxorubicin relative to the untreated control (P<0.05), and at 48 hr post-treatment with IC_{50} of doxorubicin relative to the untreated controls (P<0.01).

Radiation exposure also promoted apoptosis in the MDA-MB-231 cell line. At 2 Gy radiation dose, a statistically significant increase in apoptotic MDA-MB-231 cells at 24 hr and 48 hr following exposure was demonstrated compared to the untreated controls (P< 0.001) as shown in Figure 3.21C. Furthermore, at 24 hr following exposure of the cells to 1 Gy radiation dose, a statistically significant apoptosis was observed compared to the untreated control (P<0.05).

The data of the annexin V assay suggest that single doxorubicin and radiation can induce apoptosis in MDA-MB-231, and this effect might be dose and time dependent.

3.8.2.2 Assessment of apoptosis in MDA-MB-231 cells induced by simultaneous combination of gedatolisib with radiation or doxorubicin utilising Annexin V assay

Following assessment of the effect of single agents to induce apoptosis in the MDA-MB-231 cells, annexin V was used to evaluate the effect of combinations to induce apoptotic MDA-MB-231 cells. The gedatolisib concentrations (0.05 μ M and 0.1 μ M) that simultaneously combined with either radiation doses (1 Gy and 2 Gy) or doxorubicin concentrations (0.005 μ M and 0.01 μ M) were evaluated using annexin V

assay. The selected doses were involved in combinations that were tested in clonogenic assay and spheroids and showed a promising cytotoxicity. Following treatment, the cells were harvested at different time points (4 hr, 24 hr and 48 hr), and the proportions of healthy, apoptotic, and necrotic cells following exposure to each combination are shown in Figures 3.22 and 3.23.

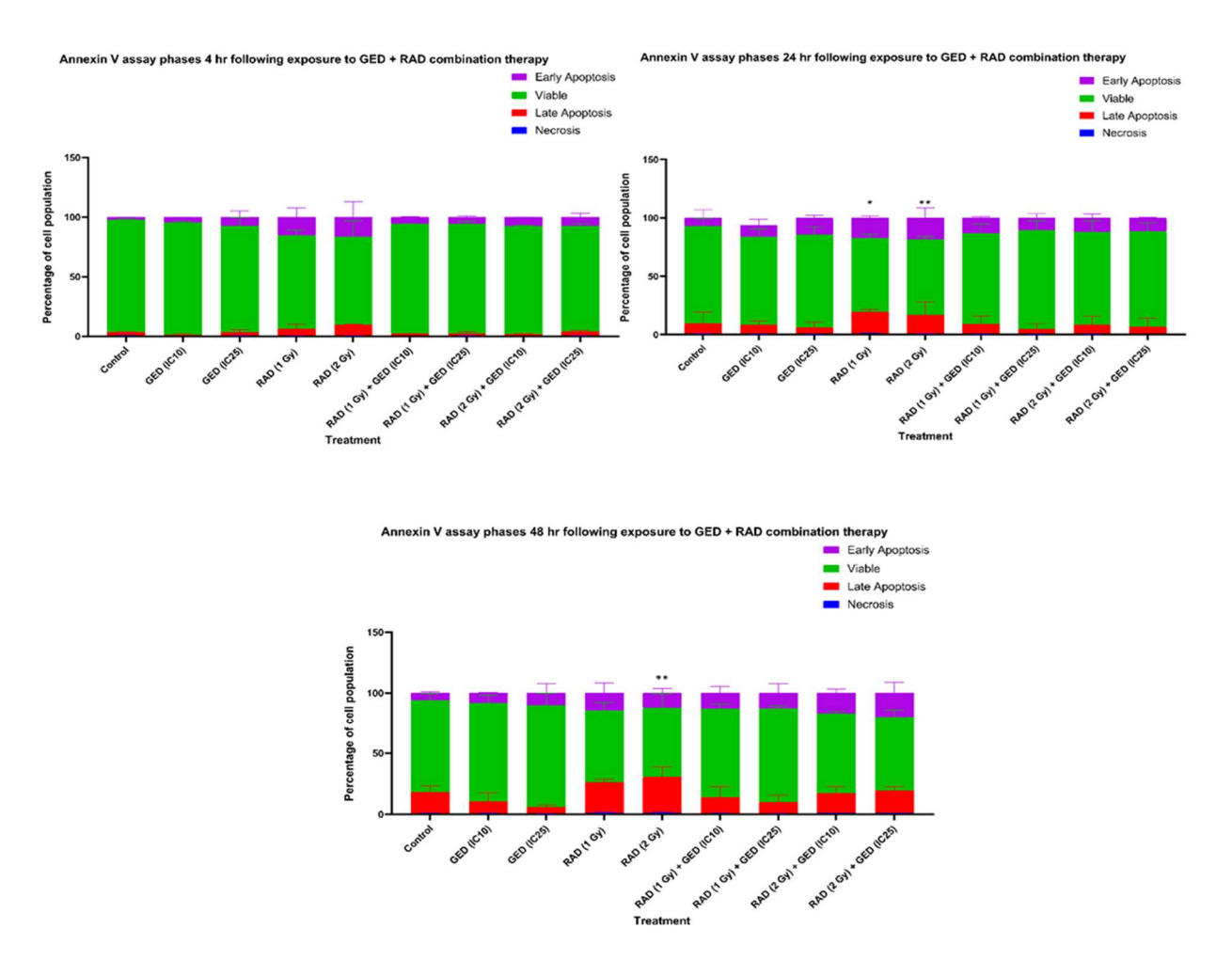


Figure 3-22 Apoptosis of MDA-MB-231 cells following treatment with simultaneous combination of gedatolisib and radiation assessed by the Annexin V assay

The distribution of viable, early apoptotic, late apoptotic, and necrotic cell populations over time following treatment with combination of gedatolisib with doxorubicin or radiation. The MDA-MB-231 cells were harvested at 4hr, 24 hr, 48 hr after treatment with low gedatolisib concentrations (05 μ M and 0.1 μ M) and low radiation doses (1Gy and 2 Gy) as mono and combination treatments. The cells were stained with Annexin V and propidium iodide to identify viable, early apoptotic, late apoptotic, and necrotic cells. Data represents the mean \pm SD for 3 independent experiments with each one performed in triplicate. Statistical analysis was employed using one-way ANOVA followed by Tukey's multiple comparisons test using GraphPad Prism 10.3.1. The difference considered statistically significant when P value < 0.05 where *P < 0.05, **P < 0.01, ***P < .001 and *****P < 0.0001.

The data in Figure 3.22 demonstrated that treatment with radiation alone with 1 Gy and 2 Gy doses resulted in statistically significant increase in the apoptotic cells at 24 hr post treatment compared to the untreated control (P<0.05). However, no one of the combination therapies showed significant apoptosis in comparison to the untreated controls and single therapy as well (P>0.05).



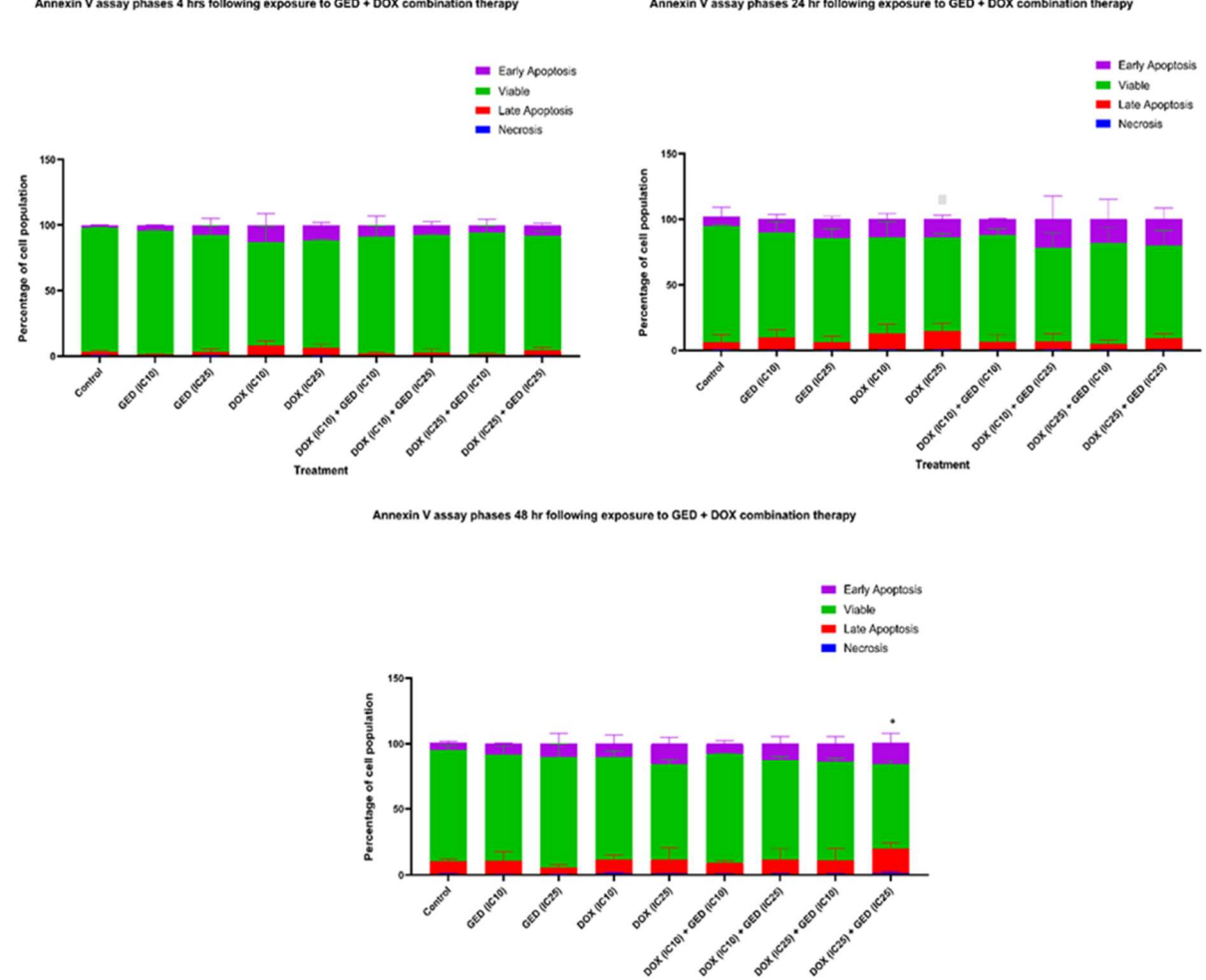


Figure 3-23 Apoptosis of MDA-MB-231 cells following treatment with simultaneous combination of gedatolisib and doxorubicin assessed by the Annexin V assay

MDA-MB-231 cells were tested by Annexin V assay following treatment with alone and a combination of low gedatolisib concentrations (05 µM and 0.1 µM) low doxorubicin concentrations (0.005 µM and 0.01 µM). The cells were harvested at 4hr, 24 hr, 48hr after treatment and stained with Annexin V and propidium iodide to identify viable, early apoptotic, late apoptotic, and necrotic cells. Data represents the mean ± SD for 3 independent experiments performed in triplicate. Statistical analysis was employed using one-way ANOVA followed by Tukey's multiple comparisons test using GraphPad Prism 10.3.1. The difference considered statistically significant when P value < 0.05 where *P < 0.05, **P < 0.01, ***P < .001 and ****P < 0.0001.

From Figure 3.23, treatment of MDA-MB-231 cells with alone 0.01 μ M doxorubicin induced a statistically significant apoptosis relative to the untreated control at 24 hr following incubation with the drug (P<0.05). However, no combination has shown statistically significant changes in apoptosis compared to the untreated control or each alone agent at any time point (P>0.05).

Taken together, these data indicate that combining of gedatolisib with radiation or doxorubicin did not show superior apoptosis than alone radiation, suggesting alternative mode of cell death.

3.8.3 Assessment of DNA damage induction in the MDA-MB-231 cell line utilising COMET assay

To further elucidate the mechanisms underpinning the cytotoxicity observed in earlier clonogenic and spheroid experiments, we subsequently evaluated the extent of DNA damage induced by alone and combination treatments utilising the COMET assay. This assay provides an important molecular insight by assessing both the induction and repair of DNA damage, identifying whether the observed cell death is associated with impaired DNA repair capacity. In this experiment, DNA damage was assessed after treatment of MDA-MB-231 cells with low concentrations of gedatolisib (IC₁₀ and IC₂₅) and doxorubicin (IC₁₀ and IC₂₅), alongside radiation doses (1 and 2 Gy) that were utilised earlier in our combination treatment experiments and revealed increased cytotoxic effects in MDA-MB-231 cells. Following treatment, the cells were harvested at different time points and processed using the COMET assay kit to investigate the DNA damage that was characterised by the presence of a tail-like shape (tail moment) in the cells. Quantification of the tail moments over time was conducted using ImageJ software to determine the DNA damage induced by treatments, as well as evaluation of the repair capacity.

3.8.3.1 Assessment of DNA damage in MDA-MB-231 cell line treated with via COMET assay following exposure to single agents of gedatolisib, doxorubicin or radiation.

To investigate the kinetics of DNA damage and repair following treatment, a COMET assay was conducted. MDA-MB-231 cells were incubated with different inhibitory concentrations of gedatolisib and doxorubicin (IC₁₀, IC₂₅, and IC₅₀) and two radiation doses (1 Gy and 2 Gy). The COMET assay was performed in cells harvested at 1 hr, 4 hr, 24 hr, and 48 hr following exposure to each treatment. The number of tail moments, reflecting the DNA damage induced by single agents, are shown in Figure 3.24A-C.

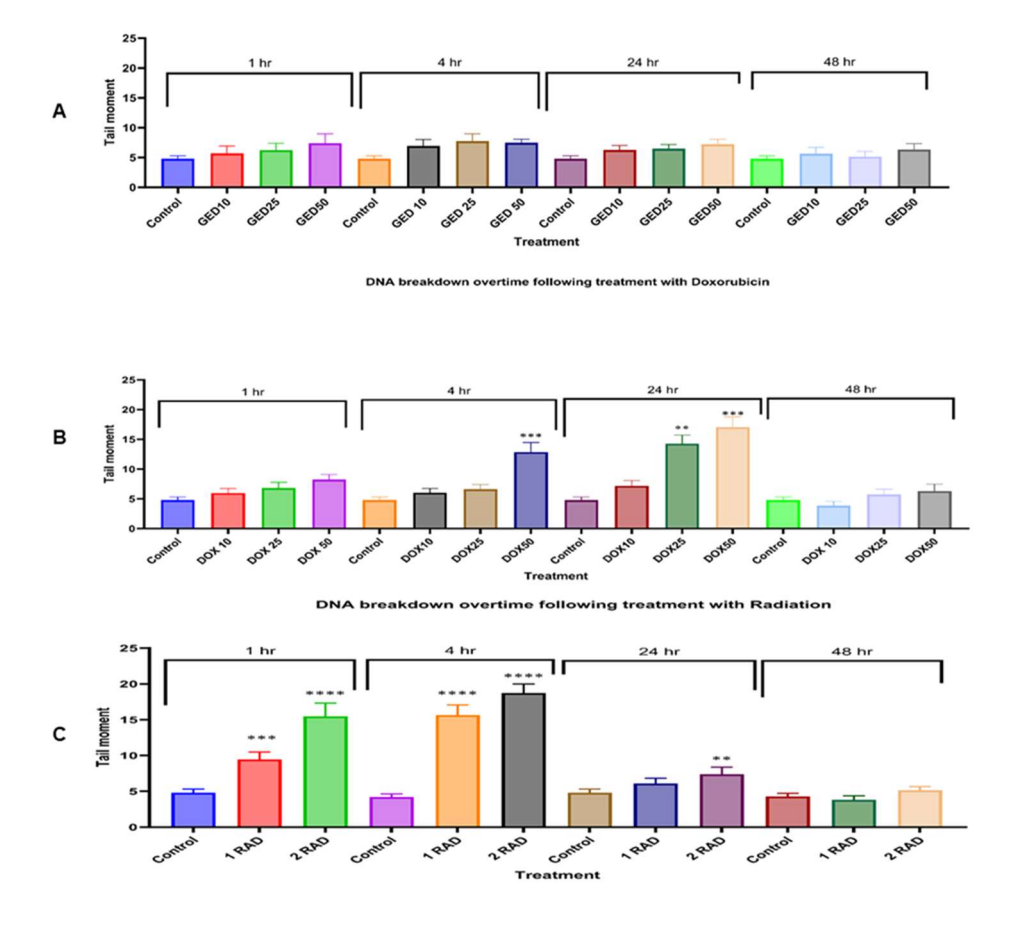


Figure 3-24 DNA damage in MDA-MB-231 cells following exposure to single agents of gedatolisib, doxorubicin or radiation assessed by COMET assay

DNA damage in MDA-MB-231 Cells over time following treatment with (A) gedatolisib concentrations (IC₁₀, IC₂₅ and IC₅₀), (B) doxorubicin concentrations (IC₁₀, IC₂₅ and IC₅₀) and (C) radiation doses (1 Gy and 2 Gy). Comet assay images were analysed using OpenComet software (1.3.1), and DNA damage was quantified as tail moments. Data represents the mean \pm SD, with 100 comets per treatment group from 3 independent experiments performed in triplicate. Statistical analysis was performed using GraphPad Prism 10.3.1 with one-way ANOVA followed by Tukey's multiple comparisons test. The difference considered significant when P value < 0.05 where *P < 0.05, **P < 0.01, ***P < 0.001 and ****P < 0.0001.

The findings revealed that gedatolisib as a single treatment did not induce significant DNA damage at any time following treatment compared to the untreated controls (P>0.05), as shown in Figure 3.24A. This may suggest the possibility of other alternative mechanisms for drug cytotoxicity.

Figure 3.24B demonstrated a statistically significant DNA damage in MDA-MB-231 cells at 24 hr following treatment with the IC_{25} of doxorubicin alone compared to the untreated control (P<0.05). Additionally, the IC_{50} of doxorubicin induced a statistically significant increase in DNA double-strand breakdown at 4 hr and 24 hr following administration relative to the untreated controls (P<0.001). The lack of significant differences in tail moments relative to the control at later time points suggests that the initial induced damage is being repaired at 48 hr following exposure to doxorubicin, as no significant changes in tail moments have been demonstrated (P>0.05) (Figure 3.24 B)

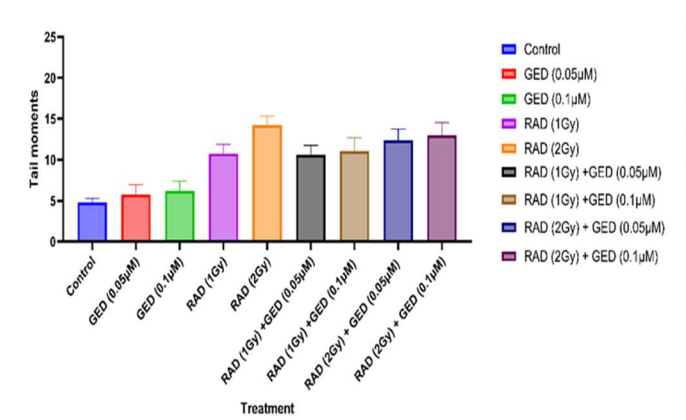
The data in Figure 3.24C displayed that both radiation doses resulted in significant DNA damage at early time points (1 hr and 4 hr) following exposure to radiation in comparison to the untreated control (P<0.0001). However, time dependent DNA repair has been demonstrated at later time points post treatment and no significant changes in tail moment induced by any radiation dose at 48 hr following treatment relative to the untreated control (P>0.05).

Taken together, individual gedatolisib administration in MDA-MB-231 cells did not cause direct DNA damage and may produce cytotoxicity through alternative mechanisms. Furthermore, the findings reinforce the capability of doxorubicin and radiation to mediate DNA damage, and this effect was dose dependent with potential repair at late time following treatment.

3.8.3.2 Assessment of DNA damage in MDA-MB-231 cell line via COMET assay following exposure to a simultaneous combination of gedatolisib with doxorubicin or radiation

Following the investigation of DNA damage induced by single-agent treatments utilising the COMET assay, combination treatments were subsequently assessed to find out whether they induce greater or more sustained DNA damage. Particularly, simultaneous combinations of gedatolisib concentrations (0.05 µM and 0.1 µM) with either doxorubicin (0.005 µM and 0.01 µM) or radiation (1 Gy and 2 Gy) were assessed. Given that both doxorubicin and radiation have been reported to induce DNA double-strand breaks, and PI3K/AKT/mTOR inhibition may impair DNA repair mechanisms, we hypothesised that these combinations would increase DNA damage compared to single treatments. MDA-MB-231 cells were treated with different combinations, accordingly, harvested at different times following treatment (1 hr, 4 hr, 24 hr, and 48 hr), and analysed via the COMET assay to quantify the tail moments. The results for combination of gedatolisib with either radiation or doxorubicin are presented in Figures 3.25A-B and 3.26A-B, respectively.

DNA breakdown 1 hr following treatment with Gedatolisib + Radiation



Tukey's multiple comparisons test	Significance	Adjusted P
		Value
Control vs. RAD (1Gy)	***	0.0004
Control vs. RAD (2 Gy)	****	<0.0001

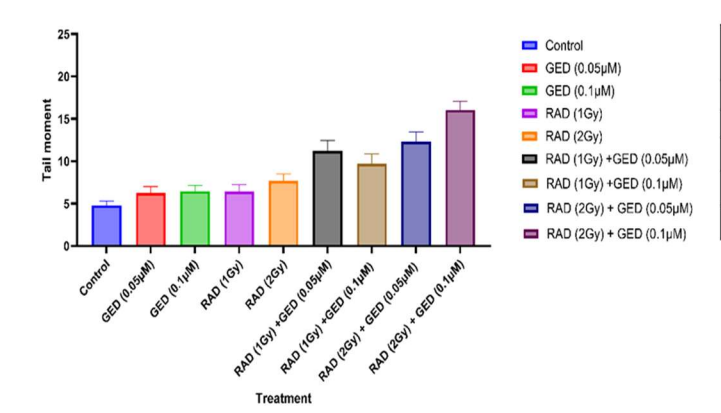
Treatment

Tukey's multiple comparisons test	Significance	Adjusted P
		Value
Control vs. RAD (1Gy)	**	0.0047
Control vs. RAD (2 Gy)	***	0.0006
RAD (1Gy) vs. RAD (2Gy) + GED (0.1μM)	**	0.0034
RAD (2Gy) vs. RAD (2Gy) +GED (0.1µM)	*	0.0241
All other comparisons	NS	

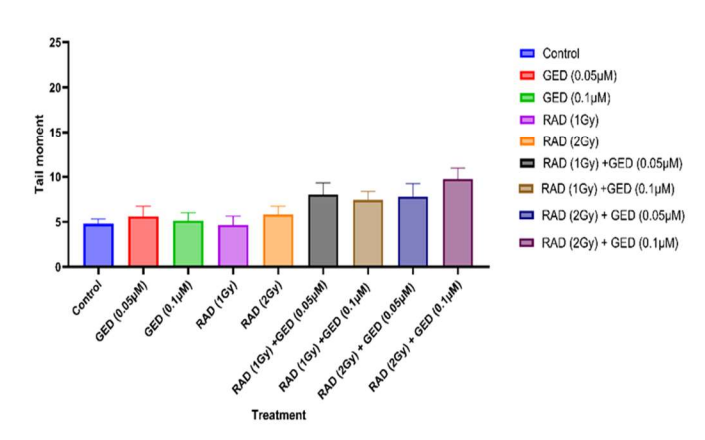
Figure 3-25-A DNA damage in MDA-MB-231 cells following treatment with a simultaneous combination of gedatolisib with radiation assessed by COMET assay

DNA damage in MDA-MB-231 Cells at 1hr and 4 hr following treatment with a combination of gedatolisib (0.05 μ M and 0.1 μ M) with radiation (1 Gy and 2 Gy). Comet assay images were analysed using OpenComet software (1.3.1), and DNA damage was quantified as tail moments. Data represent the mean \pm SD, with 100 comets per treatment group from 3 independent experiments performed in triplicate. Statistical analysis was performed using GraphPad Prism 10.3.1 with one-way ANOVA followed by Tukey's multiple comparisons test. The difference considered significant when P value < 0.05 where *P < 0.05, **P < 0.01, ***P < 0.001 and ****P < 0.0001.

DNA breakdown 24 hr following treatment with Gedatolisib + Radiation



Tukey's multiple comparisons test	Significance	Adjusted P
		Value
Control vs. RAD (2Gy) + GED (0.05µM)	**	0.0047
Control vs. RAD (2Gy) + GED (0.1µM)	***	0.0002
RAD (1Gy) vs. RAD (2Gy) + GED (0.1μM)	**	0.0067
RAD (2Gy) vs. RAD (2Gy) +GED (0.1µM)	**	0.0034



Tukey's multiple comparisons test	Significance	Adjusted P
		Value
Control vs. RAD (2Gy) + GED (0.1µM)	***	0.0006
RAD (1Gy) vs. RAD (2Gy) + GED (0.1µM)	**	0.0012
RAD (2Gy) vs. RAD (2Gy) +GED (0.1µM)	**	0.0070
All other comparisons	NS	

Figure 3-26-B DNA damage in MDA-MB-231 cells following treatment with a simultaneous combination of gedatolisib with radiation assessed by COMET assay

DNA damage in MDA-MB-231 Cells at 24 hr and 48 hr following treatment with a combination of gedatolisib (0.05 μ M and 0.1 μ M) with radiation (1 Gy and 2 Gy). Comet assay images were analysed using OpenComet software (1.3.1), and DNA damage was quantified as tail moments. Data represent the mean \pm SD, with 100 comets per treatment group from 3 independent experiments performed in triplicate. Statistical analysis was performed using GraphPad Prism 10.3.1 with one-way ANOVA followed by Tukey's multiple comparisons test. The difference considered significant when P value < 0.05 where *P < 0.05, **P < 0.01, ***P < 0.001 and ****P < 0.0001.

The data in Figure 3.25-A disclosed that at the 1 hr time point, both radiation doses utilised alone or combined with gedatolisib resulted in a statistically significant DNA damage in comparison to the untreated controls (P<0.01). The combinations of 0.1 μ M gedatolisib with 2 Gy radiation resulted in significant increase in tail moments at all investigated time points in comparison to the untreated control (P<0.001). Furthermore, Figure 3.25-B demonstrated an extended effect for combination treatment in minimising DNA repair where combination of 0.1 μ M gedatolisib with 2 Gy radiation showed a statistically significant increase in tail moments at 24 hr and 48 hr after treatment in comparison to the untreated controls (P<0.01) and each single agent (P<0.05).

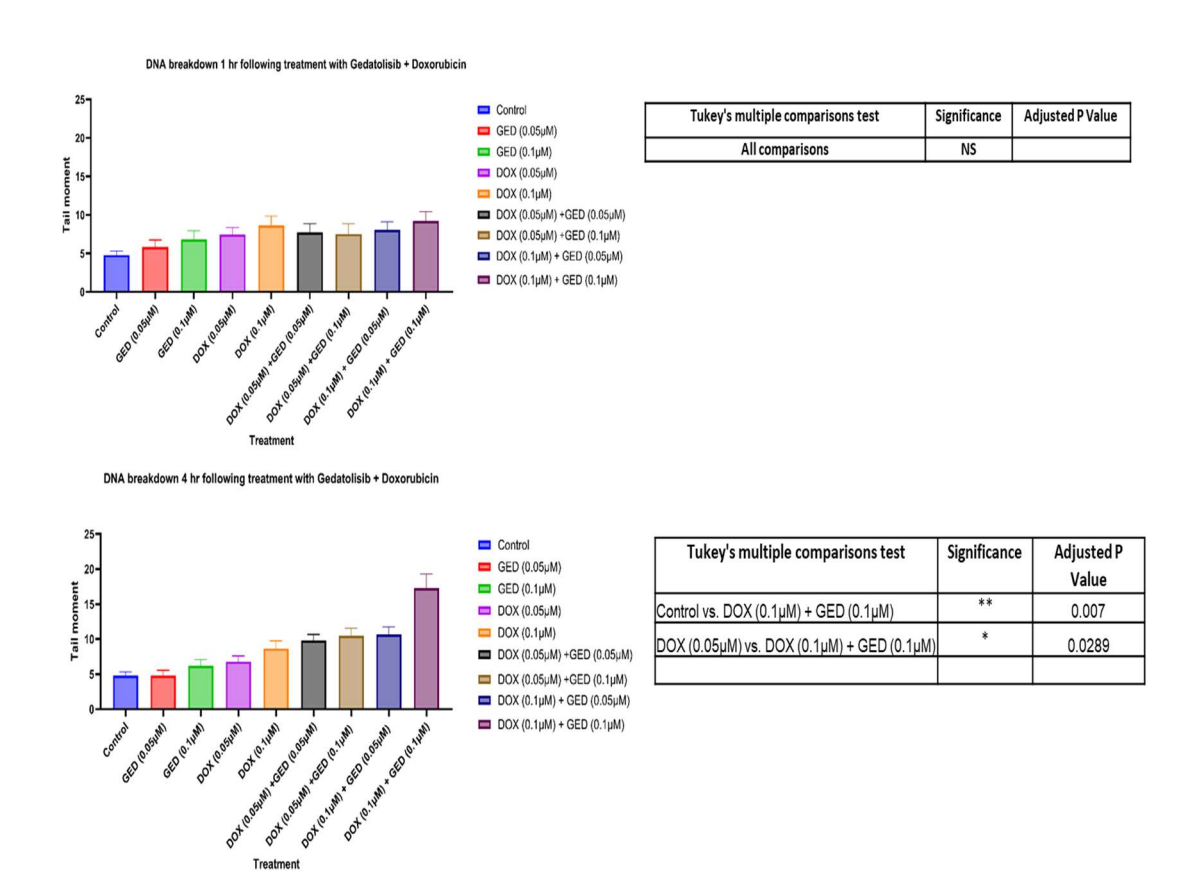


Figure 3-27-A DNA damage in MDA-MB-231 cells following treatment with a simultaneous combination of gedatolisib with doxorubicin assessed by COMET assay

DNA damage in MDA-MB-231 Cells at 1 hr and 4 hr following treatment with a combination of gedatolisib (0.05 μ M and 0.1 μ M) with doxorubicin (0.05 μ M and 0.1 μ M). Comet assay images were analysed using OpenComet software (1.3.1), and DNA damage was quantified as tail moments. Data represent the mean \pm SD, with 100 comets per treatment group from 3 independent experiments performed in triplicate. Statistical analysis was performed using GraphPad Prism 10.3.1 with one-way ANOVA followed by Tukey's multiple comparisons test. The difference considered significant when P value < 0.05 where *P < 0.05, **P < 0.01, ***P < 0.001 and ****P < 0.0001.

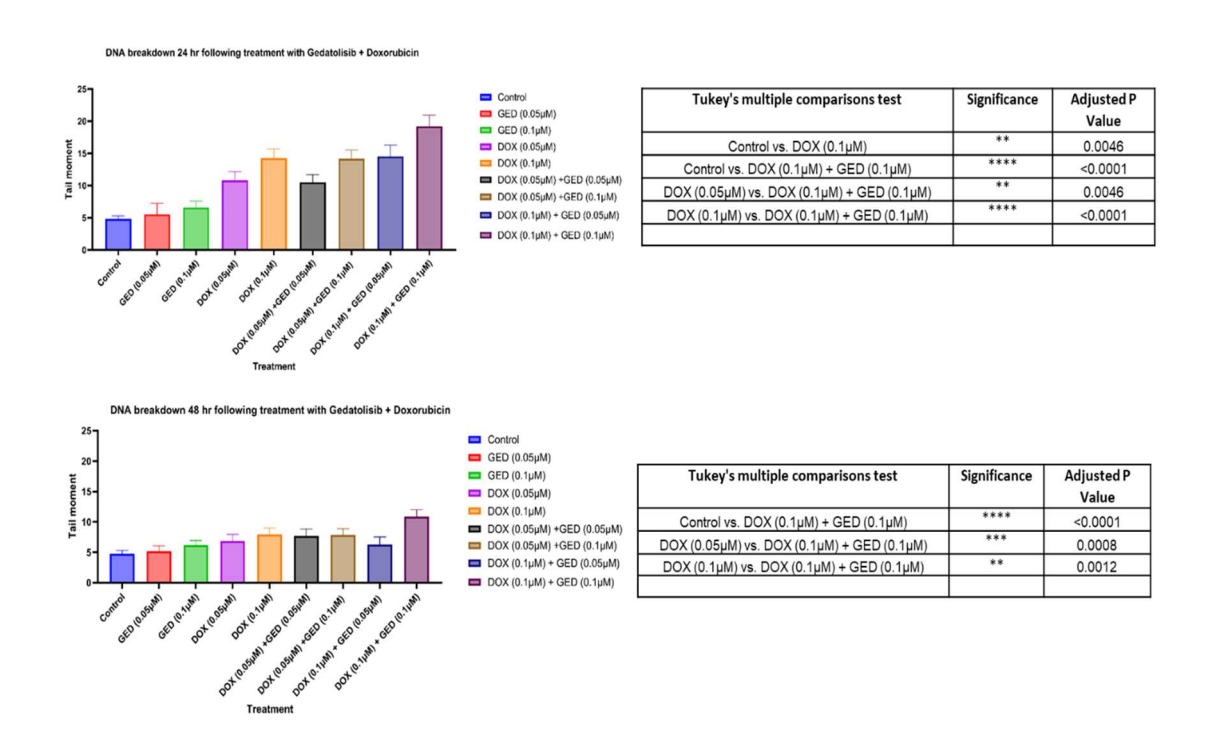


Figure 3-28-B DNA damage in MDA-MB-231 cells following treatment with a simultaneous combination of gedatolisib with doxorubicin assessed by COMET assay

DNA damage in MDA-MB-231 Cells at 24 hr and 48 hr following treatment with a combination of gedatolisib (0.05 μ M and 0.1 μ M) with doxorubicin (0.05 μ M and 0.1 μ M). Comet assay images were analysed using OpenComet software (1.3.1), and DNA damage was quantified as tail moments. Data represent the mean \pm SD, with 100 comets per treatment group from 3 independent experiments performed in triplicate. Statistical analysis was performed using GraphPad Prism 10.3.1 with one-way ANOVA followed by Tukey's multiple comparisons test. The difference considered significant when P value < 0.05 where *P < 0.05, **P < 0.01, ***P < 0.001 and ****P < 0.0001.

From Figure 3.26-A, the current findings revealed that at 4 hr time point, a combination of 0.1 µM gedatolisib and 0.01 µM doxorubicin resulted in a statistically significant increase in tail moments in comparison to the untreated control (P<0.01). Furthermore, this combination has shown a statistically significant increase in DNA damage in MDA-MB-231 cells at 24 hr and 48 hr following exposure to therapy in comparison to the untreated controls (P<0.001), and each alone drug (P<0.05) Figure 3.26-A. The assay results indicated the role of combination treatment in decreasing the DNA repair and extending DNA double-strand breaks.

Collectively, the COMET assay data elucidated the mechanistic insights into the extent and sustain of DNA damage in MDA-MB-231 cells induced by single combination treatments. While individual treatment with doxorubicin or radiation caused quantifiable DNA strand breaks, the demonstrated damage was relatively small, and in some instances, transient. Conversely, combining gedatolisib with either doxorubicin or radiation resulted in a statistically significant increase in tail moments across different time points, indicating improved and sustained DNA damage. These findings reinforce the hypothesis that inhibiting the PI3K/Akt/mTOR pathway can impair DNA repair mechanisms.

The representative images for the COMET assay showing the tail moments of the cells treated with potential combinations of gedatolisib with either doxorubicin or radiation are shown in Figure 3.27

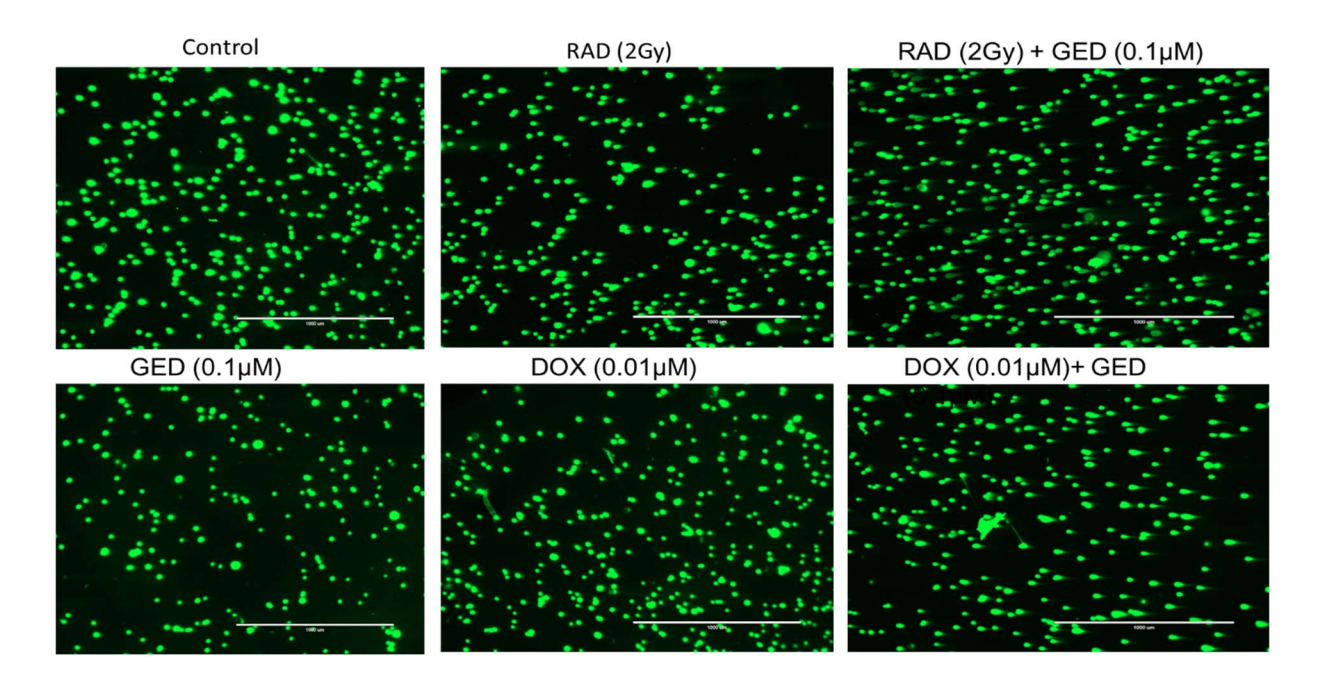
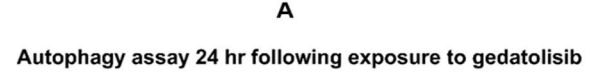


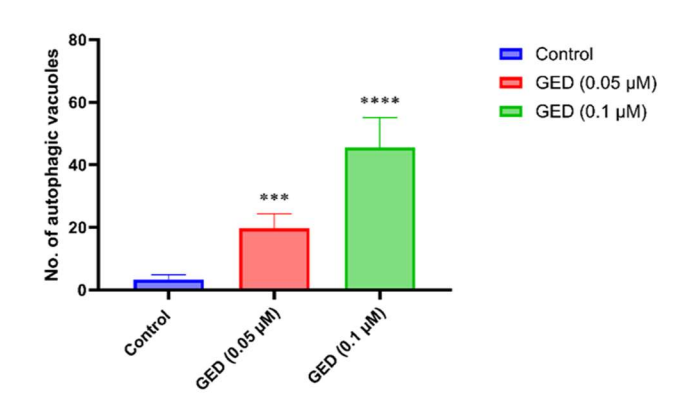
Figure 3-27 MDA-MB-231 Representative images for COMET assay.

Representative images for COMET assay in MDA-MB-231 cells at 48hr following exposure to single and combination of 0.1 μ M gedatolisib with 2 Gy radiation or 0.01 Gy irradiation. The samples were imaged using an EVOS microscope at 4X magnification, and the tail moments were measured by the Image J plugin OpenComet (Gyori et al., 2014)

3.8.4 Assessment of the effect of gedatolisib on autophagy in the MDA-MB-231 cell line

In the previous experiments, clonogenic assay has shown that gedatolisib reduced clonogenic survival of MDA-MB-231 cells, and its inhibitory concentrations were determined. Additionally, the spheroid growth was also impaired when treated with gedatolisib alone. However, the mechanisms underlying these gedatolisib effects as single agent was not identified in the earlier mechanistic experiments. Interestingly, combining gedatolisib with radiation or doxorubicin produced synergistic effects, hence, further investigation for mechanistic insight of gedatolisib alone is required. It has been reported in the literature that gedatolisib may induce autophagy, an alternative mode of cell death, where cells break down and recycle their own components(Guo and Pei 2019; Z. Xu et al. 2020). In this experiment, an autophagy assay was utilised to investigate the effect of gedatolisib in inducing autophagy in the MDA-MB-231 cell line. The cells were incubated with 0.05 μM and 0.1 μM the of gedatolisib, the concentrations that involved in combinations, and harvested at two time points (24 hr and 48 hr) post treatment, and the autophagy assay was performed as described in section 2.15. The stained autophagic vacuoles were imaged by confocal microscopy and quantified by ImageJ software, and the results are shown in Figure 3.27





Autophagy assay 48 hr following exposure to gedatolisib

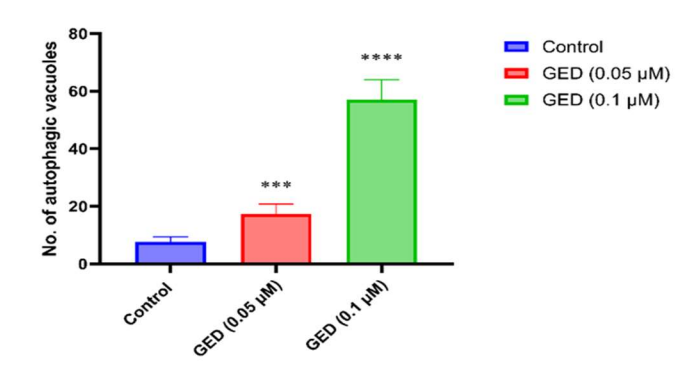


Figure 3-29-A Assessment of autophagy induction by gedatolisib.

The figure demonstrates the autophagic vacuoles in MDA-MB-231 Cells over time, evaluated by Autophagy assay, following exposure to different concentrations (IC $_{10}$ and IC $_{25}$) of gedatolisib as a single therapy. (A) Bar chart for the number of autophagic vacuoles in the treated and untreated cells. (B) Representative images for the autophagic vacuoles imaged by Leica Microsystems SP8 confocal microscope. Data represent the mean \pm SD of the number of autophagy vacuoles in the treated cell line for 3 independent experiments with each one performed in triplicate. Statistical analysis was undertaken using one-way ANOVA with Tukey's multiple comparisons test, and it was performed using GraphPad Prism 10.3.1. The difference considered significant when P value < 0.05 where *P < 0.05, **P < 0.01, ***P < 0.001 and ****P < 0.0001.

В Green channel Channels merged Blue channel (Autophagic vacuoles) **Untreated control** Autophagic Gedatolisib (0.05 μM) Gedatolisib (0.1 μM)

Figure 3-29-B Autophagic vacuoles following treatment with gedatolisib.

Representative images for the autophagic vacuoles imaged by Leica Microsystems SP8 confocal microscope.

The assay results suggested that both drug concentrations tested resulted in significant increase in number of autophagic vesicles at 24 hr and 48 hr post treatment in comparison to untreated controls (P<0.0001) as shown in Figure 3.27. Furthermore, the number of autophagic vacuoles increased in a concentration dependent manner where 0.1 μ M gedatolisib demonstrated higher induction of autophagy relative to 0.05 μ M of the drug (P<0.0001).

3.8.5 Evaluation the effect of gedatolisib on the expression of PI3K/Akt/mTOR pathway using western blot analysis.

Gedatolisib is a targeted drug that has recently utilised in therapeutic strategies of different types of cancer(Colombo *et al.*, 2021; Wilson *et al.*, 2021; Skolariki *et al.*, 2022). It primarily works as a dual node inhibitor of PI3K/mTOR signalling pathway. In this experiment, western blot analysis was utilised to assess the effects of low gedatolisib concentrations (0.05 μM and 0.1 μM) on Akt protein expression mainly activated by PI3K and mTORC2 proteins. These concentrations were tested because of their involvement in the combination experiments, demonstrating promising synergistic effects when simultaneously administered with radiation or doxorubicin. Thus, we aimed to investigate whether these low concentrations inhibit its targeted pathway (PI3K/mTOR). MDA-MB-231 cells were incubated with gedatolisib concentrations (0.05 μM and 0.1 μM) and harvested at different time points (1 hr, 4 hr, 24 hr and 48 hr) post treatment to quantify the protein expression at each time point as described in section 2.14, and the results are shown in Figure 3.28

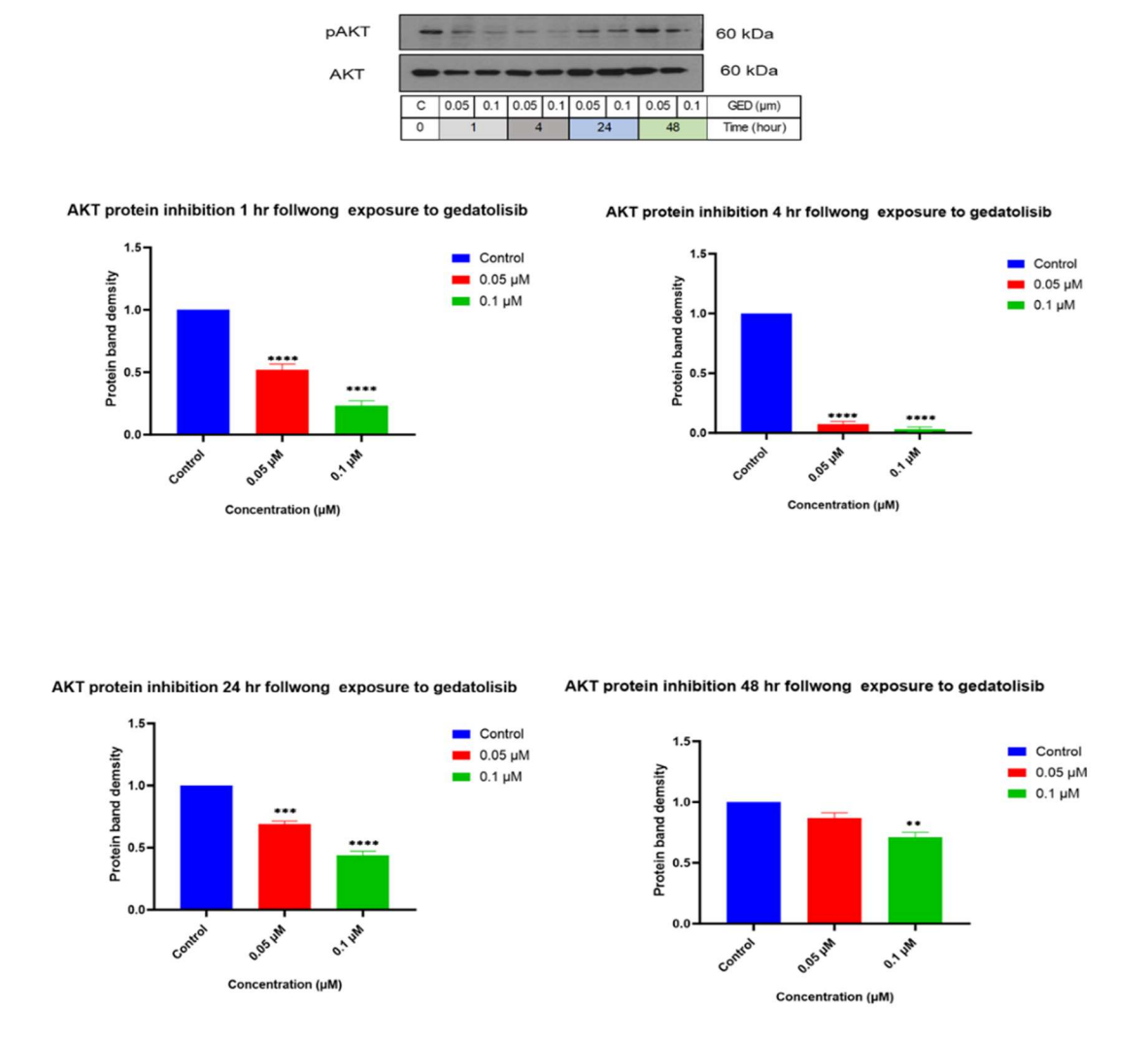


Figure 3-30 Evaluation of the effect of gedatolisib on the expression of Akt protein in MDA-MB-231 cells using western blot analysis

Signal intensity of AKT protein expression in MDA-MB-231 cells over time was assessed by western blot analysis following incubation with 0.05 μ M and 0.1 μ M of gedatolisib alone. The blots are representative of the bands of Akt protein expression. The band densities were quantified utilising ImageJ software and plotted as A: 1 h, B: 4 hr, C: 24 hr and D: 48 hr after treatment. Data represents the mean plus SD of the band densities in the treated cell line normalized to control for 3 independent experiments performed in triplicate. Statistical analysis was performed using GraphPad Prism 10.3.1 with one-way ANOVA with Tukey's multiple comparisons test. The difference considered significant when P value < 0.05 where *P < 0.05, **P < 0.01, ***P < 0.001 and ****P < 0.0001.

These data suggest that incubation of MDA-MB-231 cells with both gedatolisib concentrations tested decreased the Akt protein expression at 1 hr, 4 hr, and 24 hr following treatment in comparison to the untreated controls (P<0.0001) as shown in figure 3.28. However, 0.1 µM of gedatolisib was the only concentration that induced statistically significant reduction in Akt protein abundance relative to the untreated control (P<0.01) at all time points following treatment, suggesting that the inhibition was dose dependent.

Taken together, these data suggest that low gedatolisib concentrations inhibited their targeted pathway (PI3k/mTOR), reflecting their capability in reducing clonogenic survival and spheroid growth of MDA-MB-231 cells via inhibiting this pathway.

3.9 Discussion

Triple negative breast cancer is an aggressive subtype of breast cancers constituting 15-20% of all breast cancer cases (Das *et al.*, 2022; Pont, Marqués and Sorolla, 2024). Several types of cancer therapies including anthracyclines, taxanes and radiotherapy have been utilised in the management of TNBC. However, most of the therapies failed due to the lack of drug receptors and tumour heterogeneity, resulting in unmet clinical need (Zhu *et al.*, 2023). Consequently, there has been a growing shift in both preclinical and clinical research toward investigating targeted therapeutic strategies in TNBC (De Francesco *et al.*, 2022; Mustafa *et al.*, 2024). In this context, the current project evaluated treatments with distinct mechanisms of action, including the dual PI3K/mTOR inhibitor gedatolisib, the DNA-damaging agent doxorubicin, and ionising radiation, used alone and in combination. It was hypothesised that combining gedatolisib with these agents could improve therapeutic outcomes in TNBC.

Baseline characteristics of TNBC cell line

As per all experiments in our laboratory, we firstly identify the doubling time of the assessed cell lines because the literature doubling times characterised in different laboratories of the same cell lines vary with lab conditions, serum batches and growth conditions. The published doubling times for MDA-MB-231 vary with culture conditions but are commonly reported to be approximately 25-30 hr (German Collection of Microorganisms and Cell Cultures GmbH, 2025.), and the 28.1 and 25.5 hr were the doubling times of MDA-MB-231 cell line identified by Biswenger *et al.*, 2018 and Carneiro *et al.*, 2023, respectively. However, the slightly longer DT observed in the present work may reflect differences in experimental conditions including the cell culture vessels, the initial cell seeding density, the type of culture media and its additives, and the passage number for the assessed cells, which may

impact proliferation rates and can lengthen the apparent doubling time. The doubling time in our hands was consistent from project inception to completion.

The response to single-agents treatment

Gedatolisib is a dual PI3K/mTOR inhibitor that targets a central signalling pathway implicated in cancer cell growth and survival, particularly in triple-negative breast cancer (TNBC) (Khan et al., 2019b; Zhang et al., 2024; Garg et al., 2025). It has been reported that gedatolisib exert antiproliferative, antimetabolic and anti-invasive effects in a diverse of breast cancer models and patient derived xenograft mainly mediated by targeting pan PI3K isoforms, mTORC complex 1 and 2, thereby diminishing the probability of adaptive resistance (Rossetti et al., 2024). These drug features supported its inclusion in the current project. The data of clonogenic assay revealed a significant anti-proliferative effect of gedatolisib in MDA-MB-231 cell line, producing an IC_{50} below 1 μ M. This finding aligns with prior studies showing a potent effect of gedatolisib with TNBC models (Mallon et al., 2011; Rossetti et al., 2024). The powerful antiproliferative effect reflected by the clonogenic survival curve reinforce the hypothesis that inhibiting PI3K/Akt/mTOR pathway can significantly reduce the long-term survival potential of TNBC cells. A subsequent tumour spheroid, a threedimensional model assay, was utilised to further evaluate the clonogenic survival findings in a more complex model. The spheroid data showed that sub-micromolar range of gedatolisib concentrations resulted in significant growth reduction, although higher concentrations compared to clonogenic assay were required to show a comparable growth inhibition. These findings are in consistent with the previous studies disclosing that the complex structure of spheroids may hinder drug penetration and diffusion, thereby reducing therapeutic effectiveness (Lee and Cha, 2020; Garnique et al., 2024). This behaviour highlights the role of complex microenvironment architecture in decreasing the therapeutic response rather than

intrinsic resistance. Collectively, these findings revealed that gedatolisib has potent effect in inhibiting the growth of MDA-MB-231 cells. However, incorporating several models including ex-vivo and patient derived xenograft should be utilised to confirm its in vitro efficacy and avoid the overestimated effectiveness based on simple models.

Doxorubicin is a potent cytotoxic agent that utilised in the treatment of several types of cancer, and its cytotoxicity is mediated by inhibition of topoisomerase II and generation of oxygen reactive oxygen species as well as its role as DNA intercalating agent (Rawat et al., 2021; Pogorzelska et al., 2023; Smoots et al., 2024). By interfering with DNA replication and transcription, doxorubicin can trigger programmed cell death (apoptosis) in cancer cells with enhanced proliferation. Doxorubicin remains one of the standard therapeutic options in the treatment of triple negative breast cancer as well as other types of tumours due to its various molecular activities. In current project, a potent cytotoxicity of doxorubicin in the MDA-MB-231 cell line was demonstrated utilising with the IC₅₀ below 1 μM. From the literature, variable values for the IC₅₀ of doxorubicin in the MDA-MB-231 cell line have been reported. Some of the studies such as (Lovitt, Shelper and Avery, 2018; Mielczarek et al., 2019) demonstrated that the IC₅₀ of doxorubicin in MDA-MB-231 cell line were 0.087µM and 0.073µM, respectively. However, other studies such as (Wan et al., 2021; Abrahams, Gerber and Hiss, 2024) reported an IC₅₀ more than 0.1µM. Most of the literature studies calculate the IC50 from the cell viability assays such as MTT assay, whereas our IC50 was calculated using a clonogenic assay, which is considered a more accurate and biologically relevant method for assessing long-term proliferative potential and survival following drug exposure. Three-dimensional spheroid assays provided further insight into the efficacy of doxorubicin. Compared to clonogenic assays, spheroids exhibited reduced sensitivity, consistent with prior study demonstrating that breast cancer cell lines, including MDA-MB-231, are less

responsive to doxorubicin under 3D culture conditions (Lovitt *et al.*, 2018). This reduced sensitivity may be attributed to impaired drug penetration, altered cell-cell interactions, and reduced proliferation rates within the spheroid architecture.

Despite its clinical efficacy in breast cancer treatment, doxorubicin is associated with significant systemic toxicity such as cardiotoxicity, presenting significant risks during long-term treatment (Cavanagh *et al.*, 2024; Dewidar *et al.*, 2024; Kciuk *et al.*, 2023). These risks underscore the importance of optimising combination strategies that can enhance tumour-specific efficacy while potentially reducing systemic burden. Recent studies have shown that combining doxorubicin with DNA repair inhibitors can yield synergistic responses in TNBC models (Cavanagh *et al.*, 2024).

The limitation of the current assessment is represented by the absence of positive control to verify the sensitivity of the assay under our experimental conditions, and this can be considered in future studies to improve reproducibility and strength the assay validity.

The cytotoxicity of radiation in MDA-MB-231 cells was confirmed by clonogenic assays, which demonstrated a clear dose-dependent reduction in survival Fraction. The linear–quadratic (LQ) survival curve (Figure 3.4) showed progressive loss of clonogenic capacity with increasing dose, with the greatest effect observed at 10 Gy. Fitting of the LQ model yielded α = 0.227, β = 0.023, and an α/β ratio of 9.79. This relatively high α/β value indicates a strong contribution of the linear (α) component of cell killing, consistent with the notion that MDA-MB-231 cells exhibit significant sensitivity to single-dose exposures and respond in a manner typical of acutely responding tissues or aggressive tumour phenotypes.

The cytotoxic effect of radiation in MDA-MB-231 cells was evaluated by clonogenic assays, which revealed a dose-dependent reduction in survival fractions (Figure 3.4). The linear–quadratic (LQ) survival curve (Figure 3.4) showed progressive loss of clonogenic capacity with increasing dose, with the greatest effect observed at 10 Gy.

Fitting of the survival fractions with LQ model resulted in $\alpha = 0.227$, $\beta = 0.023$, and an α/β ratio of 9.79. The relatively high α/β value suggests that cell killing by the single hit or linear (α) component was predominant. This pattern is a characteristic of acutely responding tissues and aggressive tumour phenotypes (McMahon, 2019; Ahire et al., 2023). However, previous studies have demonstrated lower α/β ratios, for instance, Zhou et al. (2020) reported $\alpha = 0.1682$ and $\beta = 0.05468$ for the MDA-MB-231 cells, yielding an α/β nearly 3.1. Another study assessing combining sinensetin with Xirradiation in the MDA-MB-231 cell line found $\alpha = 0.0797$, $\beta = 0.076$, giving α/β around 1.05 (Rezakhani et al., 2020). In comparison with our findings, these lower ratios suggest a relatively greater contribution of the quadratic (β) component and enhanced repairing of sublethal DNA damage, which is inconsistent with our results of α/β = 9.79. Such discrepancies may indicate variations in experimental conditions, including clonogenic assay protocols, cell passage number, X-radiation machines, and culture conditions. These differences in the values of LQ parameters reflect the variability in in vitro radiosensitivity measurements. In spheroid assays, radiation also induced a clear dose-dependent effect. Compared with untreated controls, escalating doses induced a progressive reduction in spheroid growth, and at the highest assessed dose (6 Gy) this effect resulted in noticeable spheroid shrinkage.

Collectively, these data highlight that MDA-MB-231 cells demonstrate moderate intrinsic radiosensitivity in clonogenic assays and displayed dose dependent decrease in the growth of spheroids that better mimic the tumour microenvironment. Importantly, giving the higher doses required to induce spheroid shrinkage, this underscores the translational challenge of achieving effective tumour control in the complex and physiologically relevant 3D model. Furthermore, the spheroid findings underscore the clinical challenge of achieving durable tumour control in TNBC with radiotherapy alone and justifies investigation of radiosensitisation strategies, including combinations with PI3K/mTOR inhibitors, which have shown promise in

disrupting DNA repair and survival signalling pathways (Kuger *et al.*, 2014; Wanigasooriya et al., 2020; Liu *et al.*, 2021).

Efficacy of gedatolisib-based combination therapies in MDA-MB-231 cells

The cytotoxicity of gedatolisib, doxorubicin, and radiation as alone treatment in the MDA-MB-231 cell line was demonstrated with effects being dose- and concentration-dependent. While high doses are clinically efficacious, they often induce systemic toxicity, compromising patient compliance and therapeutic outcomes (Wang and Tepper, 2021; Liu *et al.*, 2025; Verginadis *et al.*, 2025). Moreover, TNBC cell lines including MDA-MB-231 activate compensatory survival pathways to recover after treatment avoiding cell death (Ku *et al.*, 2022; Abrahams, Gerber and Hiss, 2024). The combination strategies were therefore designed to target distinct mechanisms, aiming to enhance efficacy while minimizing drug exposure and toxicity.

In the current study and in the context of radiation, combining low gedatolisib concentrations with clinically relevant doses of ionising radiation resulted in a significant reduction in clonogenic survival, particularly at 0.1 µM gedatolisib with 2 Gy radiation. This agrees with prior study reported that PI3K/Akt/mTOR signalling promotes radioresistance in TNBC by maintaining cyclin D1 expression and attenuating apoptosis, whereas treatment with MK-2206, an Akt inhibitor, potentiated radiation induced-apoptosis (Johnson *et al.*, (2020). The synergistic effect of gedatolisib and radiation, as indicated by the combination index analysis in the current project, is further supported by reports showing that dual PI3K/mTOR inhibition (e.g., PKI-402) sensitises breast cancer cells, including MDA-MB-231, to radiation (Gasimli *et al.*, 2023). Interestingly, inhibition of mTOR alone (e.g., with rapamycin) was insufficient to reverse radioresistance in TNBC cells, with radiosensitivity restored only when Akt1 was concurrently suppressed (Holler *et al.*, 2016). This provides a mechanistic rationale for the superior efficacy of gedatolisib, which simultaneously

dual nodes of PI3K and mTOR, preventing feedback activation and promoting radiosensitivity in our model.

Similarly, when combined with doxorubicin, gedatolisib demonstrated synergistic antiproliferative effects at sub-cytotoxic concentrations, both in clonogenic and spheroid assays. This finding is particularly relevant and critically important if it can be translated into clinical settings given the dose-limiting cardiotoxicity associated with doxorubicin as well as development of doxorubicin resistance (Eralp et al., 2024; Keshandehghan et al., 2024). By enhancing the cytotoxic effect of low-dose doxorubicin, gedatolisib offers a potential means to preserve efficacy while minimising systemic toxicity. In support of our findings, a Phase 1 clinical trial investigating mTOR inhibitors (temsirolimus or everolimus) combined with liposomal doxorubicin and bevacizumab in patients with advanced metaplastic TNBC—a clinically identifiable surrogate for the mesenchymal subtype—demonstrated that objective responses were restricted to patients harbouring PI3K pathway aberrations, highlighting the potential of targeting the PI3K/AKT/mTOR pathway to enhance chemotherapy efficacy (Basho et al., 2017). Furthermore, preclinical studies using phytochemical agents, including curcumin, piperine, and Rumex vesicarius extract, have demonstrated synergistic cytotoxic effects when combined with doxorubicin, primarily through modulation of the PI3K/Akt/mTOR signalling pathway (Ghanem et al., 2022; Hakeem et al., 2024; Sarkar et al., 2024). Although these studies employed natural compounds, the underlying mechanism aligns with our findings that direct dual PI3K/mTOR inhibition using gedatolisib can enhance the antitumour efficacy of doxorubicin in TNBC models, thereby highlighting the translational potential of targeting this pathway to improve chemotherapy outcomes.

Taken together, these findings highlight the therapeutic value of targeting PI3K/mTOR signalling as a strategy to overcome intrinsic resistance mechanisms

and augment the effects of both chemotherapy and radiotherapy in TNBC. Importantly, the concordance between our in vitro results and published preclinical and clinical evidence strengthens the translational relevance of these combinations. However, the current study was limited to a single cell line, and further validation across multiple TNBC models, alongside mechanistic assays, is warranted to more definitively establish the robustness of these observations.

Mechanistic Insights into the effects of single-agents and combination therapies

The results from clonogenic survival and spheroid growth assays demonstrated that the combination of gedatolisib with doxorubicin or radiation produced significantly greater cytotoxicity in MDA-MB-231 cells compared to single-agent treatments. These findings prompted further investigation into the cellular mechanisms underpinning the demonstrated synergistic effect. To investigate how these agents interact at the molecular and cellular levels, a series of mechanistic assays were performed, assessing effects on cell cycle progression, apoptosis, DNA damage, autophagy, and signalling pathways. Integrating these mechanistic insights with the efficacy data is expected to provide a more comprehensive understanding of how PI3K/mTOR inhibition can potentiate conventional therapies and highlight therapeutic opportunities.

Cellular Stress Responses – Cell Cycle Arrest and Apoptosis

Cell cycle analysis showed various responses of stress adaptation across treatments. The data showed no significant cell cycle arrest following treatment with gedatolisib, suggesting that other mechanisms may mediate the antiproliferative effect of this drug in MDA-MB-231 rather than classical checkpoint blockade. However, prior studies demonstrated G0/G1 arrest in cell treated with PI3K/Akt/mTOR inhibitors such as DHW-208 and NVP-BEZ235 which was potentially via downregulation of cyclin D1 (Kuger *et al.*, 2014; Wang *et al.*, 2020). Interestingly, phytochemicals targeting the same pathway, such as ampelopsin and DMC, have instead been shown to trigger G2/M arrest through suppression of cyclin B1 and Cdc2 (Meng *et al.*, 2023; Jiang *et al.*, 2024). These discrepancies suggest that the precise point of cell cycle interference may rely on drug structure, incubation time with the treatment and cellular context.

The accumulation of cells at G2/M was displayed after incubation with doxorubicin with a significant dose and time dependent induction. This finding aligns with earlier reports assessing the cell cycle distribution in response of MDA-MB-231 cells to doxorubicin (Newell *et al.*, 2019; Novais *et al.*, 2021). Combining of gedatolisib with doxorubicin enhanced the G2/M arrest, suggesting shift of cells away from G1 and augmenting of doxorubicin mediating G2/M accumulation. In support to our findings, Sarkar *et al.* (2024b) reported an additive effect when curcumin combined with doxorubicin, which support the notion of improving the sensitivity of TNBC cells to G2/M-specific chemotherapies by targeting PI3K/Akt/mTOR signalling pathway. In the context of single agent treatment, radiation showed a robust induction of G2/M arrest at 24 and 48 hours. This effect is possibly associated with established DNA damage checkpoint activation (Hargrave *et al.*, 2022). Furthermore, this induced arrest was significantly prolonged when gedatolisib combined with radiation compared to radiation alone. This finding consistent with prior study demonstrated an enhanced radiosensitivity in nasopharyngeal carcinoma cells treated with gedatolisib

(PKI-587) with persistent G2/M accumulation and DNA damage (Liu *et al.*, 2015). Collectively, these results highlight how dual PI3K/mTOR inhibition amplifies the cytostatic impact of doxorubicin and radiation, even when minimal cell cycle changes are seen with single gedatolisib treatment.

Annexin V assay analysis provided another evidence of treatment effects. Doxorubicin triggered a dose-dependent apoptotic response, particularly noted at its IC_{50} concentration and extended across 24–48 hours following treatment. Moreover, when combined with gedatolisib, an enhanced apoptosis at concentrations below IC_{50} levels were demonstrated, suggesting that pathway inhibition can sensitize cells to lower doses of chemotherapy. Similar enhancement was reported in leiomyosarcoma, where a dual PI3K/mTOR (BEZ235), enhanced doxorubicin-induced apoptosis both *in vitro* and *in vivo* (Babichev et al., 2016).

Radiation induced apoptosis in a dose- and time-dependent fashion, with 2 Gy producing more sustained apoptotic events than 1 Gy. Interestingly, combining gedatolisib with radiation did not substantially increase apoptotic events beyond radiation alone, suggesting that in this context, the benefit of dual treatment may rely more on enforcing cell cycle arrest and impairing repair, rather than directly promoting apoptosis.

DNA Damage and Repair Dynamics

The COMET assay highlighted differences in DNA damage induction and repair kinetics across treatments. Gedatolisib monotreatment did not produce significant DNA damage, consistent with its role as a signalling inhibitor rather than a genotoxic agent. In contrast, doxorubicin generated measurable DNA breaks within 4 hours, reflected by increased tail moments, with partial repair evident by 48 hours. These findings align with reports demonstrating doxorubicin-induced double-strand breaks measured via γ-H2AX (Bodenstine *et al.*, 2016; Lee *et al.*, 2020). Importantly, the

restoration of baseline levels by 48 hours underscores the robust DNA repair capacity of TNBC cells, which may contribute to resistance.

When combined with gedatolisib, doxorubicin-induced DNA damage was both amplified and sustained, suggesting that PI3K/mTOR inhibition compromises DNA repair pathways. This is consistent with Lee *et al.* (2020), who showed that the phytocompound arctigenin enhanced doxorubicin-induced DNA damage via suppression of PI3K/Akt/mTOR signalling. Such findings support a mechanistic rationale in which gedatolisib prevents recovery from drug-induced stress, thereby sensitising TNBC cells to chemotherapy.

Our study revealed that the double strands DNA damage of MDA-MB-231 cells at 1 hr and 4 hr induced following exposure to radiation alone and measured by COMET assay was identified. This effect was dose dependent where 2 Gy dose induced more DNA damage than 1 Gy dose, reflected by higher number of tail moments. These results were compatible with other study data by Mahmoud et al., (2023) which displayed that radiation has direct interaction with DNA and indirect effect through increasing ROS resulting in increased levels of phosphorylated H2AX at 4 hr and 24 hr following irradiation. In the current project, comet assay analysis showed higher tail moments at 4 hr compared to 1 hr following to radiation exposure. Unexpected, delays in peak DNA damage have also been demonstrated utilising alternative assays. For instance, Sharma et al. (2015), revealed that while DNA damage usually peaked at 2 hr post-irradiation, in some subgroups the maximum response was delayed to 4 hr before declining towards baseline by 24 hr. This suggests that some factors may contribute to the delayed DNA damage detection, including the prolonged generation of reactive oxygen species, complex DNA damage and inter-individual variation in the kinetics of DNA repair (Willkinson et al., 2023; Mavragani et al., 2017). In this study, simultaneous administration of gedatolisib with radiation in MDA-MB-231 cells resulted in significantly greater tail moments across all time points following

treatment compared to radiation alone, suggesting that gedatolisib may impair DNA repair mechanisms. Supporting to these findings, previous studies revealed that dual inhibition of mTORC1 and Akt1 using rapamycin and MK-2206 impaired non-homologous end joining (NHEJ) repair and increased residual DNA double-strand breaks, resulting in enhanced radiosensitisation (Holler *et al.*,(2016b)

Taken together, these results suggest that gedatolisib enhances the cytotoxicity of doxorubicin and radiation not by inducing DNA damage on its own, but by preventing efficient repair, prolonging checkpoint arrest, and thereby tipping the balance toward cell death.

Adaptive Survival Mechanisms and Pathway Modulation

In addition to cell cycle arrest and DNA damage, adaptive processes such as autophagy emerged as important modulators of therapy response. The PI3K/Akt/mTOR pathway is a central regulator of both proliferation and adaptive survival processes, including autophagy, which plays a critical role in therapy resistance (Ortega et al., 2020; Wylaź et al., 2023; Li et al., 2024). To investigate whether gedatolisib, dual node inhibitor of PI3K/Akt/mTOR pathway, modulates these responses in MDA-MB-231 cells, autophagy induction and pathway activity were assessed. Gedatolisib induced a dose and time-dependent accumulation of autophagic vacuoles. These findings align with Guo and Pei (2019), who demonstrated that tetrandrine, a phytochemical, induced autophagy in MDA-MB-231 cells via downregulation of the PI3K/Akt/mTOR pathway. Their study emphasizes the central role of this pathway in regulating autophagy and supports our observation that gedatolisib, a dual PI3K/mTOR inhibitor, induces autophagy in a dose-dependent manner in TNBC cells.

Western blot analysis confirmed that gedatolisib effectively suppressed Akt phosphorylation at both IC_{10} and IC_{25} doses, with the strongest inhibition observed at early to intermediate post-treatment. Partial recovery at later time points indicates the

activation of compensatory signalling loops, such as feedback upregulation of upstream receptor tyrosine kinases (Chandarlapaty, 2012; Park *et al.*, 2020). This dynamic adaptation suggests that while gedatolisib is effective at pathway inhibition, the rebound of signalling activity could attenuate long-term efficacy unless countered by combination therapy.

Taken together, these findings suggest that the efficacy of gedatolisib is mediated, at least in part, through its ability to modulate autophagy, a key adaptive survival process in TNBC. By inducing autophagy in a dose-dependent manner, gedatolisib appears to disrupt cellular homeostasis and compromise recovery from stress, thereby amplifying the cytotoxic effects of doxorubicin and radiation. This mechanistic insight provides a strong rationale for the observed therapeutic benefit of combining PI3K/mTOR inhibition with conventional treatments in aggressive breast cancer subtypes.

Collectively, the current findings of this study offer substantial evidence that targeting the PI3K/Akt/mTOR pathway with gedatolisib not only exerts significant antiproliferative effects on MDA-MB-231 cells but also enhances the efficacy of conventional therapies such as doxorubicin and radiation. Furthermore, these results support the rationale for combining PI3K/mTOR inhibition with standard treatments and pave the way for developing more effective, mechanism-driven combination strategies in aggressive breast cancer subtypes.

Although the assessed combinations demonstrated promising results, there were limitations for the current study represented by no positive control to compare with the treatment and only one TNBC cell line was assessed. Hence, addressing these limitations may give more robustness for the current data.

Chapter 4

4 Establishment of an MDA-MB-231 radioresistant cell line and assessment of the response of the therapy resistant cell line to single and combination therapy of gedatolisib, doxorubicin and radiation

4.1 Introduction

Therapy resistance represents a clinical challenge in the management of triplenegative breast cancer (TNBC), contributing to disease progression, recurrence, and
poor patient outcomes. TNBC frequently develops resistance despite initial
responsiveness to standard treatments, including chemotherapy, targeted therapy,
and radiotherapy (Sarno et al., 2023; Mustafa et al., 2024). This resistance can arise
through various mechanisms, including enhanced DNA repair, evasion of apoptosis,
and activation of compensatory survival pathways (Bai et al., 2021; De Francesco et
al., 2022). Among different therapeutic agents, resistance to radiotherapy is of
particular concern, as it limits the efficacy of a widely used treatment approach in
TNBC. Several molecular alterations have been implicated in the development of
radioresistance, including activation of the PI3K/Akt/mTOR pathway, overexpression
of DNA repair proteins, and alterations in apoptotic regulators (Gray et al., 2019; Deng
et al., 2023b; Yu et al., 2023).

To the best of our knowledge, there are no treatment options currently available for TNBC patients who develop resistance following initial standard therapy. Following the emergence of resistance to chemotherapy or radiotherapy, the tumour typically recurs with increased aggressiveness and limited response to therapeutic interventions (Bai et al., 2021; De Francesco et al., 2022). This therapeutic gap potentially contributes to the poor prognosis and high mortality rates associated with TNBC, particularly in cases of metastatic or recurrent disease. Addressing this critical gap necessitates the development of novel therapeutic strategies specifically targeting therapy resistance pathways in cancer, and generating treatment resistant TNBC cells is essential to develop such therapies.

Establishing a radioresistant TNBC cell line is, therefore, an important first step in this journey. This cell line can be utilised to investigate a series of biological characteristics, genetic variations, and metabolic disturbances that accompany the

induction of resistance to radiotherapy. Furthermore, this cell line can be used to assess the radiosensitisation effect of single and combination chemotherapies.

Utilising the clonogenic assay, a range of gedatolisib and doxorubicin concentrations and radiation doses were tested as a single therapy to evaluate the cytotoxicity of each therapy and to demonstrate the IC_{50} of the drugs and D_{50} of radiation and to compare these between the parental MDA cell line and the generated radiation resistant cell line. Based on these values (IC_{50} and D_{50}), different combination therapies were designed to be evaluated to identify if there is any suitable combination that work better than single therapy.

4.2 Aims

- 1. To develop and validate a radiation resistant cell line with a suggested name (RR-MDA-MB-231).
- To compare the efficacy of single and combination treatments of gedatolisib with doxorubicin or radiation in this RR-MDA-MB-231 cell line utilising clonogenic assay and clonogenic spheroids

4.2.1 Hypothesis

For the current work, we hypothesised that:

- 1- The established radioresistant MDA-MB-231 cell line would show more survival following exposure to radiation than the parent MDA-MB-231 cell line.
- 2- The developed combination treatments involving gedatolisib with either doxorubicin or radiation that showed enhanced cytotoxicity in the parent cell line would retain its efficacy in the derived radioresistant MDaA-MB-231 cell line.

4.3 Results

4.3.1 Establishment of Radioresistant MDA-MB-231 cells.

To ensure the establishment and characterization of the radioresistant (RR-MDA-MB-231) cell line prior to proceeding to further experiments, a series of validation steps were performed. Firstly, clonogenic survival assays was used and the data demonstrated significantly higher survival fractions of derived RR-MDA-MB-231 compared to the parental wild-type cells (WT-MDA-MB-231) post exposure to ionizing radiation which confirmed the radioresistant phenotype. Secondly, the doubling time of each cell line was calculated to assess the proliferative capacity of the two cell populations. To calculate the doubling time, the numbers of RR-MDA-MB-231 and the parent WT-MDA-MB-231 cells were counted daily at 24-hour intervals following cell seeding time (which is considered 0 hr). The data revealed significant differences in growth kinetics, and the growth curves for both cell lines are shown in Figure 4.1. Finally, the assessment of cell morphology under phase-contrast microscopy displayed that RR-MDA-MB-231 cells showed a relatively altered morphology compared to WT-MDA-MB-231 cells, suggesting their phenotypic difference. Collectively, these evaluations confirmed the radioresistant characteristics of the RR-MDA line prior to subsequent analyses.

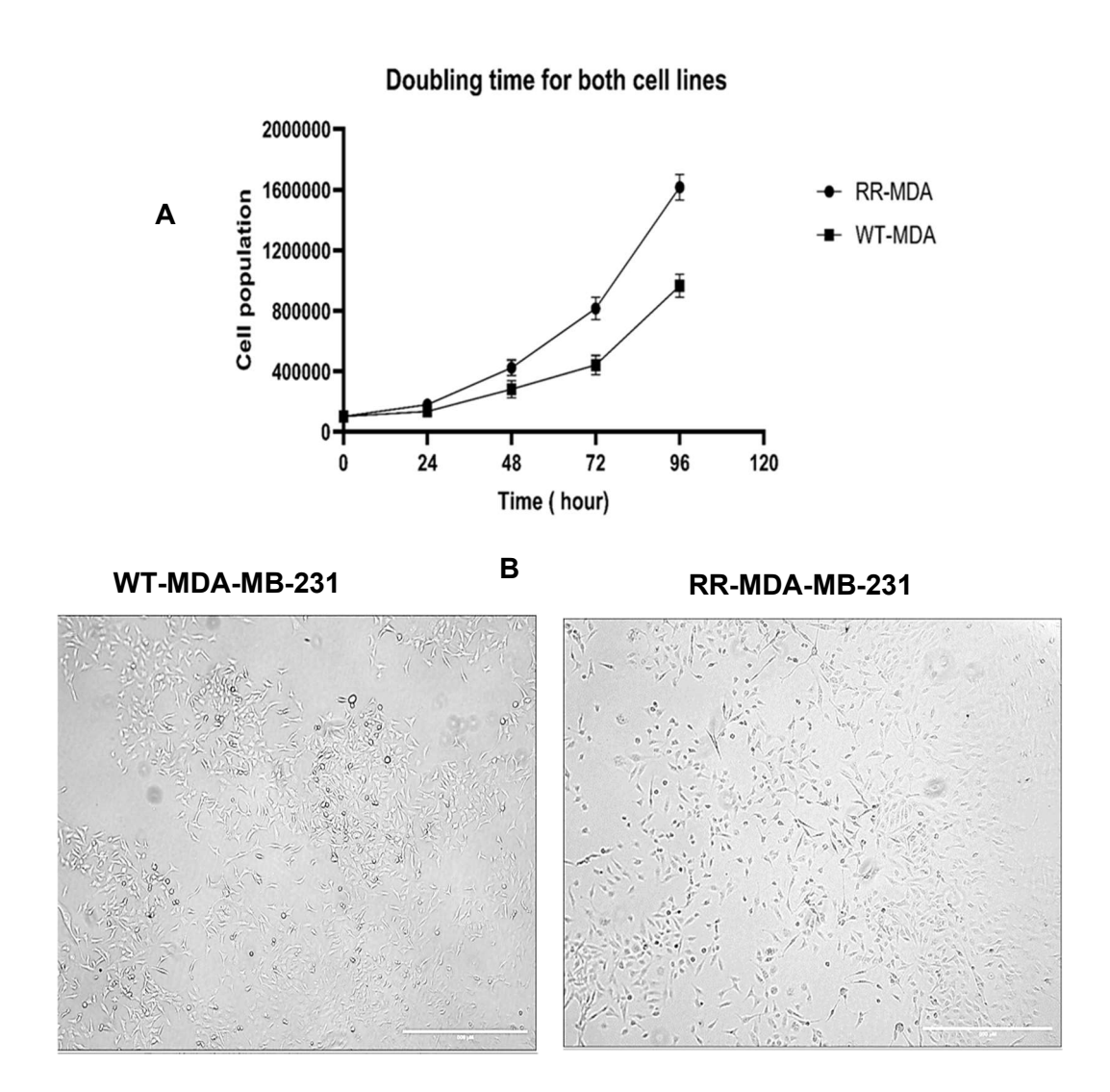


Figure 4-1 Characteristics of radioresistant and parent MDA-MB-231 cells.

A: The growth curves for radioresistant and parent MDA-MB-231 cells show the cell population harvested at different time points following starting point cell seeding. Five T25 flasks for each cell line were seeded with 100000 cells per flask, and the cells were harvested at 24-hour time intervals following seeding and counted using a haemocytometer. Data represent the mean ± SD of 3 independent experiments and each one performed in triplicate. Doubling time was calculated from the growth curve utilising the exponential growth equation in Excel 2016. The growth curve figure was plotted using GraphPad Prism 10.3.1.B: The cell population morphology imaged by EVOS microscope.

The data demonstrated a significant change in the growth pattern of the established radioresistant and its parental MDA-MB-231 cell lines. The calculated doubling time

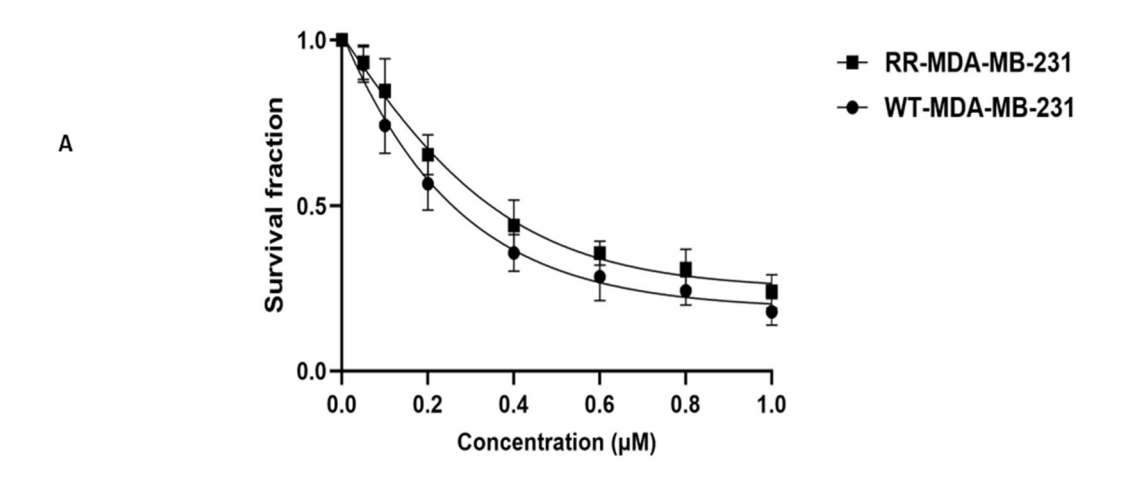
for WT-MDA-MB-231 cells in this experiment was 34 hr, while for the RR-MDA-MB-231 cell line, it was 25 hr.

4.3.2 Clonogenic assay for radioresistant (RR)-MDA-MB-231 cell line following exposure to single therapy.

To investigate the cytotoxicity of single therapies including gedatolisib, doxorubicin and radiation in the radioresistant MDA-MB-231 cell line and comparing the cytotoxicity behaviour with its parental cell line, a clonogenic assay was performed. The main goal of this assay was the evaluation of single therapeutic effectiveness in terms of toxicity, measured by the ability of radioresistant cells to form colonies following exposure to single therapy. Additionally, the inhibitory concentrations (IC_{50} , IC_{25} and IC_{10}) of each individual therapy required for further experiments were calculated based on the data of this assay.

4.3.2.1 Clonogenic survival of RR- MDA-MB-231 and wild type cell lines following treatment with gedatolisib alone

Utilising a clonogenic survival assay, the effect of gedatolisib in the RR-MDA-MB-231 cell line was evaluated. A range of gedatolisib concentrations 0.05 -1 μ g (0.05, 0.2, 0.4, 0.6, 0.8, 1 μ g) was assessed, where RR-MDA-MB-231 cells were incubated with escalating concentrations of gedatolisib as described in section 2.7. The data are shown in Figure 4.2



IC	WT-MDA-MB-231	RR-MDA-MB-231
IC ₅₀	0.249 (μΜ)	0.326 (μM)
IC ₂₅ (μM)	0.124 rounded to 0.1 (μM)	0.16 (µM)
IC ₁₀ (μM)	0.0498 rounded to 0.05 (μM)	0.08 (µM)

В

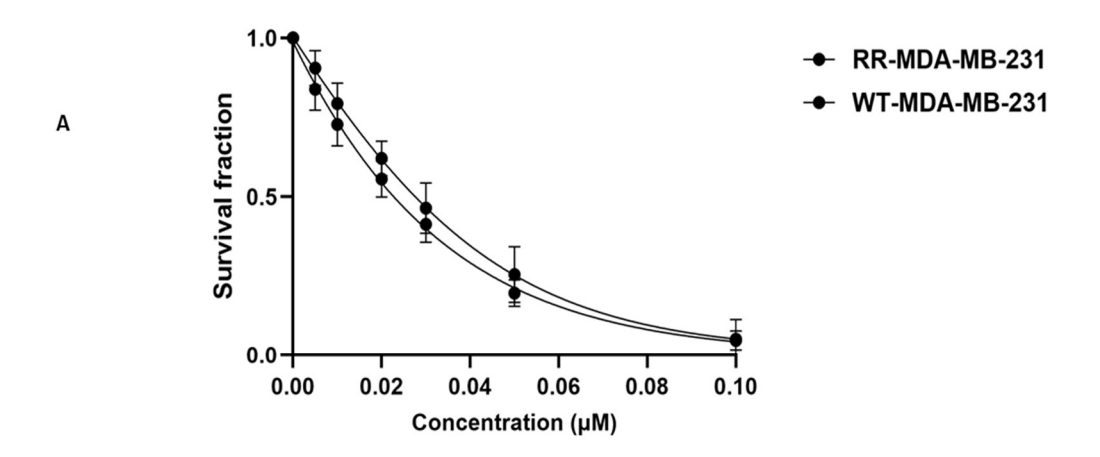
Figure 4-2 Survival fraction curves of the resistant and wild type MDA-MB-231 cell lines following treatment with gedatolisib.

A: Clonogenic survival fractions of RR-MDA-MB-231 and wild type cells following exposure to a range of gedatolisib concentrations (0.05, 0.1, 0.2, 0.4, 0.6, 0.8, 1 μM). Data represents the mean ± SD of 3 independent experiments with each experiment performed in triplicate. PE for resistant and wild type cell lines in this experiment were 59±6% and 50±4%, respectively. Statistical analysis was performed using GraphPad Prism 10.3.1 B: The inhibitory concentrations (ICs) of gedatolisib in RR-MDA-MB-231 and wild type cell lines.

Figure 4.2 displays the dose-response curves of gedatolisib in wild-type (WT) and radioresistant (RR) MDA-MB-231 cells. At increased concentrations of gedatolisib, the RR-MDA-MB-231 cells showed consistently higher survival fractions compared to wild type cells, suggesting reduced sensitivity to the drug in the resistant cell line, as expected. Although the IC_{50} value of gedatolisib was higher in the RR-MDA-MB-231 cells than in the wild type cells, this difference was not statistically significant (P>0.05). Furthermore, survival differences between the two investigated cell lines at all the assessed gedatolisib concentrations were not statistically significant (p > 0.05), suggesting that although a tendency of reduced sensitivity was identified, it was not confirmed statistically (P>0.05).

4.3.2.2 Clonogenic survival of RR- MDA-MB-231 and wild type cell lines following treatment with doxorubicin alone

To evaluate the cytotoxicity of doxorubicin in the RR-MDA-MB-231 cell line, a clonogenic survival assay was conducted. The cells were exposed to a range of 0.005 - 0.1 μ M (0.005, 0.01, 0.02, 0.03, and 0.1 μ M) doxorubicin concentrations. The survival fraction curve as well as the ICs of doxorubicin are shown in Figure 4.3



	IC	WT-MDA-MB-231	RR-MDA-MB-231	
В	IC ₅₀	0.023 (μΜ)	0.035 (μΜ)	
	IC ₂₅ (μM)	0.011 rounded to 0.01 (μM)	0.0175 rounded to 0.02 (μM)	
	IC ₁₀ (μM)	0.0046 rounded to 0.005 (μM)	0.0087 rounded to 0.01 (μM)	

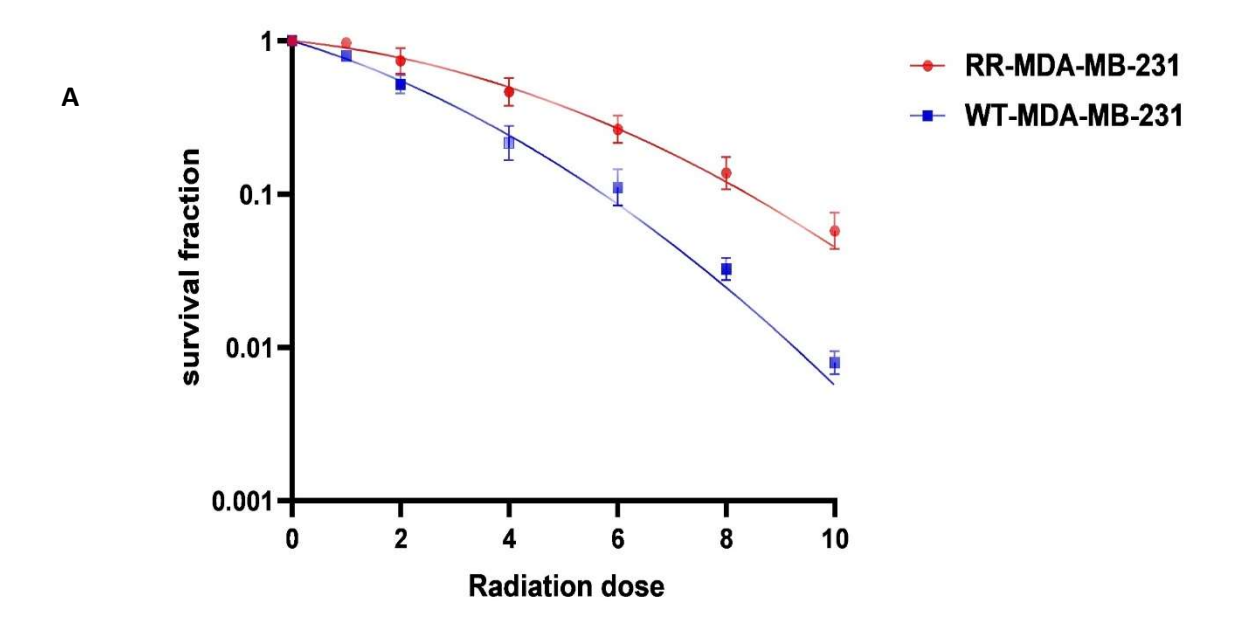
Figure 4-3 Survival fraction curves of the resistant and wild type MDA-MB-231 cell lines following treatment with doxorubicin.

A: Clonogenic survival fractions of RR-MDA-MB-231 and wild type cells following exposure to a range of doxorubicin concentrations (0.005, 0.01, 0.02, 0.03, 0.05, 0.1μM). Data represents the mean ± SD of 3 independent experiments with each experiment performed in triplicate. PE for resistant and wild type cell lines in this experiment were 59±6% and 50±4%, respectively. Statistical analysis was performed using GraphPad Prism 10.3.1 B: The inhibitory concentrations (ICs) of doxorubicin in RR-MDA-MB-231 and wild type cell lines.

Figure 4.3 displays the cytotoxic effects of doxorubicin in both RR-MDA-MB-231 and wild-type cell lines. As anticipated, doxorubicin reduced cell survival in both cell lines, and this effect was dose-dependent, where the higher assessed concentration $(0.1\mu\text{M})$ resulted in higher survival reduction in both cell lines. Although the IC₅₀ value of doxorubicin was higher in the RR-MDA-MB-231 cell line compared to the wild type, this difference was not statistically significant (P>0.05). Additionally, survival differences at individual doxorubicin concentrations were not statistically significant between the two cell lines. This suggests that despite the tendency of the RR cell line toward reduced sensitivity to doxorubicin, the difference lacked statistical significance.

4.3.2.3 Clonogenic survival of RR- MDA-MB-231 and wild type cell lines following treatment with radiation alone

To assess the survival of RR-MDA-MB-231 and parental MDA-MB-231 cells following exposure to radiation, a clonogenic assay was performed for the two cell lines post treatment with a range of X-radiation doses (1, 2, 4, 6, 8, 10 Gy). The survival fractions were fitted with the linear quadratic model and the curves for both cell lines as are displayed in Figure 4.4



Cell line	α	β	α/β
WT-MDA-MB-231	0.246 ± 0.024	0.022 ± 0.007	9.05
RR-MDA-MB-231	0.084 ± 0.026	0.027± 0.005	3.66
t-test	P<0.05	P>0.05	P<0.05

В

Figure 4-4 Linear quadratic survival curve of resistant and parental MDA-MB-231 cells exposed to radiation.

Clonogenic survival of RR-and WT-MDA-MB-231 cells following exposure to a range of radiation doses (1, 2, 4, 6, 8, 10 Gy). The survival curves were fitted by linear quadratic model. Data represents the mean ± SD of 3 independent experiments with each experiment performed in triplicate. PE for resistant and wild type cell lines in this experiment were 63±4% and 52±3%, respectively Statistical analysis was performed using GraphPad Prism 10.3.1. PE of MDA-MB-231 cells for this experiment was 53±4%

Figure 4.4 shows the survival curves of RR-MDA-MB-231 and WT-MDA-MB-231 cells fitted to the linear quadratic model following treatment with increasing doses of ionising radiation. The data revealed a higher survival fraction of RR-MDA-MB-231 cells across all the investigated doses compared to WT-MDA cells, supporting their acquired radioresistant. As shown in the table of LQ parameters, RR-MDA cells had a lower α value, reflecting reduced sensitivity to the initial lethal damage induced by radiation. Additionally, an altered and relatively higher β value of RR-MDA-MB-231 cells indicates an enhanced capacity in repairing sublethal DNA damage. Moreover, the significant lower α/β ratio demonstrated in RR-MDA cells compared to WT-MDA suggests an increased radiation—induced damage repair capacity and an overall shift toward resistance.

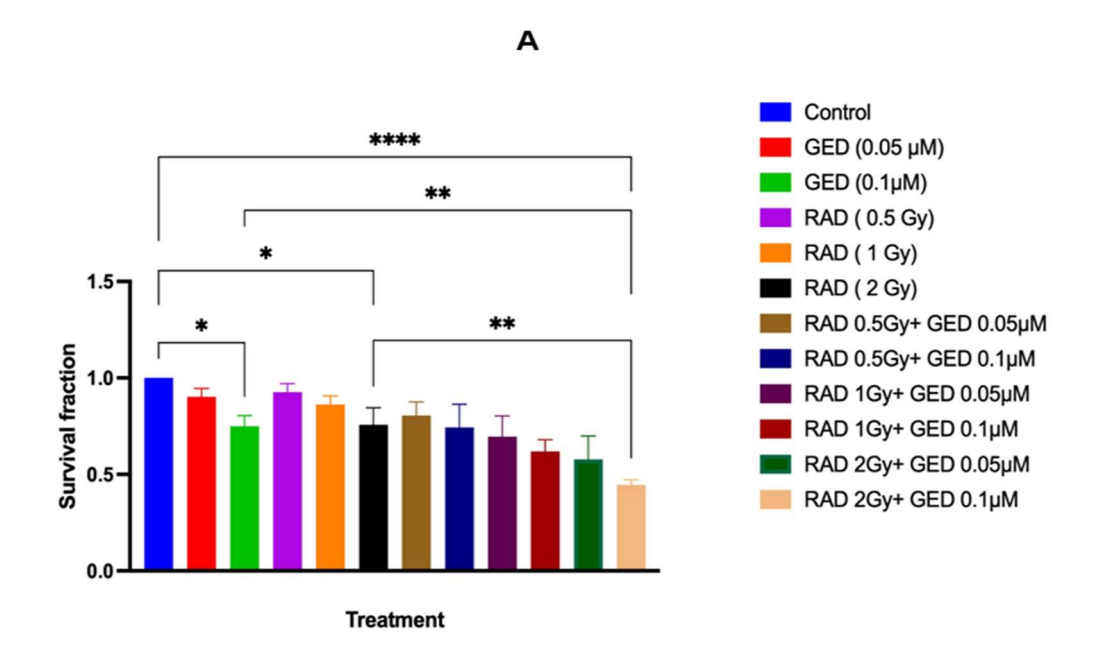
The survival curves shown in Figure 4.4 show the response of RR-MDA-MB-231 and wild type cell lines to increasing doses of radiation. The RR-MDA-MB-231 cells showed greater resistance to radiation, with consistently higher survival fractions at all the tested doses compared to the wild type. The reduction in the sensitivity is reflected in the calculated ED₅₀ values, where the dose required to reduce survival by 50% was 1.759 Gy for the wild-type cells and 3.269 Gy for the radioresistant cells, and this difference was statistically significant (P<0.001). This indicates that approximately double the radiation dose was required to achieve the same level of cytotoxicity in the resistant cell line, suggesting a successful development of a radioresistant phenotype.

4.3.3 Assessment of combination therapy effectiveness in the radioresistant (RR)- MDA-MB-231 cell line

To evaluate the effectiveness of combination therapy in the RR-MDA-MB-231 cell line, the treatment regimens utilising low doses of drugs and radiation were designed Given that there was no statistically significant difference in the IC_{50} values of gedatolisib and doxorubicin between the wild-type and RR-MDA-MB-231 cell lines, the same concentrations previously selected for combination treatments in the parental MDA-MB-231 cell line (chapter 3) were applied. This strategy minimises experimental variability and enables a clear comparison of treatment responses between the two cell lines. For radiation, doses of 0.5 Gy, 1 Gy, and 2 Gy were utilised consistently in both cell lines, where 2 Gy dose represents the standard daily fraction of radiation used in clinical settings, thus improving the translational relevance of the findings.

4.3.3.1 Clonogenic survival assay for (RR)- MDA-MB-231 cell line following exposure to gedatolisib and radiation combination therapy

The RR-MDA-MB-231 cell survival was evaluated following exposure simultaneous combination of radiation and gedatolisib, utilising clonogenic assay. Based on the IC₅₀ of gedatolisib (0.31 μ M), two concentrations of this drug, 0.05 μ M and 0.1 μ M that were around the IC₁₀ and IC₂₅ of the drug, respectively, were selected to combine with three low radiation doses, 0.5 Gy, 1 Gy, and 2 Gy. The survival fractions following exposure to different combinations are shown in Figure 4.5



В

Tukey's multiple comparison test	P (*)	Below	P-value
		threshold?	
Control vs. GED (0.1 µM)	*	Yes	0.0155
Control vs. RAD (2 Gy)	*	Yes	0.0215
GED (0.1 μM) vs. RAD 2 Gy+0.1 μM GED	**	Yes	0.0021
RAD (2 Gy) vs. RAD 2 Gy+0.1 µM GED	**	Yes	0.0015

Figure 4-5 Survival of RR-MDA-MB-231 cells following combination treatment with gedatolisib and radiation.

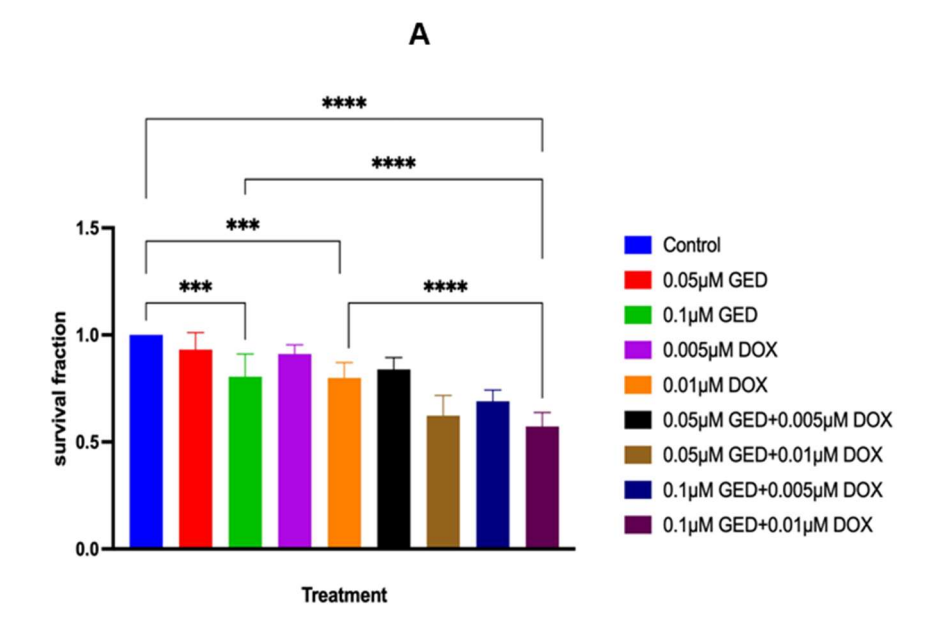
A: RR-MDA-MB-231 cell survival fractions following exposure to a simultaneous combination of 0.05 and 0.1 μ M gedatolisib with 0.5Gy, 1Gy and 2Gy radiation. Data represents the mean \pm SD of the survival fraction of the treated cells normalised to the untreated control for 3 independent experiments with each experiment performed in triplicate. PE for RR-MDA-MB-231 cell line in this experiment were 61 \pm 3%. Statistical analysis was done using one-way ANOVA. B: Tukey's multiple comparisons test to determine significance, which was undertaken using GraphPad Prism 10.3.1 and the difference considered significant when P value < 0.05 where *P < 0.05, **P < 0.01, ***P < 0.001 and *****P < 0.0001.

The data in Figure 4.5 demonstrated that the survival fractions were decreased significantly when the cells were treated with 0.1 µM gedatolisib or 2 Gy radiation alone compared to the untreated control (p < 0.05). In the statistical analysis of combinations, at the lower doses, combining of 0.05 µM gedatolisib and 0.5 Gy radiation significantly reduced survival compared to 0.5 Gy radiation alone (p < 0.05) but not compared to 0.05 μ M GED alone (p > 0.05), suggesting a low benefit from the combination at this level. Furthermore, following treatment with combination of 0.1 µM gedatolisib with 0.5 Gy radiation, the survival fraction was reduced significantly relative to control (P<0.05); however, no statistically significant difference was shown when compared to either 0.1 μ M gedatolisib or 0.5 Gy radiation alone (p > 0.05), suggesting that the combination at this level does not provide a clear advantage. Interestingly, the combination of 0.1 µM gedatolisib with 2 Gy radiation resulted in the greatest cytotoxic effect, demonstrating a statistically significant reduction in survival compared to both 0.1µM gedatolisib alone (p < 0.01) and 2 Gy radiation alone (p < 0.01). Moreover, the best combination effect at this dose level (0.1µM gedatolisib and 2 Gy radiation) supports its potential therapeutic relevance and suggests further translational investigations. The full statistical comparison table for the investigated doses and combinations are shown in the Appendix.

These findings confirm our hypothesis that combining gedatolisib with radiation would enhance cytotoxicity in the radioresistant MDA-MB-231 cell line, with the greatest reduction in cell survival demonstrated at 0.1 µM gedatolisib combined with 2 Gy radiation. This significant combination advantage reinforces the strategy of targeting different pathways as a potential approach to overcome therapy resistance in TNBC.

4.3.3.2 Clonogenic survival assay for (RR)- MDA-MB-231 cell line following exposure to gedatolisib and doxorubicin combination therapy

The effectiveness of gedatolisib and doxorubicin combination therapy in the RR-MDA-MB-231 cell line was assessed via clonogenic survival assay. Two concentrations that were around the IC $_{10}$ and IC $_{25}$ of each drug, gedatolisib (0.05 and 0.1 μ M) and doxorubicin (0.005 and 0.01 μ M), were combined and concomitantly incubated with RR-MDA-MB-231 cells for 48 hrs. The survival fractions following exposure to different combination regimens are shown in Figure 4.6



В

Tukey's multiple comparison test	P (*)	Below threshold?	P-value
Control vs. 0.1µM GED	***	Yes	0.0005
Control vs. 0.01µM DOX	***	Yes	0.0003
0.1μM GED vs. 0.1μM GED+0.01μM DOX	****	Yes	<0.0001
0.01μM DOX vs. 0.1μM GED+0.01μM DOX	****	Yes	<0.0001

Figure 4-6 Survival of RR-MDA-MB-231 cells following combination treatment with gedatolisib and doxorubicin.

A: RR-MDA-MB-231 cell survival fractions following treatment with a simultaneous combination of $0.05\mu\text{M}$ and $0.1\mu\text{M}$ gedatolisib with $0.005\mu\text{M}$ and $0.01\mu\text{M}$ doxorubicin. Data represents the mean \pm SD of the survival fraction of the treated cells normalised to the untreated control for 3 independent experiments with each experiment performed in triplicate. PE for RR-MDA-MB-231 cell line in this experiment were 59 \pm 5%. Statistical analysis was done using one-way ANOVA. B: Tukey's multiple comparisons test to determine significance, which was undertaken using GraphPad Prism 10.3.1 and the difference considered significant when P value < 0.05 where *P < 0.05, **P < 0.01, ***P < 0.001 and *****P < 0.0001.

The clonogenic survival data in Figure 4.6 revealed that treatment of RR-MDA-MB-231 cell line with low concentrations of gedatolisib and doxorubicin as a drug alone, did not significantly decrease the survival fraction compared to the untreated control (P>0.05). Nevertheless, 0.1µM gedatolisib alone significantly reduced survival compared to the untreated control (P < 0.01), in addition to the survival reduction after treatment with 0.01µM doxorubicin alone (P < 0.01). For the combinations, combining of 0.05 µM gedatolisib with 0.005 µM doxorubicin significantly reduced survival compared to the untreated control (P<0.01); however, this effect was not statistically significantly different when compared to either 0.05 μM gedatolisib alone or 0.005 μM doxorubicin alone (P > 0.05), suggesting a lack of augmented effect at this dose level. Figure 4.6 displayed that the combination of 0.1 µM gedatolisib with 0.01 µM doxorubicin produced the greatest survival reduction in RR-MDA-MB-231 cells, which was statistically significant when compared to both drugs alone (P<0.0001). suggesting that this combination was the most potent among the assessed combinations. The full statistical comparison table for the investigated concentrations of monotreatment and their combinations for the RR-MDA-MB-231 cell line are shown in the Appendix.

Collectively, the current findings confirmed our proposed hypothesis by demonstrating that rationally designed combinations utilising low doses (below the IC₅₀) of both gedatolisib and doxorubicin can significantly improve treatment effectiveness in radioresistant TNBC cells, suggesting a promising translational strategy to overcome therapeutic resistance.

4.3.3.3 Clonogenic survival assay for (RR)- MDA-MB-231 cell line following exposure to scheduled combination of gedatolisib and radiation

The clonogenic assay data demonstrated that the combination of gedatolisib with radiation was more beneficial in inducing cell killing than each treatment alone. The RR-MDA-MB-231 cells simultaneously exposed to 2Gy radiation and 0.1 µM gedatolisib showed the lowest survival compared to the untreated control and each single agent. To assess the effect of this combination when they administered preand post each other, a clonogenic survival assay for scheduled combination was utilised. The survival fractions data for the simultaneous treatment, gedatolisib first and radiation first treatment are shown in Figure 4.7

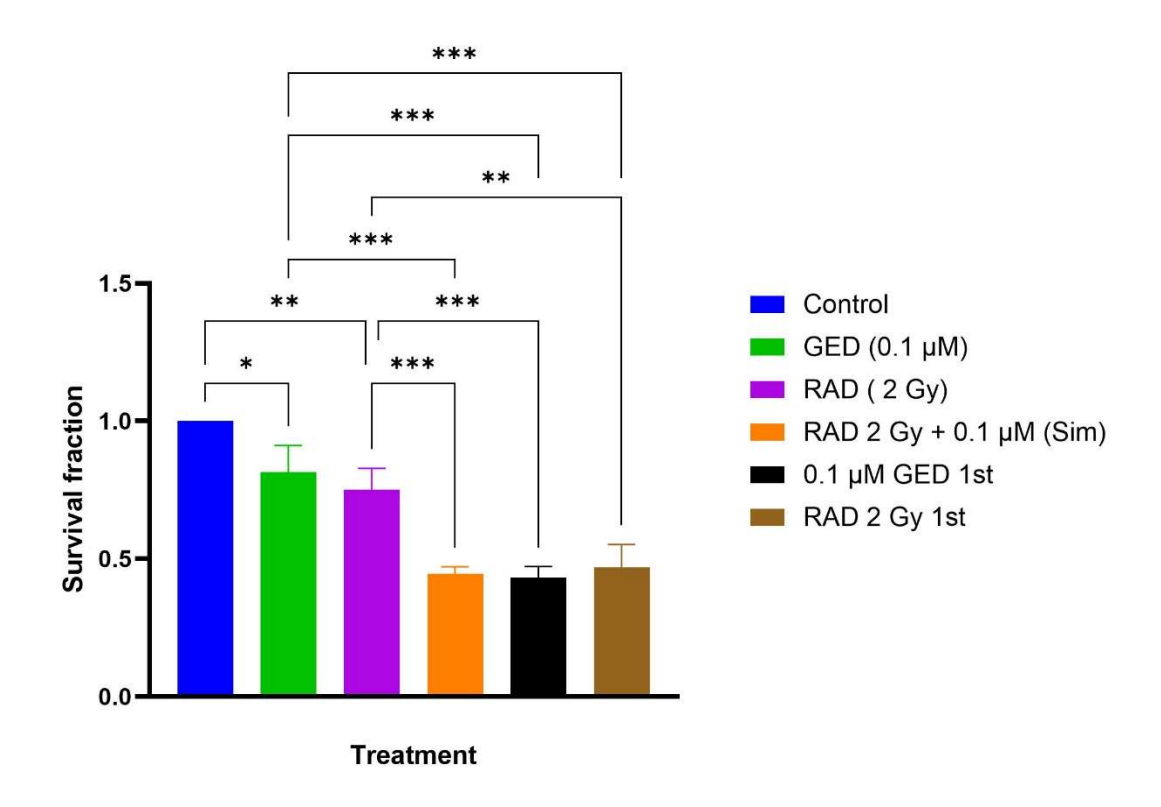


Figure 4-7 Survival fraction of RR-MDA-MB-231 cells exposed to gedatolisib –radiation scheduled combination therapy.

RR-MDA-MB-231 cell survival fractions following exposure to scheduled combinations of 0.1 μ M gedatolisib (GED) with 2 Gy radiation (RAD). Data represents the mean \pm SD of the survival fraction of the treated cells normalised to the untreated control for 3 independent experiments performed in triplicate. Statistical analysis was done using one-way ANOVA with Tukey's multiple comparisons test performed by GraphPad Prism 10.3.1. The difference considered significant when P value < 0.05 where *P < 0.05, **P < 0.01, ***P < 0.001 and ****P < 0.0001.

The clonogenic survival assay assessing the scheduled combination of 0.1 μM gedatolisib (GED) with 2 Gy radiation (RAD) in RR-MDA-MB-231 cells demonstrated a statistically significant reduction in cell survival across all scheduled combinations compared to the untreated control (P<0.0001) (Figure 4.7). Furthermore, treatment with 0.1 μM gedatolisib alone and 2Gy radiation alone significantly decreased survival fractions relative to the untreated control, with P<0.05 and P<0.01, respectively. However, the highest reduction in clonogenic survival was demonstrated in the combination treatment groups.

Simultaneous combination of 0.1 μ M gedatolisib and 2Gy radiation resulted in a highly significant decrease in survival compared to the untreated control (P < 0.0001) and each single treatment (P<0.001). Similarly, the subsequent administration of 0.1 μ M gedatolisib followed by 2Gy radiation (GED 1st) or vice versa (RAD 1st), both resulted in statistically significant low survival compared to the untreated control (P < 0.000) for both combinations, as well as when compared to 0.1 μ M gedatolisib (P < 0.001 for both combinations) and 2Gy radiation alone (P <0.001and P <0.01, respectively). Interestingly, there were no statistically significant differences among the three scheduled combinations, suggesting that the improved therapeutic effect was consistent across different treatment modalities.

Collectively, these findings highlight the potential therapeutic benefit of combining gedatolisib with radiation in overcoming resistance in TNBC. The consistency of improved cytotoxicity across all scheduled combinations suggests the reliability of this combination in improving radiosensitisation of TNBC cells. It also shows that the schedule of treatments is not essential in the efficacy of the combination.

4.3.3.4 Clonogenic survival assay for (RR)- MDA-MB-231 cell line following exposure to scheduled combination of gedatolisib and doxorubicin

Based on the data of gedatolisib-doxorubicin combination shown in Figure 4.4, the concurrent administration of 0.1 µM gedatolisib and 0.01 µM doxorubicin resulted in lower RR-MDA-MB-231 cell survival than single agents and other combinations. The clonogenic survival assay was utilised to investigate whether giving doxorubicin first or gedatolisib first would induce RR-MDA-MB-231 cell killing more than the administration of both drugs simultaneously, and the results are displayed in Figure 4.8

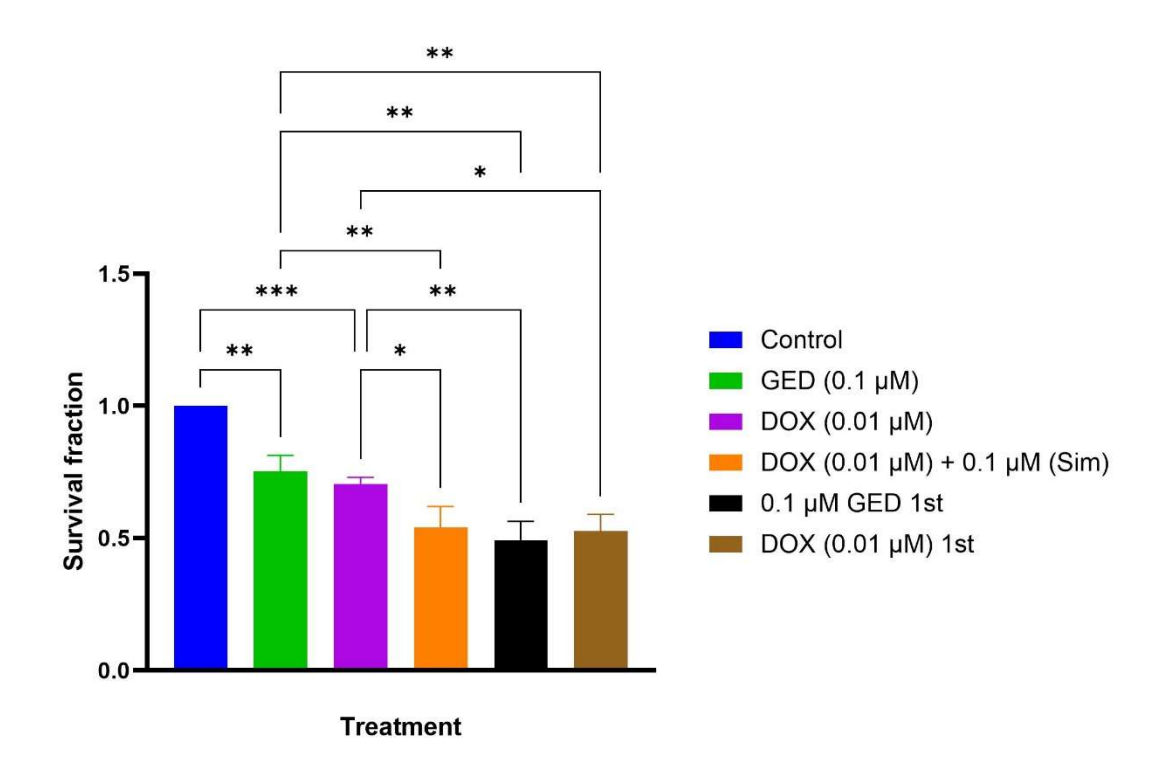


Figure 4-8 Survival fraction of RR-MDA-MB-231 cells exposed to gedatolisib-doxorubicin scheduled combinations.

RR-MDA-MB-231 cell survival fractions following treatment with scheduled combination therapy of 0.1 μ M gedatolisib (GED) with 0.01 μ M doxorubicin (DOX). Data represents the mean \pm SD of the survival fraction of the treated cells normalised to the untreated control for 3 independent experiments performed in triplicate. Statistical analysis was done using one-way ANOVA with Tukey's multiple comparisons test performed by GraphPad Prism 10.3.1. The difference considered significant when P value < 0.05 where *P < 0.05, **P < 0.01, ***P < 0.001 and ****P < 0.0001.

Figure 4.8 revealed that treatment of RR-MDA-MB-231 cells with 0.1 µM gedatolisib alone or 0.01 µM doxorubicin alone significantly decreased the survival compared to the untreated control (P < 0.01, P < 0.001, respectively. The clonogenic survival for the assessed scheduled combinations with 0.1 µM gedatolisib and 0.01 µM doxorubicin demonstrated a significant reduction in cell survival of RR-MDA-MB-231 cells compared to the untreated control (P<0.0001 for all scheduled combinations) (Figure 4.8). The simultaneous combining of 0.1 µM gedatolisib with 0.01 µM doxorubicin produced a statistically significant reduction in clonogenic survival relative to gedatolisib alone (P <0.01) and doxorubicin alone (P<0.05). Likewise, sequential administration of 0.1 µM gedatolisib first (GED 1st) or 0.01 µM doxorubicin first (DOX 1st) also resulted in significant survival reduction compared to either drug alone. Particularly, GED 1st reduced survival significantly compared to single treatments (P <0.01), while DOX 1st also decreased clonogenic survival in comparison to individual gedatolisib (P< 0.01) and individual doxorubicin (P<0.05). Despite the demonstrated improvement in the cytotoxic effects, there was no statistically significant difference in the clonogenic survival among the three scheduled combinations themselves. Taken together, these results underscore the potential advantages of combining gedatolisib and doxorubicin in reducing the survival of radioresistant TNBC cells, suggesting that the administration time may be flexible without impacting therapeutic effectiveness.

To contextualise the findings and directly compare the efficacy of single and combination treatments between the parental (WT-MDA-MB-231) and radioresistant (RR-MDA-MB-231) cell lines, a summary table was provided (Table 4.1) This comparison particularly focuses on the two most effective combinations produced greater survival reduction demonstrated in both cell lines, 0.1 µM gedatolisib with 0.01 µM doxorubicin and 0.1 µM gedatolisib with 2 Gy radiation. The table summarises the

survival fractions, statistical differences, and a comparative interpretation of response between the two cell lines, providing insight into whether these combinations maintain their efficacy in the resistant phenotype and highlighting their potential translational relevance.

Treatment Group	WT-MDA- MB-231 (Mean ± SD)	RR-MDA-MB- 231 (Mean ± SD)	Statistical Comparison (P value)	Comparative Outcome Summary
GED (0.1 μM)	0.77± 0.07	0.81 ± 0.06	ns (P = 0.998)	Comparable survival reduction in both cell lines
DOX (0.01 μM)	0.63± 0.08	0.77 ± 0.05	ns (P = 0.976)	Similar overall sensitivity, no significant difference identified
RAD (2Gy)	0.49 ± 0.06	0.757 ± 0.07	** (P =0.0014)	Significant survival reduction in (WT) compared to (RR)
GED + DOX (Simultaneous)	0.44± 0.063	0.54 ± 0.064	ns (P = 0.858)	Slightly greater reduction in WT compared to RR
GED + RAD (Simultaneous)	0.37 ± 0.036	0.45 ± 0.02	ns (P = 0.983)	Comparable survival reduction in both cell lines

Table 4.1 Comparative clonogenic survival of wild type (WT) and RR-MDA-MB-231 cells following single and combination treatments.

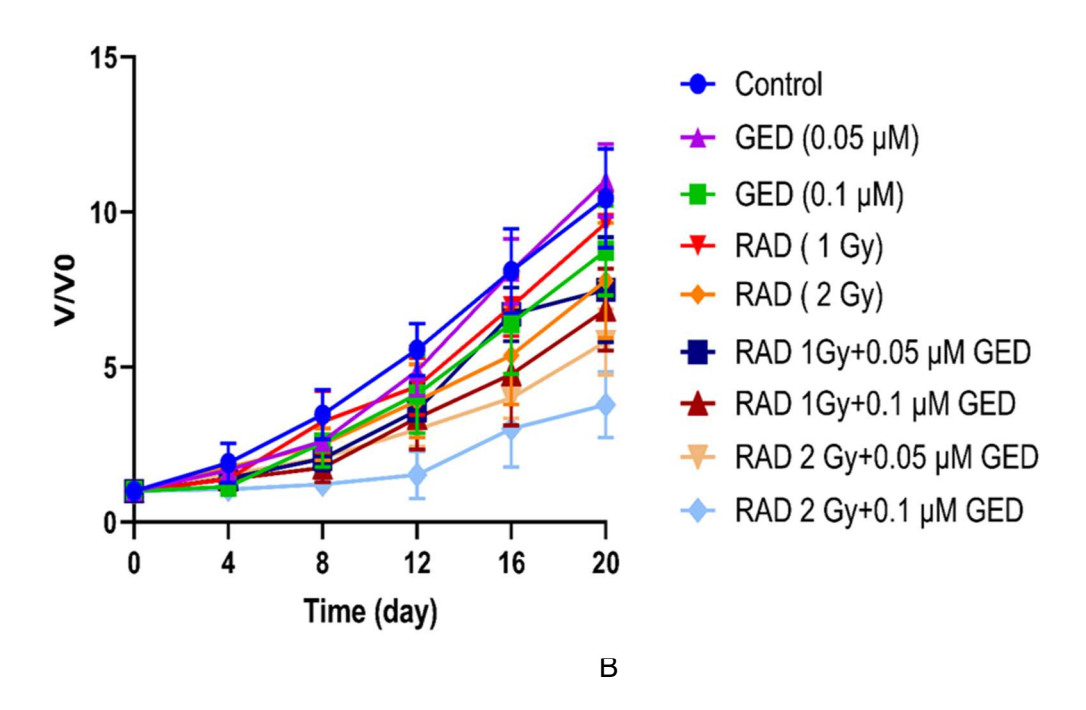
4.3.4 Evaluation of the effect of gedatolisib, doxorubicin, and radiation treatments alone and in combination using (RR)- MDA-MB-231 spheroids.

Following the cytotoxicity assessment of gedatolisib - radiation or doxorubicin combination therapy by two dimensional clonogenic assay, three-dimensional tumour spheroids have been employed to evaluate the effectiveness of these therapeutic regimens in terms of tumour growth retardation. The concentrations of gedatolisib and doxorubicin as well as the radiation doses assessed in the clonogenic survival assay were also assessed in tumour spheroids to investigate their effectiveness in a more complex model which is more representative of tumours in vivo. Spheroids were imaged every 3-4 days following treatment with single and combination therapy to measure the volume and monitor the growth development at different time intervals.

4.3.4.1 Evaluation of the effect of gedatolisib and radiation treatments alone and in combination using (RR)- MDA-MB-231 spheroids

The RR-MDA-MB-231 spheroids were exposed to a single and combination of 0.05 and 0.1 µM gedatolisib with 1 and 2 Gy radiation doses, with both treated and untreated spheroids being monitored for growth over 2-3 weeks. The changes in spheroids volumes at different time points (every 3-4 days) relative to the initial volume (time 0) were measured which reflects the tumour spheroids growth. The growth curves of RR-MDA-MB-231 spheroids exposed to single and different combination therapies of gedatolisib plus radiation as well as the untreated controls are shown in Figure 4.9A. The statistical comparisons among assessed single and combination therapy are shown in Figure 4.9B. To visualize the tumour spheroid growth, the images of representative spheroids at different time points for different assessed groups are shown in Figure 4.10.





Tukey's multiple comparison test	P (*)	Below threshold?	P-value
Control vs. GED (0.1 µM)	**	Yes	0.0029
Control vs. RAD 2 Gy)	****	Yes	<0.0001
Control vs. RAD 2 Gy+0.1 µM GED	****	Yes	<0.0001
GED (0.1 μM) vs. RAD 2 Gy+0.1 μM GED	****	Yes	<0.0001
RAD (2 Gy) vs. RAD 2 Gy+0.1 µM GED	****	Yes	<0.0001

Figure 4-9 Growth curve of RR-MDA-MB-231 spheroids following exposure to a combination of gedatolisib and radiation.

A: The RR-MDA-MB-231 spheroids growth curves following exposure to a combination of 0.05 and 0.1 μ M of gedatolisib with 1 Gy and 2 Gy of radiation. Spheroids were imaged every 3-4 days to measure their volume (V), and V/V₀ represents the change in the volume at each time point (day X) over the initial volume (day 0). Data represents an average of V/V₀ ± SD at different time points. 24 spheroids were assessed for each treatment group, and 3 independent experiments were performed. The Statistical analysis was performed using GraphPad Prism 10.3.1 with two-way ANOVA. B: Tukey's multiple comparisons test, and the difference was considered significant when P value < 0.05 where *P < 0.05, **P < 0.01, ***P < 0.001 and ****P < 0.0001

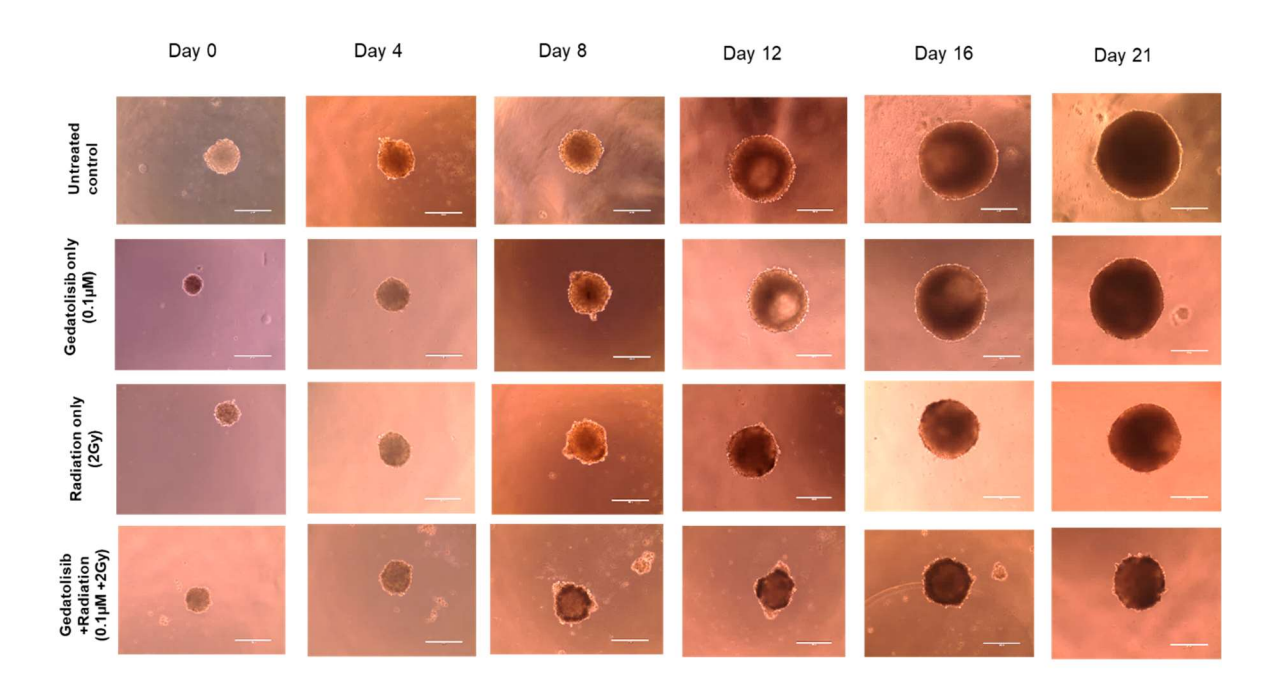


Figure 4-10 RR-MDA-MB-231 representative spheroids images treated with gedatolisib and radiation combination.

Representative MDA-MB-231 tumour spheroids images following exposure to single and combination of 0.1 μ M gedatolisib with 2 Gy radiation. Spheroid were imaged by EVOS microscope with 10X power lens.

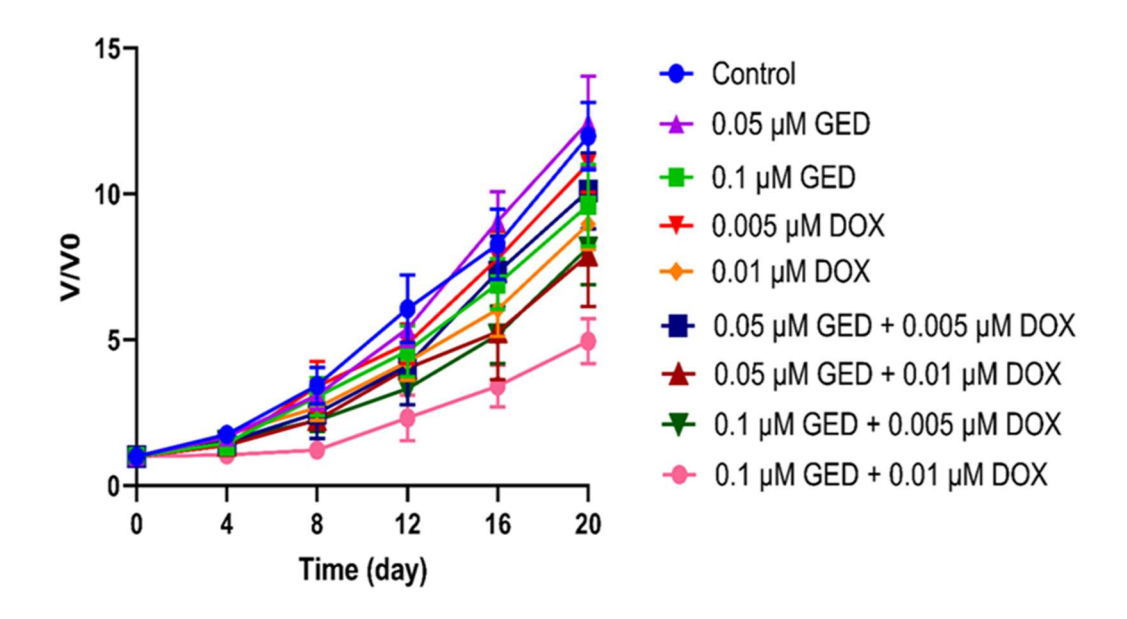
The RR-MDA-MB-231 spheroid growth was assessed post-treatment with 0.05 µM and 0.1 µM gedatolisib, 1 Gy and 2 Gy radiation, and their combinations. Spheroids exposed to either 0.05 µM gedatolisib or 1 Gy radiation alone displayed no statistically significant differences in volumes compared to the untreated controls (P > 0.05), implying limited efficacy as single treatments at these doses. However, 0.1 µM gedatolisib or 2 Gy radiation alone significantly decreased spheroid volume relative to the untreated control (P< 0.0001 and P < 0.05, respectively). Furthermore, the combination of 0.05 µM gedatolisib with 1 Gy radiation significantly reduced spheroid volume compared to the untreated control (P < 0.0001), but not when compared to either agent alone (P > 0.05). Similarly, combining 0.1 µM gedatolisib with 1 Gy radiation significantly decreased spheroid growth in comparison to the untreated control (P < 0.0001), however, no statistically significant differences relative to 0.1 μM gedatolisib alone (P > 0.05). Interestingly, the higher demonstrated reduction of spheroid volume was shown when 0.1 µM gedatolisib was simultaneously combined with 2Gy radiation, resulting in significantly lower spheroid growth than the untreated control and both single agents (P < 0.001). The full statistical comparison table for the investigated doses and concentrations of monotreatment and their combinations in the RR-MDA-MB-231 cell line are shown in the Appendix.

Taken together, these findings underscore that the combination of gedatolisib and radiation improves the therapeutic effectiveness in RR-MDA-MB-231 spheroids, with the 0.1 µM gedatolisib + 2Gy radiation combination producing the highest spheroid volume reduction effect.

4.3.4.2 Evaluation of the effect of gedatolisib and doxorubicin treatments alone and in combination using (RR)- MDA-MB-231 spheroids

To assess the effectiveness of gedatolisib-doxorubicin combination therapy, the RR-MDA-MB-231 spheroids were incubated with single and combination of 0.05 μ M and 0.1 μ M gedatolisib with 0.005 μ M and 0.01 μ M doxorubicin. The spheroids were imaged every 3-4 days to measure the volume (V), and the treated and untreated spheroids were monitored for growth over 2-3 weeks. The changes in spheroids volumes at different time points (every 3-4 days) relative to the initial volume (time 0) were measured as V/V0 which reflects the tumour spheroids growth. Figure 4.11.A displays the spheroidal growth curves for the single and combination therapy and the statistical comparisons among assessed single and combination therapies are shown in Figure 4.11.B. The representative spheroids treated with gedatolisib-doxorubicin as single and combination therapy and imaged at different time points are shown in Figure 4.12





В

Tukey's multiple comparison test	Below	Р	P-value
	threshold?	(*)	
Control vs. 0.1 µM GED	Yes	****	<0.0001
Control vs. 0.01 µM DOX	Yes	****	<0.0001
0.1 μM GED vs. 0.1 μM GED + 0.01 μM DOX	Yes	****	<0.0001
0.01 μM DOX vs. 0.1 μM GED + 0.01 μM DOX	Yes	****	<0.0001

Figure 4-11 Growth curve of RR-MDA-MB-231 spheroids treated with single and combination of gedatolisib and doxorubicin.

A: The RR-MDA-MB-231 spheroids growth curves following exposure to a combination of 0.05 and 0.1 μ M of gedatolisib with 0.005 μ M and 0.01 μ M doxorubicin. Spheroids were imaged every 3-4 days to measure their volume (V), and V/V₀ represents the change in the volume at each time point (day X) over the initial volume (day 0). Data represents an average of V/V₀ ± SD at different time points. 24 spheroids were assessed for each treatment group, and 3 independent experiments were performed. The Statistical analysis was performed using GraphPad Prism 10.3.1 with two-way ANOVA. B: Tukey's multiple comparisons test, and the difference was considered significant when P value < 0.05 where *P < 0.05, **P < 0.01, ***P < 0.001 and ****P < 0.0001

Figure 4.11 revealed that treatment of RR-MDA-MB-231 spheroids with 0.05 μ M gedatolisib or 0.005 μ M doxorubicin alone did not significantly reduce the spheroid volume compared to the untreated controls (P > 0.05). Combining of these low concentrations (0.05 μ M GED + 0.005 μ M DOX) produced a significant reduction in spheroid volume compared to untreated control (P < 0.0001), however, no statistically significant difference was found compared to each drug alone (P > 0.05), suggesting minimal advantages at this concentration level of combination.

Increasing the concentrations of each drug produced a pronounced decrease in spheroid volume. Notably, administration of $0.1\mu\text{M}$ gedatolisib or $0.01\mu\text{M}$ doxorubicin as an individual treatment significantly reduced spheroid volume compared to the untreated controls (P<0.0001), while combining them with lower doses resulted in a significant decrease in spheroid volume. Among these, $0.05\,\mu\text{M}$ GED + $0.01\,\mu\text{M}$ DOX, $0.1\,\mu\text{M}$ GED + $0.005\,\mu\text{M}$ DOX, and $0.1\,\mu\text{M}$ GED + $0.01\,\mu\text{M}$ DOX all produced statistically significant reductions in spheroid volume compared to the untreated control (P < 0.0001). Importantly, the combination of $0.1\,\mu\text{M}$ gedatolisib and $0.01\,\mu\text{M}$ doxorubicin showed a statistically significant difference in comparison to the untreated control (P < 0.0001) and to each drug administered alone (P < 0.0001), inducing the highest RR-MDA-MB-231 spheroid volume reduction. The full statistical comparison table for the investigated concentrations of monotreatment and their combinations in the RR-MDA-MB-231 cell line are shown in the Appendix.

Collectively, the data suggest a beneficial combination of gedatolisib with doxorubicin in decreasing the RR-MD-MB-231 spheroid growth, particularly the combination of 0.1µM gedatolisib with 0.01 µM doxorubicin. This effect supports our hypothesis that combining gedatolisib with doxorubicin or radiation improves the treatment outcomes in radioresistant TNBC.

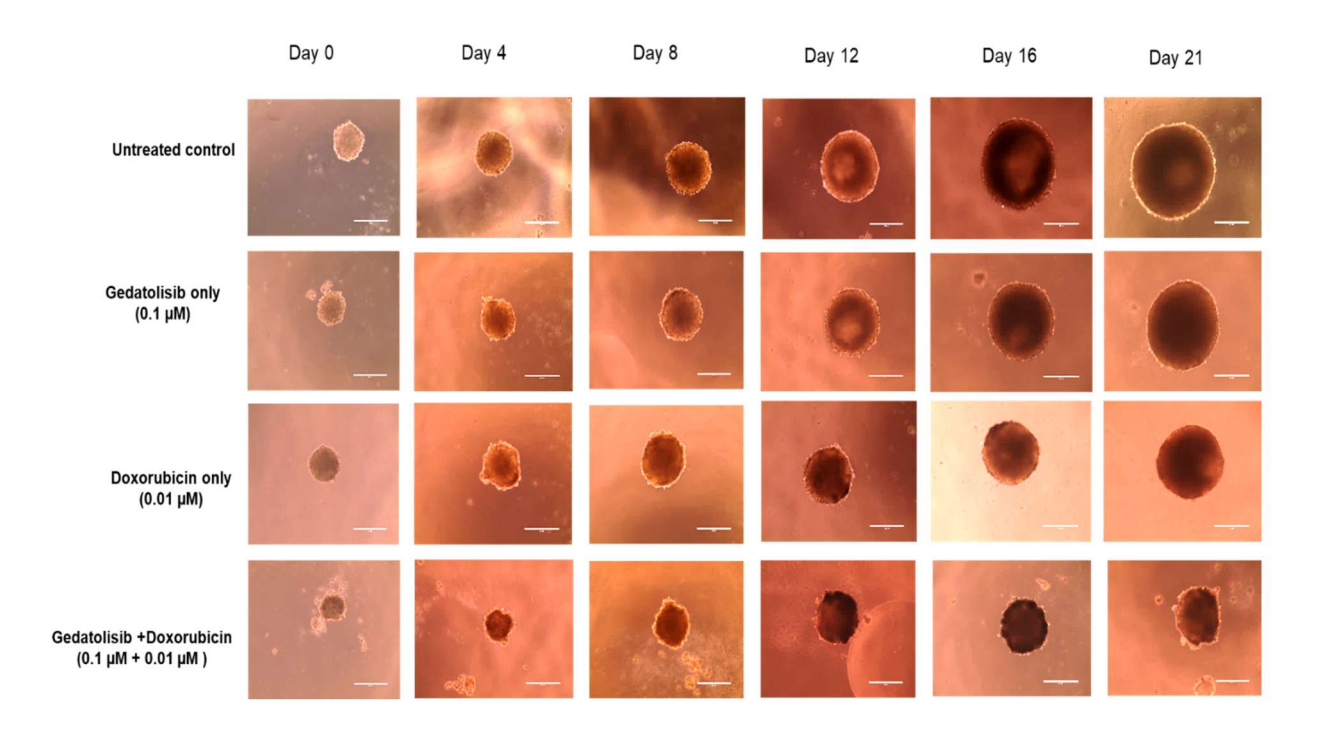


Figure 4-12 RR-MDA-MB-231 spheroids images across different time points following treatment with Gedatolisib-Doxorubicin combination therapy.

Representative MDA-MB-231 tumour spheroids images following incubation with single and combination of 0.1 μ M gedatolisib with 0.01 μ M doxorubicin. Spheroid were imaged by EVOS microscope with 10X power lens.

To compare the behaviour of the wild type and the radioresistant MDA-MB-231 cell lines following exposure to the combination of gedatolisib with either doxorubicin or radiation, a summary table was generated (Table 4.2). We focus on the combination that showed the best results in both cell lines spheroids, 0.1 μ M gedatolisib with 0.01 μ M doxorubicin, and 0.1 μ M gedatolisib with 2 Gy radiation. Therefore, the following table summarises the comparative spheroid volume changes (V/V₀) at the final time point (20 days after exposure to treatments) across both cell lines for these selected

combinations, providing a direct comparison of treatment responses between WT and RR-MDA-MB-231 spheroids.

Treatment Group	WT-MDA-MB- 231(V/V ₀ ± SD)	RR-MDA-MB- 231(V/V ₀ ± SD)	Statistical Comparison (P value)	Comparative Outcome Summary
Untreated control	11.98 ± 1.06	12.29 ± 0.74	ns (P = 0.937)	Comparable baseline growth between cell lines
GED (0.1 μM)	8.35 ± 1.40	9.61 ± 1.28	ns (P = 0.81)	Comparable spheroid volume reduction in both cell lines
DOX (0.01 μM)	9.44 ± 0.62	8.96 ± 0.78	ns (P = 0.976)	Volume reduction in both types of spheroids, with no statistically significant difference
RAD (2Gy)	6.42 ± 1.47	8.31±1.32	* (P =0.037)	V/V0 was higher and statistically significant in RR compared to WT.
GED + DOX (Simultaneous)	3.76 ± 0.68	4.95 ± 0.71	ns (P = 0.751)	Comparable spheroid volume reduction in both cell lines
GED + RAD (Simultaneous)	2.58 ± 1.04	3.78 ± 0.95	ns (P = 0.897)	Volume reduction was demonstrated in both cell lines, with no statistical differences.

Table 4.2 Comparative spheroid volume change (V/V_0) in WT- and RR-MDA-MB-231 at 20 days following treatment with Single agents and their combinations.

4.3.5 Evaluation of the mechanistic effect of single and combination treatments in RR-MDA-MB-231 Cells

The earlier experiments using clonogenic and spheroid assays demonstrated that treatment of the RR-MDA-MB-231 cells with a combination of gedatolisib and either radiation or doxorubicin resulted in a reduction of clonogenic survival and spheroid volume. However, the molecular mechanisms by which these combinations exert their effects and enhance treatment outcomes remain unidentified. Mechanistic assays, including cell cycle distribution, DNA damage, and apoptotic induction, were performed to elucidate the mechanisms driving responses of the RR-MDA-MB-231 cells to treatments.

4.3.5.1 Evaluation of RR-MDA-MB-231 cell cycle progression following treatment with a combination of gedatolisib with doxorubicin or radiation

To investigate the impact of gedatolisib, doxorubicin, radiation, and their combination on RR-MDA-MB-231 cell cycle progression, a flow cytometry-based cell cycle assay analysis was conducted at different time points following treatment. Based on the data of clonogenic and spheroids, the combination of 0.1 µM gedatolisib and 2 Gy radiation had the best cell growth inhibition activity from the assessed combination therapies. Additionally, a higher cell survival reduction resulted following treatment with a combination of 0.1 µM gedatolisib with 0.01 µM doxorubicin compared to each drug alone. The clonogenic and spheroid data suggest a promising combination of 0.1 µM gedatolisib with either 2Gy radiation or 0.01 µM doxorubicin, inducing higher cell killing than other assessed combinations. Therefore, the cell cycle assay was performed to evaluate the effect of these combinations and their single agents on cell cycle phase distribution. The RR-MDA-MB-231 cells were harvested at different time

points following exposure to different combination therapies to demonstrate the cell population at each phase, as described in section 2.11. The distribution of cells across S/G1, G1, S, and G2/M phases was counted and are shown in Figure 4.13 A-B

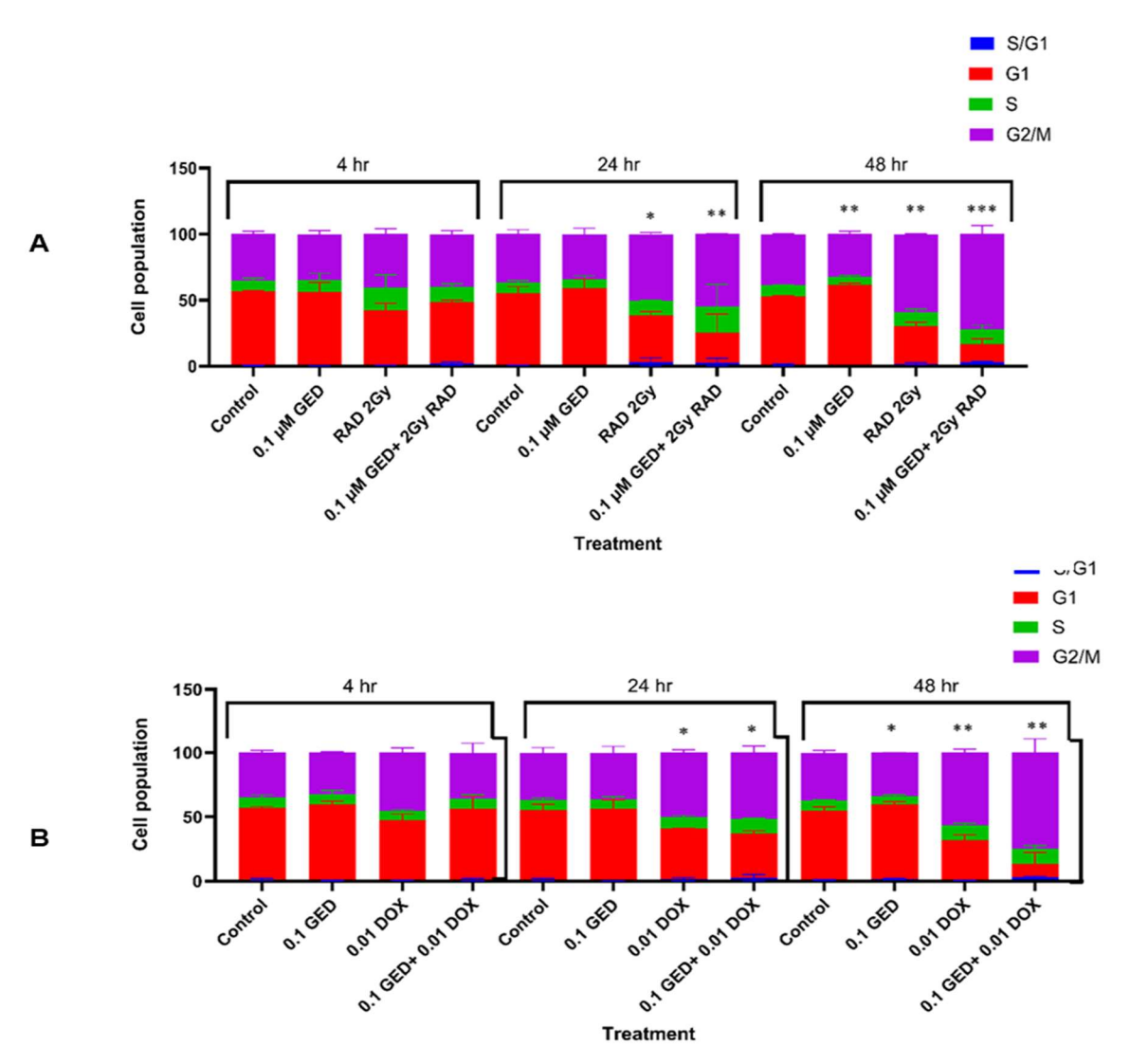


Figure 4-13 RR-MDA-MB-231 Cell cycle phases distribution following treatment with a simultaneous combination of gedatolisib with radiation or doxorubicin

The distribution of RR-MDA-MB-231 across the phases of the cell cycle over time following exposure to (A) 0.1 μ M of gedatolisib and 2 Gy radiation (B) 0.1 μ M of gedatolisib and 0.01 μ M doxorubicin, both as a single and in combination. Data represents the mean \pm SD of the cell population in each phase of the treated cells

that normalized to control for 3 independent experiments performed in triplicate. Statistical analysis was done using one-way Anova with Tukey's multiple comparisons test and it was performed using GraphPad Prism 10.3.1. The difference considered significant when P value < 0.05 where *P < 0.05, **P < 0.01, ***P < 0.001 and ****P < 0.0001.

The data demonstrated no significant changes in the cell cycle distribution of the cells at 4hr post treatment (P>0.05), which indicates that gedatolisib, doxorubicin, and radiation did not significantly alter cell cycle distribution or induce significant cell cycle arrest soon after treatment of RR-MDA-MB-231 cells. At 24 hr following treatment, there was a statistically significant accumulation of cells at G2/M phase of the cycle in groups treated with 2 Gy radiation, 0.01 µM doxorubicin and combination of gedatolisib with doxorubicin and radiation compared to untreated control (P<0.05). However, gedatolisib alone did not induce significant shifts in the phase distribution at this time point. A statistically significant accumulation at G2/M phase was also noted at 48hr following treatment with single radiation and doxorubicin as well as their combination with gedatolisib, compared to untreated control(P<0.01), which indicates a prolonged cell cycle arrest at this phase. Administration of gedatolisib alone increased cell accumulation at the G1 cell cycle phase compared to single radiation and doxorubicin alone, as well as their combination at 48 post treatment (P<0.05).

Taken together, these findings revealed that gedatolisib alone exerts no statistically significant impact on early cell cycle progression in RR-MDA-MB-231 cells, however, its combination with doxorubicin or radiation significantly enhances G2/M phase arrest at later time points, suggesting a potential mechanism by which treatment combinations impede cell division and improve therapeutic effectiveness in radioresistant TNBC.

4.3.5.2 Assessment of Apoptosis induction in RR-MDA-MB-231 cell line following exposure to single and combination treatments using Annexin V assay

An Annexin V assay was conducted to investigate the apoptotic effect of single and combination gedatolisib with either radiation or doxorubicin in RR-MDA-MB-231 cells. The cells were exposed to 0.01 µM gedatolisib, 2 Gy radiation, 0.01 µM doxorubicin and their combination (Ged +Rad and GED+ Dox). The cells were harvested at 4hr, 24hr and 48hr following treatment to assess the apoptotic response to the single and combination therapy. The proportion of the RR-MDA-MB-231 cells in early and late apoptosis following exposure to single and combination treatments are shown in Figures 4.16 A-B.

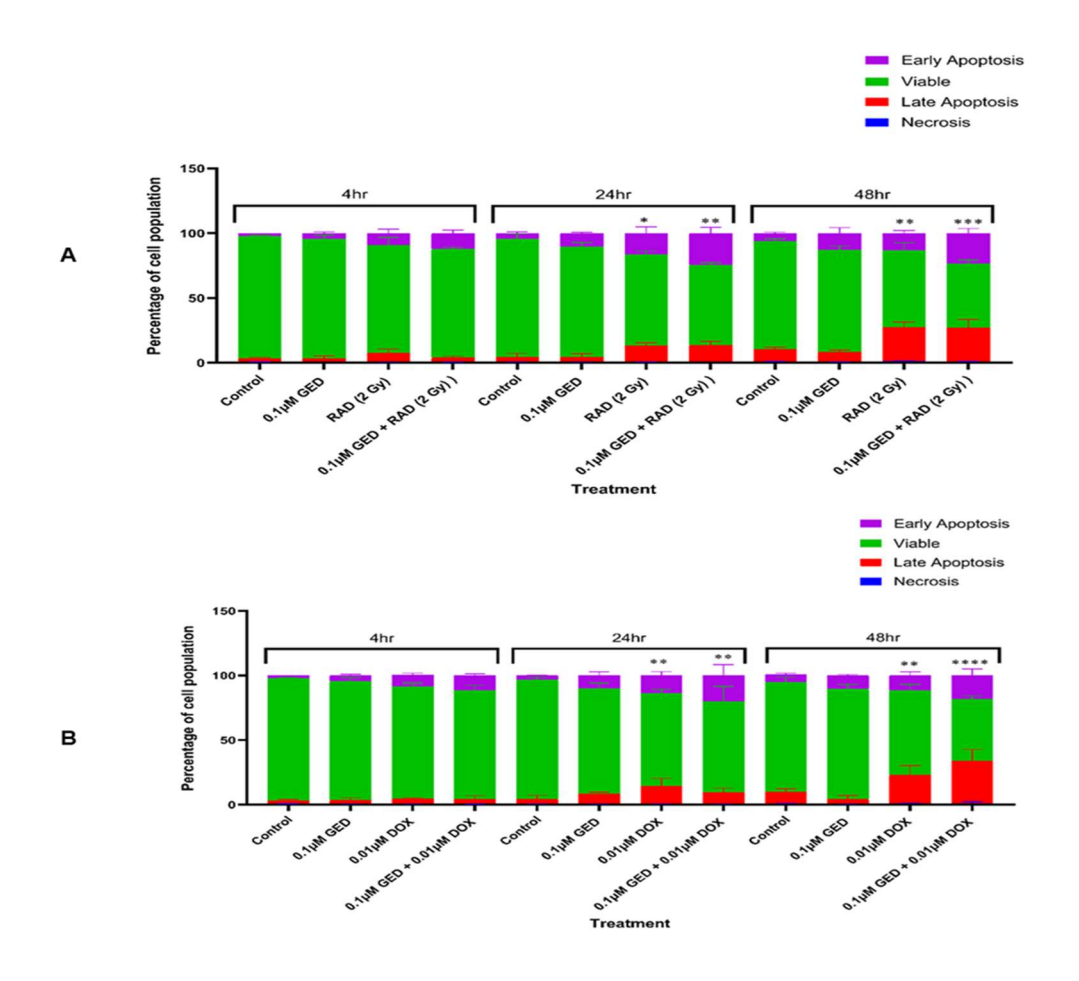


Figure 4-14 Apoptosis of MDA-MB-231 cells following treatment with simultaneous combination of gedatolisib with radiation or doxorubicin assessed by the Annexin V assay

RR-MDA-MB-231 cells were tested by Annexin V assay following exposure to (A) 0.1 μ M gedatolisib, 2 Gy radiation and their combination (B) 0.1 μ M gedatolisib, 0.01 μ M doxorubicin and their combination. The cells were harvested at 4hr, 24 hr, 48hr after treatment and stained with Annexin V and propidium iodide to identify viable, early apoptotic, late apoptotic and necrotic cells Data represents the mean plus SD of the cell population in each phase of the treated cells for 3 independent experiments performed in triplicate. Statistical analysis was employed using one-way ANOVA followed by Tukey's multiple comparisons test using GraphPad Prism 10.3.1. The difference considered statistically significant when P value < 0.05 where *P < 0.05, **P < 0.01, ***P < .001 and ****P < 0.0001.

The data in Figure 4.14 revealed variations in the apoptosis of RR-MDA-MB-231 cells to single and combination therapy of gedatolisib with radiation and doxorubicin. At 4hr after treatment which represents the early response of the cells, there were no significant variations in the cell proportions undergoing apoptosis in the treatment groups compared to the untreated control(P<0.05). This indicates low apoptosis induction at this early stage and some drugs may take time to induce programmed cell death. At 24 hr following treatment, the cells exposed to single treatments of radiation and doxorubicin and their combination with gedatolisib (gedatolisib + radiation and gedatolisib + doxorubicin) had a statistically significant proportion at early apoptosis compared to the untreated control (P<0.05). Furthermore, the cells treated with radiation or doxorubicin alone and harvested 48 hr after treatment, there was a significantly higher proportion of the late apoptotic cells compared to the untreated control (P<0.001). The combination of gedatolisib with radiation induced a significantly higher apoptosis than radiation alone (P<0.05) (Figure 4.14A). Additionally, cells treated with gedatolisib-doxorubicin combination showed a statistically significant increase in apoptosis compared to the untreated control (P<0.001) and doxorubicin alone (P<0.05) (Figure 4.14B). In cells treated with gedatolisib alone, there was no significant apoptosis difference in apoptosis across different time points (P>0.05).

Collectively, the data suggest that gedatolisib can improve apoptotic responses when combined with radiation or doxorubicin, supporting its mechanistic role in sensitizing resistant cells to cytotoxic agents.

4.3.5.3 Assessment of DNA damage in RR-MDA-MB-231 cells following exposure to combination of gedatolisib with doxorubicin and radiation utilising COMET assay

To investigate if the drop in clonogenic survival is a consequence of DNA damage in RR-MDA-MB-231 cells treated with gedatolisib, doxorubicin, radiation and their combinations, a COMET assay was performed. The RR-MDA-MB-231 cells were harvested at different time points following treatment with 0.01 µM gedatolisib, 2 Gy radiation, 0.01 µM doxorubicin and their combination (Ged +Rad and GED+ Dox), and run in a single cell gel electrophoresis as described in section 2.13. The electrophoresed cells were imaged and the presence of tail moments around the cells indicated double strand DNA damage which then was measured using ImageJ software. The tail moments were quantified for each group of treatment and control, and the data are shown in Figures 4.15 A-B

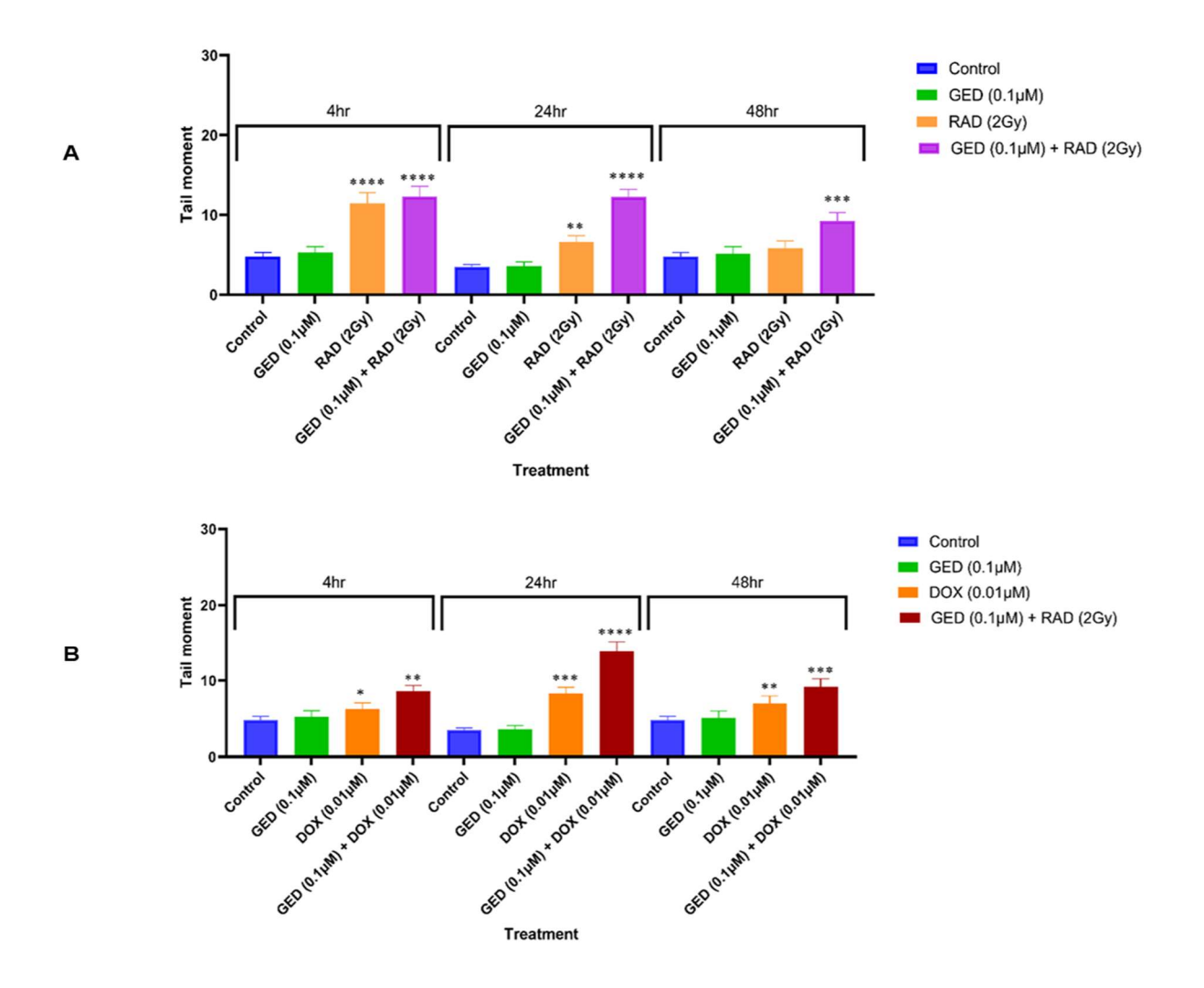


Figure 4-15 DNA damage in RR-MDA-MB-231 cells following treatment with a simultaneous combination of gedatolisib with radiation or doxorubicin assessed by COMET assay

Tail moment lengths of RR-MDA-MB-231 cells over time evaluated by COMET assay at 4hr, 24hr and 48hr following treatment with (A) 0.1 μ M gedatolisib, 2 Gy radiation and their combination (B) 0.1 μ M gedatolisib, 0.01 μ M doxorubicin and their combination. Data represents the mean \pm SD of the tail moments in the treated cell line for 3 independent experiments performed in triplicate. Statistical analysis was performed using GraphPad Prism 10.3.1 with one-way ANOVA and Tukey's multiple comparisons test. The difference considered significant when P value < 0.05 where *P < 0.05, **P < 0.01, ***P < 0.001 and ****P < 0.0001.

From Figure 4.15 we can observe that there are limited tail moments in the RR.MDA-MB-231 control cells that had no treatment, indicating minimal DNA damage and reflecting intact nuclear DNA integrity. However, the RR-MDA-MB-231 cells treated with doxorubicin or radiation alone displayed a statistically significant greater tail moments compared to untreated control and (P<0.001). Furthermore, treatment radiation alone induced a significantly higher DNA damage at 4hr compared to 48hr post-treatment (P < 0.05), suggesting that the initial damage may be partially repaired over time. The treatment with 0.1 µM gedatolisib alone did not induce significant DNA damage compared to untreated control across the investigated time points, indicating that gedatolisib does not directly induce DNA double strand breaks. However, combining 0.1µM gedatolisib with 2Gy radiation resulted in a statistically significant increase in tail moments at 4hr, 24hr and 48hr post treatment relative to radiation alone (P<0.05, P<0.001and P<0.0001, respectively) and untreated control (P<0.0001 at all-time points), suggesting a persistent DNA damage that may be partially repaired. Moreover, a combination of 0.1µM gedatolisib with 0.01µM doxorubicin produced greater tail moments compared to doxorubicin alone at all investigated time points (P<0.01, P<0.0001 and P<0.001, respectively), possibly reflecting attenuated DNA repair mechanisms after treatment with this combination.

Collectively, the current results indicate that while gedatolisib does not induce direct DNA damage g, its use in combination with radiation or doxorubicin significantly increased DNA damage in RR-MDA-MB-231 cells, potentially by impairing DNA repair pathways and thereby sensitizing resistant cells to genotoxic treatments.

To provide a comparative summary of the mechanistic responses observed in wild-type (WT) and radioresistant (RR) MDA-MB-231 cell lines following treatment with selected single agents and their combinations, a summary table is provided below. Key findings from cell cycle distribution, apoptosis induction (Annexin V assay), and

DNA damage (COMET assay) are summarised to elucidate variations in treatment effectiveness between the two cell lines.

4.3.5.4 Assessment of the effect of gedatolisib on autophagy in the RR-MDA-MB-231 cell line

The cytotoxic effect of gedatolisib in the RR-MDA-MB-231 cell line was demonstrated utilising clonogenic assay and spheroid growth delay experiments. Mechanistic assays, including Annexin V, cell cycle analysis, and COMET assay, were performed to investigate the mechanisms by which the single and combination treatments induced cell death. However, gedatolisib as a single agent did not induce statistically significant changes in the apoptosis, suggesting that this drug may induce cell death via other mechanisms. An Autophagy assay was therefore conducted, as we hypothesised that gedatolisib treatment would induce autophagy in RR-MDA-MB-231 cells, thus decreasing the cell survival and spheroid growth. The cells were incubated with 0.05 μ M and 0.1 μ M (IC₁₀ and IC₂₅) of gedatolisib and harvested at 24 hr and 48 hr post treatment as described in section 2.15. The stained autophagic vacuoles were imaged by confocal microscopy and quantified by ImageJ software, and the results are shown in Figure 4.17

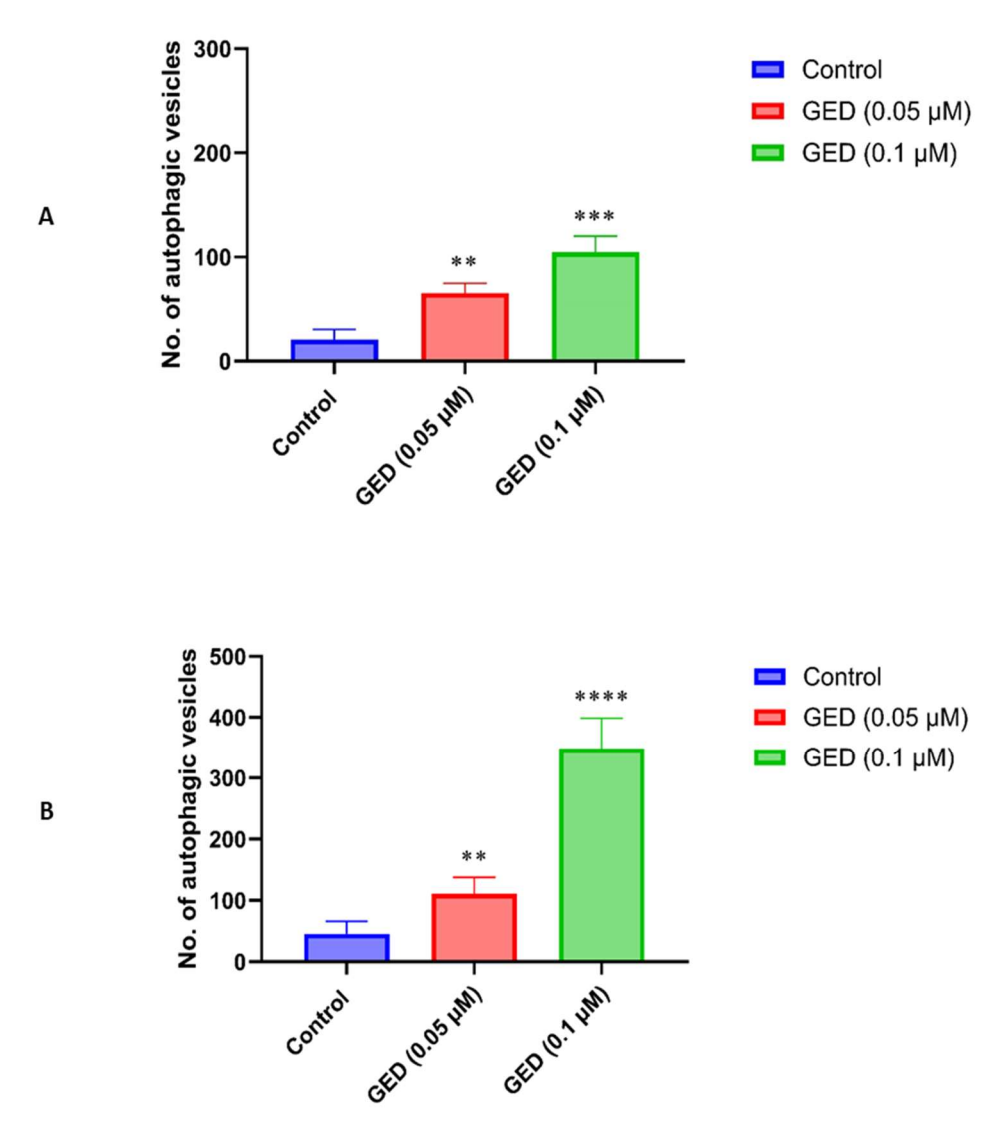


Figure 4-16 Assessment of induction of autophagy by gedatolisib in RR-MDA-MB-231 cells utilising an autophagy assay.

Autophagy vesicles in RR-MDA-MB-231 cells at different time points were evaluated by Autophagy assay following exposure to 0.05 μ M and 0.1 μ M (around IC₁₀ and IC₂₅, respectively) of gedatolisib as a single agent. The autophagy vacuoles were quantified utilising Image software and plotted as A: 24 hr and B: 48 hr after treatment. Data represents the mean \pm SD of the number of autophagy vesicles in the treated cell line for 3 independent experiments performed in triplicate. Statistical analysis was performed using GraphPad Prism 10.3.1 with one-way ANOVA with Tukey's multiple comparisons test. The difference considered significant when P value < 0.05 where *P < 0.05, **P < 0.01, ***P < 0.001 and ****P < 0.0001.

From Figure 4.17, the data showed that both drug concentrations tested (0.05 μ M and 0.1 μ M) resulted in a significant increase in the number of autophagy vacuoles in the treatment group compared to untreated controls (P<0.001), supporting our hypothesis that gedatolisib induced autophagy. Additionally, 0.1 μ M gedatolisib produced significantly more autophagy vacuoles than 0.05 μ M gedatolisib (P<0.001) at 24 hr and 48 hr following treatment indicating the concentration dependent induction of autophagy.

Taken together, the results indicate that gedatolisib induces an effective, concentration-dependent autophagic response in RR-MDA-MB-231 cells, confirming our hypothesis that autophagy is a key non-apoptotic mechanism underpinning the RR-MDA-MB-231 cell killing by gedatolisib.

4.3.5.5 Evaluation the effect of gedatolisib on the expression of PI3K/Akt/mTOR pathway in RR-MDA-MB-231 cell line using western blot analysis

Gedatolisib is a potent dual inhibitor that directly targets class I PI3K isoforms and both mTOR complexes (mTORC1 and mTORC2) within the PI3K/Akt/mTOR signalling pathway. Although gedatolisib does not directly inhibit Akt, this kinase is a critical downstream effector of PI3K activation and can also be phosphorylated by mTORC2. Thus, evaluating Akt expression provides a valuable indicator of effective PI3K/mTOR pathway inhibition. In this experiment, Western blot analysis was employed to assess the effects of low gedatolisib concentrations (0.05 µM and 0.1 µM) that were used earlier in clonogenic survival and spheroid on Akt protein levels in RR-MDA-MB-231 cells. The objective was to determine whether gedatolisib modulates Akt expression as a consequence of upstream pathway inhibition, thereby contributing to its observed effects of reducing clonogenic survival and spheroid

growth. The RR-MDA-MB-231 cells were incubated with gedatolisib and harvested at different time points after treatment to quantify the protein expression as described in section 2.14. The protein band densities at the investigated time points are shown in Figure 4.17

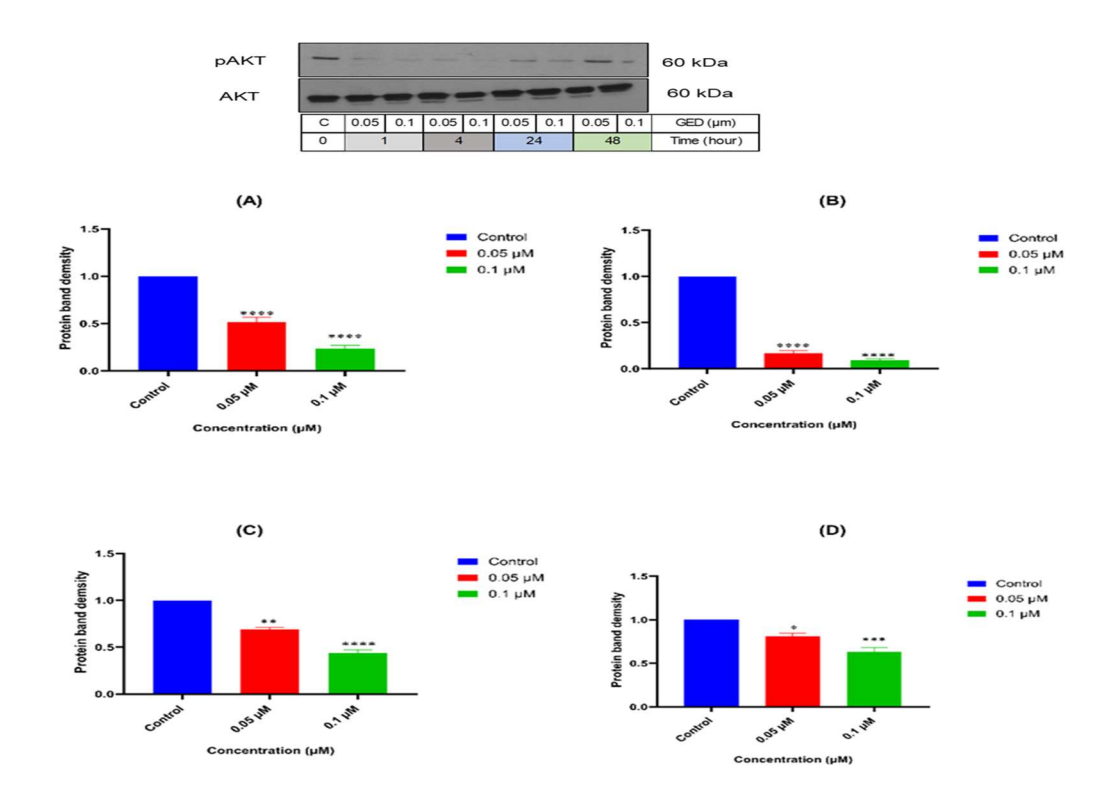


Figure 4-17 Evaluation of the effect of gedatolisib on the expression of Akt protein in RR-MDA-MB-231 cells using western blot analysis

Signal intensity of AKT protein expression in RR-MDA-MB-231 cells over time was assessed by western blot analysis following exposure to 0.05 µM and 0.1 µM of gedatolisib as a single therapy. Data represents the mean plus SD of the protein band signals in the treated and untreated (Control) cells for 3 independent experiments performed in triplicate. The band densities were quantified utilising Image software and plotted as A: 1 h, B: 4 hr, C: 24 hr and D: 48 hr after treatment. Data represents the mean plus SD of the band densities in the treated cell line normalized to control for 3 independent experiments performed in triplicate. Statistical analysis was performed using GraphPad Prism 10.3.1 with one-way ANOVA with Tukey's multiple comparisons test. The difference considered

significant when P value < 0.05 where *P < 0.05, **P < 0.01, ***P < 0.001 and ****P < 0.0001.

The data in Figure 4.17 demonstrated that Akt protein expression was significantly decreased at all the time points measured following exposure to gedatolisib in comparison to untreated controls (P<0.05), indicating a drug-induced pathway inhibition. Furthermore, 0.1 µM of gedatolisib produced a significant reduction in protein abundances relative to untreated control (P<0.001) which was also statistically greater than the other concentration (P<0.05), as shown in Figure 4.17, reflecting a concentration dependent inhibition for this pathway.

These findings revealed that even at low concentrations, gedatolisib effectively suppresses Akt expression in RR-MDA-MB-231 cells, confirming its role in inhibiting the PI3K/mTOR signalling cascade and providing mechanistic support for its observed effect of decreasing the RR-MDA-MB-231 cell survival.

The mechanistic assay comparison across the parental and radioresistant cell line are shown in table 4.3.

Treatment	Cell Line	Cell Cycle (G2/M Arrest)	Apoptosis Induction (Annexin V)	DNA Damage (Tail Moment - COMET)	Interpretative Summary
GED (0.1 μM)	WT	No significant change	No significant induction	No significant DNA damage	Minimal mechanistic activity
	RR	个 G1 phase at 48h	No significant induction	No significant DNA damage	Alters cell cycle (G1) in RR
DOX (0.01 μM)	WT	个 G2/M at 24–48h	↑ Apoptosis at 24h (P<0.05)	↑ DNA damage at 4– 24h (P<0.001), repair at 48h (NS)	Classic cytotoxic pattern
	RR	个 G2/M at 24–48h	↑ Apoptosis at 24–48h	个 DNA damage at 4— 24h, partial repair at 48h	Moderately preserved effects
RAD (2 Gy)	WT	↑ G2/M at 24–48h	↑ Apoptosis at 24–48h (P<0.001)	↑ DNA damage at 1– 4h (P<0.0001), repair by 48h (NS)	Efficient damage soon after treatment; repair observed
	RR	个 G2/M at 24–48h	↑ Apoptosis at 24–48h	↑ DNA damage at 4h, reduced by 48h	Reduced sensitivity vs WT
GED + DOX	WT	个个 G2/M arrest at 24h (P<0.0001)	No apoptosis vs DOX alone (NS)	↑ DNA damage at 4– 48h (P<0.05–0.001)	Enhanced DNA damage, not apoptosis
	RR	个 G2/M arrest at 24- 48h	↑↑ Apoptosis vs DOX (P<0.001)	↑ DNA damage at 4– 48h vs DOX (P<0.001)	Improved effect across all assays
GED + RAD	WT	个 G2/M at 24–48h	No apoptosis vs RAD (NS)	↑ DNA damage at all time points vs RAD (P<0.01–0.001)	Extended DNA damage without enhanced apoptosis
	RR	个 G2/M at 24–48h	↑↑ Apoptosis vs RAD (P<0.001)	↑ DNA damage sustained at 4–48h (P<0.001)	Potent in enhancing RAD effects

Table 4.3: Summary of key findings from mechanistic assays including cell cycle distribution, apoptosis (Annexin V), and DNA damage (COMET) in wild-type (MDA-MB-231) and radioresistant (RR-MDA-MB-231) breast cancer cell lines. It highlights treatment effects of gedatolisib, doxorubicin, and radiation, both as single agents and in combinations. "ns" = not significant (P > 0.05).

4.4 Discussion

Triple-negative breast cancer (TNBC) is an aggressive subtype of breast cancer differentiated from other subtypes by the absence of the main receptors, including oestrogen, progesterone, and human epidermal growth factor receptor 2 (HER2)(De Francesco et al., 2022; Zhu et al., 2023). Due to the absence of targeted therapies, the predominant management of triple-negative breast cancer (TNBC) relies on chemotherapy and radiotherapy(Ge et al., 2022; Ji et al., 2023). However, the higher reoccurrence rate and therapy resistance are still the major clinical challenges (Masoud and Pagès, 2017; Loria et al., 2022). The acquired resistance to radiation is a particular concern, as it may result in tumour relapses and poor patient prognoses (Wu et al., 2023; Xing and Stea, 2024). A derived radioresistant MDA-MB-231 cell line (RR-MDA) was established to investigate the biological mechanisms of radioresistance and to evaluate the potential therapeutic options. This model enables the characterization of cellular and metabolic changes that induce resistance and enhances the assessment of single and combination therapeutic strategies. The current study aims to unravel the therapeutic strategies that may overcome radioresistance and improve treatment outcomes in TNBC.

Acquired radioresistance and related growth kinetics

The data demonstrated a shorter doubling time of the radioresistant MDA-MB-231 (RR-MDA) cells compared to the wild-type (WT-MDA) cells, suggesting that the acquired resistance is associated with enhanced proliferative activity. As the cells with rapidly DNA replication are more susceptible to cytotoxic agents, this may indicate that the enhanced proliferated cells are therapeutically sensitive. This notion is supported by the clinical evidence of breast tumours response to neoadjuvant chemotherapy, where the tumours with higher proliferative phenotype had a

significant achievement of complete pathological response following treatment (Stover et al. 2016). However, this association seems to be weaker in TNBC, where proliferation-independent parameters such as cell stemness and DNA damage repair systems may be involved in phenotyping therapeutic response (Stover et al. 2016). This TNBC behaviour aligns with our finding of acquired radioresistance was accompanying enhanced proliferation enhanced. Similarly, previous studies reported that breast cancer cells resistant to radiation often develop a more aggressive phenotype characterised by increased proliferation, migration, and metabolic plasticity (Fujita et al., 2020; Wu et al., 2023). Further support to our findings arise from prior studies exhibiting that treatment-induced stress promotes the growth of aggressive cell subpopulations with increased proliferation and survival, leading to treatment failure and tumour reoccurrence (Gray et al., 2019; Wu et al., 2023). This accelerated growth may be attributed to changes in several biological processes. including alterations in cell cycle checkpoints, leading to enhanced cell cycle progression. Furthermore, Christowitz et al., (2019) showed that the failure of doxorubicin to induce cell cycle arrest in breast cancer cells was associated with enhanced tumour growth, suggesting that dysregulated cell cycle progression plays a critical role in promoting uncontrolled proliferation and treatment resistance. The activation compensatory signalling pathways such as PI3K/AKT/mTOR has been strongly associated with resistance to ionizing radiation and enhanced proliferative capacity in various solid tumours, primarily through its role in regulating glucose metabolism and sustaining energy required under stressful conditions (Deng et al., 2023b). Furthermore, Metabolic reprogramming, particularly involving mitochondrial adaptation, has been shown to play a critical role in enhancing tumour cell survival and proliferation following radiation exposure (McCann et al, 2021; Pendleton et al., 2023). By rewiring mitochondrial bioenergetics and altering cellular metabolism, cancer cells adapt to radiation-induced stress, thereby sustaining growth and

accelerating proliferation, which may contribute to the observed reduction in doubling time in radioresistant cell populations.

Collectively, the decreased doubling time demonstrated in the radioresistant MDA-MB-231 cells underscores a critical shift toward a more proliferative and adaptive tumour phenotype, highlighting the biological adaptations that may underlie resistance and emphasizing the need for targeted strategies to overcome this challenge in treatment.

The sensitivity to radiation and antiproliferative agents

The impact of single-agent treatment on clonogenic survival in the radioresistant MDA-MB-231 (RR-MDA-MB-231) cell line was evaluated using a clonogenic assay that enabled the assessment cell survival capacity following treatment with gedatolisib, doxorubicin, or radiation. The survival data revealed that gedatolisib had a dose-dependent antiproliferative effect in both the wild-type and radioresistant cell lines. However, RR-MDA-MB-231 cells required relatively higher concentrations to produce a comparable growth inhibition to parental cell line. For instance, the IC₅₀ value of gedatolisib was higher in RR-MDA-MB-231 cells, though it is statistically nonsignificant, suggesting that acquired radioresistance may be accompanied by altered sensitivity to other therapeutic agents. This elevated inhibitory concentrations may be attributed to adaptive resistance mechanisms commonly associated with PI3K/AKT/mTOR inhibition, including feedback activation of receptor tyrosine kinases (e.g., HER3, IGF-1R, EGFR), loss of PTEN, and compensatory signalling via pathways such as PDK1-SGK and PIM1, which can sustain downstream mTORC1 activity and attenuate drug efficacy (Zhang et al., 2025; Song et al., 2018; Browne and Okines, 2024). Despite this variation in antiproliferative doses, gedatolisib retained its effectiveness across the tested concentration range, suggesting its potential as a therapeutic agent for both wild-type and radioresistant TNBC.

Importantly, to the best of our knowledge, our study is the first to assess the impact of gedatolisib on the survival of the radioresistant TNBC cells, providing new insights into its therapeutic potential in this aggressive subtype.

The survival pattern of the RR-MDA-MB-231 cells in response to doxorubicin has been assessed utilising the clonogenic assay and the data showed a progressive decline in cell survival in response to treatment with escalating doxorubicin concentrations. Although a variation in the growth inhibitory concentrations of doxorubicin across cell lines was demonstrated, where the IC50 in the RR-MDA-MB-231 cells was higher compared to the wild type, it was not statistically significant, indicating that the development of resistance to radiation did not produce a substantial cross-resistance to doxorubicin. However, a cross-resistance between doxorubicin and radiation in certain breast cancer cell lines has been reported, where doxorubicinresistant MCF-7 cells revealed a correlated increase in radiation resistance, which may be attributed to improved DNA repair mechanisms and alterations in apoptosisrelated proteins, suggesting that resistance to one treatment may confer resistance to another (Luzhna et al., 2013). In contrast, the findings of our study did not show such cross-resistance in the RR-MDA-MB-231 cell line. The current data suggests that the cells may involve distinct adaptation mechanisms to develop resistance to radiation, and it does not necessarily result in decreased response to doxorubicin in this TNBC model.

In the current study, the clonogenic data analysis demonstrated significant differences in the survival Fractions between the RR-MDA-MB-231 and WT-MDA-MB-231 cells following exposure to ionizing radiation. The LQ model analysis demonstrated that RR-MDA cells showed a lower α value relative to WT-MDA cells, indicating decreased sensitivity to single hit effect. Furthermore, the β component was significantly higher in RR-MDA cells, proposing an enhanced capacity to repair sublethal DNA induced by double hits or dose-dependent (quadratic) events.

Consequently, a statistically significant low α/β ratio in RR-MDA compared to WT-MDA suggests that the RR-MDA cells have developed capability in repairing radiation induced- DNA damage and reflecting acquired resistance. These findings reinforce the acquisition of radiation resistance in the RR-MDA-MB-231 cell line, and are in alignment with previous study of Zhou et al. (2020), who revealed a decline of the α/β ratio from approximately 3.3 in wild-type MDA-MB-231 cells to below 1.0 in their radioresistant derivative, and linked that to the upregulation of genes that contribute in regulation of cell cycle and DNA damage response, specifically, CDKN1A or SOD2 genes. The demonstrated radioresistance in RR-MDA-MB-231 cells may originate from alterations in various biological processes, including improved DNA damage repair processes, dysregulation of the cell cycle, and the activation of pathways contributing to cell survival (Gray et al., 2019; To et al., 2022). Interestingly, it has been shown that breast cancer cells resistant to radiation frequently display an increase in crucial DNA repair proteins, including ATM and RAD51, which have an essential role in repairing the DNA damage induced by radiation effectively (Scully et al., 2019; García, Kirsch and Reitman, 2022; Ziyi Wang et al., 2022). Moreover, the radioresistance may be related to enhanced antioxidant defences that decrease the accumulation of reactive oxygen species (ROS) and reduce the cytotoxic effects induced by radiation (Malla et al., 2021; Dong et al., 2025). Furthermore, prior reports have been revealed that radioresistant cancer cells display metabolic adaptations, including rewiring towards glycolytic metabolism or enhancing mitochondrial function to sustain the energy required for their survival in stressful conditions (Munkácsy, Santarpia and Győrffy, 2023; Mitaishvili et al., 2024).

Alongside DNA repair mechanisms, shifting in cell signalling pathways, including the PI3K/AKT/mTOR and JNK pathway, has been found to be involved in the development of radioresistance (Costa, Han and Gradishar, 2018; Tao *et al.*, 2024; Garg *et al.*, 2025). The activation of these pathways may enhance cancer cell

survival, proliferation, and metabolism, thereby playing an important role in inducing TNBC resistance to radiation. Therefore, the therapeutic strategies implementing PI3K/AKT/mTOR inhibitor with radiotherapy may improve treatment cytotoxicity, leading to more cancer cell killing.

Collectively, despite the altered sensitivity profiles of gedatolisib and doxorubicin, both retained activity against RR-MDA-MB-231 cells, supporting our hypothesis that gedatolisib and doxorubicin could produce a pronounced antiproliferative effect in the radioresistant and its parental MDA-MB-231 cell lines. These findings underscore the need for combination therapy strategies to overcome intrinsic or acquired resistance mechanisms. In the next section, we will explore whether combining gedatolisib (a dual PI3K/mTOR inhibitor) with radiation or doxorubicin can improve treatment efficacy in radioresistant TNBC.

Targeting PI3K/mTOR pathway-based strategies to overcome radioresistance

The intrinsic heterogeneity of TNBC contributes to diverse responses of this aggressive subtype to single therapies reinforces the rational for combination approaches relying on agents with different mechanisms of action to improve therapeutic outcomes. Given the essential role of the PI3K/AKT/mTOR pathway in TNBC growth and induced therapy resistance (Zhang *et al.*, 2024), targeting this pathway with gedatolisib and combining with radiation or doxorubicin was proposed to overcome radioresistance in TNBC. The current data have shown that the combination of gedatolisib with radiation resulted in increased cytotoxicity in RR-MDA-MB-231 cells, reflected by the significant reduction in survival fractions when compared to both untreated controls and radiation alone. This augmented effect indicates a potential radiosensitising effect of gedatolisib, mainly due to its targeted inhibition of the PI3K/AKT/mTOR pathway, which has been demonstrated to play a vital role in cell survival and therapy resistance (Tao *et al.*, 2024; Garg *et al.*, 2025).

Our findings are in alignment with previous studies highlighting that targeting the PI3K/AKT/mTOR pathway can enhance the radiation effects by impeding DNA damage repair and increasing apoptosis (Khan et al., 2019a; Yang, 2024; Garg et al., 2025). By extending these observations in the radioresistant TNBC cells, the current results suggest that targeted inhibition of PI3K/Akt/mTOR pathway can improve the radiosensitivity even after developing of acquired resistance. This aligns with observations from other solid tumour studies, where Mousavikia et al., 2025 have shown that inhibiting the PI3K/AKT/mTOR pathway improved the effectiveness of radiation in colorectal cancer. Moreover, targeting of PI3K/AKT/mTOR pathway has been shown to represent a promising strategy for overcoming radioresistance in small-cell lung cancer (Deng et al., 2023b). Our clonogenic survival findings were further supported by tumour spheroid data that showed greater growth retardation following treatment with combination of gedatolisib and radiation compared to each single agent. The data provided further insight into the beneficial effects of combining gedatolisib with radiation in a more complex and physiologically relevant 3D model, although the modest comparable antiproliferative effect to clonogenic assay. This variability in the response reflects the impact of gradients such as oxygen and nutrient in the complex architecture of spheroids on the drug penetration and therapeutic response. Hence, more complex models are required for further assessment to confirm that the efficacy of this combination therapy is not a dose or context dependent.

Overall, the spheroid data complement the results of the clonogenic assay, supporting the potential of combining gedatolisib with radiation to overcome resistance and improve the outcomes of TNBC and provide the rationale for further pre-clinical and clinical studies to optimise this combination approach for treating TNBC.

The potential combination of gedatolisib with doxorubicin was evaluated as a treatment strategy in the RR-MDA-MB-231 cell line. The results of the clonogenic survival assay demonstrated enhanced cytotoxicity in RR-MDA-MB- 231 cells following exposure to gedatolisib-doxorubicin combination treatment. The efficacy of this combination was dose dependent, where the combination of higher assessed concentrations resulted in the greater reduction in clonogenic survival and spheroid growth. The increased cytotoxicity following exposure of RR-MDA-MB-231 cells to a combination of gedatolisib and doxorubicin may be attributed to the diverse modes of action of the drugs. While doxorubicin induces DNA double strand breaks, gedatolisib inhibits the PI3K/mTOR pathway, a key survival pathway that is frequently upregulated in TNBC and correlated with therapeutic resistance, underscoring potential advantages of this co-treatment strategy (Costa et al., 2018; Ciocan-Cartita et al., 2020; Kciuk et al., 2023; Zhang et al., 2024). These findings are in agreement with other studies demonstrating increasing the cancer cell sensitization to doxorubicin by targeting the PI3K/AKT/mTOR signalling pathway (Ghanem et al., 2022; Zhang et al., 2022; Agrawal, Agrawal and Chopra, 2025). Furthermore, A clinical trial led by Basho et al., 2017 assessed the safety and efficacy of everolimus or temsirolimus, the mTOR inhibitors, in combination with doxorubicin and bevacizumab in patients with advanced metaplastic TNBC, and demonstrated that both therapeutic regimens were well tolerated and resulted in better outcomes. particularly in patients with high PI3 pathway aberrations.

Taken together, the observed efficacy of the gedatolisib-doxorubicin combination in both wild-type and radioresistant MDA-MB-231 cells underscores its therapeutic potential against aggressive TNBC subtypes, including those with acquired resistance.

Mechanistic insights into gedatolisib-based combination

To explore the mechanisms underpinning the enhanced cytotoxicity demonstrated in clonogenic and spheroids, several assays have been utilised to assess the cell cycle distribution, apoptosis, DNA damage and autophagy in the RR-MDA-Mb-231 cells. Together, these assays provide a fundamental comprehension of how gedatolisib augments the effects of radiation and doxorubicin.

Cell cycle dynamics

Cell cycle analysis offers a mechanistic insight into the effects of combination therapies in terms of their abilities to impair the cell cycle progression. At the early time point (4 hr) following treatments, no statistically significant differences in RR-MDA-MB-231 cell cycle distribution were detected, suggesting that the initial response of the cells to these therapies did not rely on immediate cell cycle arrest. However, at 24 hr following treatment, radiation, or doxorubicin-alone or in combination with gedatolisib induced a significant accumulation at G2/M. This may indicate that DNA damage induced by treatments activated the G2/M checkpoint to permit DNA repair prior mitosis. This cell cycle phase arrest was sustained at 48hr, indicating prolonged DNA damage and a transition towards mitotic catastrophe. However, gedatolisib alone induced significant G1 accumulation, in consistent with previous studies demonstrating that PI3K/AKT/mTOR inhibition induces G1 arrest (Ahmed et al., 2022; Xia et al., 2023). The current findings suggest that while radiation and doxorubicin disrupt cell cycle distribution via DNA damage-driven G2/M arrest, gedatolisib may work by modulating proliferative signalling, reflecting a potential complementary mode of action.

Apoptotic response

The Annexin V assay data provided important insights into the apoptotic effects of combinations of gedatolisib with radiation or doxorubicin in the RR-MDA-MB-231 cells across different time points post-treatment. The results demonstrated no apoptosis at

the early response time point (4hr post-treatment) across treatment groups. However, significant apoptosis was shown at 24-48 hr in samples treated with radiation or doxorubicin alone, with further apoptotic enhancement shown in the combination groups (GED+RAD and GED+DOX). These findings are in alignment with previous studies revealing that targeting the PI3K/Akt/mTOR signalling pathway enhances the apoptotic effects of both radiation and doxorubicin, consequently sensitizing the cells to apoptosis-induced agent (Zhennan Wang et al., 2022; Deng et al., 2023b; Jafari et al., 2023). Mechanistically, the suppression of the PI3K/Akt/mTOR signalling pathway has been found to enhance the apoptotic effect of radiation and doxorubicin through enhancing G2/M phase arrest, the downregulation of Bcl-2, an anti-apoptotic protein, and diminishing the Akt-mediated phosphorylation of pro-apoptotic proteins, including BAD and caspase-9 (Marklein et al., 2012; Rattanapornsompong et al., 2021; Ghanem et al., 2022; Deng et al., 2023b). A recent study investigated the effects of combining curcumin with doxorubicin on the PI3K/Akt/mTOR signalling pathway in MDA-MB-231 cells showed that combination treatment significantly reduced cell survival, induced G2/M cell cycle phase arrest, and increased apoptosis compared to doxorubicin alone (Sarkar et al., 2024a).. Furthermore, the increased in apoptotic fractions demonstrated at 48 hr were correlated with the earlier determined G2/M cell arrest, and the sustained cell cycle arrest at this phase is known to push cells toward apoptotic cell death (Mardanshahi et al., 2021; Salanci et al., 2024).

DNA damage and repair

The COMET assay data displayed minimal DNA damage in the untreated control group over time, indicating intact nuclear DNA integrity, while exposure to single doxorubicin or radiation therapy produced significantly higher tail moments, reflecting substantial DNA damage. The DNA damage observed at 4 hr following treatment with radiation or doxorubicin alone was higher than that by 48hr, suggesting that radiation-induced DNA damage occurs rapidly but is subject to repair over time. In contrast,

gedatolisib as a single treatment did not show significant DNA damage, reinforcing its role as signalling modulator rather than genotoxic agent. However, combining gedatolisib with either radiation or doxorubicin resulted in significantly enhanced DNA damage 48hr, suggesting impaired DNA repair pathways, thereby enhancing the DNA damage induced by radiation or doxorubicin. In support to our findings, a previous study demonstrated that the concurrent targeting of mTORC1 and Akt was found to impair the non-homologous end joining (NHEJ) repair pathway, resulting in prolonged DNA damage and enhanced radiosensitivity (Holler et al., 2016b). A recent study evaluating the efficacy of combining PKI-402, a dual PI3K/mTOR inhibitor, with radiation in breast cancer cell lines has shown elevated y-H2AX levels, a DNA damage marker, following therapy which indicates the role of PKI-402 in sensitising the cells to radiation and increasing the cell death (Gasimli et al., 2023). These findings support our results, indicating that gedatolisib, as a dual PI3K/mTOR inhibitor, may contribute to prolonged DNA damage by disrupting the DNA repair pathways, thereby improving the effectiveness of radiation and doxorubicin in radioresistant breast cancer cells.

Modulation of PI3K/Akt/mTOR pathway and autophagy

Given that gedatolisib alone did not induce significant apoptosis, DNA damage, or cell cycle arrest, the autophagy was assessed as an alternative mechanism mediating its biological effect. The results showed that gedatolisib induced dose-dependent accumulation of autophagic vacuoles in the RR-MDA-MB-231 cells. In the context of combination therapy, the induced-autophagy may enhance the response to gedatolisib-based combinations by disrupting the cellular homoeostasis and priming damaged cells for apoptosis, leading to augmenting the cytotoxic effects of radiation and doxorubicin. These findings are in alignment with previous studies showing that targeting the PI3K/Akt/mTOR pathway could promote autophagy induction, enhancing the effectiveness of cancer therapies (Ahmed *et al.*, 2022; Wang *et al.*,

2022; Agrawal, Agrawal and Chopra, 2025). The gedatolisib-induced autophagy was further supported by western blot analysis which revealed a significant reduction in in Akt protein expression following incubation of the RR-MDA-MB-231 cells with gedatolisib.

Collectively, the results of mechanistic assays provide a comprehensive understanding of how gedatolisib enhance therapeutic responses in radioresistant MDA-MB-231 cells. Although gedatolisib alone did not induce pronounced apoptosis, DNA damage, or cell cycle arrest; its combination with radiation or doxorubicin significantly enhanced cytotoxic effects. These findings suggest that gedatolisib sensitises RR-MDA-MB-231 cells to radiation or doxorubicin potentially via modulation of key survival pathways rather than direct cell damage. The significant autophagic induction, supported by suppression of Akt expression, indicates its mechanistic role in disrupting PI3K/Akt/mTOR signalling making a cellular state more susceptible to cytotoxic agents.

In summary, gedatolisib has shown considerable antiproliferative effects in both wild-type and radioresistant MDA-MB-231 cells; however, its combination with doxorubicin or radiation significantly enhanced the cytotoxicity. These combinations effectively induced DNA damage, cell cycle arrest, and apoptosis, mechanistic effects that were limited with gedatolisib alone and only modestly observed with other single agents, highlighting the enhanced efficacy of combination treatments. These data reinforce the therapeutic rational for targeting PI3K/Akt/mTOR in combination with standard therapies in TNBC. While these results highlight the therapeutic advantages of combination strategies involving targeting PI3K/Akt/mTOR signalling, it remains likely that resistance mechanisms beyond this pathway contribute to therapy failure. To address these underlying mechanisms and identify further vulnerabilities, we next employed untargeted metabolomics to characterize the metabolic adaptations associated with radioresistance in MDA-MB-231 cells.

Chapter 5

5 Metabolomics profiling of radiotherapy resistance
MDA-MB-231 cell line

5.1 Introduction

In previous chapters we assessed a proposed novel combination therapy for TNBC in MDA-231 TNBC cells and in radiation resistant cells that were derived in this project from the parental line. As TNBC is a cancer which initially responds to therapy, but then always returns killing the patient, with the tumour resistant to therapy, we next decided to change tact and to attempt to interrogate what molecular mechanism underpin this switch to radiation resistance. The ultimate aims of these experiments were to identify pathways critical to the development of therapy resistance, to lay the groundwork for future studies that could aim to target these resistance causing pathways at the time of therapy administration. If this ultimate goal was achieved, patients' tumours may not return as resistant cancer subclones and survival from TNBC would be enhanced as this is the real clinical problem rather than the initial tumour. The cells in the body utilise thousands of chemical reactions to maintain their viability and health and to enable them to carry out their myriad functions. Cell metabolism is defined as a set of pathways that regulate these chemical reactions and the chemical components which result from these chemical reactions during metabolism are called metabolites (Klassen et al., 2017). These metabolites may include organic and inorganic compounds, lipids, amino acids, vitamins, and other biochemical molecules. The systematic study of metabolites in different biological samples such as cells, tissues and organs utilising high-throughput technologies is termed metabolomics (Kell and Oliver, 2016; Klassen et al., 2017). As metabolites represent the end products of cellular activity, metabolomics provides comprehension understanding into dynamic biological states that may not be reflected from other omics components such as genomics or proteomics alone (Danzi et al., 2023). In oncology, metabolomics is an emerging valuable tool for understanding how tumour cells rewiring metabolism to support growth, survival, and therapy resistance.

Cancer patients often undergo metabolic changes arising from tumour burden, nutritional changes, and treatment, all of which affect quality of life and clinical outcomes (Suri *et al.*, 2023). Metabolic reprogramming is now recognised as a hallmark of cancer progression, driving tumour initiation, evolution, and metastasis by supporting biosynthetic demands, enhancing redox balance, and fuelling oncogenic signalling (Pavlova and Thompson, 2016; Martinez-Outschoorn *et al.*, 2017). Consequently, metabolomics studies in oncology have shown promising potential in identifying biomarkers for various cancer pathogenesis, drug toxicity, therapeutic interventions and resistance mechanisms (Guijas *et al.*, 2018; Danzi *et al.*, 2023; Suri *et al.*, 2023).

In breast cancer, and particularly in triple-negative breast cancer (TNBC), metabolic rewiring may contribute to resistance against chemotherapy and radiotherapy. Previous studies have highlighted that changes in glucose metabolism, amino acid dependencies (aspartate and glutamate), and lipid turnover could be correlated with chemotherapy resistance in breast cancer (Xu *et al.*, 2018; Bacci *et al.*, 2019; Pranzini *et al.*, 2021).

Radiotherapy also induces severe metabolic stress by generating reactive oxygen species (ROS), inducing DNA damage, and disrupting redox homeostasis (Liu *et al.*, 2021). Tumour cells that survive radiation often reprogram their metabolism to increase ATP production, strengthen antioxidant defences, and sustain biosynthetic pathways, thereby enhancing radioresistance (Liu *et al.*, 2021; Payne, 2021). Prior studies have shown that metabolic reprogramming in different cancer cell lines mediated resistance to radiation, for instance, some metabolic pathways such as glutathione synthesis and glutamine metabolism were involved by breast cancer and glioma cells lines to survive radiation-induced stress (Cobler *et al.*, 2018; Fu *et al.*, 2019).

Radioresistance and chemoresistance are the main challenges in treatment of the triple negative breast cancer. TNBC initially responds to chemotherapy and radiotherapy; however, tumour reoccurrence due to the emergence of therapy-resistant subclones remains a clinical challenge (Lu et al., 2018; Garg et al., 2025). Most studies focus on chemoresistance, while molecular insights into radiation resistance, particularly metabolic adaptations, still require further investigation. Given TNBC is highly heterogeneous both genetically and metabolically, distinct subpopulations of cancer cells can resist treatments by activating alternative biological mechanisms, including metabolic reprogramming (Bai et al., 2021). In response to radiation-induced stress, TNBC cells may modulate their metabolism, enabling cancer cells to enhance energy production, decrease oxidative stress, and sustain biosynthetic processes essential for their viability and survival (Lu et al., 2018; Bai et al., 2021; Garg et al., 2025).

Our project particularly investigates the metabolic rewiring associated with radiation resistance in the MDA-MB-231 derived radioresistant cell line utilising an untargeted metabolomics approach to reveal novel therapeutic targets.

5.2 Aims

This study aims to investigate the metabolite alterations in established radioresistant MDA-MB-231 cell lines following radiation exposure compared to the wild-type MDA-MB-231 cell line, using an untargeted LC-MS-based approach. The further objective is to identify metabolic adaptations that possibly contribute to radioresistance, unravelling biomarkers and potential pathways that may inform novel therapeutic strategies for overcoming resistance in TNBC.

5.2.1 Hypothesis

We hypothesised that the radioresistant of derived RR-MDA-MB-231 cells are driven by distinct metabolic reprogramming compared to their parent MDA-MB-231 cell line that alters energy support, redox balance, and biosynthetic pathways. This would reveal novel biomarkers and therapeutic vulnerabilities in triple-negative breast cancer.

5.3 Results

5.3.1 Cellular metabolome of an established radioresistant and wild type triple negative breast cancer cell lines at 1hr following exposure to 2Gy radiation

To investigate cellular events in terms of metabolite abundance following exposure to radiation, an untargeted metabolomics approach utilising LC-MS technique was performed in wild type and resistant MDA-MB-231 cell lines. The generated metabolite intensities were normalised using MetaboAnalyst v6.0 webserver applying median normalisation, log 10 transformation and mean centring to minimize technical variability, correct the data skewness and standardise the data for the subsequent statistical and pathway analysis.

Prior to performing data analysis, box plots of log2-transformed abundance data with corresponding retention times were generated as part of the data inspection and quality evaluation process (Figure 5.1). The box plots have shown that metabolite levels are comparable across different samples, which is essential for identifying actual biological variations rather than technical noise, thus producing more reliable and interpretable data.

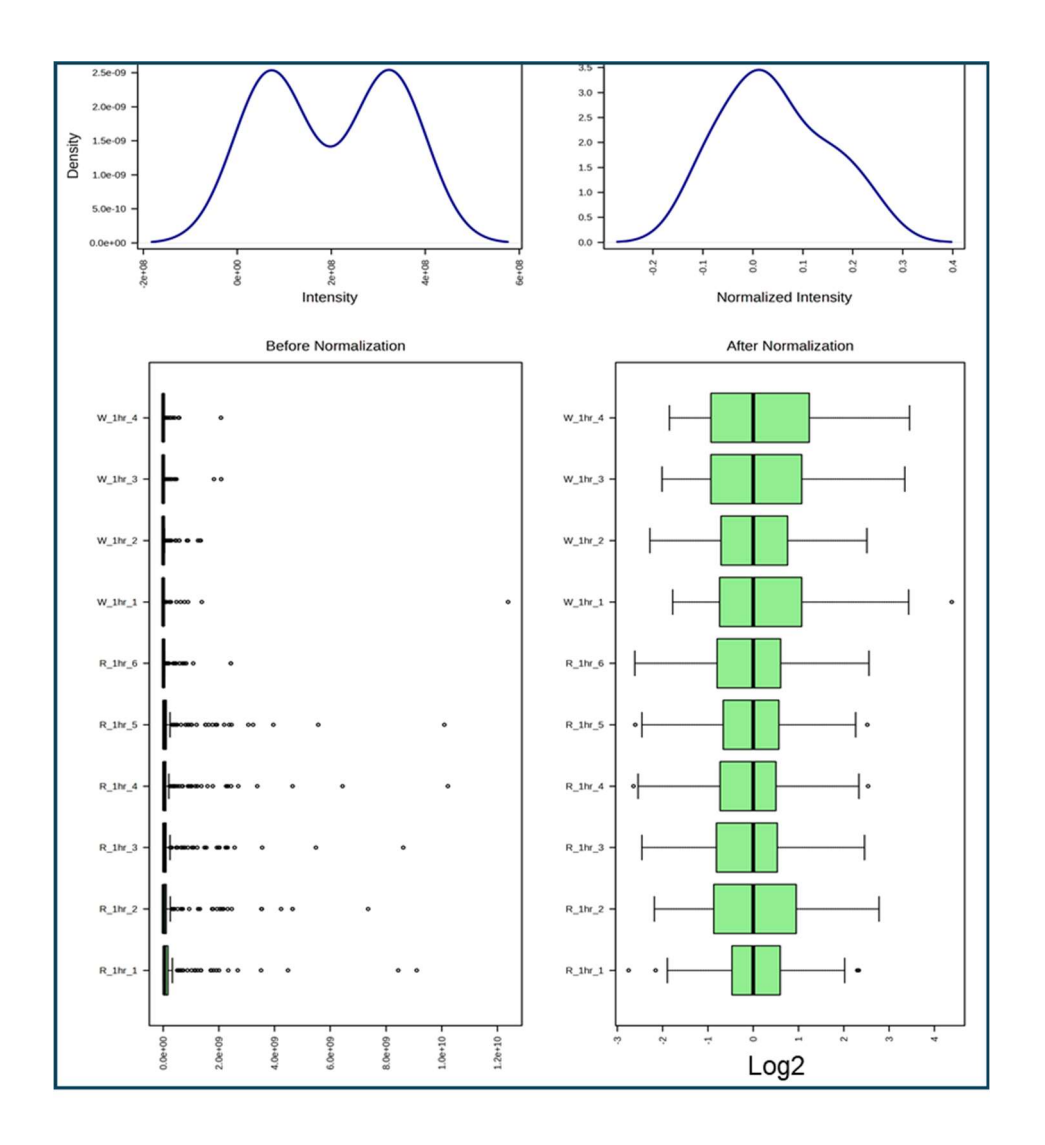


Figure 5-1 Metabolite abundance distribution after normalisation across samples in response to radiation.

Box plots of log2 area for each individual sample at 1 hr time point following exposure to 2Gy radiation. Wild type MDA-MB-231 cell samples (labelled with W) and resistant cell samples (labelled with R) were normalised by median and log2 transformation.

Figure 5.1 demonstrates that the normalization process improved data quality and comparability, indicating that subsequent analyses reflect true metabolic alterations linked to radioresistance rather than systematic bias.

5.3.1.1 Univariate and multivariate analysis

The data analysis was initiated with univariate and multivariate analysis. In multivariate analysis, all the variables (metabolites) were assessed simultaneously to assess the overall patterns and relationships within the data set. Following data normalization and preprocessing, a multivariate analysis utilising principal component analysis (PCA) and orthogonal partial least square discriminant analysis (OPLS-DA) was conducted to visualise the similarities and heterogeneities among biological samples. The data of these analyses are shown in Figure 5.2

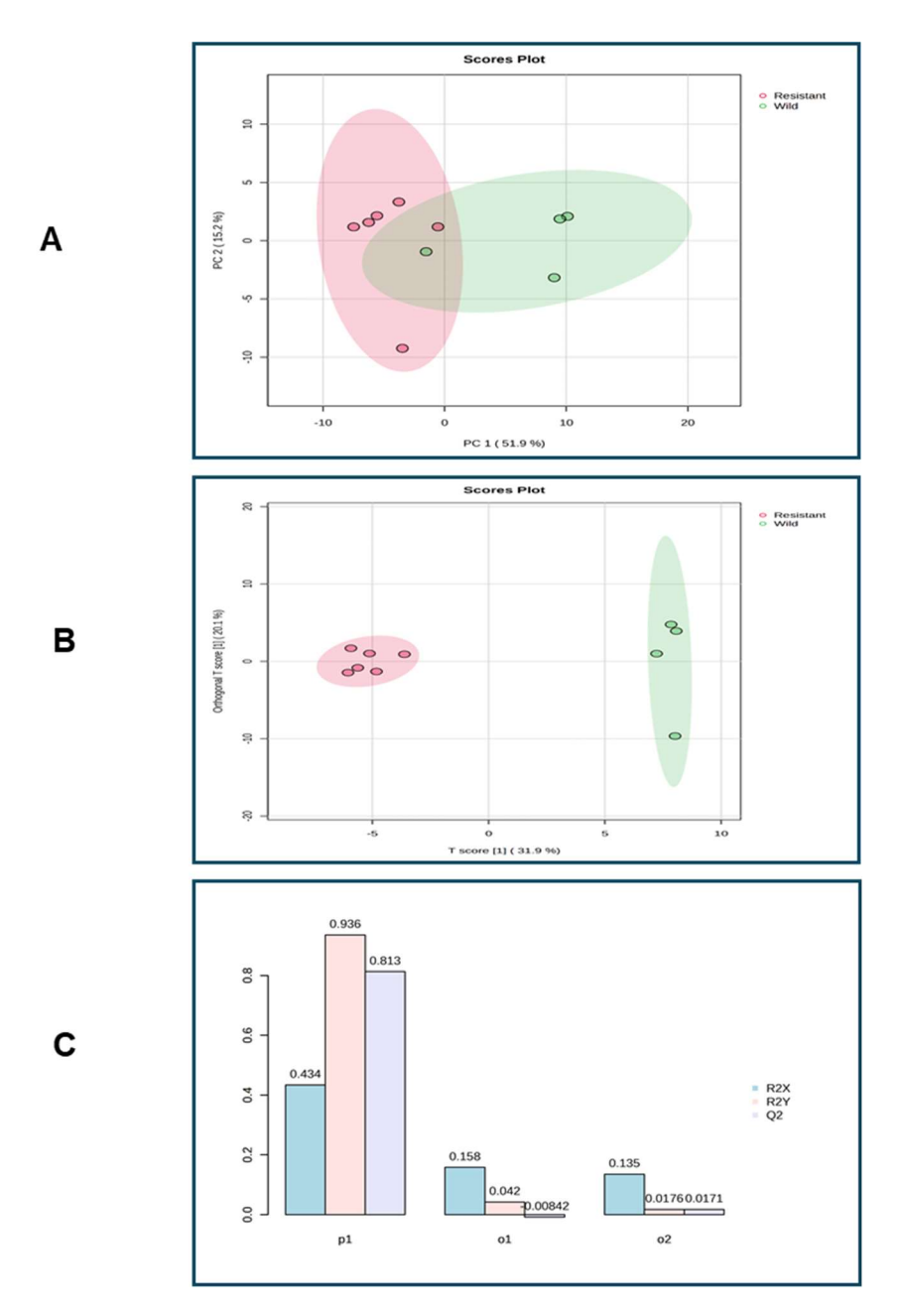


Figure 5-2 Multivariate analysis of extracted MDA-MB-231 cell samples at 1hr following exposure to radiation.

(A) PCA scatter plot shows the clustering of resistant (red) and wild type (green) cell samples (n=5 biological replicates per group). (B) OPLS-DA plot showing the separation of resistant and wild type cells as well as sub-splitting of samples within each group. (C) OPLS-DA model overview quality metrics, where R2 value reflects the model fitness and Q2 value indicates model's predictive ability. P1 indicates the main predictive variation while O1 and O2 (orthogonal component) capture the non-predictive variation or unrelated noise and background variation.

The data in Figure 5.2 showed the multivariate analysis of radioresistant and wild type MDA-MB-231 cell metabolites at 1-hour post-radiation. Panel A in the figure shows the PCA scatter plot of all samples (5 biological replicates per group), an unsupervised analysis that does not use group labels. While some separation between resistant and wild-type cells is apparent, clusters are not fully distinct. Panel B displayed the OPLS-DA scores plot, a supervised method that maximizes group distinction, where resistant and wild-type cells exhibit clear separation, demonstrating distinct metabolic signatures between the groups. Each group contained one outlier sample, which was excluded from subsequent analyses to prevent bias in metabolic data interpretation. Furthermore, panel C showed the OPLS-DA model quality metrics. The main predictive component (P1) captures most of the classdiscriminatory variation, while orthogonal components O1 and O2 represent nonpredictive background variation. The multivariate analysis model achieved a high prediction ability value and a satisfactory model fitness of ($R^2 = 0.936$ and $Q^2 = 0.813$), indicating the model's reliability and power for distinguishing between the assessed groups.

To investigate each metabolite independently, univariate analysis was employed. Several analysis including student's t-test, volcano plot and fold change were performed to assess each metabolite independently across group samples aiming to identify the significant metabolic alterations between pairwise compared groups. Unpaired two-tailed student's t-test was utilised to determine the metabolites that statistically significantly changed between the two groups with a P-value of <0.05. A fold change test was performed to measure the magnitude of the changes in metabolites between resistant and wild type MDA-MB-231 cells, as well as determining whether each independent metabolite is upregulated or downregulated. The threshold for the fold change test was set to be 2 (FC>2) or the log2 ≥ ±1 which

means that the metabolite level is upregulated when FC> 2 and downregulated when FC<0.05, and this threshold is commonly used in metabolomics studies (Pang *et al.*, 2024). A Volcano plot which combines change magnitude (fold change) and statistical p-value from the t-test was then employed to visualise the clear representation of the metabolites that have statistical and biological significance. The data are shown in Figure 5.3

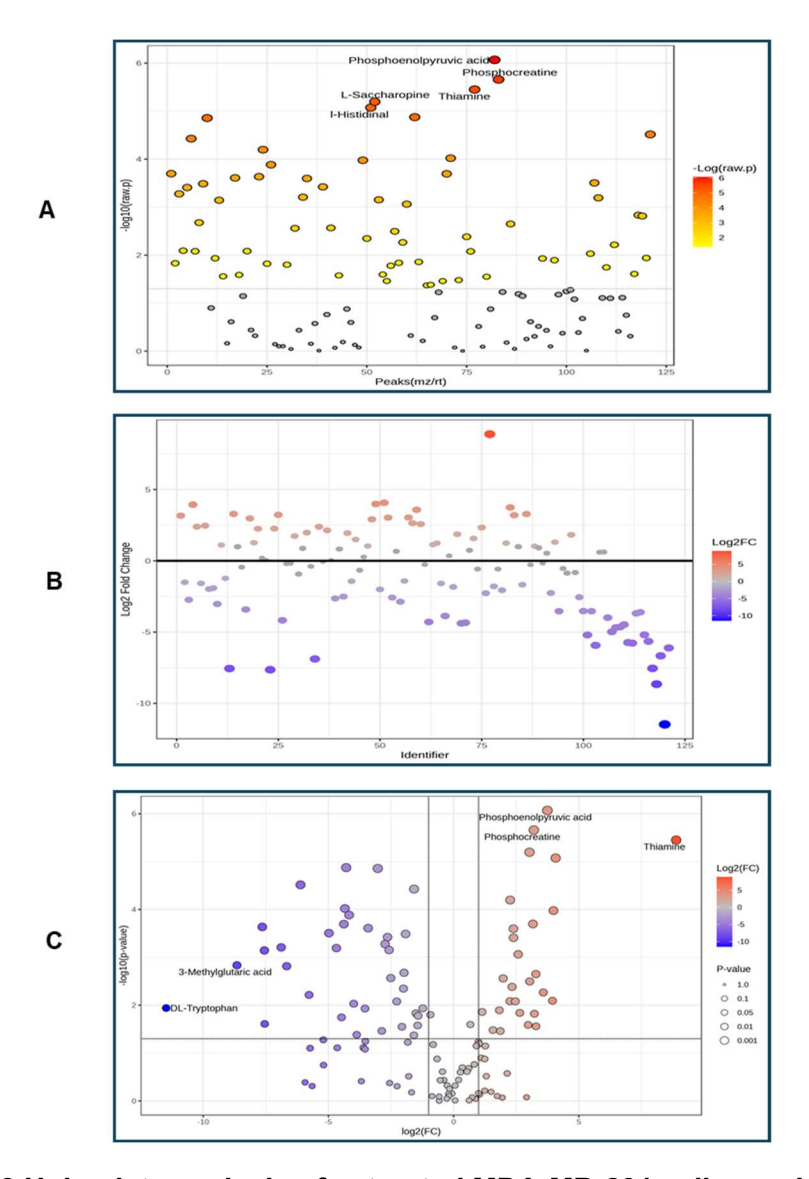


Figure 5-3 Univariate analysis of extracted MDA-MB-231 cell samples.

Metabolite abundances extracted from resistant and wild-type MDA-MB-231 cells at 1 hr following exposure to radiation were compared utilising univariate analysis. (A) Metabolites analysed with t-test were significant at P>0.05, and dots are scaled by a colour gradient from yellow (less difference) to red (high difference). (B) Fold change analysis comparing resistant to wild type cells, where the biologically significant metabolites above threshold (FC>2 or <0.05 or log2≥ ±1) are highlighted in colour ranging from blue (downregulated) to red (upregulated). (C) Volcano plot showing significantly changed metabolites combining t-test and fold change at p>0.05 and log2≥ ±1. Dots colour showing regulation (red for upregulated, and blue for downregulated), while the Dot size shows the statistical change (larger dots indicating higher difference).

Figure 5.3 A shows the significant variation in metabolites levels between resistant and wild type MDA-MB-231 cells based on t-test analysis (P<0.05). The data analysis utilising t-test revealed that 64 metabolites were significantly changed when compare resistant with wild type cells. Phosphoenolpyruvic acid, phosphocreatine, thiamine, L-saccharopine and histidinal were the metabolites with greatest degree of variance between the assessed groups. The resistant MDA-MB-231 metabolites with significant fold changes (FC>2 or the log2 ≥ ±1) when compared to wild type MDA-MB-231 cells at 1hr after exposure to radiation are shown in (Figure 5.3 B). The data analysis showed that 35 metabolites had fold change above the threshold (FC>2 or <0.05 or log2≥ ±1), suggesting their upregulation in resistance compared to wild type cells. Figure 5.3 C displays that 27 metabolites were statistically significantly different and had significant fold change in a ratio of resistant over wild type MDA-MB-231 cells at 1hr following exposure to radiation. The scattered dots in the volcano plot represent the distribution of metabolites following this test where the size and the colour of the dotes are attributed to the t-test statistics (significant: P<0.05) and the fold changes (upregulated and downregulated metabolites), respectively.

A heatmap cluster analysis was then performed to visualize the relationship between statistically significant (P<0.05) metabolites and samples in different groups. In this analysis, the metabolite abundances across samples are highlighted using a colour gradient, reflecting the upregulation and downregulation of significant metabolites where blue (downregulated) while red (upregulated). Based on the clustering of metabolites and samples, the group of samples that share a similar metabolic profile can be identified, as shown in Figure 5.4. The outlier samples were excluded to avoid interfering with metabolite expressions of another group.

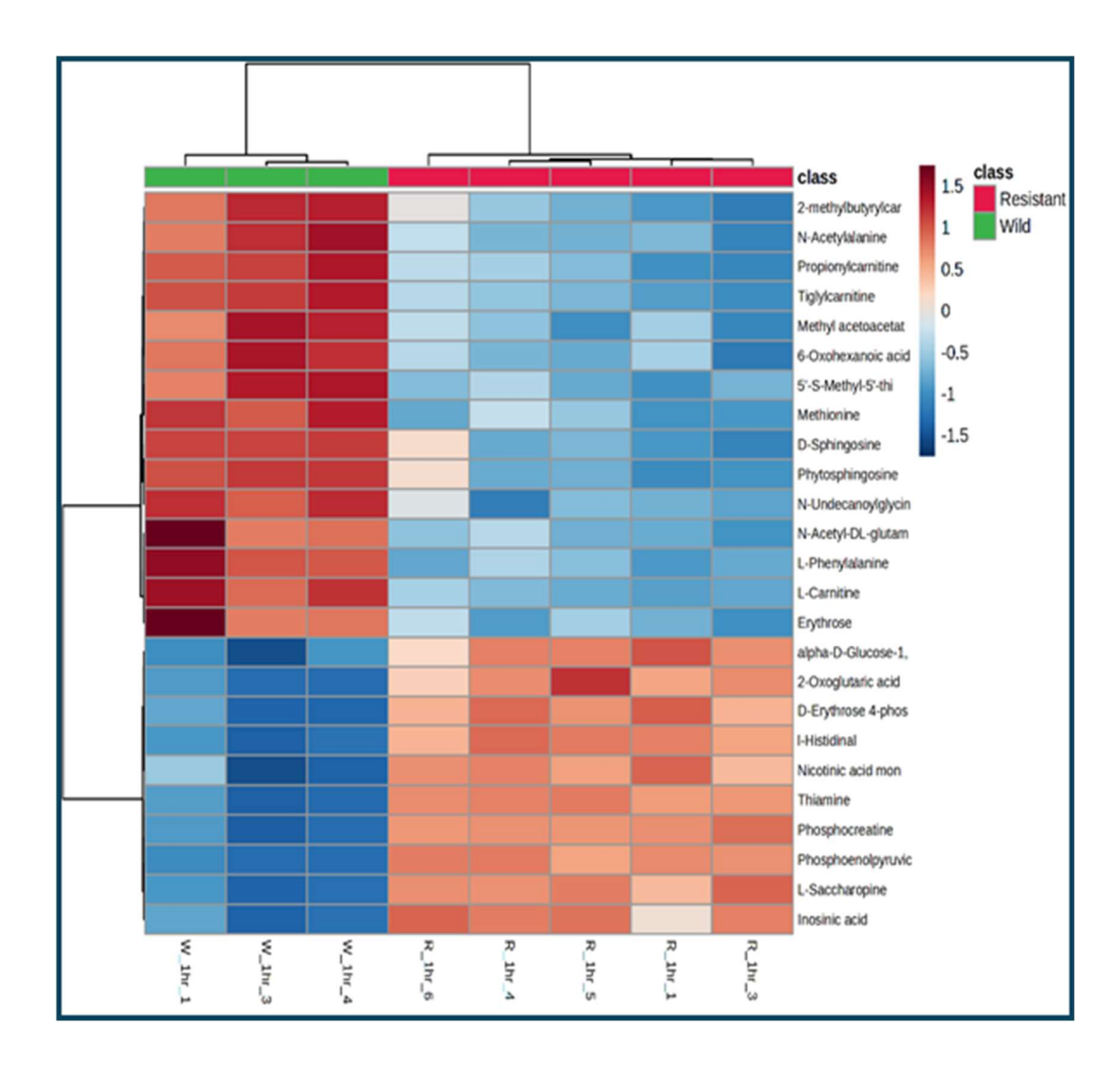


Figure 5-4 Metabolites clustering analysis.

Metabolites abundances across samples of resistant and wild type MDA-MB-231 cells at 1hr following exposure to radiation. The colours reflect the abundance of metabolites across samples ranging from blue (downregulated) to red (upregulated) with clear distinction of resistant and wild type MDA-MB-231 cell samples. The red colour gradient represent upregulation while the blue colour gradient represents the downregulation of metabolites.

Figure 5.4 showed that several metabolites including phosphocreatine, phosphoenolpyruvic acid and L-saccharopine have high abundances across resistant samples and low abundances in wild type MDA-MB-231 samples. Conversely, several metabolites such as carnitine and its derivatives including propionylcarnitine,2-methylbutylcarnitine and tiglylcarnitine as well as phenylalanine were downregulated in resistant samples and upregulated in wild type samples.

The variable importance in projection (VIP) is a statistical measure that was utilised to determine the significant individual metabolites responsible for distinguishing resistance from the wild-type group at 1hr following exposure to radiation therapy was conducted (Figure 5.5).

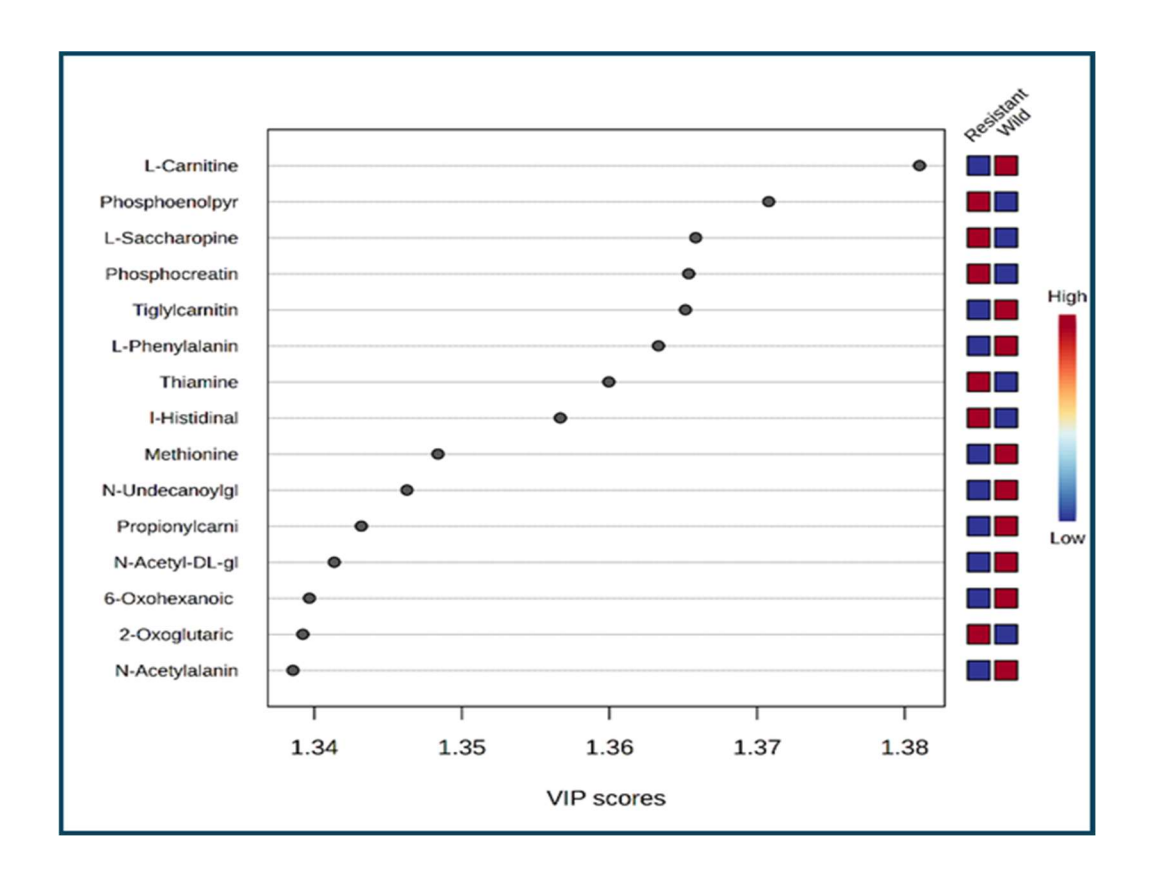


Figure 5-5 Variable importance in projection (VIP) for top 15 metabolites.

The variable importance in projection (VIP) score plot showing top 15 significant metabolites with a VIP value >1, responsible for differentiation of resistant group from wild type MDA-MB-231 group in the OPLS-DA model at 1hr following exposure to radiation. The colour code denotes the concentration of each individual metabolite in the two groups, where red indicates high concentration and blue indicates low concentration.

The VIP data analysis revealed several metabolites including phosphocreatine, phosphoenolpyruvic acid and thiamine that have higher VIP scores in the resistant group when compared to the wild-type MDA-MB-231 group. However, L-carnitine was the top metabolite in the VIP score plot which was upregulated in wild type group in comparison to resistant group. These data highlight the key metabolites that upregulated in early response of resistant cells to radiation and may contribute to inducing resistance.

5.3.1.2 Metabolite set enrichment analysis (MSEA) and Pathway analysis

The metabolite set enrichment analysis (MSEA) and pathway analysis were conducted utilising the MetaboAnalyst software to investigate the perturbation of metabolic pathways or metabolite set of biochemical processes in resistant and wild type cells at 1 hr following exposure to radiation. The metabolic pathways identified by pathway analysis and the top 25 enriched metabolite sets are shown in figure 5.6 A and B, respectively.

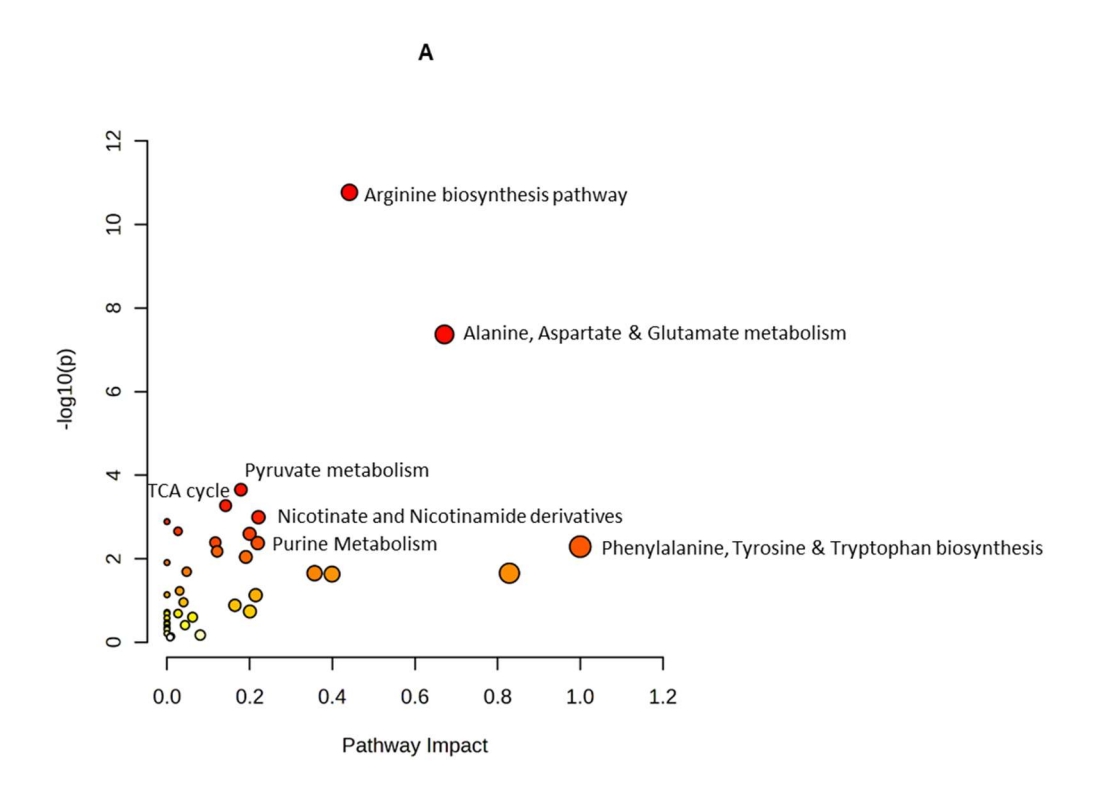
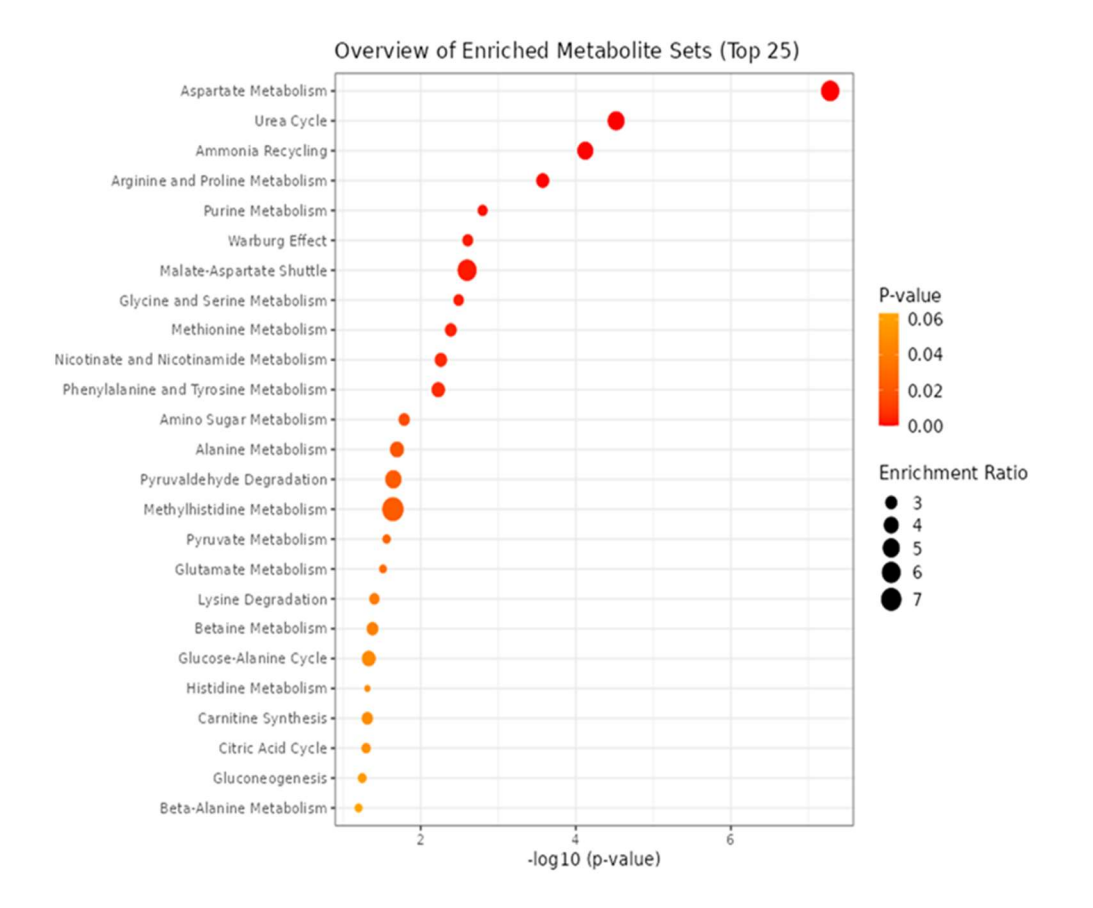


Figure 5-6 Metabolic pathway analysis and MSEA.

The pathway analysis of the metabolites identified in resistant and wild type MDA-MB-231 cells at 1hr following exposure to radiation. (A) The impact value of each identified pathway, with significantly changed pathways labelled with a P value < 0.05. (B) Represents the top 25 enriched pathways where the size and the colour are representative of the enrichment ratio and the statistical significance, respectively.

В



The data has shown that several metabolic pathways, particularly those relating to amino acid biosynthesis, were significantly perturbed in the resistant cell line compared to wild type at 1 hr following exposure to radiation. Among these, arginine biosynthesis was the most altered pathway, while phenylalanine, tyrosine and tryptophan biosynthesis had higher impact value (Figure 5.6.A). Furthermore, the metabolic set enrichment analysis identifies biochemical processes such as Warburg effect, urea cycle and ammonia recycling as top enrichment metabolite sets specifically in radioresistant cell line, suggesting a significant metabolic reprogramming following exposure to radiation (Figure 5.6.B).

5.3.1.3 Identification of potential metabolites utilising ROC to discriminate between resistant and wild type MDA-MB-231 cells.

The identification of metabolites with high discriminating potential between the assessed cell lines was conducted utilising receiver operating characteristics (ROC). The abundance of metabolites in resistant and wild type MDA-MB-231 cells at 1 hr following exposure to radiation was analysed using MetaboAnalyst software. Following this, the performance and accuracy of the model in identification of potential biomarkers was assessed via a ROC curve (Figure 5.7), which take in consideration the area under the curve, sensitivity, and specificity of each individual metabolite. The metabolic features with higher urea under the curve are shown in figure (Figure 5.7 A-C).

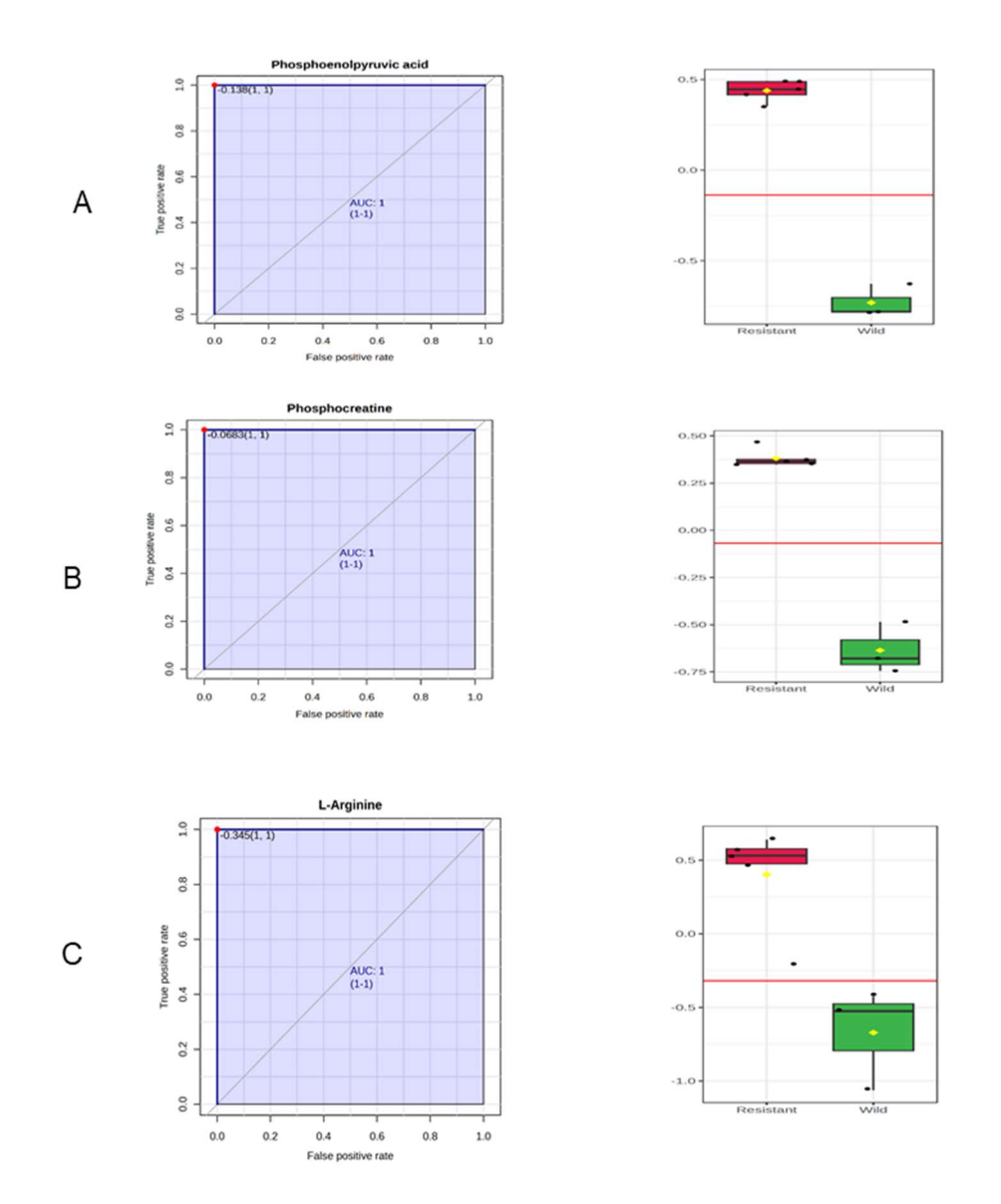


Figure 5-7 Metabolites identification utilising ROC.

Receiver operating characteristic (ROC) analysis of the top 3 metabolites with highest area under the curve differentiating radioresistant from wild type MDA-MB-231 cells 1hr following exposure to radiation. Panels (A-C) display boxplots and corresponding ROC curves for phosphoenolpyruvic acid, phosphocreatine, and β -Alanine, respectively.

Figure 5.7 has demonstrated that Phosphoenolpyruvic acid, phosphocreatine and L-Arginine were highly expressed in the radiation resistant cell line when compared to wild type MDA-MB-231 cell line at 1hr post exposure to radiation. Furthermore, the area under the curve for these metabolites was higher, indicating the sensitivity and specificity of these candidate biomarkers in discriminating between the tested groups.

5.3.2 Cellular metabolome of an established radioresistant and wild type triple negative breast cancer cell lines at 4hr following exposure to 2 Gy radiation

To assess the intermediate response of radioresistant and wild type MDA-MB-231 cells to radiotherapy, untargeted metabolomics at 4hr following exposure to radiation has been conducted.

Data normalization was performed as a pre-analysis step to make sure that the investigated samples are comparable and interpretable. Figure 5.8 shows the box plots of log2-transformed abundance data with corresponding retention times after data normalisation as part of the data inspection and quality evaluation process. In this figure, box plots revealed that the metabolites levels are comparable across different samples which is essential for a reliable model and interpretable data.

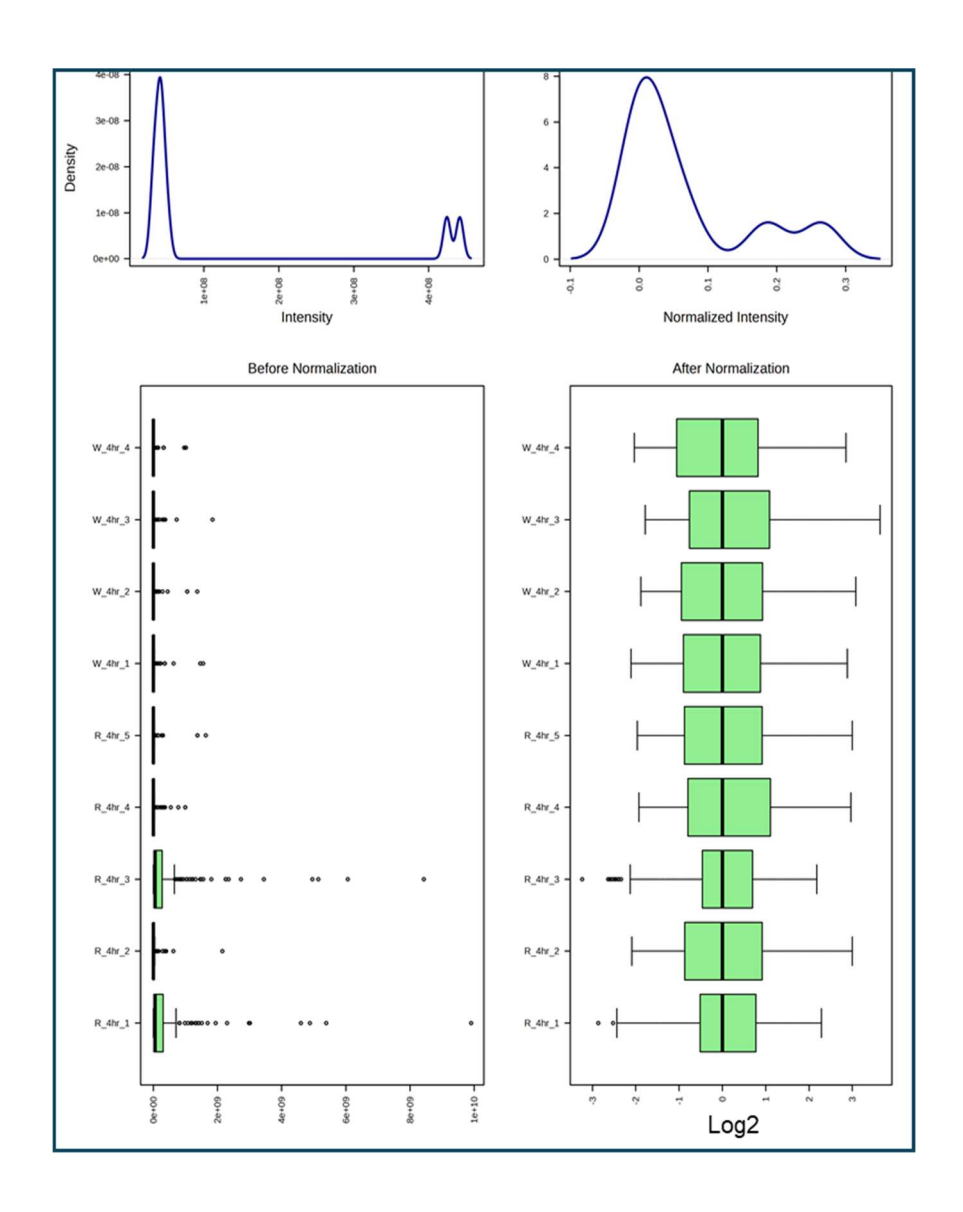


Figure 5-8 Metabolites abundances distribution across samples in response to radiation.

Box plots of log2 area for each individual sample at the 4-hr time point following exposure to 2Gy radiation. Wild-type MDA-MB-231 cell samples (labelled with W) and resistant cell samples (labelled with R) were normalised by median and log2 transformation.

Figure 5.8 revealed that data normalization improved sample comparability, indicating that subsequent analyses reflect true metabolic changes associated with radioresistance rather than systematic bias.

5.3.2.1 Univariate and multivariate analysis

The data was analysed utilising univariate and multivariate analysis. In multivariate analysis, all the features were investigated simultaneously to look at the overall patterns and relationships within data set. The unsupervised PCA, a component of multivariate analysis set, was undertaken to visualise the heterogeneity and clustering of different biological samples. The distribution and distinction among samples can be visualized in PCA scatter plot (Figure 5.9 A). The Supervised analysis using OPLS-DA was performed to determine the important metabolic profiles of samples labelled with wild type and resistant MDA-MB-231 cells (Figure 5.9 B).

The multivariate analysis appropriateness for the current data set has been assessed by model overview quality metrics as shown in (Figure 5.9 C).

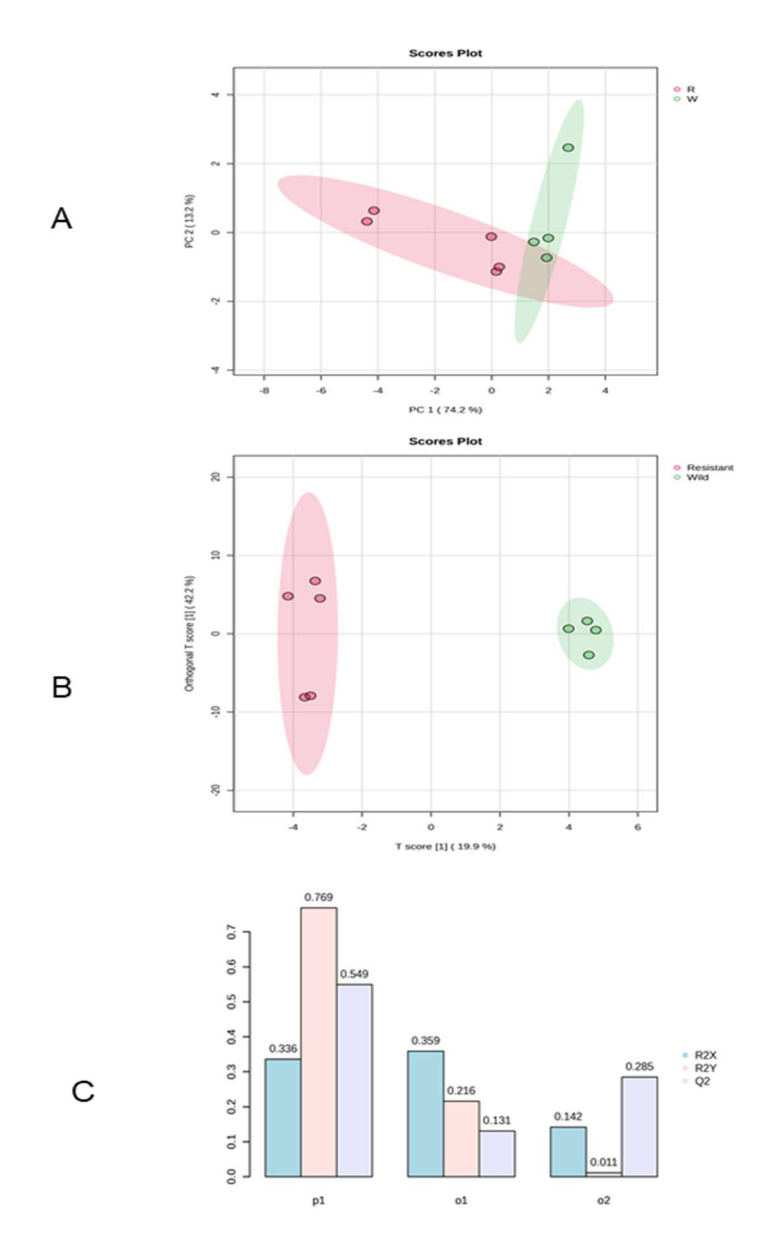


Figure 5-9 Multivariate analysis of extracted MDA-MB-231 cell samples at 4hr following exposure to radiation.

(A) PCA scatter plot showing the clustering of resistant (red) and wild type (green) cell samples (n=5 biological replicates per group). (B) OPLS-DA plot showing the separation of resistant and wild type cells as well as sub-splitting of samples within each group. (C) OPLS-DA model overview quality metrics, where R2 value reflects the model fitness and Q2 value indicates model's predictive ability. P1 indicates the main predictive variation while O1 and O2 (orthogonal component) capture the non-predictive variation or unrelated noise and background variation.

The data analysis by supervised PCA and unsupervised OPLS-DA has shown that each of the assessed groups produce a distinct metabolic profile (Figure 5.9.A-B). These analysis plots have explained the clustering of the samples in resistant group and wild type group. Figure 5.9.C displayed the quality metrics of OPLS-DA multivariate analysis model which demonstrated an eminent prediction ability value and a satisfactory model fitness of ($R^2 = 0.76$ and $Q^2 = 0.54$), suggesting that the model is reliable in distinguishing between the investigated groups.

The univariate data analysis set including t-test, volcano plot and fold change were conducted to assess the individual metabolite abundance across group samples, which will inform the alterations in metabolites between the compared groups. The statistically significant changes in metabolite expression were determined by performing t-test analysis to determine the metabolites that are statistically changed between the two groups (Figure 5.10 A). To measure the magnitude of the changes in metabolites across the investigated samples, a fold change test was performed on the recruited data of metabolites extracted from resistant and wild-type MDA-MB-231 cells. Fold change test can identify the higher and lower expression of metabolic features according to the commonly used threshold set, which was 2 (FC>2 or log2 ≥ ±1) in the current study. Figure 5.10 B shows the metabolites with different magnitude of changes, where metabolites were upregulated when FC> 2 and downregulated when FC<0.05.

To identify the metabolites with statistically significant changes (P<0.5) and significant fold changes (FC>2 or $\log 2 \ge \pm 1$), a Volcano plot was utilised, which has the algorithm combining both of t-test and fold change. Figure 5.10 C displayed the scattering of metabolites according to their p-values and fold changes.

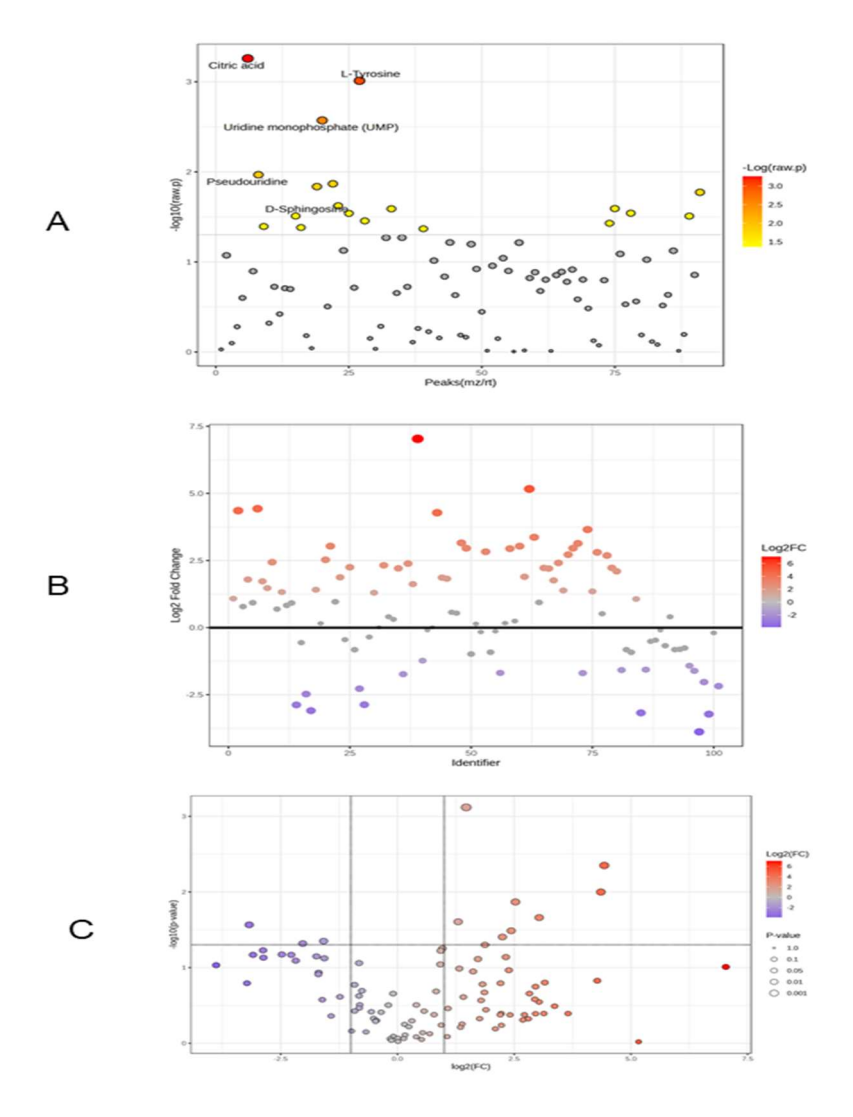


Figure 5-10 Univariate analysis of extracted MDA-MB-231 cell samples.

Metabolite abundances extracted from resistant and wild-type MDA-MB-231 cells at 4 hr following exposure to radiation were compared utilising univariate analysis. (A) Metabolites analysed with t-test were significant at P>0.05, and dots are scaled by a colour gradient from yellow (less difference) to red (high difference). (B) Fold change analysis comparing resistant to wild type cells, where the biologically significant metabolites above threshold (FC>2 or <0.05 or log2≥ ±1) are highlighted in colour ranging from blue (downregulated) to red (upregulated). (C) Volcano plot showing significantly changed metabolites combining t-test and fold change at p>0.05 and log2≥ ±1. Dots colour showing regulation (red for upregulated, and blue for downregulated), while the Dot size shows the statistical change (larger dots indicating higher difference).

Figure 5.10 A displays the metabolite abundances that have significantly changed (P>0.05) as a result of t-test analysis of metabolites extracted from resistant and wild type MDA-MB-231 cells at 4hr following exposure to radiation. The data analysis has shown that 19 metabolites were statistically significantly changed when compared resistant to wild type cells (P<0.05). Furthermore, several metabolites including citric acid, pseudouridine, L-tyrosine and uridine monophosphate were highly changed among the significant metabolites (Figure 5.10 A). The data in Figure 5.10 B demonstrated that 32 metabolic features had significant fold change (FC>2 or the $\log 2 \ge \pm 1$) when resistant compared to wild type cells. Among them, pseudouridine and citric acid were the highly upregulated metabolites in resistant cells compared to wild type MDA-MB-231 cells. The data analysis utilising volcano plot revealed that 11 metabolites were statistically significant (P<0.05) and had significant fold changes in a ratio of resistant/ wild type cells (Figure 5.10 C).

To assess the relationship between metabolites and the investigated samples, heatmap cluster analysis was conducted. This test can identify the samples that share similar metabolic profile and visualise the metabolites abundances using gradient colour, where the significant metabolites with blue colour are downregulated while red colour are upregulated. Figure 5.11 displays the clustering of metabolites based on their relations with the samples as well as their expression in a gradient colour manner. The outlier samples were excluded to avoid interfering with metabolite expressions of another group.

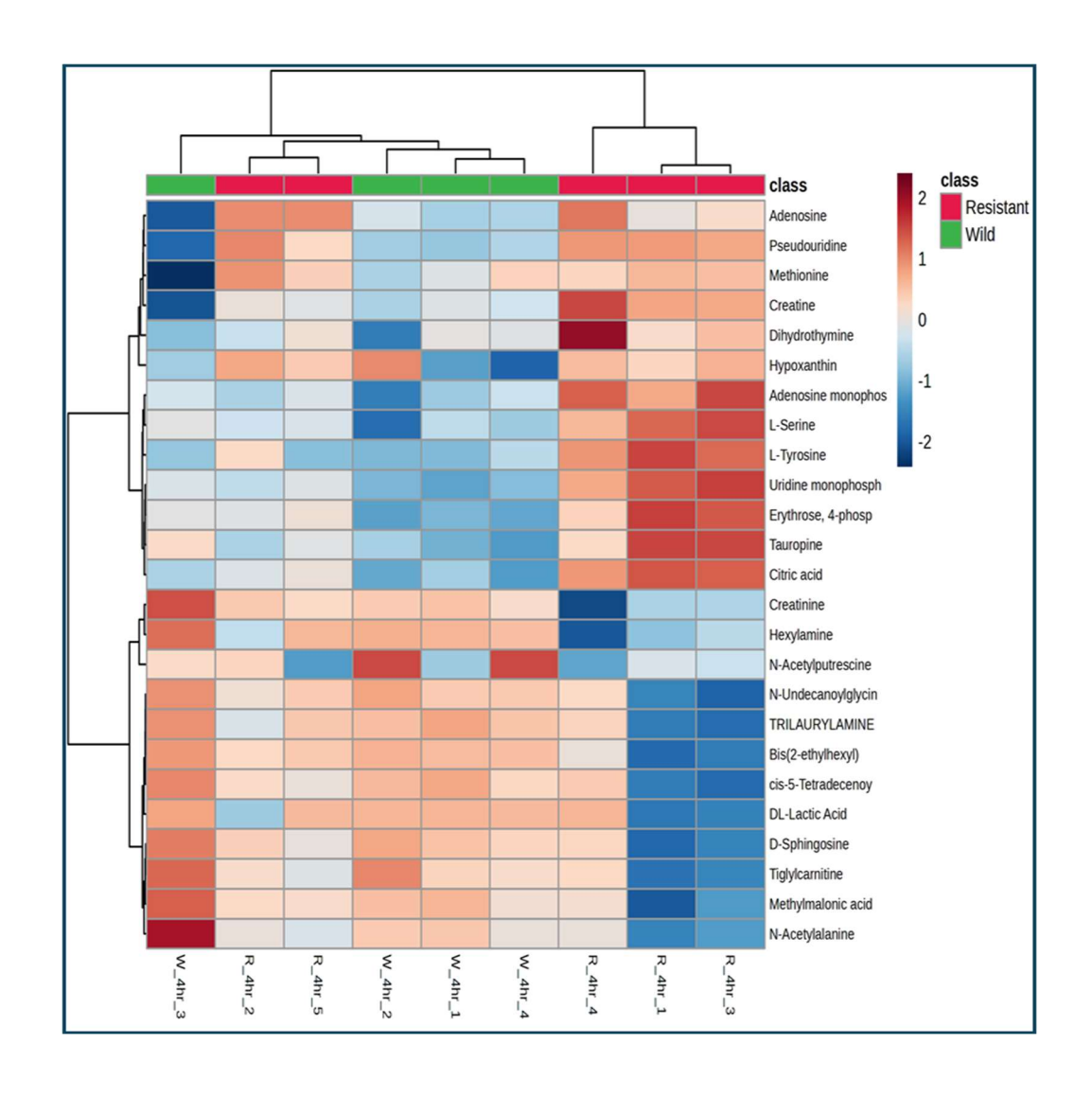


Figure 5-11 Metabolites clustering analysis.

Metabolites abundances across samples of resistant and wild type MDA-MB-231 cells at 4hr following exposure to radiation. The colours reflect the abundance of metabolites across samples ranging from blue (downregulated) to red (upregulated) with clear distinction of resistant and wild type MDA-MB-231 cell samples. The red colour gradient represent upregulation while the blue colour gradient represents the downregulation of metabolites.

Figure 5.11 shows that several metabolites, including Adenosine, Pseudouridine, Citric acid, and Hypoxanthine, are expressed more strongly in resistant samples than in wild-type MDA-MB-231 samples. However, metabolic features such as DL-lactic acid, Tiglylcarnitine, and N-acetylalanine were downregulated in resistant cells.

The variable importance in projection (VIP), a statistical metric, was performed to identify which key features contributed to discriminating the resistant group from the wild type at 4 hours following exposure to radiation. Figure 5.12 displays the top 15 metabolites, with their abundances reflected by coloured boxes that differentiate the resistant from the wild-type group.

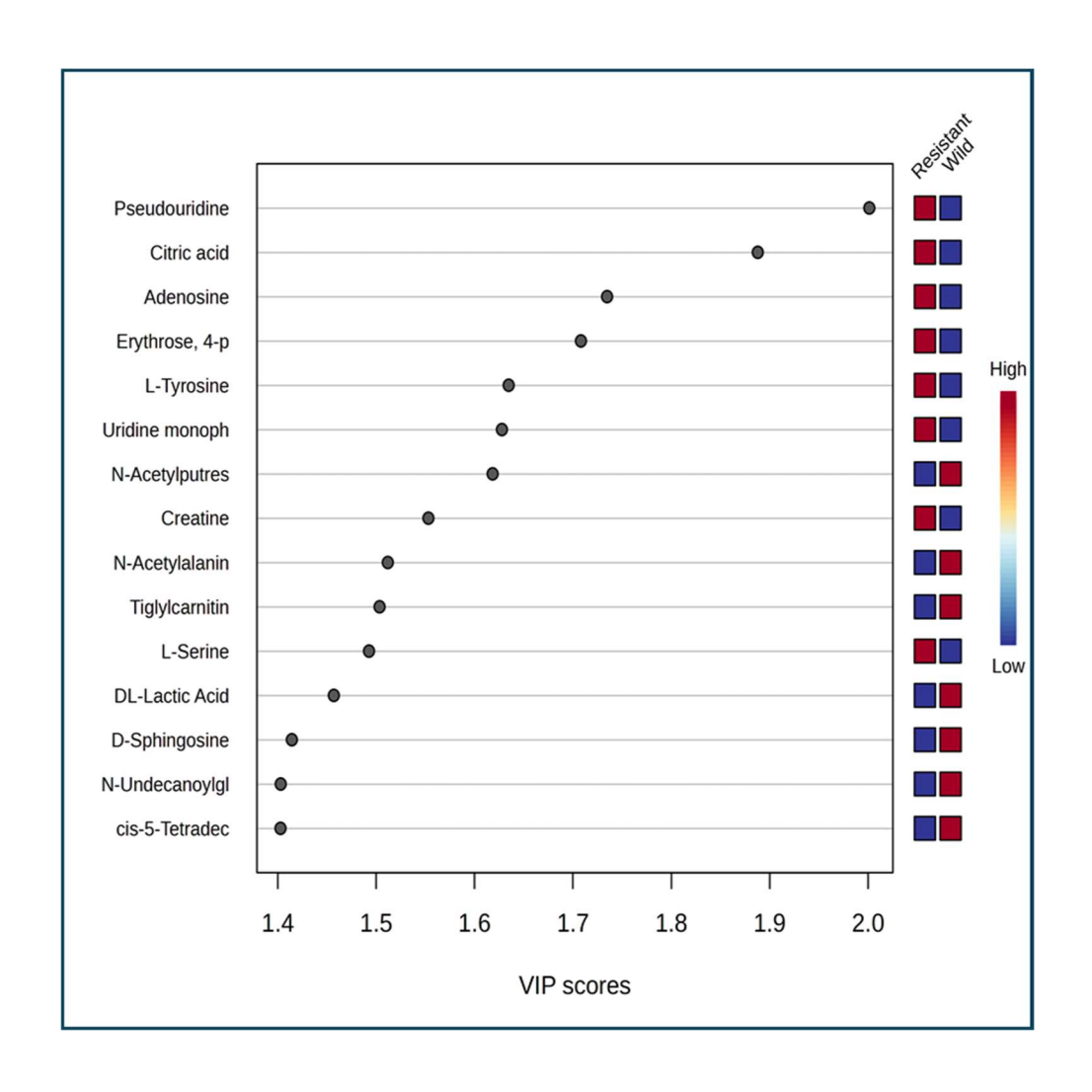


Figure 5-12 Variable importance in projection (VIP) for top 15 metabolites.

The variable importance in projection (VIP) score plot showing top 15 significant features responsible for differentiation of resistant group from wild type MDA-MB-231 group in the OPLS-DA model at 4hr following exposure to radiation. The colour code denotes the concentration of each metabolite in the two groups, where red indicates high concentration and blue indicates low concentration.

The data analysis has highlighted several amino acids, including L-Tyrosine and L-Serine, pseudouridine, and citric acid as metabolites with high VIP score, reflecting the capability of these metabolites in distinguishing between the assessed groups following exposure to radiation. Furthermore, these metabolites were highly expressed in resistant cells compared to wild-type MDA-MB-231, suggesting their contribution to inducing radioresistance.

5.3.2.2 Metabolite set enrichment analysis (MSEA) and Pathway analysis

Utilising the MetaboAnalyst website, metabolite set enrichment analysis (MSEA) and pathway analysis were performed to assess the alterations in metabolic pathways or metabolic sets of biochemical events in resistant and wild-type MDA-MB-231 cells. The metabolic pathways identified by pathway analysis and the top 25 enriched metabolite sets at 4 hr following exposure to radiation are shown in Figure 5.13 A and B, respectively.

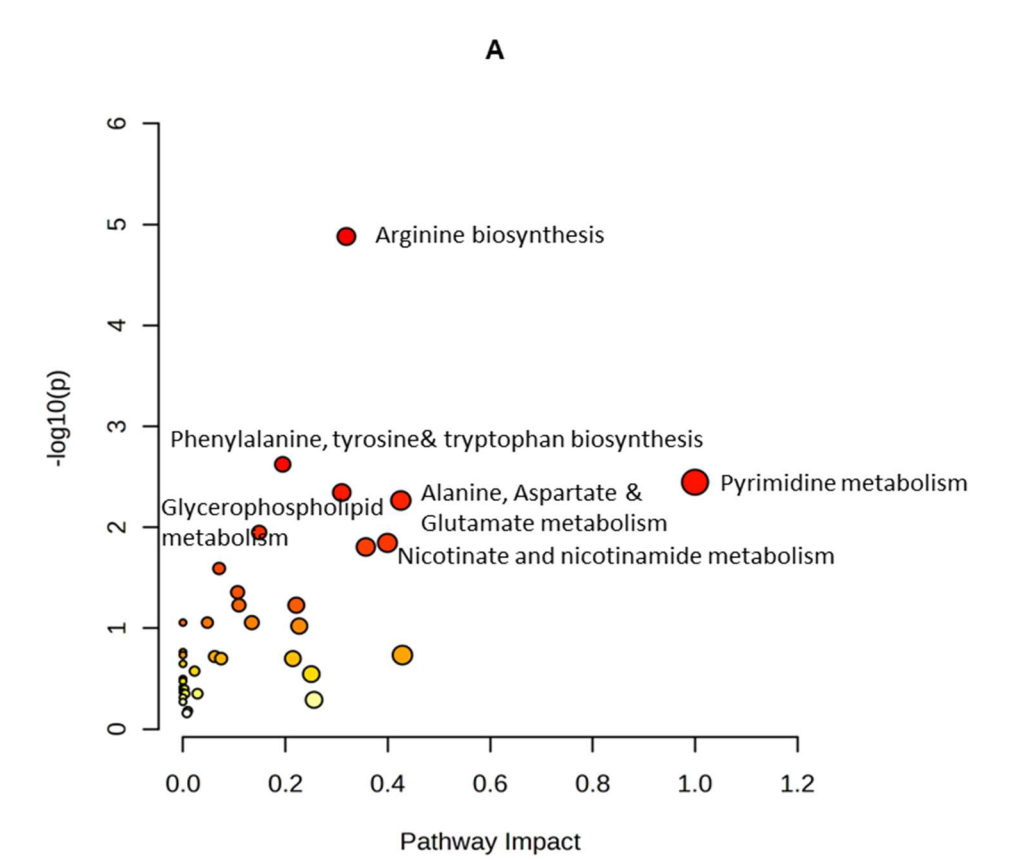
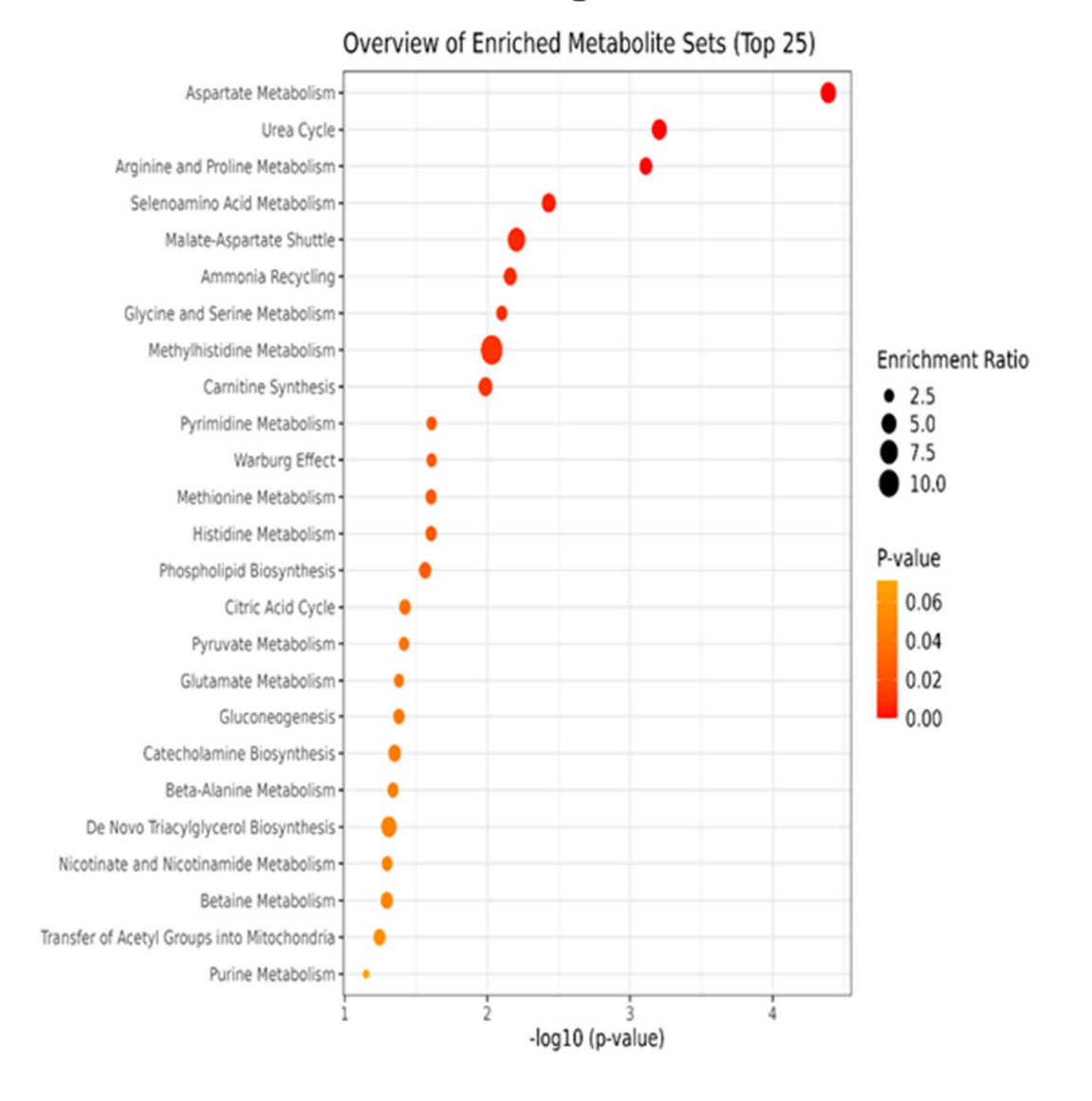


Figure 5-13 Metabolic pathway analysis and MSEA.

The pathway analysis of the metabolites identified in resistant and wild type MDA-MB-231 cells at 4hr following exposure to radiation. (A) The impact value of each identified pathway, where the labelled pathways were significantly changed (P value <0.05). (B) The top 25 enriched pathways where the size and the colour represent the enrichment ratio and the statistical significance, respectively.





The pathway analysis for metabolites has shown the alterations in biological behaviour of several metabolic pathways, particularly those associated with amino acid biosynthesis, in resistant and wild type MDA-MB-231 cells at 4hr following exposure to radiation. Among these pathways, arginine biosynthesis was the highly altered pathway in the resistant cell line (Figure 5.13.A). Additionally, biochemical events, including aspartate metabolism, urea cycle and ammonia recycling were identified as the top enriched metabolite sets in radioresistant MDA-MB-231 cells (Figure 5.13.B).

5.3.2.3 Identification of potential metabolites utilising ROC to discriminate between resistant and wild type MDA-MB-231 cells.

The receiver operating characteristics (ROC), a statistical measure, was performed to identify the key metabolites with high potential differentiation between the investigated groups. The expression of metabolites in resistant and wild type MDA-MB-231 cells at 4hr post exposure to radiation was determined utilising the MetaboAnalyst webserver. Thereafter, the model's precision and performance in identifying candidate biomarkers were assessed by employing a ROC curve that considers the area under the curve, sensitivity, and specificity of each individual metabolite (Figure 5.14).

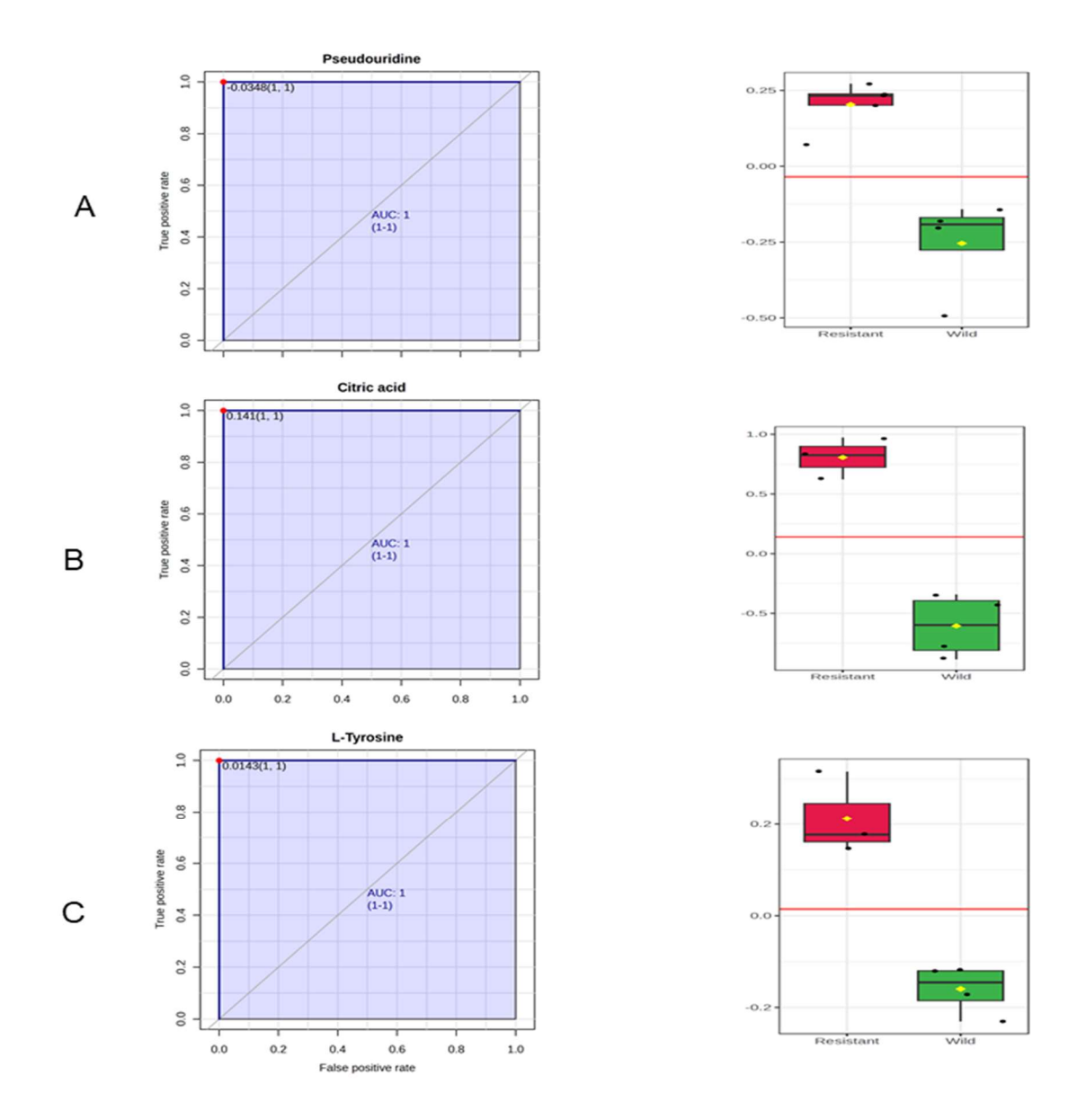


Figure 5-14 Biomarkers identification utilising ROC.

Receiver operating characteristic (ROC) analysis of the top 3 metabolites with highest area under the curve differentiating radioresistant from wild type MDA-MB-231 cells 4hr following exposure to radiation. Panels (A-C) display boxplots and corresponding ROC curves for Pseudouridine, Citric acid and L-Tyrosine, respectively.

Figure 5.14 has shown that Pseudouridine, Citric acid and L-Tyrosine were upregulated in resistant samples compared to wild type MDA-MB-231 cell samples at 4hr post treatment with 2Gy radiation. Furthermore, these metabolites had higher area under the curve that reflect the sensitivity and specificity of these potential biomarkers in differentiation of the assessed groups.

5.3.3 Cellular metabolome of an established radioresistant and wild type triple negative breast cancer cell lines at 24hr following exposure to 2Gy radiation

The late metabolic response of radioresistant and wild type MDA-MB-231 cell lines following exposure to radiation was evaluated utilising untargeted metabolomics. The cellular samples were extracted at 24hr post treatment with radiotherapy.

The raw data was normalised to eliminate any technical noises or other biases that are not related to true biological variations. As part of data inspection and quality assessment, Figure 5.15 displays the box plots of logarithmic transformed data abundances with matched retention times following data normalisation.

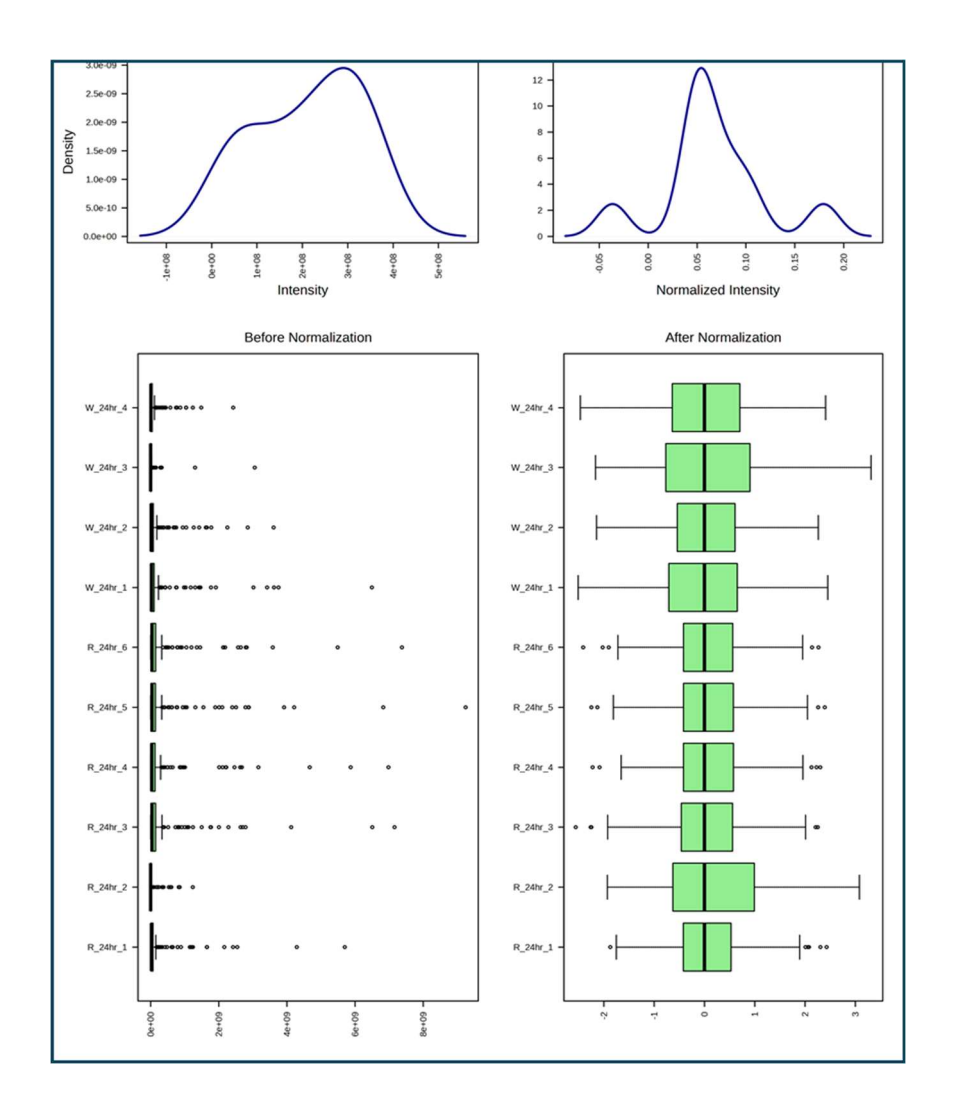


Figure 5-15 Metabolites abundances distribution across samples in response to radiation.

Box plots of log2 area for each individual sample at 24 hr time point following exposure to 2Gy radiation. Wild type MDA-MB-231 cell samples (labelled with W) and resistant cell samples (labelled with R) were normalised by median and log2 transformation.

In Figure 5.15, box plots demonstrated that the features abundances are comparable across different samples, which means that the observed alterations in metabolites expression reflect the biological differences rather than technical variations.

5.3.3.1 Univariate and multivariate analysis

The principal component analysis (PCA), an unsupervised multivariate test, was performed to assess the statistical behaviour of the recruited samples in terms of clustering that reflects the similarities and differences among them. Figure 5.16 A displays the clustering and scattering of the assessed samples in the PCA plot. Furthermore, another multivariate test called OPLS-DA was then conducted, which employs the supervised analysis of the samples, considering the labelling of sample groups. The clustering of samples sharing similar metabolic characteristics following the OPLS-DA test is shown in Figure 5.16. B. Additionally, the performance and quality of the OPLS-DA model in the differentiation of resistant and wild-type MDA-MB-231 cell samples are shown in (Figure 5.16. C).

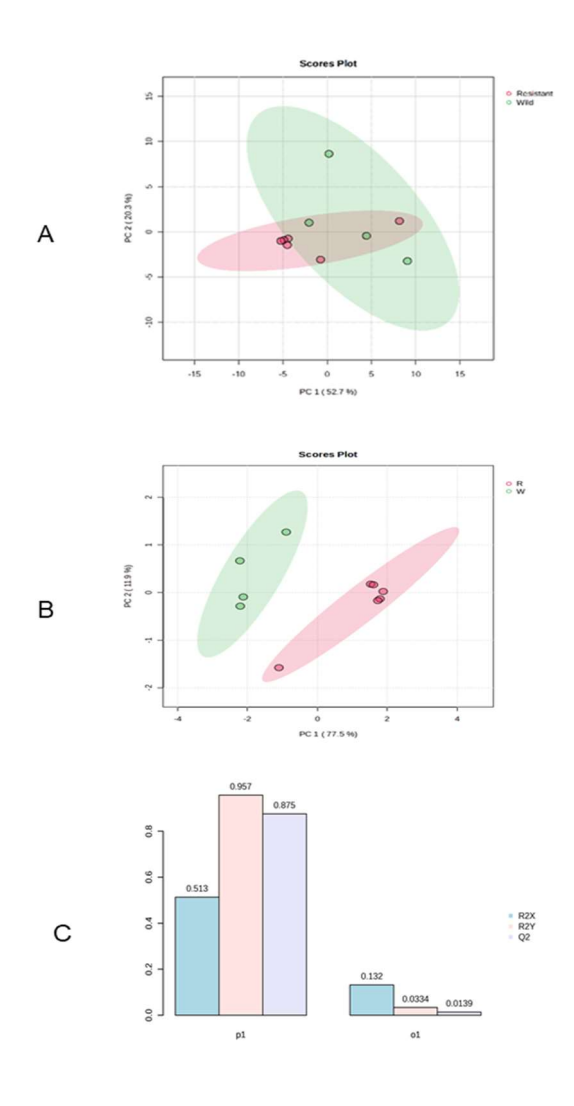


Figure 5-16 Multivariate analysis of extracted MDA-MB-231 cell samples at 24hr following exposure to radiation.

(A) PCA scatter plot shows the clustering of resistant (red) and wild type (green) cell samples (n=5 biological replicates per group). (B) OPLS-DA plot showing the separation of resistant and wild type cells and sub-splitting of samples within each group. (C) OPLS-DA model overview quality metrics, where the R2 value reflects the model's fitness and the Q2 value indicates the model's predictive ability. P1 indicates the main predictive variation, while O1 and O2 (orthogonal component) capture the non-predictive variation or unrelated noise and background variation.

The data analysis utilising multivariate models, unsupervised PCA and supervised OPLS-DA, has shown the separation of investigated groups of samples as well as clustering of samples within each individual group (Figure 5.16.A-B), which indicate that the biological differences are comparable between groups. The performance and quality metrics of these analysis models shown in (Figure 5.16.C) have demonstrated a significant prediction value and satisfactory model fitness ($R^2 = 0.957$ and $Q^2 = 0.875$), reflecting the reliability of the model in discriminating between the investigated groups.

To assess the biological behaviour of individual metabolites across different samples, data analysis utilising univariate model measures comprised of t-test, volcano plot, and fold change was performed. Figure 5.17 displays the distribution of the individual metabolites in the analysis plots based on their t-test statistical significance (P<0.05), magnitude of changes (FC>2 or $\log 2 \ge \pm 1$) and volcano behaviour test that combines both of t-test and fold change thresholds.

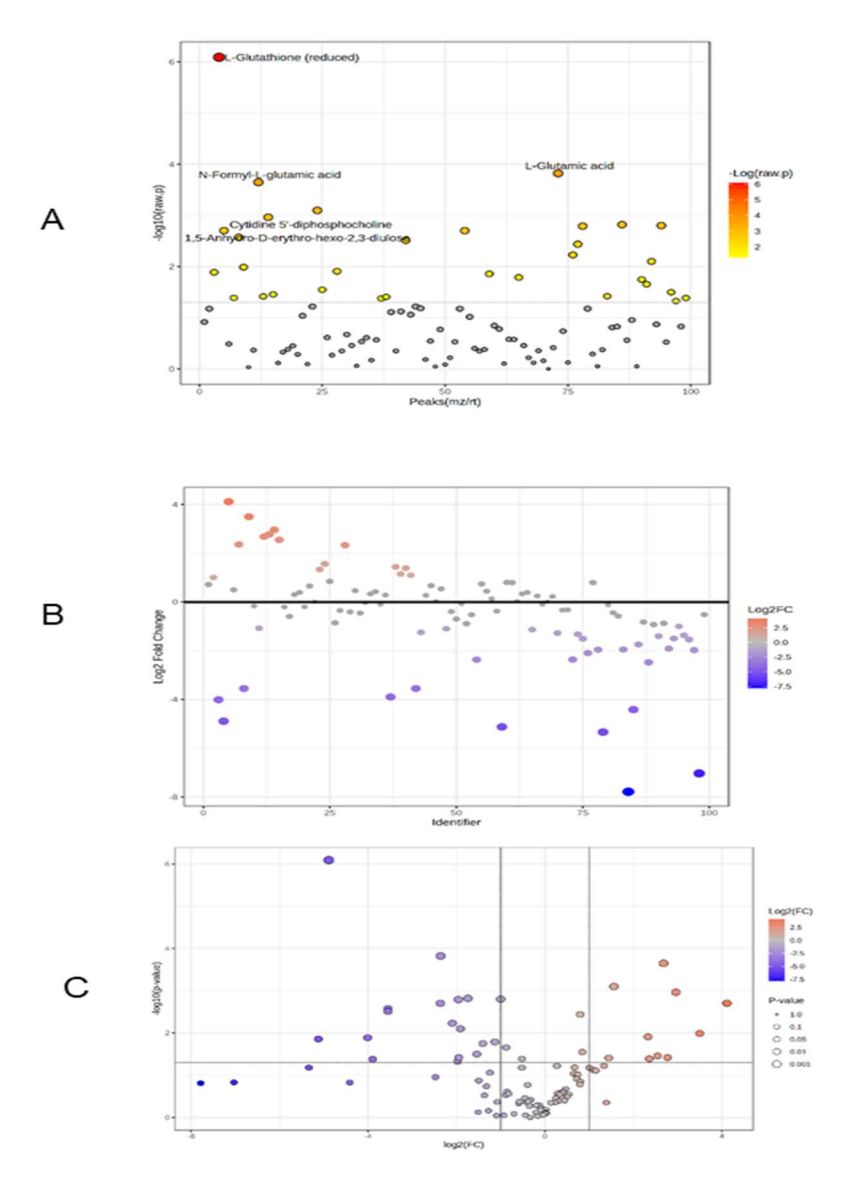


Figure 5-17 Univariate analysis of extracted MDA-MB-231 cell samples.

Metabolite abundances extracted from resistant and wild-type MDA-MB-231 cells at 24 hr following exposure to radiation were compared utilising univariate analysis. (A) Metabolites analysed with t-test were significant at P>0.05, and dots are scaled by a colour gradient from yellow (less difference) to red (high difference). (B) Fold change analysis comparing resistant to wild type cells, where the biologically significant metabolites above threshold (FC>2 or <0.05 or log2≥ ±1) are highlighted in colour ranging from blue (downregulated) to red (upregulated). (C) Volcano plot showing significantly changed metabolites combining t-test and fold change at p>0.05 and log2≥ ±1. Dots colour showing regulation (red for upregulated, and blue for downregulated), while the Dot size shows the statistical change (larger dots indicating higher difference).

Figure 5.17 A has shown the metabolites scattering based on their statistical differences across samples following t-test analysis. The data revealed that 31 metabolites extracted from resistant and wild type MDA-MB-231 cells at 24hr following exposure to radiation were significantly changed when comparing the resistant to wild type cells (P<0.05). Additionally, some metabolites including Glutathione (reduced) were highly changed than other statistically significant metabolites and were highlighted in (Figure 5.17 A).

The data analysis revealed that 43 metabolites had a significant magnitude of change $(FC>2 \text{ or the log2} \ge \pm 1)$ as visualised in Figure 5.17 B. In this plot, L-lysine, Thiamine, and L-histidine abundances were higher in the resistant than wild type MDA-MB-231 cells. Volcano plot analysis demonstrated that Cytidine 5'-diphosphocholinemetabolites and 3-Phosphoglyceric acid changed significantly (P<0.05) and showed significant fold changes in a resistant group compared to wild type (Figure 5.17 C).

Heatmap cluster analysis was utilised to assess the abundances of metabolites across the tested samples. This analysis tool employs gradient colour to visualise the concentration of metabolites over the samples, ranging from blue (downregulated) to red (upregulated). In Figure 5.18, the metabolites are clustered according to their relationship with the samples as well as their expression represented in a gradient colour pattern. The outlier samples were excluded to avoid interfering with metabolite expressions of another group.

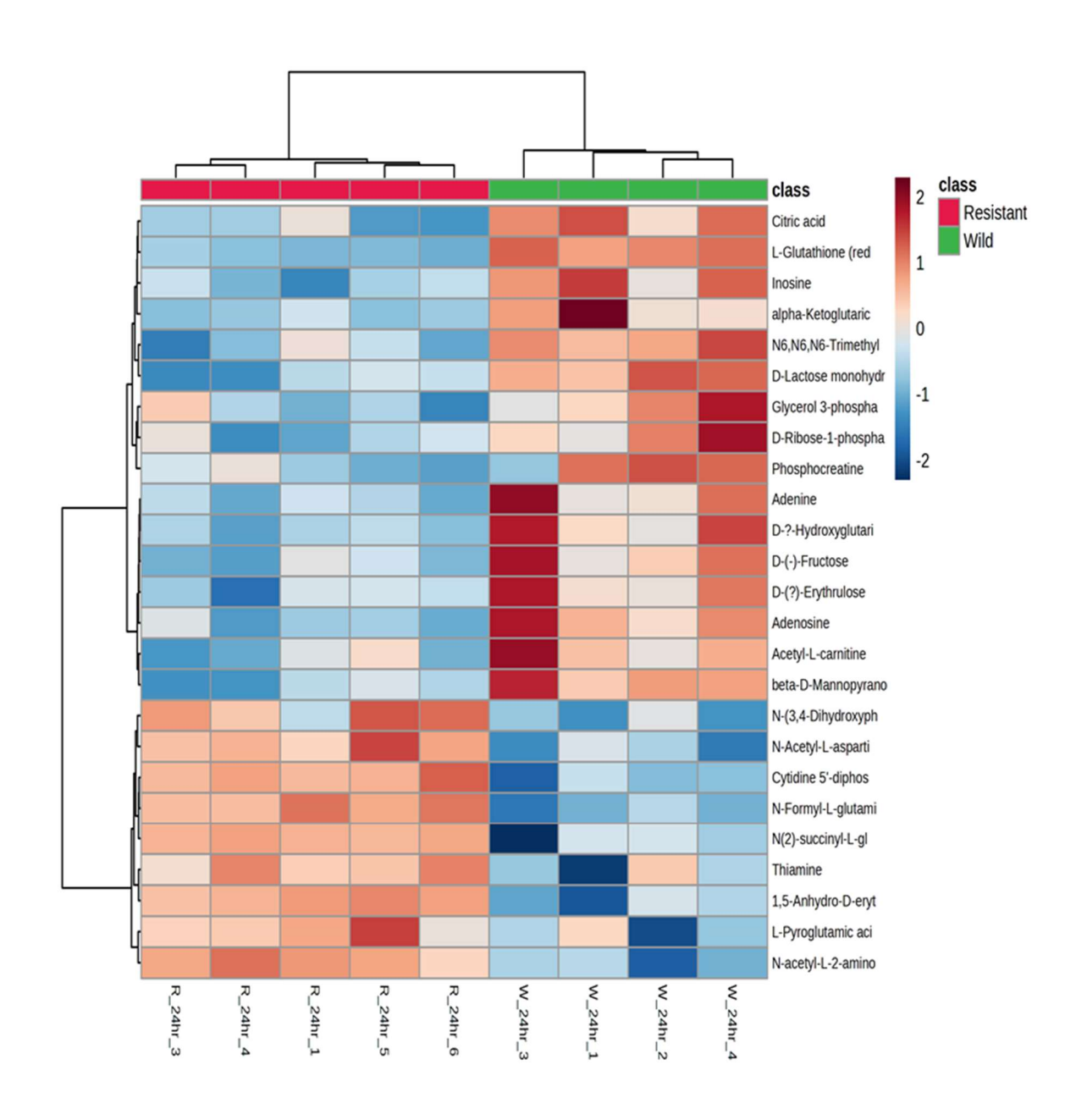


Figure 5-18 Metabolites clustering analysis.

Metabolites abundances across samples of resistant and wild type MDA-MB-231 cells at 24hr following exposure to radiation. The colours reflect the abundance of metabolites across samples, with a clear distinction between resistant and wild-type MDA-MB-231 cell samples. The red colour gradient represents upregulation while the blue colour gradient represents the downregulation of metabolites.

Figure 5.18 has demonstrated higher abundances of N-succinyl-L-glutamic acid, Cytidine 5'-diphosphocholine, and Thiamine in resistant samples compared to wild type MDA-MB-231 samples. Nevertheless, several metabolites including L-Glutathione, Glycerol 3-phosphate and Citric acid had higher levels in wild type cells and lower levels in resistant cells.

To identify which key metabolites contributed to the differentiation of the resistant group from wild wild-type MDA-MB-231 group, a statistical tool called Variable Importance in Projection (VIP) has been utilised. The top 15 discriminating metabolites with their levels represented by colour codes are shown in Figure 5.19.

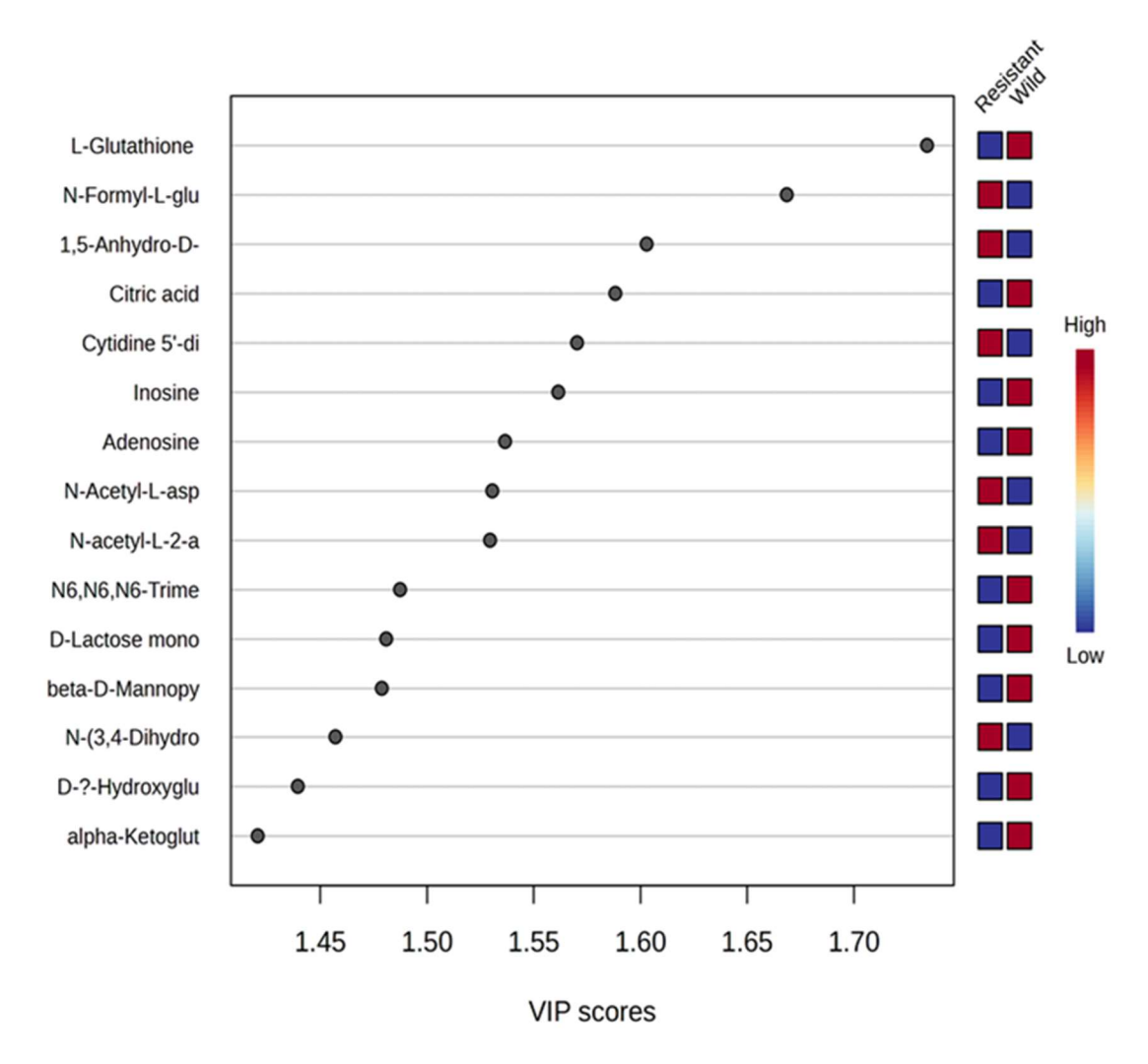


Figure 5-19 Variable importance in projection (VIP) for top 15 metabolites.

The variable importance in projection (VIP) score plot showing top 15 significant features responsible for differentiation of resistant group from wild type MDA-MB-231 group in the OPLS-DA model at 24hr following exposure to radiation. The colour code denotes the concentration of each metabolite in the two groups, where red indicates high concentration and blue indicates low concentration.

Figure 5.19 demonstrated the metabolites with higher VIP score including Cytidine 5'-diphosphocholine and N-Acetyl-L-Aspartate. These metabolites were capable to discriminate between the assessed groups in OPLS-DA model. Moreover, the concentration of these top differentiated metabolites was higher in the resistant group compared to wild type MDA-MB-231 group.

5.3.3.2 Metabolite set enrichment analysis (MSEA) and Pathway analysis

The variations in biochemical processes and metabolic pathways of resistant and wild type MDA-MB-231 cells at 24hr following exposure to radiation was evaluated employing the metabolite set enrichment analysis (MSEA) and pathway analysis tools in the MetaboAnalyst webserver. Figure 5.20 displays the metabolic pathways determined via pathway analysis and the top 25 enriched metabolite sets at 24hr following exposure to radiation.

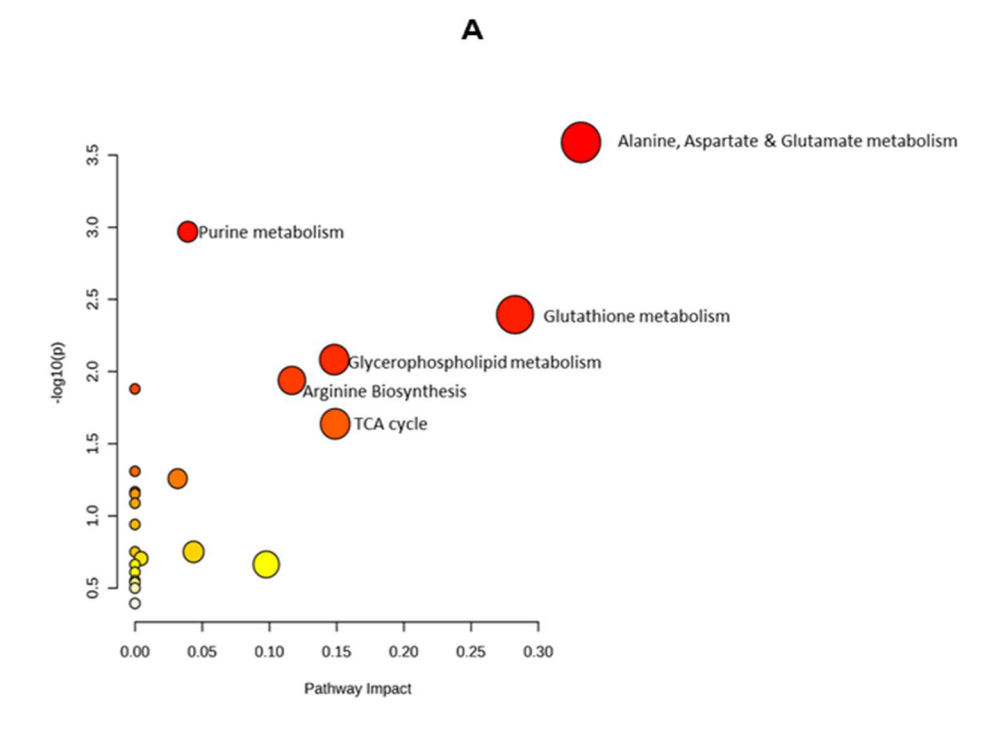


Figure 5-20 Metabolic pathway analysis and MSEA.

The pathway analysis of the metabolites identified in resistant and wild type MDA-MB-231 cells at 24hr following exposure to radiation. **(A)** The impact value of each identified pathway, where the labelled pathways were significantly changed (P value <0.05). **(B)** The top 25 enriched pathways where the size and the colour represent the enrichment ratio and the statistical significance, respectively.

В

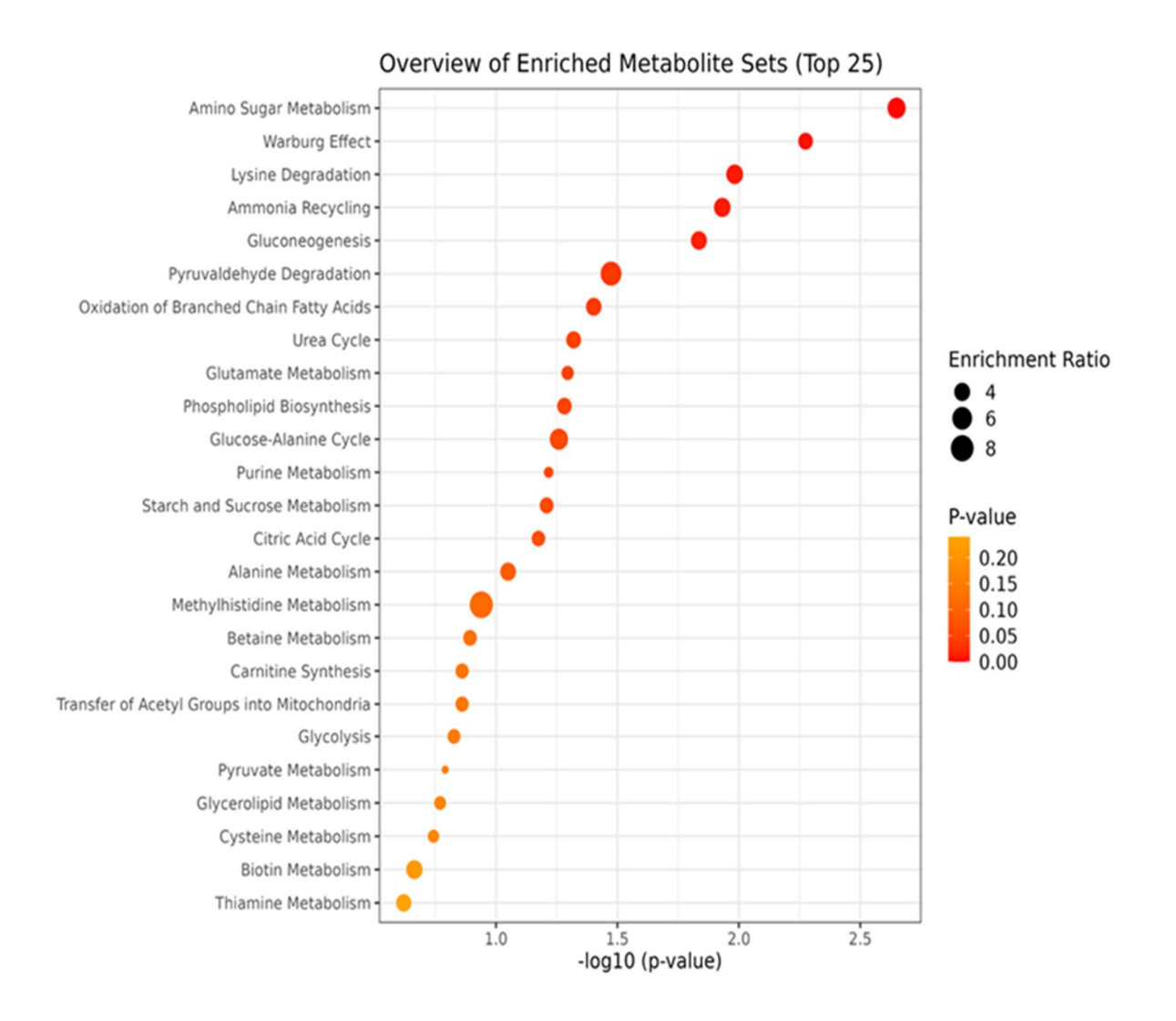


Figure 5.20.A demonstrated the perturbation of several metabolic pathways, including Alanine-Aspartate-Glutamate metabolism, Glutathione metabolism, Arginine biosynthesis, and TCA cycle at 24hr following exposure of resistant and wild type MDA-MB-231 cells to radiation. The pathway with higher significant alteration and higher impact value in the resistant cells was Alanine-Aspartate-Glutamate metabolism. Furthermore, the enrichment set analysis revealed that the biochemical

process including Warburg effect, ammonia recycling and gluconeogenesis were highlighted as the top involved cellular events in the resistant cells (Figure 5.20.B).

5.3.3.3 Identification of potential metabolites utilising ROC to discriminate between resistant and wild type MDA-MB-231 cells.

To determine the key metabolites discriminating between the sample groups, the statistical tool called the receiver operating characteristic (ROC) was utilised. The box plots and ROC curves for potential metabolites that differentiate the resistant from wild type MDA-MB-231 samples at 24hr post exposure to radiation are shown in Figure 5.21. The sensitivity, specificity, and urea under the curve of each particular metabolite were all represented via ROC curve.

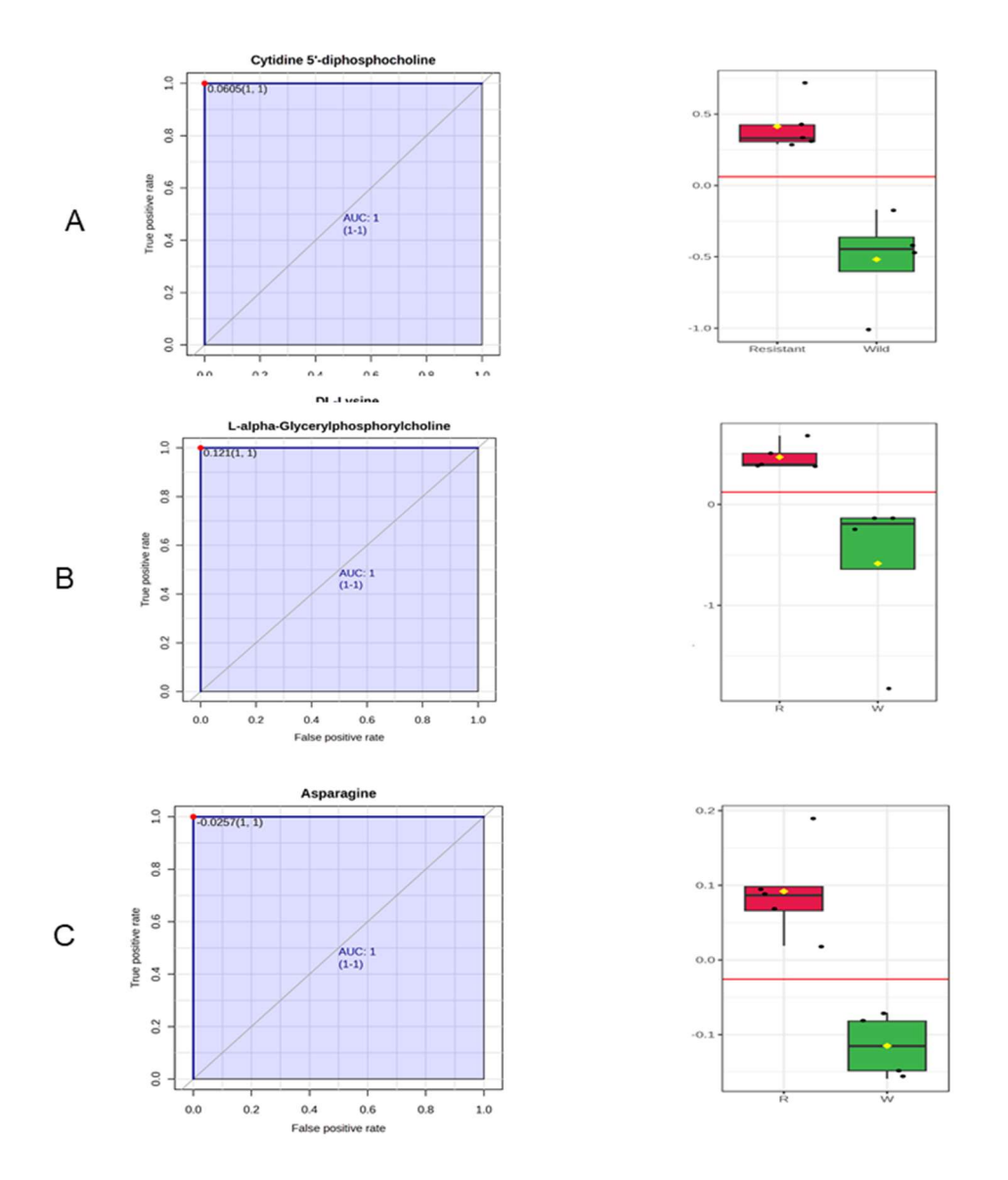


Figure 5-21 Metabolites identification utilising ROC

Receiver operating characteristic (ROC) analysis of the top 3 metabolites with highest area under the curve differentiating radioresistant from wild type MDA-MB-231 cells 24hr following exposure to radiation. Panels (A-C) display boxplots and corresponding ROC curves for Cytidine 5'-diphosphocholine, L-alpha-Glycerylphosphorylcholine and Asparagine, respectively.

Figure 5.21 demonstrated that the levels of Cytidine 5'-diphosphocholinemetabolites, N-Acetyl-L-Aspartic acid and N-succinyl-L-glutamic acid are higher in resistant samples when compared to wild type MDA-MB-231 cell samples at 24hr following exposure to radiation dose. Furthermore, the area under the curve for these metabolites was higher, indicating the sensitivity and specificity of candidate biomarkers in discriminating the evaluated sample groups.

5.4 Discussion

Metabolic reprogramming refers to the process by which cancer cells modulate their metabolism to meet the increased demands for energy, biosynthesis, and survival in stressful environments (Liu *et al.* 2024b). It is one of the particular features of triple negative breast cancer contributing to its aggressiveness and poor prognosis (Gandhi and Das, 2019; Wang, Jiang and Dong, 2020; Munkácsy, Santarpia and Győrffy, 2023). TNBC cells undergo substantial metabolic alterations to meet their increasing energy demand, supporting rapid proliferation, stress adaptation, and therapeutic resistance. The comprehension of metabolic reprogramming, particularly in the context of TNBC resistance to radiotherapy, can disclose potential therapeutic vulnerabilities that can be targeted to reverse the resistance and improve therapeutic outcomes for this aggressive breast cancer subtype(Kim, Fahmy and Haffty, 2024). In the current study, a metabolomics approach was used to identify altered metabolic pathways contributing to the radiotherapy resistance of triple-negative breast cancer cell lines, which will inform potential therapeutic targets to overcome radiotherapy resistance.

Liquid-chromatography mass spectrometry was utilised to assess the cellular metabolome following exposure of resistant and wild-type MDA-MB-231 cell lines to radiation. The metabolic alterations were investigated at three distinct phases: early response (1 hr following exposure), intermediate response (4 hr following exposure), and late response (24 hr following exposure).

5.4.1 Early Response of Resistant and Wild type MDA-MB-231 cells to radiation

The early response of resistant MDA-MB-231 cell lines at 1hr following exposure to radiation revealed several perturbations of metabolic pathways in comparison to the

wild type cells. Multivariate and univariate analysis consistently differentiated between radioresistant and parental cell line and highlighted several key metabolites including phosphoenolpyruvate and phosphocreatine, and enrichment of pathways such as arginine biosynthesis and glutamine/glutamate metabolism as drivers for early response following exposure to radiation. The robustness of these statistical findings reinforces the interpretation of metabolic reprograming in the resistant cells that enable them to endure radiation induced stress.

Energy buffering: Phosphocreatine and phosphoenolpyruvate were identified among the highest VIP score metabolites, suggesting their potential contribution to inducing resistance to radiation. These metabolites are essential in several biochemical processes, including glycolysis, antioxidant defence, and energy metabolism.

Upregulation of phosphocreatine in the radioresistant cell line might indicate effective energy storage or improved energy balancing mechanisms in response to radiationinduced stress. To the best of our knowledge, this study is the first to suggest a potential association between phosphocreatine and radiation resistance in triplenegative breast cancer (TNBC), highlighting a novel area for further investigation. Despite limited evidence for direct association between phosphocreatine and radiation, a previous study investigating cisplatin-resistant MDA-MB-231 cells identified higher phosphocreatine/creatine ratios, suggesting that this metabolic shift may represent a broader resistance strategy in triple-negative breast cancer (TNBC)(Carneiro et al., 2023). Furthermore, creatine kinase brain-type (CKB), the enzyme responsible for phosphocreatine synthesis, has been shown to enhance doxorubicin resistance in MDA-MB-231 cells via activation of TGF-β signalling, a pathway known to facilitate survival (Son et al., 2022). This suggests that alongside its metabolic role, phosphocreatine may also activate signalling cascades that reinforce resistance. Further support arises from HER2-positive breast cancer studies, where mitochondrial creatine kinase 1 phosphorylation was shown to activate

the phosphocreatine shuttle, enabling sustained proliferation in trastuzumab-resistant cells (Kurmi *et al.*, 2018). Although conducted in a different subtype, it emphasises a broader relevance of phosphocreatine-driven metabolic adaptations in therapeutic resistance. Collectively, these findings reinforce the hypothesis that phosphocreatine upregulation in the resistant TNBC model represents a crucial metabolic adaptation with potential functional implications in radiation resistance.

Enhanced glycolysis: in our study, phosphoenolpyruvate (PEP), a key intermediate in the glycolytic pathway, was significantly upregulated in the radioresistant MDA-MB-231 triple-negative breast cancer (TNBC) cell line compared to the parental wild-type counterpart. This accumulation of PEP suggests a shift toward enhanced glycolytic activity, a hallmark of metabolic reprogramming commonly observed in therapyresistant cancers (Liu et al. 2024b). PEP, produced by enolase and subsequently converted to pyruvate via pyruvate kinase, generates ATP to meet the energy demand for highly proliferative and stressed cells (Qian et al., 2017a; Liu et al., 2023). The increase in PEP levels may reflect an adaptive mechanism to support the high energy demands of resistant cells, allowing them to maintain survival under stressful conditions such as irradiation. Phosphoenolpyruvate carboxykinase2 (PCK2) is an important enzyme that helps cancer cells reprogram their metabolism by producing phosphoenolpyruvate (PEP) from TCA cycle intermediates. In triple-negative breast cancer (TNBC), PCK2 plays a crucial role in metabolic reprogramming, particularly in relation to PEP production, where its upregulation was correlated with enhanced TNBC cell growth and metastasis (Gunasekharan et al., 2024). Besides its role in energy production, recent studies have highlighted that PCK2, and PEP can influence cellular behaviour through promoting activation of signalling pathways. For instance, PCK2 knockdown resulted in decreased cell proliferation and downregulation of mTOR signalling (Chang et al., 2025). Moreover, higher levels of PCK2 were associated with increased cell invasion and migration of TNBC cells, as well as

elevated expression of epithelial-to-mesenchymal transition (EMT) markers. These effects were found to be induced by the activation of the TGF-β/SMAD3 signalling pathway (Chang *et al.*, 2025). In a previous study on colon cancer cells, it was found that increased PEP levels could indirectly raise calcium levels inside the cell, promoting the activation of c-Myc, a protein that regulates many genes involved in cell growth and metabolism (Moreno-felici *et al.*, 2020). The clinical relevance of glycolytic reprogramming was highlighted by findings from other cancers, where elevated levels of upstream glycolytic enzymes like enolase (ENO1), which catalyses PEP production, have been associated with cisplatin resistance in gastric cancer (Qian *et al.*, 2017b). Additionally, therapeutic strategies targeting glycolysis, such as the use of 2-deoxyglucose, have shown radiosensitising effects in highly glycolytic and radioresistant cervical cancers (Rashmi *et al.*, 2018).

Taken together, our findings suggest that the upregulation of PEP may contribute to the radioresistance of TNBC cells by supporting their energy demands and activating survival-related pathways.

Arginine metabolism: the data analysis demonstrated that arginine biosynthesis was one of the most significantly altered pathways in the radioresistant MDA-MB-231 breast cancer cell line compared to its wild-type counterpart. This pathway was notably enriched by arginine and lysine, the upregulated amino acids in the radioresistant cells, suggesting a metabolic shift associated with resistance to radiation-induced stress. Due to the potential role of arginine in modulating reactive oxygen species, the elevated arginine levels in resistant cells may enhance their ability to mitigate oxidative stress, as an early adaptation following radiation exposure (Ji et al. 2019b; Kus et al. 2018). In alignment with our findings, a metabolomics study showed that arginine and proline metabolism were significantly dysregulated in doxorubicin-resistant MDA-MB-231 cells, further indicating that reprogramming of arginine metabolism is a common metabolic adaptation in resistant TNBC

phenotypes, whether induced by chemotherapy or radiation (Rushing, Molina and Sumner, 2023).

Arginine serves as a substrate for nitric oxide synthase (NOS), facilitating the production of nitric oxide (NO), which can modulate reactive oxygen species (ROS) and contribute to cellular defence mechanisms (Chen et al. 2021). Interestingly, a clinical study in brain metastases showed that l-arginine supplementation prior to radiotherapy enhanced radiation response via a NO-mediated mechanism, where metabolic reprogramming led to reduced glycolysis, depletion of ATP and NAD+, and impaired DNA repair through GAPDH inhibition and PARP activation (Marullo et al., 2021b). In addition to its role in redox homeostasis, arginine is a key precursor in polyamine biosynthesis, where it is converted to ornithine and subsequently to putrescine, spermidine, and spermine, the polyamines that are essential for DNA stabilization, chromatin structure, and efficient DNA repair(Chen et al. 2021; Roci et al. 2019). The polyamine production, fuelled by arginine abundance, may support the proliferation and survival of resistant cells following exposure to cytotoxic agents such as ionizing radiation (Tang et al. 2018). In support of these findings, Huang et al. (2015) reported that inhibition of arginine-producing enzymes in MCF-7 and MDA-MB-231 cells significantly suppressed cancer cell growth, reinforcing the notion that arginine metabolism plays a central role in tumour survival and progression.

Taken together, the demonstrated enrichment of the arginine biosynthesis pathway in radioresistant cells likely reflects an adaptive mechanism to counteract oxidative damage and promote post-radiation survival. This metabolic reprogramming not only facilitates DNA repair and redox balance but may also represent a potential therapeutic target for sensitising resistant cells to radiotherapy.

Glutamine/Glutamate dependencies: the current study demonstrated significant alterations in the interrelated pathways of alanine, aspartate, and glutamate metabolism in the radioresistant TNBC cell line compared to wild-type control. Several

key intermediate metabolites, including glutamine, glutamate, pyruvate, and L-acetylaspartate, were significantly upregulated in the resistant group. Glutamine, a central metabolite in cancer metabolism that serve as core for essential processes, acting as a precursor for glutamate, which supports amino acid biosynthesis and provide ornithine for arginine metabolism (Majumdar et al., 2016; Nguyen et al., 2019; Gallo et al., 2025). Moreover, glutamate promotes metabolic flow into the TCA cycle via its conversion into α-ketoglutarate, providing an important metabolic hub that link between amino acid metabolism and energy production (Halama and Suhre, 2022; Jin et al., 2023; Wang et al., 2024). These metabolic shifts suggest that glutamate and its derivatives play an essential role in sustaining proliferation and supporting redox homeostasis in resistant cells. The current findings are supported by a recent study demonstrating that TNBC cells resistant to doxorubicin and cisplatin displayed enhanced glutaminase activity and glutamate accumulation, which mitigated the oxidative stress and enhanced cell survival (Choi et al., 2025). Their strategy of dual inhibition of glutaminase (GLS) and glutamate export has effectively disrupted redox balance and sensitized both parental and chemoresistant TNBC cells to chemotherapies (Choi et al., 2025). Similarly, Lampa et al. (2017) demonstrated that proliferation of triple-negative breast cancer (TNBC) cells with deregulated glutamine metabolism depend heavily on glutaminase. Moreover, their study showed that GLS knockdown significantly impaired TNBC tumour growth both in vitro and in vivo, while targeted inhibition of GLS inhibition (via CB-839) reduced mTOR signalling and produced synergism when combined with everolimus (mTOR inhibitor).

Collectively, the elevated levels of glutamate and interconnected intermediate metabolites suggest that the radioresistant MDA-MB-231 cells have enhanced their metabolic capability to support anabolic biosynthesis and maintain cellular homeostasis, enabling them to endure and recover from the radiation-induced damage.

Mitochondrial reprograming: In parallel, TCA cycle intermediates, including citrate, α-ketoglutarate, and phosphoenolpyruvate, were significantly upregulated in the resistant cell line, suggesting an increased activity of this central energy-producing pathway. The enhanced TCA activity may support ATP production necessary for DNA repair, chromatin remodelling, and ion transport, all of which are essential for cellular recovery following radiation exposure (Inigo, Deja, and Burgess 2021;Wu *et al.* 2024). In support to our findings, Winter *et al.* (2023) revealed that the TCA cycle was the most upregulated pathway in persistent MDA-MB-231 cells, generated after long-term exposure to sequential chemotherapeutic agents (epirubicin, cyclophosphamide and then paclitaxel), accompanied by enhanced oxidative phosphorylation. These cells displayed a shift toward a pyruvate metabolism, suggesting enhanced mitochondrial utilisation of pyruvate to sustain OXPHOS. Importantly, inhibition of pyruvate entry into mitochondria using UK-5099 impaired OXPHOS and re-sensitized the persistent cells to chemotherapeutic agents (Winter *et al.*, 2023).

Taken together, the metabolic upregulation of glutamine—glutamate pathways and the TCA cycle reflects an adaptive mechanism used by radioresistant TNBC cells to meet higher energy and biosynthetic demands following radiation exposure. These pathways represent promising metabolic targets to overcome resistance and improve treatment efficacy.

5.4.2 Intermediate Response of Resistant and Wild type MDA-MB-231 Cells to Radiation

To delineate the evolving metabolic profile following radiotherapy, an intermediate time point (4 hours) following irradiation was selected for comparative metabolomic analysis of wild-type and radioresistant MDA-MB-231 cells. This time frame was selected to capture metabolic trajectories contributing to radiation resistance. Distinct metabolic patterns emerged between resistant and wild type cells. Multivariate and univariate analysis have as shown a distinctive metabolic pattern for each of the resistant and wild-type cells.

Pyrimidine metabolism: the data analysis demonstrated significant alterations of key metabolites involved in pyrimidine metabolism, including Uridine diphosphate (UDP), Uridine monophosphate (UMP) and pseudouridine. These metabolites were upregulated in resistant cells compared to wild type cells, suggesting enhanced pyrimidine nucleotide synthesis. Pyrimidine metabolism is essential for DNA and RNA synthesis, which is particularly important for cells undergoing DNA damage due to several factors, including exposure to radiation (Jongmyung et al. 2024). Pseudouridine, the most abundant RNA modification, plays a central role in stabilizing RNA structure, enhancing translation and transcription processes, and facilitating ribosome function processes that are crucial during stress recovery and cellular adaptation(Jia et al. 2025). The current findings are in alignment with another study by Fang et al. (2022), who identified a prognostic biomarker in breast cancer, represented by pseudouridine synthase 1 (PUS1), an enzyme responsible for catalysing the isomerization of uridine to pseudouridine. Their study showed that PUS1 is highly expressed in triple-negative breast cancer and significantly associated with poor clinical outcomes. Functionally, PUS1 enhanced cell proliferation, invasion, and survival in MDA-MB-231 and BT-549 cells, while its knockdown impaired these

phenotypes and downregulated key cancer-related pathways including PI3K/Akt/mTOR (Fang et al., 2022).

Interestingly, our findings contrast with those of Carneiro *et al.* (2023), who reported downregulation of pseudouridine and uridine diphosphate in cisplatin-resistant MDA-MB-231 cells. This discrepancy may reflect differences in therapeutic modality and analytical approach. While cisplatin resistance may involve long-term suppression of nucleotide turnover, our data displayed an early ongoing response to radiation, during which pyrimidine metabolites (pseudouridine, UDP and UMP) accumulation potentially supports RNA stability and repair. Moreover, their utilising of NMR-based metabolomics, less sensitive to low-abundance polar than LC-MS platform, may partly elucidate these differences.

Together, these studies underscore the importance of pyrimidine metabolism in therapy-resistant TNBC and highlight its role as a functional mediator of resistance and a therapeutic target.

Amino acid shifts: the data has shown that alterations in amino acid metabolism were notable in radio-resistant cells. L-Arginine, L-Citrulline, N-Acetylornithine and L-Serine were overexpressed in resistant cells compared to wild type cells, suggesting their contribution to radiotherapy resistance. These key metabolites enriched the arginine biosynthesis pathway, which also was identified as one of the most significantly altered pathways in radioresistant cell line. Its persistent at 4hr indicates an ongoing role radioresistant adaptation. The upregulation of arginine in radioresistant cells may enhance production of nitric oxide (NO), an important mediator of oxidative stress mitigation, potentially improving survival under stressful conditions such as radiation exposure (Chen *et al.* 2021; Fung *et al.* 2025). Furthermore, the overexpression of N-Acetylornithine, polyamine precursor, suggesting the metabolic shift toward polyamine biosynthesis that potentially involved

in DNA stabilization and repair, particularly as a recovery following genotoxic stress (Geck *et al.*, 2020).

Mitochondrial activity: The current findings revealed significant alterations in key tricarboxylic acid (TCA) cycle metabolites in radioresistant MDA-MB-231 cells. Citrate was significantly upregulated in resistant cells following exposure to radiation, suggesting enhanced TCA cycle activity. This upregulation likely reflects a shift toward mitochondrial ATP production to meet the higher energy demand associated with stressful conditions, such as genotoxic stress(Wang et al. 2025; Wu et al. 2024). In parallel, elevated levels of creatine and phosphocreatine were demonstrated in resistant cells compared to wild type 4 hr following exposure to radiation, suggesting an adaptive mechanism to buffer and maintain ATP levels under metabolically stressful conditions, particularly following radiation exposure (Carneiro et al. 2023, Son et al. 2022)

Collectively, the significantly altered metabolites were interrelated to the pathways of pyrimidine metabolism, arginine biosynthesis and TCA cycle. This suggests that these pathways may be central to the adaptive mechanisms of radioresistant cells 4hr after irradiation, improving their capacity for energy production, redox balance, DNA repair, and survival.

5.4.3 Late Response (24 hr post irradiation) of Resistant and Wild type MDA-MB-231 Cells to Radiation

The 24hr time point provides insight into enduring metabolic alterations underpinning prolonged radiation resistance. The metabolic profile at 24 hr time point reflects the ongoing adaptive mechanisms supporting resistant cell survival under radiation stress. Samples were extracted at 24hr post irradiation to assess later metabolic changes, reflecting the long-term impact of radiation. Statistical analysis of the data

identified asparagine, glycerylphosphocholine and cytidine diphosphate as key metabolites that were upregulated in the radioresistant MDA-MB-231 cells compared to wild type cells.

Asparagine dependency: The demonstrated upregulation of asparagine in radioresistant MDA-MB-231 cells may reflect a broader metabolic reprogramming that supports survival under radiation-induced stress, where asparagine has been increasingly recognized as a key modulator of cancer progression and metastasis (Knott et al., 2018). It is synthesized from aspartate via asparagine synthetase (ASNS), which is upregulated in various cancers(Lomelino et al., 2017). Interestingly, Knott et al. (2018) reported that ASNS is important for in vitro breast cancer cell (4T1) migration and in vivo lung metastasis, with asparagine directly promoting epithelialto-mesenchymal transition. Likewise, Yoo et al. (2024) showed that castrationresistant prostate cancer cells, commonly emerging following resistance to androgen receptor inhibitors, depend on asparagine biosynthesis for their survival, with ASNS expression driven by mTORC1 signalling. Asparagine depletion impaired survival in these prostate cells, suggesting its role in maintaining protein synthesis, redox balance, and stress endurance (Yoo et al., 2024). Moreover, asparagine has been shown to induce glutamine synthetase (GLUL) expression, promoting de novo glutamine biosynthesis to support protein synthesis and enhance cell survival (Liu et al. 2020; Luo et al 2018; Pavlova et al. 2018).

Taken together, the upregulation of asparagine in radioresistant MDA-MB-231 cells may not only reflect a metabolic shift in amino acid interconversion and nitrogen balance, while also implicating asparagine in DNA repair, survival, and invasiveness.

Choline-phospholipid metabolism: Our study demonstrated a significant upregulation of glycerophosphocholine (GPC) in radioresistant MDA-MB-231 cells compared to their wild-type counterparts, suggesting a potential role for choline phospholipid

metabolism in the adaptive response to radiotherapy. GPC is involved in membrane phospholipid turnover, and its accumulation may reflect remodelling and repair mechanisms, processes essential for maintaining cellular integrity under oxidative stress (Sonkar *et al.*, 2019; Bi *et al.*, 2024). In alignment with our findings, Lu *et al.* (2022) demonstrated elevated GPC levels in paclitaxel-resistant epithelial ovarian cancer xenografts, attributed to the downregulation of catabolic enzymes GPCPD1 and GDE1, which normally degrade GPC. The study further reported that dysregulated choline metabolism, as evidenced by increased total choline level, was a hallmark of chemoresistant tumours (Lu *et al.* 2022). Furthermore, Tressler *et al.* (2025) identified the GPC/phosphocholine ratio as a marker of TNBC response to various chemotherapeutic agents. This indicates that altered GPC levels may be associated with sensitivity or resistance to therapy depending on the cellular context and therapeutic type. In our study, the upregulation of GPC may reflect a resistance phenotype to radiation that potentially facilitates phospholipid recycling, membrane repair and cell survival following cellular stress.

In parallel, our study revealed a significant upregulation of cytidine 5'-diphosphocholine (CDP-choline) in radioresistant MDA-MB-231 cells compared to wild type. CDP-choline is a central intermediate in the Kennedy pathway, which is responsible for the biosynthesis of phosphatidylcholine, the main cell membrane phospholipid (Phyu et al. 2018; Saito et al. 2022). Its upregulation in the resistant cells suggests increased membrane biosynthesis and repair essential for maintaining cellular integrity under oxidative stress induced by radiation. This remodelling potentially maintains membrane stability, facilitate intracellular transport, and support signalling mechanisms that drive cell growth and survival (Yao et al., 2023). In support of our findings, Krug et al. (2024) showed that malignant T follicular helper cells in angioimmunoblastic T-cell lymphoma are highly dependent on the CDP-choline pathway, and inhibiting of this metabolic pathway decreased tumour viability.

Taken together, the dual upregulation of both a biosynthetic precursor (CDP-choline) and a degradation product (GPC) suggests a high rate of phospholipid cycling, a hallmark of metabolic plasticity. Such remodelling could provide the structural flexibility and biosynthetic resources for adaptation, reinforcing the resistant phenotype.

5.4.4 Metabolic Pathways Potentially Driving Overall Resistance to Radiotherapy

Resistance of TNBC cells to radiotherapy is a complex process that involves different but interconnected metabolic adaptations across early, intermediate, and late response phases. The early response reflected rapid energy/redox adaptations, the intermediate emphasised enhanced nucleotide synthesis for DNA repair, while the late response involved prolonged metabolic shifts essential for long-term survival and proliferation.

Three metabolic pathways, including Arginine biosynthesis, the TCA cycle and Alanine-Aspartate- glutamate metabolism were perturbed over time, highlighting their involvement in the acquired radiation resistance of MDA-MB-231 cells.

Arginine biosynthesis has emerged as a significantly altered pathway over time (Figure 5.6-A, 5.13-A, and 5.20-A). The ongoing activation of this pathway across the phases implies its intricate role in both immediate and delayed cellular adaptation to radiation. The consistent upregulation of key metabolites such as L-arginine may enhance resistance-related mechanisms, including nitric oxide (NO) production and polyamine biosynthesis, both of which are critical for mitigating oxidative damage and maintaining genomic stability. Our results are aligned with previous studies investigating the impact of arginine metabolism on modulating stress responses (Cheng *et al.*, 2018; Vidal *et al.*, 2023). Both studies have shown that the arginine starvation of the MDA-MB-231 cell line has been found to induce non-canonical

endoplasmic reticulum stress and mitochondrial distress, resulting in the inhibition of cancer cell growth. However, such findings highlight that arginine biosynthesis preserves mitochondrial homeostasis and protein folding under stress, consistent with its activation in radioresistant cells.

TCA cycle dynamics: the current findings revealed that the TCA cycle pathway was significantly altered in radioresistant MDA-MB-231 cells compared to wild type across different time points following exposure to 2 Gy radiation (Figure 5.6-A and 5.13-A). The TCA cycle is essential for cancer cell proliferation and survival under stressful conditions, including exposure to radiation, serving as a central hub for the metabolic interconversion of amino acids, glucose and lipids (Wu et al. 2024). The current data demonstrated that the levels of citrate and 2-oxoluglutrate (α-ketoglutarate), the important intermediates of TCA, were significantly upregulated in resistant cells compared to wild type in early and intermediate response phases. Their upregulation in the resistant group underlines their important roles in MDA-MB-231 cell proliferation and survival following exposure to radiation. Citrate generates Acetyl-CoA for lipid biosynthesis and membrane formation, while α-Ketoglutarate supports energy metabolism and anabolic bioprocesses. Moreover, it serves as an essential link between the TCA cycle and amino acid metabolism, working as a substrate for transamination reactions that enable the interconversion of amino acids including alanine, aspartate, and glutamate. It has been demonstrated that higher levels of citrate and α-ketoglutarate have contributed to the biosynthesis of amino acids, nucleotides and fatty acids in several types of cancers, including non-small cell lung cancer, glioblastoma and basal breast cancer (Cluntun et al., 2017; Wang et al., 2019; J. yuan Zhang *et al.*, 2021).

Collectively, our data suggests that the metabolic upregulation of TCA intermediates, including citrate and α -ketoglutarate, in radioresistant MDA-MB-231 cells contributes

to sustain metabolic reprogramming that may underpin their enhanced capacity for repair, proliferation, and resistance to radiotherapy.

Alanine-Aspartate-Glutamate metabolism: In the current study, alterations in the alanine, aspartate, and glutamate metabolism pathway were consistently identified in the radioresistant group across early, intermediate, and late response phases (Figure 5.6-A, 5.13-A and 5.20-A), underscoring their essential role in metabolic reprogramming following exposure to radiation. The sustained enrichment of alanine, aspartate, and glutamate metabolism suggests its critical role in promoting metabolic reprogramming that supports cellular survival and recovery under genotoxic stress (Fan et al., 2016; Wang et al., 2025). In our study, several key metabolites within alanine, aspartate, and glutamate axis, including glutamate, aspartate, asparagine, and pyruvate, were found to be upregulated in the radioresistant MDA-MB-231 group compared to wild type group. These metabolites may contribute to essential cellular functions such as TCA cycle replenishment, redox balance, and the biosynthesis of nucleotides and other macromolecules, thereby directly linking amino acid metabolism to DNA repair and proliferative recovery (Bacci et al. 2019; Xiao et al. 2022) . Their coordinated elevation suggests enhanced metabolic flexibility, enabling resistant cells to maintain survival, repair DNA damage, and adapt to radiationinduced stress.

In support to our findings, Carneiro *et al.*, (2023) metabolomics study employing NMR has shown that higher levels of N-acetyl aspartic acid, phosphocreatine, as well as TCA cycle dynamics were part of the metabolic reprograming in MDA-MB-231 cell line resistant to cisplatin. Rushing et al., (2023) have assessed the altered metabolic pathways in the doxorubicin-resistant MDA-MB-231 cell line. They demonstrated a perturbation in several metabolic pathways across doxorubicin-resistant cell lines, including arginine biosynthesis and alanine-aspartate-glutamate metabolism,

indicating that resistant cells exploit these pathways to sustain their growth and evade the cytotoxic effect of doxorubicin. The convergence between resistance to doxorubicin and radiation suggests that arginine biosynthesis and alanine-aspartate-glutamate metabolism pathways could represent cross-cutting metabolic features that enable tumour cells to survive under different forms of treatment-induced stress. This supports the potential of targeting these metabolic nodes to overcome resistance in aggressive breast cancer subtypes.

The metabolic adaptation of cancer cells to different conditions may involve the activation of diverse downstream cell signalling pathways. For example, arginine and aspartate have been demonstrated to enhance the activation of PI3K/Akt/mTOR pathway while α-Ketoglutarate has an important role in activation of IKKβ and nuclear factor kB (NF-kB) (Chen *et al.* 2021; X. Wang *et al.* 2019). The intracellular glutamate, generated via glutaminolysis, serves diverse roles in cancer cells, including indirect activation of mTORC1 by enhancing arginine biosynthesis via cyclization into proline which is then converted to ornithine (the precursor for arginine biosynthesis), contribution to the TCA cycle by converting to α-Ketoglutarate, and direct conversion to glutathione, collectively supporting proliferation (Halama and Suhre, 2022; D. Wang et al., 2024). Furthermore, in a comprehensive metabolomics study of TNBC clinical samples, N-acetyl-aspartyl-glutamate was demonstrated as a crucial metabolite promoting tumour growth (Xiao et al., 2022). Furthermore, it has been revealed that the inhibition of N-acetyl-aspartyl-glutamate conversion to glutamate could restrict the growth of lymphoma and ovarian cancer (Nguyen et al., 2019). Taken together, these insights support our findings that the upregulation of glutamate, α-ketoglutarate, and aspartate-related metabolites in radioresistant MDA-MB-231 cells may enhance survival through activation of pro-growth signalling pathways and improved metabolic plasticity following radiation exposure.

Collectively, our findings suggest that metabolic reprogramming via amino acids interconversion pathways including arginine biosynthesis, alanine-aspartate-glutamate metabolism as well as TCA cycle dynamics, have a potential role in driving the resistance of MDA-MB-231 cell line to radiotherapy. The intermediate metabolites in these pathways may activate signalling cascade including PI3K/Akt/mTOR, IKKβ and nuclear factor kB (NF-kB) to sustain cell proliferation and survival. Targeting these pathways or their metabolic drivers may contribute to reverse the radioresistance in TNBC.

6	General discussion, Conclusion and Future Works

6.1 General discussion

Triple-negative breast cancer (TNBC) is a challenging and aggressive subtype of breast cancer, representing approximately 15-20% of all breast cancers. This complex subtype is characterised by the absence of typical receptors, including oestrogen receptor (ER), progesterone receptor (PR), and human epidermal growth factor receptor 2 (HER2), leading to the absence of its response to endocrine therapy or HER2-targeted agents. The high recurrence rates, early metastatic capacity, and poor prognosis are the main challenges of TNBC. Hence, the development of alternative therapeutic strategies is essential.

Currently, chemotherapies, including anthracyclines (e.g., doxorubicin) and radiotherapy, remain the primary treatment for TNBC in clinical settings (Chen *et al.* 2025; Gupta *et al.* 2020; Won and Spruck 2020). However, resistance to treatment, particularly the emergence of radiation-resistant TNBC subpopulations, significantly impairs the long-term effectiveness of these therapies, resulting in therapy failure and disease progression. Combination therapy strategies are developing to enhance the cytotoxicity of therapy, reduce resistance, and improve patient survival (Lee *et al.*, 2020; Han *et al.*, 2023).

The current study aimed to assess the role of gedatolisib, a dual inhibitor of the PI3K/Akt/mTOR pathway, in enhancing the therapeutic effectiveness and overcoming the radioresistance in TNBC when combined with standard therapies. Moreover, the metabolomics approach has been utilised to determine the metabolic fingerprint of wild and resistant TNBC cell lines, leading to the identification of metabolic pathways contributing to the development of radioresistance.

6.1.1 Therapeutic effectiveness of combining gedatolisib with doxorubicin or radiation in MDA-MB-231 cell line

The effectiveness of the combination of gedatolisib with doxorubicin or radiation, as was assessed in both wild-type (WT) and radioresistant (RR) MDA-MB-231 cell lines utilising two dimensional clonogenic survival assay and three-dimensional tumour spheroid, as well as mechanistic assays underpinning mechanisms mediated cytotoxicity. The clonogenic survival assays showed that RR-MDA cells demonstrated enhanced survival and resistance to radiation compared to WT-MDA cells, indicating their acquired radioresistant phenotype which was supported by morphological changes and lower doubling time of RR-MDA cells than WT cells. Single agent treatment with low doses of gedatolisib, doxorubicin, or radiation resulted in relative reductions in survival fractions of exposed cell lines compared to the untreated control. However, combining gedatolisib with either radiation or doxorubicin at these low-level doses has shown enhanced effectiveness in decreasing colony formation and delaying spheroid growth in both cell lines. Interestingly, while RR-MDA-MB-231 cells displayed significant resistance to radiation alone compared to the parent cell line, the co-treatment of gedatolisib diminished the acquired resistance, suggesting that dual PI3K/mTOR inhibition may overcome intrinsic resistance mechanisms. Furthermore, combining gedatolisib, a targeted inhibitor of PI3K/mTOR pathway, with doxorubicin resulted in significant survival colonies reduction and spheroid growth retardation in both cell lines compared to each single agent, reflecting the enhanced cytotoxicity following combination. In clinical terms, this might mean that combining gedatolisib with standard therapies may improve outcomes in patients with recurrent or refractory TNBC who have radioresistance.

This finding is interesting in the context of TNBC, where PI3K/Akt/mTOR signalling is frequently activated, driving survival and treatment resistance. Previous studies have

shown that PI3K/mTOR inhibition can radiosensitize cancers by impairing DNA repair and altering checkpoint responses (Chang *et al.* 2022; Song *et al.* 2022). The present thesis confirms and extends this, showing that radiosensitisation occurs not only in wild-type cells but persists in a radioresistant derivative. This suggests that targeting PI3K/mTOR signalling may remain effective even after resistance emerges, an important observation for therapeutic strategy design.

Mechanistic assays provided further understanding of the mechanisms by which the therapies exert their effects on the cells. The Annexin V assay revealed that gedatolisib monotherapy did not significantly induce apoptosis in both cell lines. However, its combination with doxorubicin or radiation induced a significant increase in apoptotic cell death, indicating the ability of gedatolisib to augment the effects of these standard therapies in TNBC cells. Furthermore, cell cycle analysis revealed that the combination of gedatolisib with radiation or doxorubicin produced enhanced G2/M arrest, particularly in RR cells, which possibly contributed to the recognized synergistic effect of combination therapy. Since single gedatolisib treatment did not significantly induce DNA damage or apoptosis in both cell lines, its contribution to enhancing the effectiveness of combination therapy was further investigated utilising an autophagy assay. The data have shown that RR-MDA-MB-231 cells treated with gedatolisib demonstrated increased autophagic activity, suggesting the underlying mechanism of the drug-induced cell death. The collective results demonstrate the benefit of adding the PI3K/Akt/mTOR pathway inhibitors in the treatment of TNBC, as gedatolisib enhances the effectiveness of standard therapies by inducing a different mechanism of cell death than traditional therapies. Moreover, gedatolisib may increase the radiosensitivity in both investigated cell lines by suppressing the PI3K/Akt/mTOR pathway, which could be a survival pathway utilised by radioresistant cells.

resistance. As many previous studies assessing targeting inhibition of PI3K/mTOR pathway as a radiosensitisation approach have been performed in parental or relatively sensitive breast cancer models, the current study revealed that gedatolisib retains efficacy in an experimentally derived radioresistant MDA-MB-231 cell line. Both clonogenic survival and spheroid volume assays showed that the addition of gedatolisib has improved treatment sensitivity in resistant cells in comparison with their parent cell line. This is a valuable advance because clinical resistance rarely arises in treatment-naïve tumours but instead emerges following exposure to therapy. By directly addressing this resistant phenotype, the study provides stronger translational relevance than models limited to treatment-sensitive cells. Comparable dual PI3K/mTOR inhibitors, such as PKI-402, have shown radiosensitising activity in breast cancer cell lines (Gasimli et al., 2023), but studies particularly targeting acquired radioresistance are still little. Thus, this thesis contributes to filling an important gap in literature by demonstrating that dual pathway inhibition can meaningfully resensitize resistant TNBC cells, supporting its potential utility in the clinical management of recurrent or refractory disease.

Importantly, a significant contribution of this work lies in its focus on acquired

6.1.2 Metabolic reprograming as driver of radioresistance

An important finding of this thesis was identifying that metabolic rewiring represents an essential mechanism underpinning the radioresistance of TNBC cells. In RR-MDA-MB-231 cells, significant alterations were identified including amino acid metabolism, arginine biosynthesis, alanine—aspartate—glutamate metabolism, and TCA cycle intermediates. These metabolic shifts could serve in diverse cellular processes such as enabling enhanced redox buffering, prolonged generation of biosynthetic precursors, and ensuring the sustained production of ATP under

genotoxic-induced stress, which collectively supports cell survival following radiation exposure. These results are consistent with growing evidence that metabolic reprograming is crucial for inducing therapy resistance in cancer. For instance, prior study demonstrated that radioresistant MDA-MB-231 cells have enhanced their antioxidant capacity and promoted survival following exposure to radiation by increasing glutathione (GSH) biosynthesis via upregulation of cysteine, glutamine, and glycine metabolism (Lee *et al.*, 2021). Furthermore, the upregulation of glutathione biosynthesis genes such as SLC7A11 and CTH driven by eIF2α/ATF4 axis has been found to play an essential role in maintaining redox homeostasis and mediating TNBC radioresistance (Bai *et al.*, 2021). These mechanisms support our findings that RR-MDA-MB-231 resistant cells rewire amino acid metabolism toward redox buffering and energy stabilization under genotoxic stress.

Critically, a key advance from the current project is the acknowledgement that the metabolic reprograming of radioresistant TNBC cells represents a dynamic and temporarily coordinated adaptive response and not a single or static metabolic shift. For instance, the rapid enrichment of phosphocreatine and phosphoenolpyruvate following exposure to radiation indicates increased energy buffering and glycolytic support during acute stressful conditions, with the abundances of pyrimidine nucleotides that enhance DNA and RNA synthesis required for damage repair. In late adaptive response, 24hr after irradiation, elevated levels of asparagine and glycerophosphocholine suggests sustained adaptations in amino acid and membrane lipid metabolism, supporting cell membrane integrity, proliferation, and survival. These findings highlight the metabolic flexibility of resistant cells as they shift from acute stress response to cell recovery and growth.

Collectively, the metabolomics data of the current project provides a comprehension insights and translational direction, suggesting the role of metabolic plasticity not only

as a hallmark of TNBC aggressiveness but also as a therapeutic vulnerability that can be targeted to improve the radiosensitivity.

6.2 Conclusions

Triple-negative breast cancer (TNBC) remains one of the most aggressive breast cancer subtypes characterised by the absence of ER, PR, and HER2 targets. Conventional treatments such as anthracycline-based chemotherapy and radiotherapy are widely used; however, resistance frequently emerges, leading to tumour recurrence, metastasis, and poor survival. Hence, the management of subtype is challenging in clinical setting which highlight the critical need to new therapeutic strategies that rely on using of targeted therapies alongside identification of new therapeutic vulnerabilities. The current thesis addressed that challenge by assessing the effectiveness of gedatolisib, a dual PI3K/mTOR inhibitor, in combination with standard therapies, doxorubicin or radiation, in both wild-type and radioresistant MDA-MB-231 cells. Through clonogenic survival and spheroid growth assays, these combinations resulted in significant reduction of survival colonies and spheroid growth retardation. Furthermore, mechanistic assays have further demonstrated that gedatolisib has significantly enhanced G2/M arrest, increased apoptosis, and impaired DNA repair when combined with doxorubicin or radiation compared to each single treatment. Importantly, gedatolisib as a single treatment did cause significant apoptosis or DNA damage in both cell lines, however, it increased autophagic activity, which may function as another cell-death mechanism and as a process that sensitize the cells for cytotoxic agents.

Taken together, these findings unravel the therapeutic advantage of targeting the PI3K/mTOR pathway in improving the treatment outcomes of TNBC, particularly in the strategy for overcoming acquired radioresistance.

Beyond therapeutic assays, a critical advance of the current project represented by the incorporation of untargeted metabolomics to interrogate the metabolic adaptations underpinning radioresistance. This approach identified that radioresistant MDA-MB-231 cells undergo interconnected reprogramming of amino acid and central carbon metabolism, particularly within arginine biosynthesis, alanine—aspartate—glutamate metabolism, and TCA cycle flux. These metabolic alterations support cells to mitigate the radiation induced stress by maintaining redox homeostasis, ATP production and abundance of biosynthetic precursors.

Collectively, the findings of this thesis highlight that although the standard treatments alone have limited effect against resistant TNBC, rationally designed combination strategies, particularly co-treatment of PI3K/mTOR inhibitors with DNA-damaging agents, resulted in significant improvements in cytotoxicity. At the same time, the identification of metabolic rewiring as a hallmark of resistance suggests new avenues for innovative therapeutic approaches such as incorporation of metabolic inhibitors or combination regimens targeting these adaptive pathways.

6.3 Future works

While the current project offers significant advancements, several limitations have to be acknowledged. The results were generated utilising a single TNBC cell line and its derived radioresistant cells, restricting the validity across the heterogeneity of TNBC. Furthermore, while different assays were conducted to investigate the mechanisms mediating effect, no positive control radiosensitiser was included for comparison. Additionally, the initial translational conclusions are limited due to the lack of *in vivo* or clinical trials. Based on these strengths and limitations, several potential research avenues are suggested for future work:

1. Expansion across TNBC cell lines

To confirm the reliability of the current results, the potential combination of gedatolisib with doxorubicin or radiation requires further assessment in other TNBC cell lines with diverse molecular features to identify whether inhibiting of PI3K/mTOR pathway improve the cytotoxicity in both of parent and radioresistance cells.

2. Validation in pre-clinical models

Subsequent validations of these combinations in xenograft or patient derived tumour are required to confirm the effectiveness of these combination therapies in more physiologically relevant models.

3. Targeting metabolic vulnerabilities

The metabolic alterations demonstrated in the current project offer a rationale for therapeutic interventions. For instance, targeting glutamine metabolism, arginine metabolism, and TCA entry points can be evaluated as potential approaches to reduce the metabolic capacity of radioresistant cells.

4. Integration of omics approaches and biomarker discovery

Broadening the analytical approaches further than metabolomics will be essential to provide a systems-level comprehension of TNBC resistance. Incorporating transcriptomic and proteomic datasets with metabolomic profiles could identify the regulatory frameworks connecting metabolic shifts to signalling pathways.

5. Clinical and translational validation

Clinically, employing untargeted metabolomics to TNBC patient samples scheduled for radiotherapy and performing the assessment pre- and post-irradiation would validate the metabolic fingerprints of radioresistance and contribute to the development of novel predictive biomarkers for patient stratification and personalised therapy approach. Translationally, the preclinical data of combination therapy, *in vitro* and *in vivo*, need to be validated in clinical studies to assess whether the proposed

combining of gedatolisib with standard therapies can achieve tumour control, prevent reoccurrence, and improve the overall survival.

7 References

- Abrahams, B., Gerber, A. and Hiss, D.C. (2024) 'Combination Treatment with EGFR Inhibitor and Doxorubicin Synergistically Inhibits Proliferation of MCF-7 Cells and MDA-MB-231 Triple-Negative Breast Cancer Cells In Vitro', *International Journal of Molecular Sciences* 2024, Vol. 25, Page 3066, 25(5), p. 3066. Available at: https://doi.org/10.3390/IJMS25053066.
- Aebi, S, et al., (2022). Locally advanced breast cancer. *Breast (Edinburgh, Scotland)*, 62 Suppl 1(Suppl 1), S58–S62. https://doi.org/10.1016/j.breast.2021.12.011
- Abramson, V.G. et al. (2015) 'Subtyping of triple-negative breast cancer: Implications for therapy', Cancer, 121(1), pp. 8–16. Available at: https://doi.org/10.1002/cncr.28914.
- Adams, S. et al. (2020) 'Patient-reported outcomes from the phase III IMpassion130 trial of atezolizumab plus nab-paclitaxel in metastatic triple-negative breast cancer', Annals of Oncology, 31(5), pp. 582–589. Available at: https://doi.org/10.1016/j.annonc.2020.02.003.
- Agelidis, A. et al. (2025) 'Triple-negative breast cancer on the rise: breakthroughs and beyond', Breast Cancer: Targets and Therapy, 17, pp. 523–529. doi:10.2147/BCTT.S516125.
- Agrawal, M., Agrawal, S.K. and Chopra, K. (2025) 'Overcoming drug resistance in ovarian cancer through PI3K/AKT signalling inhibitors', Gene, 948, p. 149352. Available at: https://doi.org/10.1016/J.GENE.2025.149352.
- Ahmed, S.A. et al. (2022) 'Anticancer Effects of Fucoxanthin through Cell Cycle Arrest, Apoptosis Induction, Angiogenesis Inhibition, and Autophagy Modulation', International Journal of Molecular Sciences 2022, Vol. 23, Page 16091, 23(24), p. 16091. Available at: https://doi.org/10.3390/IJMS232416091.
- Ahire, V. et al. (2023) 'Radiobiology of combining radiotherapy with other cancer treatment modalities', in Radiobiology Textbook, pp. 311–386.
- Al-Saraireh, Y.M. et al. (2021) 'Cytochrome 4Z1 expression is associated with unfavorable survival in triple-negative breast cancers', Breast Cancer: Targets and Therapy, 13, pp. 565–574. Available at: https://doi.org/10.2147/BCTT.S329770/ASSET/D2C39D98-BCEB-43B1-A47B-F45444454296/ASSETS/IMAGES/DBCT_A_34675653_F0003_C.JPG.
- Alés-Martínez, J.E. et al. (2024) 'Olaparib plus trastuzumab in HER2-positive advanced breast cancer patients with germline BRCA1/2 mutations: The OPHELIA phase 2 study', Breast, 77, p. 103780. Available at: https://doi.org/10.1016/j.breast.2024.103780.
- Alnahhas, I. et al. (2020) 'Characterizing benefit from temozolomide in MGMT promoter unmethylated and methylated glioblastoma: a systematic review and meta-analysis', Neuro-Oncology Advances, 2(1), pp. 1–7. Available at:

- https://doi.org/10.1093/noajnl/vdaa082.
- Altman, B.J., Stine, Z.E. and Dang, C. V. (2016) 'From Krebs to clinic: Glutamine metabolism to cancer therapy', Nature Reviews Cancer, 16(10), pp. 619–634. Available at: https://doi.org/10.1038/nrc.2016.71.
- Ananieva, E.A. and Wilkinson, A.C. (2018) 'Branched-chain amino acid metabolism in cancer', Current Opinion in Clinical Nutrition and Metabolic Care, 21(1), pp. 64–70. Available at: https://doi.org/10.1097/MCO.0000000000000430.
- Andrieu, G.P. et al. (2019) 'BET protein targeting suppresses the PD-1/PD-L1 pathway in triple-negative breast cancer and elicits anti-tumour immune response', Cancer Letters, 465(April), pp. 45–58. Available at: https://doi.org/10.1016/j.canlet.2019.08.013.
- Asselain, B. et al. (2018) 'Long-term outcomes for neoadjuvant versus adjuvant chemotherapy in early breast cancer: meta-analysis of individual patient data from ten randomised trials', The Lancet Oncology, 19(1), pp. 27–39. Available at: https://doi.org/10.1016/S1470-2045(17)30777-5.
- Babichev, Y. et al. (2016) 'PI3K/AKT/mTOR inhibition in combination with doxorubicin is an effective therapy for leiomyosarcoma', Journal of Translational Medicine, 14(1), pp. 1–12. Available at: https://doi.org/10.1186/S12967-016-0814-Z/FIGURES/6.
- Bacci, M. et al. (2019) 'Reprogramming of Amino Acid Transporters to Support Aspartate and Glutamate Dependency Sustains Endocrine Resistance in Breast Cancer', Cell Reports, 28(1), pp. 104-118.e8. Available at: https://doi.org/10.1016/j.celrep.2019.06.010.
- Bai, X. et al. (2021) 'Triple-negative breast cancer therapeutic resistance: Where is the Achilles' heel?', Cancer Letters, 497, pp. 100–111. Available at: https://doi.org/10.1016/j.canlet.2020.10.016.
- Bai X. et al. (2021) 'Activation of the eIF2α/ATF4 axis drives triple-negative breast cancer radioresistance by promoting glutathione biosynthesis'. Redox Biol, 43:101993. doi: 10.1016/j.redox.2021.101993. Epub 2021 Apr 28. PMID: 33946018; PMCID: PMC8111851.
- Balko, J.M. et al. (2014) 'Molecular profiling of the residual disease of triple-negative breast cancers after neoadjuvant chemotherapy identifies actionable therapeutic targets', Cancer Discovery, 4(2), pp. 232–245. Available at: https://doi.org/10.1158/2159-8290.CD-13-0286.
- Bardia, A. et al. (2019) 'Sacituzumab Govitecan-hziy in Refractory Metastatic Triple-Negative Breast Cancer', New England Journal of Medicine, 380(8), pp. 741–751. Available at: https://doi.org/10.1056/nejmoa1814213.
- Basho, R.K. et al. (2017) 'Targeting the PI3K/AKT/mTOR Pathway for the Treatment of Mesenchymal Triple-Negative Breast Cancer: Evidence From a Phase 1 Trial of mTOR Inhibition in Combination With Liposomal Doxorubicin and Bevacizumab', JAMA Oncology, 3(4), pp. 509–515. Available at: https://doi.org/10.1001/JAMAONCOL.2016.5281.

- Beatty, A. et al. (2018) 'Metabolite profiling reveals the glutathione biosynthetic pathway as a therapeutic target in triple-negative breast cancer', Molecular Cancer Therapeutics, 17(1), pp. 264–275. Available at: https://doi.org/10.1158/1535-7163.MCT-17-0407.
- Beckers, R.K. et al. (2016) 'Programmed death ligand 1 expression in triple-negative breast cancer is associated with tumour-infiltrating lymphocytes and improved outcome', Histopathology, 69(1), pp. 25–34. Available at: https://doi.org/10.1111/his.12904.
- Beniey, M., Haque, T. and Hassan, S. (2019) 'Translating the role of PARP inhibitors in triple-negative breast cancer', Oncoscience, 6(1–2), pp. 287–288. Available at: https://doi.org/10.18632/oncoscience.474.
- Bhardwaj, A. et al. (2018). 'The isomiR-140-3p-regulated mevalonic acid pathway as a potential target for prevention of triple negative breast cancer. Breast cancer research: BCR, 20(1), 150. https://doi.org/10.1186/s13058-018-1074-z
- Bi, Y. et al. (2024) 'Glycerophospholipid-driven lipid metabolic reprogramming as a common key mechanism in the progression of human primary hepatocellular carcinoma and cholangiocarcinoma', Lipids in health and disease, 23(1), p. 326. Available at: https://doi.org/10.1186/S12944-024-02298-4.
- Biswenger, V. et al. (2018) 'Characterization of EGF-guided MDA-MB-231 cell chemotaxis in vitro using a physiological and highly sensitive assay system.' PLOS ONE, 13(6), e0198330. https://doi.org/10.1371/journal.pone.0198330
- Bodenstine, T.M. et al. (2016) 'Nodal expression in triple-negative breast cancer: Cellular effects of its inhibition following doxorubicin treatment', Cell Cycle, 15(9), pp. 1295–1302. Available at: https://doi.org/10.1080/15384101.2016.1160981.
- Bouchard, G. et al. (2016) 'Stimulation of triple negative breast cancer cell migration and metastases formation is prevented by chloroquine in a pre-irradiated mouse model', BMC cancer, 16(1). Available at: https://doi.org/10.1186/S12885-016-2393-Z.
- Boutros, C. et al. (2016) 'Safety profiles of anti-CTLA-4 and anti-PD-1 antibodies alone and in combination', Nature Reviews Clinical Oncology, 13(8), pp. 473–486. Available at: https://doi.org/10.1038/nrclinonc.2016.58.
- Bray, F. et al. (2024) 'Global cancer statistics 2022: GLOBOCAN estimates of incidence and mortality worldwide for 36 cancers in 185 countries', CA: A Cancer Journal for Clinicians, 74(3), pp. 229–263. Available at: https://doi.org/10.3322/caac.21834.
- Brett, J.O. et al. (2021) 'ESR1 mutation as an emerging clinical biomarker in metastatic hormone receptor-positive breast cancer', Breast cancer research: BCR, 23(1). Available at: https://doi.org/10.1186/S13058-021-01462-3.
- Brix, N. et al. (2020) 'The clonogenic assay: robustness of plating efficiency-based analysis is strongly compromised by cellular cooperation'. Radiation oncology (London, England), 15(1), 248. https://doi.org/10.1186/s13014-020-01697-y
- Broege, A. et al. (2024) 'Functional Assessments of Gynecologic Cancer Models Highlight Differences Between Single-Node Inhibitors of the PI3K/AKT/mTOR Pathway and a Pan-PI3K/mTOR Inhibitor, Gedatolisib'. Cancers, 16(20), 3520. https://doi.org/10.3390/cancers16203520

- Browne, I.M. and Okines, A.F.C. (2024) 'Resistance to Targeted Inhibitors of the PI3K/AKT/mTOR Pathway in Advanced Ooestrogen-Receptor-Positive Breast Cancer', Cancers 2024, Vol. 16, Page 2259, 16(12), p. 2259. Available at: https://doi.org/10.3390/CANCERS16122259.
- Burstein, M.D. et al. (2016) 'HHS Public Access', 21(7), pp. 1688–1698. Available at: https://doi.org/10.1158/1078-0432.CCR-14-0432.Comprehensive.
- Brunt, A.M., Haviland, J.S., Wheatley, D.A., Sydenham, M.A., Bloomfield, D.J., Chan, C., Cleator, S., Coles, C.E., Donovan, E., Fleming, H., Glynn, D., Goodman, A., Griffin, S., Hopwood, P., Kirby, A.M., Kirwan, C.C., Nabi, Z., Patel, J., Sawyer, E., Somaiah, N., Syndikus, I., Venables, K., Yarnold, J.R., Bliss, J.M. and FAST-Forward Trial Management Group, 2023. *One versus three weeks hypofractionated whole breast radiotherapy for early breast cancer treatment: the FAST-Forward phase III RCT*. Health Technology Assessment, [online] 27(36). Available at: https://doi.org/10.3310/WWBF1044
- Caciolla, J. et al. (2021) 'Balanced dual acting compounds targeting aromatase and oestrogen receptor α as an emerging therapeutic opportunity to counteract oestrogen responsive breast cancer', European Journal of Medicinal Chemistry, 224, p. 113733. Available at: https://doi.org/10.1016/j.ejmech.2021.113733.
- Cancer research UK, https://www.cancerresearchuk.org/health-professional/cancer-statistics/statistics-by-cancer-type/breast-cancer#breastcs0, Accessed May 2025.
- Candas-Green, D. et al. (2020) 'Dual blockade of CD47 and HER2 eliminates radioresistant breast cancer cells', Nature communications, 11(1). Available at: https://doi.org/10.1038/S41467-020-18245-7.
- Carlisi, D. et al. (2017) 'Parthenolide prevents resistance of MDA-MB231 cells to doxorubicin and mitoxantrone: the role of Nrf2', Cell Death Discovery, 3(1), pp. 1–12. Available at: https://doi.org/10.1038/cddiscovery.2017.78.
- Carneiro, T.J. et al. (2023) 'Disclosing a metabolic signature of cisplatin resistance in MDA-MB-231 triple-negative breast cancer cells by NMR metabolomics', Cancer Cell International, 23(1), pp. 1–17. Available at: https://doi.org/10.1186/S12935-023-03124-0/FIGURES/7.
- Caron, M.C. et al. (2019) 'Poly (ADP-ribose) polymerase-1 antagonizes DNA resection at double-strand breaks', Nature Communications, 10(1). Available at: https://doi.org/10.1038/s41467-019-10741-9.
- Caswell-Jin, J.L. et al. (2018) 'Change in Survival in Metastatic Breast Cancer with Treatment Advances: Meta-Analysis and Systematic Review', JNCI Cancer Spectrum, 2(4), pp. 1–10. Available at: https://doi.org/10.1093/jncics/pky062.
- Cavanagh, R.J. et al. (2024) 'Free drug and ROS-responsive nanoparticle delivery of synergistic doxorubicin and olaparib combinations to triple negative breast cancer models', Biomaterials Science, 12(7), pp. 1822–1840. Available at: https://doi.org/10.1039/D3BM01931D.
- Chandarlapaty, S. (2012) 'Negative feedback and adaptive resistance to the targeted therapy of cancer', Cancer Discovery, 2(4), pp. 311–319. Available at:

- https://doi.org/10.1158/2159-8290.CD-12-0018.
- Chang, L. et al. (2014) 'PI3K/Akt/mTOR pathway inhibitors enhance radiosensitivity in radioresistant prostate cancer cells through inducing apoptosis, reducing autophagy, suppressing NHEJ and HR repair pathways'. Cell Death Dis 5, e1437. https://doi.org/10.1038/cddis.2014.415
- Chang, T.M. et al. (2025) 'PCK2 promotes invasion and epithelial-to-mesenchymal transition in triple-negative breast cancer by promoting TGF-β/SMAD3 signalling through inhibiting TRIM67-mediated SMAD3 ubiquitination', Cancer biology & therapy, 26(1), p. 2478670. Available at: https://doi.org/10.1080/15384047.2025.2478670.
- Chen, C.L. et al. (2021) 'Arginine Signalling and Cancer Metabolism', Cancers, 13(14), p. 3541. Available at: https://doi.org/10.3390/CANCERS13143541.
- Chen, F. et al. (2019) 'Extracellular vesicle-packaged HIF-1α-stabilizing IncRNA from tumour-associated macrophages regulates aerobic glycolysis of breast cancer cells', Nature Cell Biology, 21(4), pp. 498–510. Available at: https://doi.org/10.1038/s41556-019-0299-0.
- Chen, S. et al. (2023) 'Estimates and Projections of the Global Economic Cost of 29 Cancers in 204 Countries and Territories From 2020 to 2050', JAMA Oncology, 9(4), pp. 465–472. Available at: https://doi.org/10.1001/JAMAONCOL.2022.7826.
- Chen, Ziqi et al. (2025) 'Classifications of triple-negative breast cancer: insights and current therapeutic approaches', Cell & bioscience, 15(1). Available at: https://doi.org/10.1186/S13578-025-01359-0.
- Cheng, C.T. et al. (2018) 'Arginine starvation kills tumour cells through aspartate exhaustion and mitochondrial dysfunction', Communications biology, 1(1). Available at: https://doi.org/10.1038/S42003-018-0178-4.
- Choi, H. et al. (2025) 'Disruption of redox balance in glutaminolytic triple negative breast cancer by inhibition of glutaminase and glutamate export', Neoplasia (New York, N.Y.), 61, p. 101136. Available at: https://doi.org/10.1016/J.NEO.2025.101136.
- Chou, T.C. (2010) 'Drug combination studies and their synergy quantification using the choutalalay method', Cancer Research, 70(2), pp. 440–446. Available at: https://doi.org/10.1158/0008-5472.CAN-09-1947.
- Choy C. et al. (2016) Inhibition of β 2-adrenergic receptor reduces triple-negative breast cancer brain metastases: The potential benefit of perioperative β -blockade. Oncol Rep, 35(6):3135–42.
- Christowitz, C. et al. (2019) 'Mechanisms of doxorubicin-induced drug resistance and drugresistant tumour growth in a murine breast tumour model', BMC Cancer, 19(1), pp. 1–10. Available at: https://doi.org/10.1186/S12885-019-5939-Z/FIGURES/5.
- Ciocan-Cartita, C.A. et al. (2020) 'New insights in gene expression alteration as effect of doxorubicin drug resistance in triple negative breast cancer cells', Journal of Experimental and Clinical Cancer Research, 39(1), pp. 1–16. Available at: https://doi.org/10.1186/S13046-020-01736-2/FIGURES/11.

- Claudino, W. et al. (2007) 'Metabolomics: available results, current research projects in breast cancer, and future applications'. Journal of clinical oncology: official journal of the American Society of Clinical Oncology, 25(19), 2840–2846. https://doi.org/10.1200/JCO.2006.09.7550
- Cluntun, A.A. et al. (2017) 'Glutamine Metabolism in Cancer: Understanding the Heterogeneity', Trends in cancer, 3(3), p. 169. Available at: https://doi.org/10.1016/J.TRECAN.2017.01.005.
- Cobler L. et al. (2018) 'xCT inhibition sensitizes tumours to γ-radiation via glutathione reduction'. Oncotarget, 17;9(64):32280-32297. doi: 10.18632/oncotarget.25794. PMID: 30190786; PMCID: PMC6122354.
- Colombo, I. et al. (2021) 'Phase I dose-escalation study of the dual PI3K-mTORC1/2 inhibitor gedatolisib in combination with paclitaxel and carboplatin in patients with advanced solid tumours', Clinical Cancer Research, 27(18), pp. 5012–5019. Available at: https://doi.org/10.1158/1078-0432.CCR-21-1402/672323/AM/PHASE-1-DOSE-ESCALATION-STUDY-OF-THE-DUAL-PI3K.
- Correia, A.S., Gärtner, F. and Vale, N. (2021a) 'Drug combination and repurposing for cancer therapy: the example of breast cancer', Heliyon, 7(1). Available at: https://doi.org/10.1016/j.heliyon.2021.e05948.
- Correia, A.S., Gärtner, F. and Vale, N. (2021b) 'Drug combination and repurposing for cancer therapy: the example of breast cancer', Heliyon, 7(1), p. e05948. Available at: https://doi.org/10.1016/J.HELIYON.2021.E05948.
- Cortazar, P. et al. (2014) 'Pathological complete response and long-term clinical benefit in breast cancer: The CTNeoBC pooled analysis', The Lancet, 384(9938), pp. 164–172. Available at: https://doi.org/10.1016/S0140-6736(13)62422-8.
- Costa, R.L.B., Han, H.S. and Gradishar, W.J. (2018) 'Targeting the PI3K/AKT/mTOR pathway in triple-negative breast cancer: a review', Breast Cancer Research and Treatment, 169(3), pp. 397–406. Available at: https://doi.org/10.1007/S10549-018-4697-Y/TABLES/1.
- Cucciniello, L. et al. (2023) 'Oestrogen deprivation effects of endocrine therapy in breast cancer patients: Incidence, management and outcome', Cancer Treatment Reviews, 120, p. 102624. Available at: https://doi.org/10.1016/J.CTRV.2023.102624.
- Curtius, K., Wright, N. A., & Graham, T. A. (2017). Evolution of Premalignant Disease. Cold Spring Harbor perspectives in medicine, 7(12), a026542. https://doi.org/10.1101/cshperspect.a026542
- Dagogo-Jack, I. and Shaw, A.T. (2018) 'Tumour heterogeneity and resistance to cancer therapies', Nature Reviews Clinical Oncology, 15(2), pp. 81–94. Available at: https://doi.org/10.1038/nrclinonc.2017.166.
- Danzi, F. et al. (2023) 'To metabolomics and beyond: a technological portfolio to investigate cancer metabolism', Signal Transduction and Targeted Therapy 2023 8:1, 8(1), pp. 1–22. Available at: https://doi.org/10.1038/s41392-023-01380-0.
- Das, A. et al. (2022) 'Repurposing Drugs as Novel Triple-negative Breast Cancer

- Therapeutics', Anti-cancer agents in medicinal chemistry, 22(3), pp. 515–550. Available at: https://doi.org/10.2174/1871520621666211021143255.
- Deng, H. et al. (2023a) 'PI3K/AKT/mTOR pathway, hypoxia, and glucose metabolism: Potential targets to overcome radioresistance in small cell lung cancer', Cancer Pathogenesis and Therapy, 1(1), pp. 56–66. Available at: https://doi.org/10.1016/J.CPT.2022.09.001/ASSET/6FDF7DD4-2DB3-451F-B5C4-35209A8BA2A5/ASSETS/GRAPHIC/2949-7132-01-01-009-F002.PNG.
- Deng, H. et al. (2023b) 'PI3K/AKT/mTOR pathway, hypoxia, and glucose metabolism: Potential targets to overcome radioresistance in small cell lung cancer', Cancer Pathogenesis and Therapy, 1(1), pp. 56–66. Available at: https://doi.org/10.1016/J.CPT.2022.09.001.
- De Vera, A.A. & Reznik, S.E. (2019) 'Combining PI3K/Akt/mTOR inhibition with chemotherapy. In: A. Ahmad, ed. Protein Kinase Inhibitors as Sensitizing Agents for Chemotherapy'. 1st ed. Cambridge, MA: Academic Press, pp.229–242. https://doi.org/10.1016/B978-0-12-816435-8.00014-6
- Dewidar, S.A. et al. (2024) 'Enhanced therapeutic efficacy of doxorubicin/cyclophosphamide in combination with pitavastatin or simvastatin against breast cancer cells', Medical Oncology, 41(1), pp. 1–12. Available at: https://doi.org/10.1007/S12032-023-02248-7/FIGURES/6.
- Dias, K. et al. (2017) 'Claudin-low breast cancer; clinical & pathological characteristics', PLoS ONE, 12(1), pp. 1–17. Available at: https://doi.org/10.1371/journal.pone.0168669.
- Dong, R. et al. (2025) 'Role of Oxidative Stress in the Occurrence, Development, and Treatment of Breast Cancer', Antioxidants 2025, Vol. 14, Page 104, 14(1), p. 104. Available at: https://doi.org/10.3390/ANTIOX14010104.
- Du Y, Huang L. (2025) Efficacy and safety of platinum-based, anthracycline-free neoadjuvant chemotherapy for triple-negative breast cancer: a systematic review and meta-analysis. Discov Oncol.;16:1567. doi:10.1007/s12672-025-03435-w
- Dupuy, F. et al. (2015) 'PDK1-dependent metabolic reprogramming dictates metastatic potential in breast cancer', Cell Metabolism, 22(4), pp. 577–589. Available at: https://doi.org/10.1016/j.cmet.2015.08.007.
- EDGE, S. B. & COMPTON, C. C. (2010). The American Joint Committee on Cancer: the 7th edition of the AJCC cancer staging manual and the future of TNM. Ann Surg Oncol, 17, 1471-4.
- Eliassen, F.M. et al. (2023) 'Importance of endocrine treatment adherence and persistence in breast cancer survivorship: a systematic review', BMC Cancer, 23(1), pp. 1–12. Available at: https://doi.org/10.1186/S12885-023-11122-8/FIGURES/3.
- Eralp, T.N., Sevinc, A. and Mansuroglu, B. (2024) 'Combination therapy application of Abemaciclib with Doxorubicin in triple negative breast cancer cell line MDA-MB-231', Cellular and Molecular Biology, 70(2), pp. 169–177. Available at: https://doi.org/10.14715/CMB/2024.70.2.24.
- Fabi, F. et al. (2021) 'Pharmacologic inhibition of Akt in combination with chemotherapeutic

- agents effectively induces apoptosis in ovarian and endometrial cancer cell lines', Molecular Oncology, 15(8), pp. 2106–2119. Available at: https://doi.org/10.1002/1878-0261.12888.
- Fan, Y. et al. (2016) 'Human plasma metabolomics for identifying differential metabolites and predicting molecular subtypes of breast cancer', Oncotarget, 7(9), pp. 9925–9938. Available at: https://doi.org/10.18632/oncotarget.7155.
- Fang, Z. et al. (2022) 'PUS1 is a novel biomarker for predicting poor outcomes and triple-negative status in breast cancer', Frontiers in Oncology, 12(November), pp. 1–13. Available at: https://doi.org/10.3389/fonc.2022.1030571.
- Ferreira Almeida, C. et al. (2020) 'Oestrogen receptor-positive (ER+) breast cancer treatment: Are multi-target compounds the next promising approach?', Biochemical Pharmacology, 177(March), p. 113989. Available at: https://doi.org/10.1016/j.bcp.2020.113989.
- De Francesco, E.M. et al. (2022) 'Triple-negative breast cancer drug resistance, durable efficacy, and cure: how advanced biological insights and emerging drug modalities could transform progress', Expert opinion on therapeutic targets, 26(6), pp. 513–535. Available at: https://doi.org/10.1080/14728222.2022.2094762.
- Forgie B et al., (2024) 'Vitality, viability, long-term clonogenic survival, cytotoxicity, cytostasis and lethality: what do they mean when testing new investigational oncology drugs?' Discov Oncol, 5;15(1):5. doi: 10.1007/s12672-023-00857-2. PMID: 38180601; PMCID: PMC10769964.
- Franceschini, G. et al. (2007). Update in the treatment of locally advanced breast cancer: a multidisciplinary approach. Eur Rev Med Pharmacol Sci, 11, 283-9.
- Franken, N. et al. (2006) 'Clonogenic assay of cells in vitro'. Nature Protocols, 1(5), pp.2315–2319. https://doi.org/10.1038/nprot.2006.339
- Fribbens, C. et al. (2016) 'Plasma ESR1 Mutations and the treatment of oestrogen receptor-Positive advanced breast cancer', Journal of Clinical Oncology, 34(25), pp. 2961–2968. Available at: https://doi.org/10.1200/JCO.2016.67.3061.
- Fujita, M. et al. (2020) 'Metabolic characterization of aggressive breast cancer cells exhibiting invasive phenotype: Impact of non-cytotoxic doses of 2-DG on diminishing invasiveness', BMC Cancer, 20(1), pp. 1–13. Available at: https://doi.org/10.1186/S12885-020-07414-Y/FIGURES/6.
- Fumagalli, C. et al. (2014) 'Prevalence and clinicopathologic correlates of o6-methylguanine-dna methyltransferase methylation status in patients with triple-negative breast cancer treated preoperatively by alkylating drugs', Clinical Breast Cancer, 14(4), pp. 285–290. Available at: https://doi.org/10.1016/j.clbc.2014.02.010.
- Fu S. et al. (2019) 'Glutamine Synthetase Promotes Radiation Resistance via Facilitating Nucleotide Metabolism and Subsequent DNA Damage Repair'. Cell Rep ;28(5):1136-1143.e4. doi: 10.1016/j.celrep.2019.07.002. PMID: 31365859.
- Fung, T.S., Ryu, K.W. and Thompson, C.B. (2025) 'Arginine: at the crossroads of nitrogen metabolism.', The EMBO journal, 44(5), pp. 1275–1293. Available at:

- https://doi.org/10.1038/S44318-025-00379-3/ASSET/1C811331-DAC7-45F5-9BAE-1723C7AEFB2D/ASSETS/GRAPHIC/44318 2025 379 FIG7 HTML.PNG.
- Gallo, M. et al. (2025) 'Metabolic Profiling of Breast Cancer Cell Lines: Unique and Shared Metabolites'. Available at: https://doi.org/10.3390/ijms26030969.
- Gandhi, N. and Das, G.M. (2019) 'Metabolic reprogramming in breast cancer and its therapeutic implications', Cells, 8(2). Available at: https://doi.org/10.3390/CELLS8020089.
- García, M.E.G., Kirsch, D.G. and Reitman, Z.J. (2022) 'Targeting the ATM Kinase to Enhance the Efficacy of Radiotherapy and Outcomes for Cancer Patients', Seminars in Radiation Oncology, 32(1), pp. 3–14. Available at: https://doi.org/10.1016/J.SEMRADONC.2021.09.008.
- Garg, P. et al. (2015). Current definition of locally advanced breast cancer. Current oncology (Toronto, Ont.), 22, e409-e410.
- Garg, P. et al. (2024) 'Emerging Therapeutic Strategies to Overcome Drug Resistance in Cancer Cells'. Cancers, 16(13), 2478. https://doi.org/10.3390/cancers16132478
- Garg, P. et al. (2025) 'Strategic advancements in targeting the PI3K/AKT/mTOR pathway for Breast cancer therapy', Biochemical Pharmacology, 236, p. 116850. Available at: https://doi.org/10.1016/J.BCP.2025.116850.
- Garg, P.et al.(2025) 'Metabolic reprogramming in breast cancer: Pathways driving progression, drug resistance, and emerging therapeutics'. Biochimica et biophysica acta. Reviews on cancer, 1880(5), 189396. Advance online publication. https://doi.org/10.1016/j.bbcan.2025.189396
- Garnique, A. del M.B. et al. (2024) 'Two-Dimensional and Spheroid-Based Three-Dimensional Cell Culture Systems: Implications for Drug Discovery in Cancer', Drugs and Drug Candidates 2024, Vol. 3, Pages 391-409, 3(2), pp. 391–409. Available at: https://doi.org/10.3390/DDC3020024.
- Gasimli, R. et al. (2023) 'The effects of PKI-402 on breast tumour models' radiosensitivity via dual inhibition of PI3K/mTOR', International Journal of Radiation Biology, 99(12), pp. 1961–1970.

 Available at: https://doi.org/10.1080/09553002.2023.2232019/ASSET/5BC19CCE-0BE9-4CF1-B771-1CB1E69DD0EE/ASSETS/GRAPHIC/IRAB_A_2232019_F0007_B.JPG.
- Ge, J. et al. (2022) 'The advance of adjuvant treatment for triple-negative breast cancer', Cancer Biology and Medicine, 19(2), pp. 187–201. Available at: https://doi.org/10.20892/j.issn.2095-3941.2020.0752.
- Geck, R.C. et al. (2020) 'Inhibition of the polyamine synthesis enzyme ornithine decarboxylase sensitizes triple-negative breast cancer cells to cytotoxic chemotherapy', The Journal of Biological Chemistry, 295(19), p. 6263. Available at: https://doi.org/10.1074/JBC.RA119.012376.
- Ghanem, A. et al. (2022) 'Rumex Vesicarius L. extract improves the efficacy of doxorubicin in triple-negative breast cancer through inhibiting Bcl2, mTOR, JNK1 and augmenting p21 expression', Informatics in Medicine Unlocked, 29, p. 100869. Available at:

- https://doi.org/10.1016/J.IMU.2022.100869.
- Gianni, L. et al. (2016) '5-year analysis of neoadjuvant pertuzumab and trastuzumab in patients with locally advanced, inflammatory, or early-stage HER2-positive breast cancer (NeoSphere): a multicentre, open-label, phase 2 randomised trial', The Lancet Oncology, 17(6), pp. 791–800. Available at: https://doi.org/10.1016/S1470-2045(16)00163-7.
- Girardi F *et al* (2025). Omitting anthracyclines for the adjuvant treatment of patients with triple-negative breast cancer: A non-inferiority meta-analysis. Breast.;83:104524. doi: 10.1016/j.breast.2025.104524
- Goldenberg, D.M., Stein, R. and Sharkey, R.M. (2018) 'The emergence of trophoblast cell-surface antigen 2 (TROP-2) as a novel cancer target', Oncotarget, 9(48), pp. 28989–29006. Available at: https://doi.org/10.18632/oncotarget.25615.
- Gong, Y. et al. (2021) 'Metabolic-Pathway-Based Subtyping of Triple-Negative Breast Cancer Reveals Potential Therapeutic Targets', Cell Metabolism, 33(1), pp. 51-64.e9. Available at: https://doi.org/10.1016/j.cmet.2020.10.012.
- Gray, M. et al. (2019) 'Development and characterisation of acquired radioresistant breast cancer cell lines', Radiation Oncology, 14(1), pp. 1–19. Available at: https://doi.org/10.1186/S13014-019-1268-2/FIGURES/8.
- Guijas, C. et al. (2018) 'Metabolomics activity screening for identifying metabolites that modulate phenotype', Nature Biotechnology 2018 36:4, 36(4), pp. 316–320. Available at: https://doi.org/10.1038/nbt.4101.
- Gunasekharan, V. et al. (2024) 'Phosphoenolpyruvate carboxykinase-2 (PCK2) is a therapeutic target in triple-negative breast cancer', Breast Cancer Research and Treatment, 208(3), pp. 657–671. Available at: https://doi.org/10.1007/S10549-024-07462-Z/FIGURES/7.
- Guo, L. et al. (2023) 'Breast cancer heterogeneity and its implication in personalized precision therapy', Experimental Hematology and Oncology, 12(1), pp. 1–27. Available at: https://doi.org/10.1186/s40164-022-00363-1.
- Guo, Y. and Pei, X. (2019) 'Tetrandrine-Induced Autophagy in MDA-MB-231 Triple-Negative Breast Cancer Cell through the Inhibition of PI3K/AKT/mTOR Signalling', Evidence-Based Complementary and Alternative Medicine, 2019(1), p. 7517431. Available at: https://doi.org/10.1155/2019/7517431.
- Gupta, G.K. et al. (2020) 'Perspectives on triple-negative breast cancer: Current treatment strategies, unmet needs, and potential targets for future therapies', Cancers, 12(9), pp. 1–33. Available at: https://doi.org/10.3390/cancers12092392.
- Gyori, B. et al. (2014) 'OpenComet: An automated tool for comet assay image analysis', Redox Biology, 2, pp. 457–465. doi: 10.1016/j.redox.2013.12.020.
- Heikal, L. et al. (2024). Microneedles integrated with atorvastatin-loaded pumpkisomes for breast cancer therapy: a localized delivery approach. Journal of Controlled Release, 376, pp.354–368. Available at: https://doi.org/10.1016/j.jconrel.2024.10.013

- Hakeem, A.N. et al. (2024) 'Piperine enhances doxorubicin sensitivity in triple-negative breast cancer by targeting the PI3K/Akt/mTOR pathway and cancer stem cells', Scientific Reports 2024 14:1, 14(1), pp. 1–16. Available at: https://doi.org/10.1038/s41598-024-65508-0.
- Halama, A. and Suhre, K. (2022) 'Advancing Cancer Treatment by Targeting Glutamine Metabolism—A Roadmap', Cancers, 14(3). Available at: https://doi.org/10.3390/CANCERS14030553.
- Hammershoi Madsen, A.M. et al. (2024) 'Targeted Treatment of Metastatic Triple-Negative Breast Cancer: A Systematic Review', The Breast Journal, 2024(1), p. 9083055. Available at: https://doi.org/10.1155/2024/9083055.
- Han, H. *et al.* (2023) Early-Stage Triple-Negative Breast Cancer Journey: Beginning, End, and Everything in Between. ASCO Educational Book.;43. doi:10.1200/EDBK 390464
- Han, D. et al. (2024). Targeting Hypoxia and HIF1α in Triple-Negative Breast Cancer: New Insights from Gene Expression Profiling and Implications for Therapy. Biology, 13(8), 577. https://doi.org/10.3390/biology13080577
- Hanahan, D. & Weinberg, R.A., 2000. The hallmarks of cancer. Cell, 100(1), pp.57–70. doi:10.1016/S0092-8674(00)81683-9.
- Hanahan, D., & Weinberg, R. A. (2011). Hallmarks of cancer: the next generation. Cell, 144(5), 646–674. https://doi.org/10.1016/j.cell.2011.02.013
- Hanahan D. (2022). Hallmarks of Cancer: New Dimensions. Cancer discovery, 12(1), 31–46. https://doi.org/10.1158/2159-8290.CD-21-1059
- Hao, C. et al. (2025) 'PI3K/AKT/mTOR inhibitors for hormone receptor-positive advanced breast cancer', Cancer Treatment Reviews, 132, p. 102861. Available at: https://doi.org/10.1016/J.CTRV.2024.102861.
- Hargrave, S.D. et al. (2022) 'Cell Fate following Irradiation of MDA-MB-231 and MCF-7 Breast Cancer Cells Pre-Exposed to the Tetrahydroisoquinoline Sulfamate Microtubule Disruptor STX3451', Molecules, 27(12). Available at: https://doi.org/10.3390/MOLECULES27123819/S1.
- Hassan, A., Aubel, C. (2025). The PI3K/Akt/mTOR Signalling Pathway in Triple-Negative Breast Cancer: A Resistance Pathway and a Prime Target for Targeted Therapies. Cancers, 17(13), 2232. https://doi.org/10.3390/cancers17132232
- Hasanovic, A. and Mus-Veteau, I. (2018) 'Targeting the Multidrug Transporter Ptch1 Potentiates Chemotherapy Efficiency', Cells, 7(8), p. 107. Available at: https://doi.org/10.3390/cells7080107.
- Hatano, Y. et al. (2020) 'Molecular Trajectory of BRCA1 and BRCA2 Mutations', Frontiers in Oncology, 10(March), pp. 1–10. Available at: https://doi.org/10.3389/fonc.2020.00361.
- He, Y. et al. (2021) 'Targeting Pl3K/Akt signal transduction for cancer therapy', Signal Transduction and Targeted Therapy 2021 6:1, 6(1), pp. 1–17. Available at: https://doi.org/10.1038/s41392-021-00828-5.

- Hennigs, A. et al. (2016) 'Prognosis of breast cancer molecular subtypes in routine clinical care: A large prospective cohort study', BMC Cancer, 16(1), pp. 1–9. Available at: https://doi.org/10.1186/s12885-016-2766-3.
- Holler, M. et al. (2016a) 'Dual targeting of Akt and mTORC1 impairs repair of DNA double-strand breaks and increases radiation sensitivity of human tumour cells', PLoS ONE, 11(5). Available at: https://doi.org/10.1371/JOURNAL.PONE.0154745.
- Hoppe, R. et al. (2025) 'Lessons learned from a candidate gene study investigating aromatase inhibitor treatment outcome in breast cancer', npj Breast Cancer 2025 11:1, 11(1), pp. 1–15. Available at: https://doi.org/10.1038/s41523-025-00733-y.
- Hou, Y. et al. (2019) 'PD-L1 and CD8 are associated with deficient mismatch repair status in triple-negative and HER2-positive breast cancers', Human Pathology, 86, pp. 108–114. Available at: https://doi.org/10.1016/j.humpath.2018.12.007.
- Howell, A. and Howell, S.J. (2023) 'Tamoxifen evolution', British Journal of Cancer 2023 128:3, 128(3), pp. 421–425. Available at: https://doi.org/10.1038/s41416-023-02158-5.
- Huang, H.L. et al. (2015) 'Argininosuccinate lyase is a potential therapeutic target in breast cancer', Oncology reports, 34(6), pp. 3131–3139. Available at: https://doi.org/10.3892/OR.2015.4280.
- Huang, Z. et al. (2025) 'Neoadjuvant Strategies for Triple Negative Breast Cancer: Current Evidence and Future Perspectives', MedComm Future Medicine, 4(1), p. e70013. Available at: https://doi.org/10.1002/MEF2.70013.
- Ibrar, M. et al. (2022) 'Breast Cancer Survivors' Lived Experience of Adjuvant Hormone Therapy: A Thematic Analysis of Medication Side Effects and Their Impact on Adherence', Frontiers in Psychology, 13, p. 861198. Available at: https://doi.org/10.3389/FPSYG.2022.861198/BIBTEX.
- Inigo, M., Deja, S. and Burgess, S.C. (2021) 'Ins and Outs of the TCA Cycle: The Central Role of Anaplerosis', Annual Review of Nutrition. Annu Rev Nutr, pp. 19–47. Available at: https://doi.org/10.1146/annurev-nutr-120420-025558.
- Iweala, E.E.J. et al. (2024) 'Targeting c-Met in breast cancer: From mechanisms of chemoresistance to novel therapeutic strategies', Current research in pharmacology and drug discovery, 7. Available at: https://doi.org/10.1016/J.CRPHAR.2024.100204.
- Jafari, S. et al. (2023) 'Synergistic effect of chrysin and radiotherapy against triple-negative breast cancer (TNBC) cell lines', Clinical & translational oncology: official publication of the Federation of Spanish Oncology Societies and of the National Cancer Institute of Mexico, 25(8), pp. 2559–2568. Available at: https://doi.org/10.1007/S12094-023-03141-5.
- Jakhmola-Mani, R. et al. (2024) 'Drug Repurposing and Molecular Insights in the Fight Against Breast Cancer', Biomedical and Pharmacology Journal, 17(2), pp. 831–861. Available at: https://doi.org/10.13005/BPJ/2907.
- Ji, J. et al. (2023) 'Triple-negative breast cancer cells that survive ionizing radiation exhibit an Axl-dependent aggressive radioresistant phenotype', Experimental and

- Therapeutic Medicine, 26(3), pp. 1–13. Available at: https://doi.org/10.3892/etm.2023.12147.
- Ji, X. et al. (2019a) 'Chemoresistance mechanisms of breast cancer and their countermeasures', Biomedicine & Pharmacotherapy, 114, p. 108800. Available at: https://doi.org/10.1016/J.BIOPHA.2019.108800.
- Ji, X. et al. (2019b) 'Chemoresistance mechanisms of breast cancer and their countermeasures', Biomedicine & pharmacotherapy = Biomedecine & pharmacotherapie, 114. Available at: https://doi.org/10.1016/J.BIOPHA.2019.108800.
- Jia, D. et al. (2019) 'Elucidating cancer metabolic plasticity by coupling gene regulation with metabolic pathways', Proceedings of the National Academy of Sciences of the United States of America, 116(9), pp. 3909–3918. Available at: https://doi.org/10.1073/pnas.1816391116.
- Jia, S. et al. (2025) 'Deciphering the pseudouridine nucleobase modification in human diseases: From molecular mechanisms to clinical perspectives', Clinical and Translational Medicine, 15(1), p. e70190. Available at: https://doi.org/10.1002/CTM2.70190.
- Jiang, Y. et al. (2024) 'DMC triggers MDA-MB-231 cells apoptosis via inhibiting protective autophagy and PI3K/AKT/mTOR pathway by enhancing ROS level', Toxicology in Vitro, 97, p. 105809. Available at: https://doi.org/10.1016/J.TIV.2024.105809.
- Jiang, Y.Z. et al. (2019) 'Genomic and Transcriptomic Landscape of Triple-Negative Breast Cancers: Subtypes and Treatment Strategies', Cancer Cell, 35(3), pp. 428-440.e5. Available at: https://doi.org/10.1016/j.ccell.2019.02.001.
- Jiang, W. et al. (2020). Expression and clinical significance of MAPK and EGFR in triplenegative breast cancer. Oncology letters, 19(3), 1842–1848. https://doi.org/10.3892/ol.2020.11274
- Jin, J. et al. (2023) 'Targeting glutamine metabolism as a therapeutic strategy for cancer', Experimental & Molecular Medicine 2023 55:4, 55(4), pp. 706–715. Available at: https://doi.org/10.1038/s12276-023-00971-9.
- Johnson, J. et al. (2020) 'Targeting PI3K and AMPKα Signalling Alone or in Combination to Enhance Radiosensitivity of Triple Negative Breast Cancer', Cells, 9(5). Available at: https://doi.org/10.3390/CELLS9051253.
- Kciuk, M. et al. (2023) 'Doxorubicin—An Agent with Multiple Mechanisms of Anticancer Activity', Cells, 12(4), p. 659. Available at: https://doi.org/10.3390/CELLS12040659.
- Kell, D.B. and Oliver, S.G. (2016) 'The metabolome 18 years on: a concept comes of age', Metabolomics, 12(9). Available at: https://doi.org/10.1007/S11306-016-1108-4.
- Keshandehghan, A. et al. (2024) 'Acquisition of Doxorubicin Resistance Induces Breast Cancer Cell Migration and Epithelial-Mesenchymal Transition that are Reversed by Shikonin-Metformin Synergy: Dox resistance and BC cell migration', Archives of Breast Cancer, 11(2), pp. 159–171. Available at: https://doi.org/10.32768/ABC.2024112159-171.

- Khan, M.A. et al. (2019a) 'PI3K/AKT/mTOR pathway inhibitors in triple-negative breast cancer: a review on drug discovery and future challenges', Drug Discovery Today, 24(11), pp. 2181–2191. Available at: https://doi.org/10.1016/J.DRUDIS.2019.09.001.
- Khan, M.A. et al. (2019b) 'PI3K/AKT/mTOR pathway inhibitors in triple-negative breast cancer: a review on drug discovery and future challenges', Drug Discovery Today, 24(11), pp. 2181–2191. Available at: https://doi.org/10.1016/j.drudis.2019.09.001.
- Kim, J., Harper, A., McCormack, V., Sung, H., Houssami, N., Morgan, E., Mutebi, M., Garvey, G., Soerjomataram, I. and Fidler-Benaoudia, Miranda M. (2025) 'Global patterns and trends in breast cancer incidence and mortality across 185 countries', Nature Medicine 2025, pp. 1–9. Available at: https://doi.org/10.1038/s41591-025-03502-3.
- Kim, J., Fahmy, V. and Haffty, B.G. (2024) 'Radiation therapy for triple-negative breast cancer: from molecular insights to clinical perspectives', Expert Review of Anticancer Therapy, 24(5), pp. 211–217. Available at: https://doi.org/10.1080/14737140.2024.2333320.
- Klassen, A. et al. (2017) 'Metabolomics: Definitions and Significance in Systems Biology', Advances in Experimental Medicine and Biology, 965, pp. 3–17. Available at: https://doi.org/10.1007/978-3-319-47656-8_1.
- Knott, S.R.V. et al. (2018) 'Asparagine bioavailability governs metastasis in a model of breast cancer', Nature, 554(7692), pp. 378–381. Available at: https://doi.org/10.1038/NATURE25465;TECHMETA=13,89;SUBJMETA=322,631,67;KWRD=CANCER,METASTASIS.
- Koulaouzidis, G. et al. (2021) 'Conventional cardiac risk factors associated with trastuzumabinduced cardiotoxicity in breast cancer: Systematic review and meta-analysis', Current Problems in Cancer, p. 100723. Available at: https://doi.org/10.1016/J.CURRPROBLCANCER.2021.100723.
- Ku, G.C. et al. (2022) 'Identification of Lethal Inhibitors and Inhibitor Combinations for Mono-Driver versus Multi-Driver Triple-Negative Breast Cancer Cells', Cancers, 14(16). Available at: https://doi.org/10.3390/CANCERS14164027/S1.
- Kubli, S.P. et al. (2019) 'AhR controls redox homeostasis and shapes the tumour microenvironment in BRCA1-associated breast cancer', Proceedings of the National Academy of Sciences of the United States of America, 116(9), pp. 3604–3613. Available at: https://doi.org/10.1073/pnas.1815126116.
- Kuger, S. et al. (2014) 'Novel PI3K and mTOR Inhibitor NVP-BEZ235 radiosensitizes breast cancer cell lines under normoxic and hypoxic conditions', Breast Cancer: Basic and Clinical Research, 8(1), pp. 39–49. Available at: https://doi.org/10.4137/BCBCR.S13693.
- Kurmi, K. et al. (2018) 'Tyrosine Phosphorylation of Mitochondrial Creatine Kinase 1 Enhances a Druggable Tumour Energy Shuttle Pathway', Cell Metabolism, 28(6), pp. 833-847.e8. Available at: https://doi.org/10.1016/j.cmet.2018.08.008.
- Kus, K. et al. (2018) 'Alterations in arginine and energy metabolism, structural and signalling lipids in metastatic breast cancer in mice detected in plasma by targeted metabolomics and lipidomics', Breast Cancer Research, 20(1). Available at:

- https://doi.org/10.1186/s13058-018-1075-y.
- Lampa, M. et al. (2017) 'Glutaminase is essential for the growth of triple-negative breast cancer cells with a deregulated glutamine metabolism pathway, and its suppression synergizes with mTOR inhibition', PLoS ONE, 12(9). Available at: https://doi.org/10.1371/JOURNAL.PONE.0185092.
- Larkin, J. et al. (2015) 'Combined Nivolumab and Ipilimumab or Monotherapy in Untreated Melanoma', New England Journal of Medicine, 373(1), pp. 23–34. Available at: https://doi.org/10.1056/nejmoa1504030.
- Layman, R.M. et al. (2024) 'Gedatolisib in combination with palbociclib and endocrine therapy in women with hormone receptor-positive, HER2-negative advanced breast cancer: results from the dose expansion groups of an open-label, phase 1b study', The Lancet. Oncology, 25(4), pp. 474–487. Available at: https://doi.org/10.1016/S1470-2045(24)00034-2.
- Lee, D. and Cha, C. (2020) 'Cell subtype-dependent formation of breast tumour spheroids and their variable responses to chemotherapeutics within microfluidics-generated 3D microgels with tunable mechanics', Materials Science and Engineering: C, 112, p. 110932. Available at: https://doi.org/10.1016/J.MSEC.2020.110932.
- Lee, H. et al. (2022) 'Metabolic and lipidomic characterization of radioresistant MDA-MB-231 human breast cancer cells to investigate potential therapeutic targets'. Journal of pharmaceutical and biomedical analysis, 208, 114449. https://doi.org/10.1016/j.jpba.2021.114449
- Lee J et al. (2020). Neoadjuvant Treatment for Triple Negative Breast Cancer: Recent Progresses and Challenges. Cancers (Basel).;12(6):1404. doi:10.3390/cancers12061404
- Lee, K.S. et al. (2020) 'Arctigenin enhances the cytotoxic effect of doxorubicin in MDA-MB-231 breast cancer cells', International Journal of Molecular Sciences, 21(8). Available at: https://doi.org/10.3390/ijms21082997.
- Lehmann, B.D. et al. (2016) 'Refinement of triple-negative breast cancer molecular subtypes: Implications for neoadjuvant chemotherapy selection', PLoS ONE, 11(6), pp. 1–22. Available at: https://doi.org/10.1371/journal.pone.0157368.
- Lehmann, B.D., Pietenpol, J.A. and Tan, A.R. (2015) 'Triple-Negative Breast Cancer: Molecular Subtypes and New Targets for Therapy', American Society of Clinical Oncology Educational Book, (35), pp. e31–e39. Available at: https://doi.org/10.14694/edbook am.2015.35.e31.
- Leon-Ferre, R.A. and Goetz, M.P. (2023) 'Advances in systemic therapies for triple negative breast cancer', BMJ, 381. Available at: https://doi.org/10.1136/BMJ-2022-071674.
- Li, H. et al. (2022). Hypoxia induces docetaxel resistance in triple-negative breast cancer via the HIF-1α/miR-494/Survivin signalling pathway. Neoplasia, 34, p.100843. https://doi.org/10.1016/j.neo.2022.100821
- Li, H. et al. (2024) 'Linc00707 regulates autophagy and promotes the progression of triple negative breast cancer by activation of PI3K/AKT/mTOR pathway', Cell Death

- Discovery 2024 10:1, 10(1), pp. 1–14. Available at: https://doi.org/10.1038/s41420-024-01906-7.
- Li, Y. et al. (2022) 'Global Burden of Female Breast Cancer: Age-Period-Cohort Analysis of Incidence Trends From 1990 to 2019 and Forecasts for 2035', Frontiers in Oncology, 12, p. 891824. Available at: https://doi.org/10.3389/FONC.2022.891824/FULL.
- Liedtke, C. et al. (2008) 'Response to neoadjuvant therapy and long-term survival in patients with triple-negative breast cancer', Journal of Clinical Oncology, 26(8), pp. 1275–1281. Available at: https://doi.org/10.1200/JCO.2007.14.4147.
- Lin, W.Z. et al. (2022) 'From GWAS to drug screening: repurposing antipsychotics for glioblastoma', Journal of translational medicine, 20(1). Available at: https://doi.org/10.1186/S12967-021-03209-2.
- Liu, C et al. (2025) 'Molecular classification of hormone receptor-positive /HER2-positive breast cancer reveals potential neoadjuvant therapeutic strategies'. Signal transduction and targeted therapy, 10(1), 97. https://doi.org/10.1038/s41392-025-02181-3
- Liu, P. et al. (2020) 'Glutamine synthetase promotes tumour invasion in hepatocellular carcinoma through mediating epithelial–mesenchymal transition', Hepatology Research, 50(2), pp. 246–257. Available at: https://doi.org/10.1111/hepr.13433.
- Liu, S. et al. (2024a) 'Metabolic reprogramming and therapeutic resistance in primary and metastatic breast cancer', Molecular Cancer 2024 23:1, 23(1), pp. 1–57. Available at: https://doi.org/10.1186/S12943-024-02165-X.
- Liu, S. et al. (2024b) 'Metabolic reprogramming and therapeutic resistance in primary and metastatic breast cancer', Molecular Cancer 2024 23:1, 23(1), pp. 1–57. Available at: https://doi.org/10.1186/S12943-024-02165-X.
- Liu, T. et al. (2015) 'Dual PI3K/mTOR inhibitors, GSK2126458 and PKI-587, suppress tumour progression and increase radiosensitivity in nasopharyngeal carcinoma', Molecular Cancer Therapeutics, 14(2), pp. 429–439. Available at: https://doi.org/10.1158/1535-7163.MCT-14-0548.
- Liu, X. et al. (2025) 'A comparative analysis of toxicity and treatment outcomes of adaptive radiotherapy and intensity-modulated radiotherapy in cervical cancer', Scientific reports, 15(1), p. 1609. Available at: https://doi.org/10.1038/S41598-024-85074-9;SUBJMETA=1059,4028,631,67,692;KWRD=CANCER,CANCER+THERAPY.
- Liu, Y. et al. (2021) 'Molecular mechanisms of chemo- and radiotherapy resistance and the potential implications for cancer treatment', MedComm, (August 2020), pp. 1–26. Available at: https://doi.org/10.1002/mco2.55.
- Liu, Y. et al. (2023) 'Advances in the study of aerobic glycolytic effects in resistance to radiotherapy in malignant tumours', PeerJ, 11, p. e14930. Available at: https://doi.org/10.7717/PEERJ.14930/TABLE-1.
- Liu, Z. et al. (2015) 'The upregulation of PI3K/Akt and MAP kinase pathways is associated with resistance of microtubule-targeting drugs in prostate cancer', Journal of Cellular Biochemistry, 116(7), pp. 1341–1349. Available at: https://doi.org/10.1002/jcb.25091.

- Lomelino, C.L. et al. (2017) 'Asparagine synthetase: Function, structure, and role in disease', Journal of Biological Chemistry, 292(49), pp. 19952–19958. Available at: https://doi.org/10.1074/jbc.R117.819060.
- Loria, R. et al. (2022) 'Cross-Resistance Among Sequential Cancer Therapeutics: An Emerging Issue', Frontiers in Oncology, 12, p. 877380. Available at: https://doi.org/10.3389/FONC.2022.877380/PDF.
- Lovitt, C.J., Shelper, T.B. and Avery, V.M. (2018) 'Doxorubicin resistance in breast cancer cells is mediated by extracellular matrix proteins', BMC Cancer, 18(1), pp. 1–11. Available at: https://doi.org/10.1186/S12885-017-3953-6/FIGURES/6.
- Lu, J. et al. (2022) 'In vivo detection of dysregulated choline metabolism in paclitaxel-resistant ovarian cancers with proton magnetic resonance spectroscopy', Journal of Translational Medicine, 20(1), p. 92. Available at: https://doi.org/10.1186/S12967-022-03292-Z.
- Lu, L. et al. (2018) 'Activation of STAT3 and Bcl-2 and reduction of reactive oxygen species (ROS) promote radioresistance in breast cancer and overcome of radioresistance with niclosamide', Oncogene, 37(39), pp. 5292–5304. Available at: https://doi.org/10.1038/s41388-018-0340-y.
- Luo, M., Brooks, M. and Wicha, M.S. (2018) 'Asparagine and Glutamine: Co-conspirators Fueling Metastasis', Cell Metabolism, 27(5), pp. 947–949. Available at: https://doi.org/10.1016/j.cmet.2018.04.012.
- Luzhna, L. et al. (2013) 'Molecular mechanisms of radiation resistance in doxorubicinresistant breast adenocarcinoma cells', International Journal of Oncology, 42(5), pp. 1692–1708. Available at: https://doi.org/10.3892/ijo.2013.1845.
- Mahmoud, A. et al. (2023) 'The Detection of DNA Damage Response in MCF7 and MDA-MB-231 Breast Cancer Cell Lines after X-ray Exposure', Genome Integrity, 14, p. 20220001. Available at: https://doi.org/10.14293/GENINT.14.1.001.
- McMahon, S.J. (2019) 'The linear quadratic model: usage, interpretation and challenges', Physics in Medicine & Biology, 64(1), 01TR01. doi: 10.1088/1361-6560/aaf26a.
- Maity, G. (2019) 'Aspirin suppresses tumour cell-induced angiogenesis and their incongruity'. Journal of cell communication and signalling, 13(4), 491–502. https://doi.org/10.1007/s12079-018-00499-y
- Majumdar, R. et al. (2016) 'Glutamate, Ornithine, Arginine, Proline, and Polyamine Metabolic Interactions: The Pathway Is Regulated at the Post-Transcriptional Level', Frontiers in plant science, 7(FEB2016). Available at: https://doi.org/10.3389/FPLS.2016.00078.
- Malla, R.R. et al. (2021) 'Reactive oxygen species (ROS): Critical roles in breast tumour microenvironment', Critical Reviews in Oncology/Hematology, 160, p. 103285. Available at: https://doi.org/10.1016/J.CRITREVONC.2021.103285.
- Mallon, R. et al. (2011) 'Antitumour efficacy of PKI-587, a highly potent dual PI3K/mTOR kinase inhibitor', Clinical Cancer Research, 17(10), pp. 3193–3203. Available at: https://doi.org/10.1158/1078-0432.CCR-10-1694/83633/AM/ANTITUMOUR-

EFFICACY-OF-PKI-587-A-HIGHLY-POTENT-DUAL.

- Marcus, L. et al. (2019) 'FDA approval summary: Pembrolizumab for the treatment of microsatellite instability-high solid tumours', Clinical Cancer Research, 25(13), pp. 3753–3758. Available at: https://doi.org/10.1158/1078-0432.CCR-18-4070.
- Mardanshahi, A. et al. (2021) 'The PI3K/AKT/mTOR signalling pathway inhibitors enhance radiosensitivity in cancer cell lines', Molecular Biology Reports, 48(8), pp. 1–14. Available at: https://doi.org/10.1007/S11033-021-06607-3/FIGURES/2.
- Mariotto A. et al. (2014) 'Cancer survival: an overview of measures, uses, and interpretation. Journal of the National Cancer Institute. Monographs'. (49):145-186. DOI: 10.1093/jncimonographs/lgu024. PMID: 25417231; PMCID: PMC4829054.
- Marklein, D. et al. (2012) 'Pl3K Inhibition Enhances Doxorubicin-Induced Apoptosis in Sarcoma Cells', PLOS ONE, 7(12), p. e52898. Available at: https://doi.org/10.1371/JOURNAL.PONE.0052898.
- Martinez-Outschoorn, U.E. et al. (2017) 'Cancer metabolism: A therapeutic perspective', Nature Reviews Clinical Oncology, 14(1), pp. 11–31. Available at: https://doi.org/10.1038/nrclinonc.2016.60.
- Martínez-Reza, let al. (2019). 'Calcitriol Inhibits the Proliferation of Triple-Negative Breast Cancer Cells through a Mechanism Involving the Proinflammatory Cytokines IL-1β and TNF-α'. Journal of immunology research, 2019, 6384278. https://doi.org/10.1155/2019/6384278
- Marullo, R. et al. (2021a) 'The metabolic adaptation evoked by arginine enhances the effect of radiation in brain metastases', Science Advances, 7(45), p. eabg1964. Available at: https://doi.org/10.1126/SCIADV.ABG1964.
- Marullo, R. et al. (2021b) 'The metabolic adaptation evoked by arginine enhances the effect of radiation in brain metastases', Science Advances, 7(45), pp. 1–16. Available at: https://doi.org/10.1126/sciadv.abg1964.
- Mavragani, I. *et al.* (2017) 'Complex DNA Damage: A Route to Radiation-Induced Genomic Instability and Carcinogenesis. Cancers', 9(7), 91. https://doi.org/10.3390/cancers9070091
- Masoud, V. and Pagès, G. (2017) 'Targeted therapies in breast cancer: New challenges to fight against resistance', World Journal of Clinical Oncology, 8(2), pp. 120–134. Available at: https://doi.org/10.5306/wjco.v8.i2.120.
- Mavaddat, N. et al. (2012) 'Pathology of breast and ovarian cancers among BRCA1 and BRCA2 mutation carriers: Results from the consortium of investigators of modifiers of BRCA1/2 (CIMBA)', Cancer Epidemiology Biomarkers and Prevention, 21(1), pp. 134–147. Available at: https://doi.org/10.1158/1055-9965.EPI-11-0775.
- McCann, E., O'Sullivan, J. and Marcone, S. (2021) 'Targeting cancer-cell mitochondria and metabolism to improve radiotherapy response', Translational Oncology, 14(1), p. 100905. Available at: https://doi.org/10.1016/J.TRANON.2020.100905.
- McCartney, A. et al. (2018) 'Metabolomics in breast cancer: A decade in review'. Cancer

- McGale, P. (2014). Effect of radiotherapy after mastectomy and axillary surgery on 10-year recurrence and 20-year breast cancer mortality: meta-analysis of individual patient data for 8135 women in 22 randomised trials. The Lancet, 383(9935), 2127-35.
- McGowan, D.R. et al. (2019) 'Buparlisib with thoracic radiotherapy and its effect on tumour hypoxia: A phase I study in patients with advanced non-small cell lung carcinoma', European Journal of Cancer, 113, p. 87. Available at: https://doi.org/10.1016/J.EJCA.2019.03.015.
- Medina, M.A. et al. (2020) 'Triple-negative breast cancer: A review of conventional and advanced therapeutic strategies', International Journal of Environmental Research and Public Health, 17(6), pp. 1–32. Available at: https://doi.org/10.3390/ijerph17062078.
- Meng, F. et al. (2019) 'EGFL9 promotes breast cancer metastasis by inducing cMET activation and metabolic reprogramming', Nature Communications, 10(1). Available at: https://doi.org/10.1038/s41467-019-13034-3.
- Meng, M. et al. (2023) 'Ampelopsin induces MDA-MB-231 cell cycle arrest through cyclin B1-mediated Pl3K/AKT/mTOR pathway in vitro and in vivo', Acta Pharmaceutica, 73(1), pp. 75–90. Available at: https://doi.org/10.2478/ACPH-2023-0005.
- Mielczarek, L. et al. (2019) 'In the triple-negative breast cancer MDA-MB-231 cell line, sulforaphane enhances the intracellular accumulation and anticancer action of doxorubicin encapsulated in liposomes', International Journal of Pharmaceutics, 558, pp. 311–318. Available at: https://doi.org/10.1016/J.IJPHARM.2019.01.008.
- Mills, A.M. et al. (2018) 'The relationship between mismatch repair deficiency and PD-L1 expression in breast carcinoma', American Journal of Surgical Pathology, 42(2), pp. 183–191. Available at: https://doi.org/10.1097/PAS.0000000000000949.
- Mills, J.N., Rutkovsky, A.C. and Giordano, A. (2018) 'Mechanisms of resistance in oestrogen receptor positive breast cancer: overcoming resistance to tamoxifen/aromatase inhibitors', Current Opinion in Pharmacology, 41, pp. 59–65. Available at: https://doi.org/10.1016/j.coph.2018.04.009.
- von Minckwitz, G. et al. (2017) 'Adjuvant Pertuzumab and Trastuzumab in Early HER2-Positive Breast Cancer', New England Journal of Medicine, 377(2), pp. 122–131. Available at: https://doi.org/10.1056/nejmoa1703643.
- Mitaishvili, E. et al. (2024) 'The Molecular Mechanisms behind Advanced Breast Cancer Metabolism: Warburg Effect, OXPHOS, and Calcium', Frontiers in bioscience (Landmark edition), 29(3). Available at: https://doi.org/10.31083/J.FBL2903099.
- Moreno-felici, J. et al. (2020) 'Regulate Cancer Cell Fate by Altering Cytosolic Ca 2 +', Cells, 9, pp. 1–15.
- Morse D. et al. (2005) 'Docetaxel induces cell death through mitotic catastrophe in human breast cancer cells'. Mol Cancer Ther,4(10):1495-504. doi: 10.1158/1535-7163.MCT-05-0130. PMID: 16227398.

- Mousavikia, S.N. et al. (2025) 'PI3K/AKT/mTOR Targeting in Colorectal Cancer Radiotherapy: A Systematic Review', Journal of gastrointestinal cancer, 56(1), p. 52. Available at: https://doi.org/10.1007/S12029-024-01160-1/FIGURES/3.
- Mukohara, T. (2015) 'Pi3k mutations in breast cancer: Prognostic and therapeutic implications', Breast Cancer: Targets and Therapy, 7, pp. 111–123. Available at: https://doi.org/10.2147/BCTT.S60696.
- Munkácsy, G., Santarpia, L. and Győrffy, B. (2023) 'Therapeutic Potential of Tumour Metabolic Reprogramming in Triple-Negative Breast Cancer', International journal of molecular sciences, 24(8). Available at: https://doi.org/10.3390/IJMS24086945.
- Mustafa, M. et al. (2024) 'Molecular pathways and therapeutic targets linked to triple-negative breast cancer (TNBC)', Molecular and Cellular Biochemistry, 479(4), pp. 895–913. Available at: https://doi.org/10.1007/s11010-023-04772-6.
- Nagpal, D. et al. (2023) 'Targeted therapies against breast cancer: Clinical perspectives, obstacles and new opportunities', Journal of Drug Delivery Science and Technology, 89, p. 105049. Available at: https://doi.org/10.1016/J.JDDST.2023.105049.
- Newell, M., Brun, M. and Field, C.J. (2019) 'Treatment with DHA Modifies the Response of MDA-MB-231 Breast Cancer Cells and Tumours from nu/nu Mice to Doxorubicin through Apoptosis and Cell Cycle Arrest', Journal of Nutrition, 149(1), pp. 46–56. Available at: https://doi.org/10.1093/jn/nxy224.
- Nedeljković, M., & Damjanović, A. (2019) 'Mechanisms of Chemotherapy Resistance in Triple-Negative Breast Cancer-How We Can Rise to the Challenge'. Cells, 8(9), 957. https://doi.org/10.3390/cells8090957
- Newton, E. et al. (2022). Molecular Targets of Triple-Negative Breast Cancer: Where Do We Stand? Cancers, 14(3), 482. https://doi.org/10.3390/cancers14030482
- Nguyen, T. et al. (2019) 'Uncovering the Role of N-Acetyl-Aspartyl-Glutamate as a Glutamate Reservoir in Cancer', Cell reports, 27(2), p. 491. Available at: https://doi.org/10.1016/J.CELREP.2019.03.036.
- Nishimura, Y. et al. (2017) 'Overcoming obstacles to drug repositioning in Japan', Frontiers in Pharmacology, 8(OCT). Available at: https://doi.org/10.3389/FPHAR.2017.00729.
- Noorolyai, S. et al. (2019) 'The relation between PI3K/AKT signalling pathway and cancer', Gene, 698(November 2018), pp. 120–128. Available at: https://doi.org/10.1016/j.gene.2019.02.076.
- Novais, M.V.M. et al. (2021) 'Liposomes co-encapsulating doxorubicin and glucoevatromonoside derivative induce synergic cytotoxic response against breast cancer cell lines', Biomedicine & Pharmacotherapy, 136, p. 111123. Available at: https://doi.org/10.1016/J.BIOPHA.2020.111123.
- Ocean, A.J. et al. (2017) 'Sacituzumab govitecan (IMMU-132), an anti-Trop-2-SN-38 antibody-drug conjugate for the treatment of diverse epithelial cancers: Safety and pharmacokinetics', Cancer, 123(19), pp. 3843–3854. Available at: https://doi.org/10.1002/cncr.30789.

- Omarini, C. et al. (2018) 'Neoadjuvant treatments in triple-negative breast cancer patients: Where we are now and where we are going', Cancer Management and Research, 10, pp. 91–103. Available at: https://doi.org/10.2147/CMAR.S146658.
- Olawaiye, A. B., Baker, T. P., Washington, M. K., & Mutch, D. G. (2021). The new (Version 9) American Joint Committee on Cancer tumour, node, metastasis staging for cervical cancer. CA: a cancer journal for clinicians, 71(4), 287–298. https://doi.org/10.3322/caac.21663
- Ortega, M.A. et al. (2020) 'Signal Transduction Pathways in Breast Cancer: The Important Role of Pl3K/Akt/mTOR', Journal of Oncology, 2020. Available at: https://doi.org/10.1155/2020/9258396.
- Pajonk, F., Vlashi, E., & McBride, W. H. (2010). Radiation resistance of cancer stem cells: the 4 R's of radiobiology revisited. Stem cells (Dayton, Ohio), 28(4), 639–648. https://doi.org/10.1002/stem.318
- Pang, Z. et al. (2024) 'MetaboAnalyst 6.0: towards a unified platform for metabolomics data processing, analysis and interpretation', Nucleic Acids Research, 52(W1), pp. W398–W406. Available at: https://doi.org/10.1093/NAR/GKAE253.
- Park, S.M. et al. (2020) 'Feedback analysis identifies a combination target for overcoming adaptive resistance to targeted cancer therapy', Oncogene, 39(19), pp. 3803–3820. Available at: https://doi.org/10.1038/S41388-020-1255-Y.
- Park, M. et al. (2022). Breast Cancer Metastasis: Mechanisms and Therapeutic Implications. *International journal of molecular sciences*, 23(12), 6806. https://doi.org/10.3390/ijms23126806
- Pavlova, N.N. et al. (2018) 'As Extracellular Glutamine Levels Decline, Asparagine Becomes an Essential Amino Acid', Cell Metabolism, 27(2), pp. 428-438.e5. Available at: https://doi.org/10.1016/j.cmet.2017.12.006.
- Pavlova, N.N. and Thompson, C.B. (2016) 'The Emerging Hallmarks of Cancer Metabolism', Cell Metabolism, 23(1), pp. 27–47. Available at: https://doi.org/10.1016/j.cmet.2015.12.006.
- Payne, K.K. (2021) 'Cellular stress responses and metabolic reprogramming in cancer progression and dormancy', Seminars in Cancer Biology [Preprint], (January). Available at: https://doi.org/10.1016/j.semcancer.2021.06.004.
- Peddi, P.F. (2018) 'Hormone receptor positive breast cancer: State of the art', Current Opinion in Obstetrics and Gynecology, 30(1), pp. 51–54. Available at: https://doi.org/10.1097/GCO.0000000000000424.
- Peddie, N. et al. (2021) 'The impact of medication side effects on adherence and persistence to hormone therapy in breast cancer survivors: A qualitative systematic review and thematic synthesis', Breast, 58, pp. 147–159. Available at: https://doi.org/10.1016/j.breast.2021.05.005.
- Peleg Hasson, S. et al. (2021) 'Adjuvant endocrine therapy in HER2-positive breast cancer patients: systematic review and meta-analysis', ESMO open, 6(2), p. 100088. Available at: https://doi.org/10.1016/j.esmoop.2021.100088.

- Pendleton, K.E., Wang, K. and Echeverria, G. V. (2023) 'Rewiring of mitochondrial metabolism in therapy-resistant cancers: permanent and plastic adaptations', Frontiers in Cell and Developmental Biology, 11, p. 1254313. Available at: https://doi.org/10.3389/FCELL.2023.1254313/PDF.
- Phyu, S.M., Tseng, C.C. and Smith, T.A.D. (2018) 'CDP-choline accumulation in breast and colorectal cancer cells treated with a GSK-3-targeting inhibitor', Magma (New York, N.y.), 32(2), p. 227. Available at: https://doi.org/10.1007/S10334-018-0719-3.
- Plevritis, S.K. et al. (2018) 'Association of screening and treatment with breast cancer mortality by molecular subtype in US women, 2000-2012', JAMA Journal of the American Medical Association, pp. 154–164. Available at: https://doi.org/10.1001/jama.2017.19130.
- Pogorzelska, A. et al. (2023) 'Anticancer effect and safety of doxorubicin and nutraceutical sulforaphane liposomal formulation in triple-negative breast cancer (TNBC) animal model', Biomedicine & Pharmacotherapy, 161, p. 114490. Available at: https://doi.org/10.1016/J.BIOPHA.2023.114490.
- Pont, M., Marqués, M. and Sorolla, A. (2024) 'Latest Therapeutical Approaches for Triple-Negative Breast Cancer: From Preclinical to Clinical Research', International Journal of Molecular Sciences 2024, Vol. 25, Page 13518, 25(24), p. 13518. Available at: https://doi.org/10.3390/IJMS252413518.
- Post, S.M. et al. (2021) 'TAM kinases as regulators of cell death', Biochimica et Biophysica Acta Molecular Cell Research, 1868(6), p. 118992. Available at: https://doi.org/10.1016/j.bbamcr.2021.118992.
- Pranzini, E. et al. (2021) 'Metabolic Reprogramming in Anticancer Drug Resistance: A Focus on Amino Acids', Trends in Cancer, 7(8), pp. 682–699. Available at: https://doi.org/10.1016/j.trecan.2021.02.004.
- Pushpakom, S. et al. (2019) 'Drug repurposing: progress, challenges and recommendations', Nature reviews. Drug discovery, 18(1), pp. 41–58. Available at: https://doi.org/10.1038/NRD.2018.168.
- Qian, X. et al. (2017a) 'Enolase 1 stimulates glycolysis to promote chemoresistance in gastric cancer', Oncotarget, 8(29), pp. 47691–47708. Available at: https://doi.org/10.18632/ONCOTARGET.17868.
- Qian, X. et al. (2017b) 'Enolase 1 stimulates glycolysis to promote chemoresistance in gastric cancer', Oncotarget, 8(29), pp. 47691–47708. Available at: https://doi.org/10.18632/ONCOTARGET.17868.
- Qin, J. et al. (2019) 'STAT3 as a potential therapeutic target in triple negative breast cancer: a systematic review'. J Exp Clin Cancer Res 38, 195. https://doi.org/10.1186/s13046-019-1206-z
- Quaresma, M., Coleman, M.P. and Rachet, B. (2015) '40-year trends in an index of survival for all cancers combined and survival adjusted for age and sex for each cancer in England and Wales, 1971-2011: A population-based study', The Lancet, 385(9974), pp. 1206–1218. Available at: https://doi.org/10.1016/S0140-6736(14)61396-9.

- Rachner, T. et al. (2014). 'Dickkopf-1 is regulated by the mevalonate pathway in breast cancer'. Breast cancer research: BCR, 16(1), R20. https://doi.org/10.1186/bcr3616
- Raguz, S. et al. (2013) 'Loss of O6-methylguanine-DNA methyltransferase confers collateral sensitivity to carmustine in topoisomerase II-mediated doxorubicin resistant triple negative breast cancer cells', Biochemical Pharmacology, 85(2), pp. 186–196. Available at: https://doi.org/10.1016/j.bcp.2012.10.020.
- Raninga, P. et al. (2020). Therapeutic cooperation between auranofin, a thioredoxin reductase inhibitor and anti-PD-L1 antibody for treatment of triple-negative breast cancer. International journal of cancer, 146(1), 123–136. https://doi.org/10.1002/ijc.32410
- Rashmi, R. et al. (2018) 'Radioresistant cervical cancers are sensitive to inhibition of glycolysis and redox metabolism', Cancer Research, 78(6), pp. 1392–1403. Available at: https://doi.org/10.1158/0008-5472.CAN-17-2367/653035/AM/RADIO-RESISTANT-CERVICAL-CANCERS-ARE-SENSITIVE-TO.
- Rattanapornsompong, K. et al. (2021) 'Impaired G2/M cell cycle arrest induces apoptosis in pyruvate carboxylase knockdown MDA-MB-231 cells', Biochemistry and Biophysics Reports, 25, p. 100903. Available at: https://doi.org/10.1016/J.BBREP.2020.100903.
- Rawat, P.S. et al. (2021) 'Doxorubicin-induced cardiotoxicity: An update on the molecular mechanism and novel therapeutic strategies for effective management', Biomedicine & Pharmacotherapy, 139, p. 111708. Available at: https://doi.org/10.1016/J.BIOPHA.2021.111708.
- Rezakhani, N. (2020) 'Effects of X-irradiation and sinensetin on apoptosis induction in MDA-MB-231 human breast cancer cells', International Journal of Radiation Research, 18(1), pp. 75–82. doi: 10.18869/acadpub.ijrr.18.1.75.
- Dos Reis, L.M. et al. (2019) 'Dual inhibition of glutaminase and carnitine palmitoyltransferase decreases growth and migration of glutaminase inhibition-resistant triple-negative breast cancer cells', Journal of Biological Chemistry, 294(24), pp. 9342–9357. Available at: https://doi.org/10.1074/jbc.RA119.008180.
- Ren, J.X. et al. (2019) 'Racial/ethnic differences in the outcomes of patients with metastatic breast cancer: contributions of demographic, socioeconomic, tumour and metastatic characteristics', Breast Cancer Research and Treatment, 173(1), pp. 225–237. Available at: https://doi.org/10.1007/s10549-018-4956-y.
- Ren, J.et al. (2022) 'Lysophosphatidylcholine: Potential Target for the Treatment of Chronic Pain'. International Journal of Molecular Sciences, 23(15), 8274. https://doi.org/10.3390/ijms23158274
- Robson, M. et al. (2017) 'Olaparib for Metastatic Breast Cancer in Patients with a Germline BRCA Mutation', New England Journal of Medicine, 377(6), pp. 523–533. Available at: https://doi.org/10.1056/nejmoa1706450.
- Roci, I. et al. (2019) 'Mapping metabolic events in the cancer cell cycle reveals arginine catabolism in the committed SG2M phase', Cell reports, 26(7), p. 1691. Available at: https://doi.org/10.1016/J.CELREP.2019.01.059.

- Ros, S. et al. (2020) 'Metabolic Imaging Detects Resistance to PI3Kα Inhibition Mediated by Persistent FOXM1 Expression in ER+ Breast Cancer', Cancer Cell, 38(4), pp. 516-533.e9. Available at: https://doi.org/10.1016/j.ccell.2020.08.016.
- Rossetti, S. et al. (2024) 'Gedatolisib shows superior potency and efficacy versus single-node PI3K/AKT/mTOR inhibitors in breast cancer models', npj Breast Cancer 2024 10:1, 10(1), pp. 1–15. Available at: https://doi.org/10.1038/s41523-024-00648-0.
- Rouzier, R. et al. (2005) 'Breast cancer molecular subtypes respond differently to preoperative chemotherapy', Clinical Cancer Research, 11(16), pp. 5678–5685. Available at: https://doi.org/10.1158/1078-0432.CCR-04-2421.
- Roy, M. et al. (2023) 'Molecular Classification of Breast Cancer', PET clinics, 18(4), pp. 441–458. Available at: https://doi.org/10.1016/J.CPET.2023.04.002.
- Rushing, B.R., Molina, S. and Sumner, S. (2023) 'Metabolomics Analysis Reveals Altered Metabolic Pathways and Response to Doxorubicin in Drug-Resistant Triple-Negative Breast Cancer Cells', Metabolites, 13(7). Available at: https://doi.org/10.3390/METABO13070865/S1.
- Ryu, W.-J. and Sohn, J.H., (2021). Molecular targets and promising therapeutics of triplenegative breast cancer. Pharmaceuticals, 14(10), p.1008. https://doi.org/10.3390/ph14101008
- De Sá Junior, P.L. et al. (2017) 'The Roles of ROS in Cancer Heterogeneity and Therapy', Oxidative Medicine and Cellular Longevity, 2017. Available at: https://doi.org/10.1155/2017/2467940.
- Saheed, E.S. et al. (2024) 'Mechanism of the Warburg effect and its role in breast cancer immunotherapy', Discover Medicine 2024 1:1, 1(1), pp. 1–11. Available at: https://doi.org/10.1007/S44337-024-00131-6.
- Sahu, P. (2024). Electroporation enhances cell death in 3D scaffold-based MDA-MB-231 cells treated with metformin. Bioelectrochemistry, 159, p.108734. Available at: https://doi.org/10.1016/j.bioelechem.2024.108734.
- Saito, R. de F. et al. (2022) 'Phosphatidylcholine-Derived Lipid Mediators: The Crosstalk Between Cancer Cells and Immune Cells', Frontiers in Immunology, 13, p. 768606. Available at: https://doi.org/10.3389/FIMMU.2022.768606/XML/NLM.
- Salanci, Š. et al. (2024) 'The Induction of G2/M Phase Cell Cycle Arrest and Apoptosis by the Chalcone Derivative 1C in Sensitive and Resistant Ovarian Cancer Cells Is Associated with ROS Generation', International Journal of Molecular Sciences, 25(14), p. 7541. Available at: https://doi.org/10.3390/IJMS25147541/S1.
- Sarkar, E. et al. (2024a) 'The combination of Curcumin and Doxorubicin on targeting PI3K/AKT/mTOR signalling pathway: an in vitro and molecular docking study for inhibiting the survival of MDA-MB-231', In Silico Pharmacology 2024 12:2, 12(2), pp. 1–23. Available at: https://doi.org/10.1007/S40203-024-00231-2.
- Sarkar, E. et al. (2024b) 'The combination of Curcumin and Doxorubicin on targeting PI3K/AKT/mTOR signalling pathway: an in vitro and molecular docking study for inhibiting the survival of MDA-MB-231', In Silico Pharmacology 2024 12:2, 12(2), pp.

- 1-23. Available at: https://doi.org/10.1007/S40203-024-00231-2.
- Sarlak, S., Pagès, G. and Luciano, F. (2025) 'Enhancing radiotherapy techniques for Triple-Negative breast cancer treatment', Cancer Treatment Reviews, 136, p. 102939. Available at: https://doi.org/10.1016/J.CTRV.2025.102939/ASSET/DF8EE4BD-74C4-42B7-A0EA-200489E5A45F/MAIN.ASSETS/GR4.JPG.
- Sarmiento-Salinas, F.L. et al. (2019) 'Breast cancer subtypes present a differential production of reactive oxygen species (ROS) and susceptibility to antioxidant treatment', Frontiers in Oncology, 9(JUN), pp. 1–13. Available at: https://doi.org/10.3389/fonc.2019.00480.
- Sarno, F. et al. (2023) 'Triple Negative Breast Cancer Treatment Options and Limitations: Future Outlook', Pharmaceutics 2023, Vol. 15, Page 1796, 15(7), p. 1796. Available at: https://doi.org/10.3390/PHARMACEUTICS15071796.
- Schettini, F. et al. (2016) 'Hormone Receptor/Human Epidermal Growth Factor Receptor 2-positive breast cancer: Where we are now and where we are going', Cancer Treatment Reviews, 46, pp. 20–26. Available at: https://doi.org/10.1016/j.ctrv.2016.03.012.
- Schmidt, D. et al. (2021) 'Metabolomics in cancer research and emerging applications in clinical oncology'. CA: a cancer journal for clinicians, 71(4), 333–358. https://doi.org/10.3322/caac.21670
- Schmid, P. et al. (2020) 'Capivasertib plus paclitaxel versus placebo plus paclitaxel as first-line therapy for metastatic triple-negative breast cancer: The PAKT trial', Journal of Clinical Oncology, 38(5), pp. 423–433. Available at: https://doi.org/10.1200/JCO.19.00368.
- Schuster, E.F. et al. (2023) 'Molecular profiling of aromatase inhibitor sensitive and resistant ER+HER2- postmenopausal breast cancers', Nature Communications 2023 14:1, 14(1), pp. 1–15. Available at: https://doi.org/10.1038/s41467-023-39613-z.
- Scully, R. et al. (2019) 'DNA double-strand break repair-pathway choice in somatic mammalian cells', Nature Reviews Molecular Cell Biology 2019 20:11, 20(11), pp. 698–714. Available at: https://doi.org/10.1038/s41580-019-0152-0.
- Seo, M. et al. (2023). Dual inhibition of thioredoxin reductase and proteasome is required for auranofin-induced paraptosis in breast cancer cells. Cell death & disease, 14(1), 42. https://doi.org/10.1038/s41419-023-05586-6
- Sharma, P. et al. (2015) 'High throughput measurement of γ-H2AX DSB repair kinetics in a healthy human population', PLOS ONE, 10(3): e0121083.
- Sharma P. et al. (2025) Randomized Phase II Trial of Anthracycline-free and Anthracycline-containing Neoadjuvant Carboplatin Chemotherapy Regimens in Stage I–III Triple-negative Breast Cancer (NeoSTOP). Breast.;83:104524. doi: 10.1016/j.breast.2025.104524
- Shimura, T. et al. (2014) 'AKT-mediated enhanced aerobic glycolysis causes acquired radioresistance by human tumour cells', Radiotherapy and Oncology, 112(2), pp. 302–307. Available at: https://doi.org/10.1016/j.radonc.2014.07.015.

- Su, W (2023) 'PI3K signalling-regulated metabolic reprogramming: From mechanism to application'. Biochimica et biophysica acta. Reviews on cancer, 1878(5), 188952. https://doi.org/10.1016/j.bbcan.2023.188952
- Shu, Y. et al. (2024) 'FOS-Mediated PLCB1 Induces Radioresistance and Weakens the Antitumour Effects of CD8+ T Cells in Triple-Negative Breast Cancer', Molecular Carcinogenesis [Preprint]. Available at: https://doi.org/10.1002/MC.23834.
- Singh, D. et al. (2024). Remodeling of tumour microenvironment: strategies to overcome therapeutic resistance and innovate immunoengineering in triple-negative breast cancer. Frontiers in immunology, 15, 1455211. https://doi.org/10.3389/fimmu.2024.1455211
- Skolariki, A. et al. (2022) 'Role of PI3K/Akt/mTOR pathway in mediating endocrine resistance: concept to clinic', Exploration of Targeted Anti-tumour Therapy, 3(2), p. 172. Available at: https://doi.org/10.37349/ETAT.2022.00078.
- Smith, B.D., Bellon, J.R., Blitzblau, R., Freedman, G., Haffty, B., Hahn, C., Halberg, F., Hoffman, K., Horst, K., Moran, J., Patton, C., Perlmutter, J., Warren, L., Whelan, T., Wright, J. and Jagsi, R., 2018. *Radiation therapy for the whole breast: Executive summary of an American Society for Radiation Oncology (ASTRO) evidence-based guideline*. Practical Radiation Oncology, 8(3), pp.145–152. https://doi.org/10.1016/j.prro.2018.01.012
- Smoots, S.G. et al. (2024) 'Overcoming doxorubicin resistance in triple-negative breast cancer using the class I-targeting HDAC inhibitor bocodepsin/OKI-179 to promote apoptosis', Breast Cancer Research, 26(1), pp. 1–13. Available at: https://doi.org/10.1186/S13058-024-01799-5/FIGURES/6.
- Sofianidi, A; et al. (2024) 'Triple-Negative Breast Cancer and Emerging Therapeutic Strategies: ATR and CHK1/2 as Promising Targets', Cancers 2024, Vol. 16, Page 1139, 16(6), p. 1139. Available at: https://doi.org/10.3390/CANCERS16061139.
- Son, S. et al. (2022) 'Brain type of creatine kinase induces doxorubicin resistance via TGF-β signalling in MDA-MB-231 breast cancer cells', Animal Cells and Systems, 26(5), pp. 203–213. Available at: https://doi.org/10.1080/19768354.2022.2107070.
- Song, J.H. et al. (2018) 'Mechanisms behind resistance to PI3K inhibitor treatment induced by the PIM kinase', Molecular Cancer Therapeutics, 17(12), pp. 2710–2721. Available at: https://doi.org/10.1158/1535-7163.MCT-18-0374/87722/AM/MECHANISMS-BEHIND-RESISTANCE-TO-PI3K-INHIBITOR.
- Song, L.et al. (2022) 'Everolimus (RAD001) combined with programmed death-1 (PD-1) blockade enhances radiosensitivity of cervical cancer and programmed death-ligand 1 (PD-L1) expression by blocking the phosphoinositide 3-kinase (PI3K)/protein kinase B (AKT)/mammalian target of rapamycin (mTOR)/S6 kinase 1 (S6K1) pathway'. Bioengineered, 13(4), 11240–11257. https://doi.org/10.1080/21655979.2022.2064205
- Sonkar, K. et al. (2019) 'Focus on the glycerophosphocholine pathway in choline phospholipid metabolism of cancer', NMR in biomedicine, 32(10), p. e4112. Available at: https://doi.org/10.1002/NBM.4112.

- Spini, A. et al. (2019) 'Evidence of β-blockers drug repurposing for the treatment of triple negative breast cancer: A systematic review', Neoplasma, 66(6), pp. 963–970. Available at: https://doi.org/10.4149/NEO 2019 190110N34.
- Sriramulu, S. et al. (2024) 'Present and Future of Immunotherapy for Triple-Negative Breast Cancer', Cancers 2024, Vol. 16, Page 3250, 16(19), p. 3250. Available at: https://doi.org/10.3390/CANCERS16193250.
- Staaf, J. et al. (2019) 'Whole-genome sequencing of triple-negative breast cancers in a population-based clinical study', Nature Medicine, 25(10), pp. 1526–1533. Available at: https://doi.org/10.1038/s41591-019-0582-4.
- Stine, Z.E. et al. (2022) 'Targeting cancer metabolism in the era of precision oncology', Nat. Rev. Drug Discov., 21(2), pp. 141–162. Available at: https://doi.org/10.1038/s41573-021-00339-6.
- Stover, D. (2016). 'The Role of Proliferation in Determining Response to Neoadjuvant Chemotherapy in Breast Cancer: A Gene Expression-Based Meta-Analysis'. Clinical cancer research: an official journal of the American Association for Cancer Research, 22(24), 6039–6050. https://doi.org/10.1158/1078-0432.CCR-16-0471
- Sun, Z.et al. (2024). Surgery paradigm for locally advanced breast cancer following neoadjuvant systemic therapy. Frontiers in Surgery, 11, p.1410127. https://doi.org/10.3389/fsurg.2024.1410127
- Suri, G.S. et al. (2023) 'Metabolomics in oncology', Cancer Reports, 6(3). Available at: https://doi.org/10.1002/CNR2.1795.
- Swain, S.M., Shastry, M. and Hamilton, E. (2022) 'Targeting HER2-positive breast cancer: advances and future directions', Nature Reviews Drug Discovery 2022 22:2, 22(2), pp. 101–126. Available at: https://doi.org/10.1038/s41573-022-00579-0.
- Syrnioti, A. (2024). Triple Negative Breast Cancer: Molecular Subtype-Specific Immune Landscapes with Therapeutic Implications. *Cancers*, *16*(11), 2094. https://doi.org/10.3390/cancers16112094
- Tang, L. et al. (2018) 'Role of metabolism in cancer cell radioresistance and radiosensitization methods', Journal of Experimental & Clinical Cancer Research 2018 37:1, 37(1), pp. 1–15. Available at: https://doi.org/10.1186/S13046-018-0758-7.
- Tang, Y.H. et al. (2022) 'Neuropilin-1 is over-expressed in claudin-low breast cancer and promotes tumour progression through acquisition of stem cell characteristics and RAS/MAPK pathway activation', Breast Cancer Research, 24(1), pp. 1–17. Available at: https://doi.org/10.1186/S13058-022-01501-7/FIGURES/6.
- Tao, J. et al. (2024) 'Protein disulfide isomerase family member 4 promotes triple-negative breast cancer tumourigenesis and radiotherapy resistance through JNK pathway', Breast Cancer Research, 26(1), pp. 1–17. Available at: https://doi.org/10.1186/S13058-023-01758-6/FIGURES/8.
- ter Brugge, P. et al. (2023) Homologous recombination deficiency derived from wholegenome sequencing predicts platinum response in triple-negative breast cancers. Nat Commun 14, 1958. https://doi.org/10.1038/s41467-023-37537-2

- To, N.H. et al. (2022) 'Radiation therapy for triple-negative breast cancer: emerging role of microRNAs as biomarkers and radiosensitivity modifiers. A systematic review', Breast Cancer Research and Treatment, 193(2), pp. 265–279. Available at: https://doi.org/10.1007/S10549-022-06533-3/METRICS.
- Tomioka, N. et al. (2018) 'The therapeutic candidate for immune checkpoint inhibitors elucidated by the status of tumour-infiltrating lymphocytes (TILs) and programmed death ligand 1 (PD-L1) expression in triple negative breast cancer (TNBC)', Breast Cancer, 25(1), pp. 34–42. Available at: https://doi.org/10.1007/s12282-017-0781-0.
- Tressler, C.M. et al. (2025) 'Molecular effects of clinically relevant chemotherapeutic agents on choline phospholipid metabolism in triple negative breast cancer cells', Translational Oncology, 53. Available at: https://doi.org/10.1016/j.tranon.2025.102311.
- Tripathi, V. et al. (2023) 'Therapeutic influence of simvastatin on MCF-7 and MDA-MB-231 breast cancer cells via mitochondrial depletion and improvement in chemosensitivity of cytotoxic drugs'. Advances in Cancer Biology Metastasis, 9, p.100110.
- Tseng, C.W. et al. (2018) 'Transketolase Regulates the Metabolic Switch to Control Breast Cancer Cell Metastasis via the a-Ketoglutarate Signalling Pathway', Cancer Research, 78(11), pp. 2799–2812. Available at: https://doi.org/10.1158/0008-5472.CAN-17-2906.
- De Vera, A.A. and Reznik, S.E. (2019a) Combining PI3K/Akt/mTOR Inhibition With Chemotherapy, Protein Kinase Inhibitors as Sensitizing Agents for Chemotherapy. Elsevier Inc. Available at: https://doi.org/10.1016/b978-0-12-816435-8.00014-6.
- De Vera, A.A. and Reznik, S.E. (2019b) 'Combining Pl3K/Akt/mTOR Inhibition With Chemotherapy', Protein Kinase Inhibitors as Sensitizing Agents for Chemotherapy, pp. 229–242. Available at: https://doi.org/10.1016/B978-0-12-816435-8.00014-6.
- Valenza, C. et al. (2023) 'Platinum-based chemotherapy and PARP inhibitors for patients with a germline BRCA pathogenic variant and advanced breast cancer (LATER-BC): retrospective multicentric analysis of post-progression treatments', European Journal of Cancer, 190, p. 112944. doi: 10.1016/j.ejca.2023.112944.
- Verginadis, I.I. et al. (2025) 'Radiotherapy toxicities: mechanisms, management, and future directions.', Lancet (London, England), 405(10475), pp. 338–352. Available at: https://doi.org/10.1016/S0140-6736(24)02319-5/ASSET/3EC5A359-A982-4CC8-B0A8-AFB5E5C79797/MAIN.ASSETS/GR3.SML.
- Vici, P. et al. (2016) "Triple positive" early breast cancer: An observational multicenter retrospective analysis of outcome', Oncotarget, 7(14), pp. 17932–17944. Available at: https://doi.org/10.18632/oncotarget.7480.
- Vidal, C.M. et al. (2023) 'Arginine regulates HSPA5/BiP translation through ribosome pausing in triple-negative breast cancer cells', British Journal of Cancer, 129(3), p. 444. Available at: https://doi.org/10.1038/S41416-023-02322-X.
- Wahba, H.A. and El-Hadaad, H.A. (2015) 'Current approaches in treatment of triple-negative breast cancer', Cancer Biology and Medicine, 12(2), pp. 106–116. Available at: https://doi.org/10.7497/j.issn.2095-3941.2015.0030.

- Wainberg, Z.A. et al. (2017) 'A Multi-Arm Phase I Study of the PI3K/mTOR Inhibitors PF-04691502 and Gedatolisib (PF-05212384) plus Irinotecan or the MEK Inhibitor PD-0325901 in Advanced Cancer', Targeted Oncology, 12(6), pp. 775–785. Available at: https://doi.org/10.1007/S11523-017-0530-5/FIGURES/2.
- Wan, X. et al. (2021) 'Oestrogen Receptor α Mediates Doxorubicin Sensitivity in Breast Cancer Cells by Regulating E-Cadherin', Frontiers in Cell and Developmental Biology, 9(February). Available at: https://doi.org/10.3389/fcell.2021.583572.
- Wang, B. et al. (2024) 'A glutamine tug-of-war between cancer and immune cells: recent advances in unraveling the ongoing battle', Journal of Experimental & Clinical Cancer Research 2024 43:1, 43(1), pp. 1–25. Available at: https://doi.org/10.1186/S13046-024-02994-0.
- Wang, D. et al. (2024) 'Targeting the glutamine-arginine-proline metabolism axis in cancer', Journal of Enzyme Inhibition and Medicinal Chemistry, 39(1), p. Available at: https://doi.org/10.1080/14756366.2024.2367129.
- Wang, J. and Wu, S.G. (2023) 'Breast Cancer: An Overview of Current Therapeutic Strategies, Challenge, and Perspectives', Breast Cancer: Targets and Therapy, 15, p. 721. Available at: https://doi.org/10.2147/BCTT.S432526.
- Wang, K. and Tepper, J.E. (2021) 'Radiation therapy-associated toxicity: Etiology, management, and prevention', CA: A Cancer Journal for Clinicians, 71(5), pp. 437–454.

 Available at: https://doi.org/10.3322/CAAC.21689;REQUESTEDJOURNAL:JOURNAL:15424863; WGROUP:STRING:PUBLICATION.
- Wang, M. et al. (2025) 'WTAP contributes to platinum resistance in high-grade serous ovarian cancer by up-regulating malic acid: insights from liquid chromatography and mass spectrometry analysis', Cancer & Metabolism 2025 13:1, 13(1), pp. 1–18. Available at: https://doi.org/10.1186/S40170-025-00383-5.
- Wang, S. et al. (2020) 'A novel 4-aminoquinazoline derivative, DHW-208, suppresses the growth of human breast cancer cells by targeting the PI3K/AKT/mTOR pathway', Cell Death & Disease, 11(6). Available at: https://doi.org/10.1038/S41419-020-2690-Y.
- Wang, S.S.Y. et al. (2023) 'PARP Inhibitors in Breast and Ovarian Cancer', Cancers, 15(8), p. 2357. Available at: https://doi.org/10.3390/CANCERS15082357.
- Wang, X. et al. (2019) 'α-Ketoglutarate-Activated NF-κB Signalling Promotes Compensatory Glucose Uptake and Brain Tumour Development', Molecular Cell, 76(1), pp. 148-162.e7. Available at: https://doi.org/10.1016/J.MOLCEL.2019.07.007/ATTACHMENT/A10F7CA4-5EF3-482B-8B5B-8EC7E31A93CF/MMC2.PDF.
- Wang, Ziyi et al. (2022) 'The Emerging Roles of Rad51 in Cancer and Its Potential as a Therapeutic Target', Frontiers in Oncology, 12, p. 935593. Available at: https://doi.org/10.3389/FONC.2022.935593/BIBTEX.
- Wang, Zhennan et al. (2022) 'Ursolic Acid Enhances the Sensitivity of MCF-7 and MDA-MB-231 Cells to Epirubicin by Modulating the Autophagy Pathway', Molecules (Basel, Switzerland), 27(11). Available at: https://doi.org/10.3390/MOLECULES27113399.

- Wang, Z., Jiang, Q. and Dong, C. (2020) 'Metabolic reprogramming in triple-negative breast cancer', Cancer Biology and Medicine, 17(1), pp. 44–59. Available at: https://doi.org/10.20892/j.issn.2095-3941.2019.0210.
- Wanigasooriya, K. et al. (2020) 'Radiosensitising Cancer Using Phosphatidylinositol-3-Kinase (PI3K), Protein Kinase B (AKT) or Mammalian Target of Rapamycin (mTOR) Inhibitors', Cancers, 12(5), p. 1278. Available at: https://doi.org/10.3390/CANCERS12051278.
- Wenzel, C. et al. (2025) 'Combination of cerium oxide nanoparticles and antimalarial drug chloroquine: characterization and anti-cancer potential for triple negative breast cancer'. Materials & Design, 255, p.114179. Available at: https://doi.org/10.1016/j.matdes.2025.114179
- Weth, F.R. et al. (2024) 'Unlocking hidden potential: advancements, approaches, and obstacles in repurposing drugs for cancer therapy', British Journal of Cancer, 130(5), pp. 703–715. Available at: https://doi.org/10.1038/s41416-023-02502-9.
- Whitaker, K.D. et al. (2022) 'Racial inequities in second-line treatment and overall survival among patients with metastatic breast cancer', 196, pp. 163–173. Available at: https://doi.org/10.1007/s10549-022-06701-5.
- Wilkinson, B. et al. (2023) 'The Cellular Response to Complex DNA Damage Induced by Ionising Radiation'. International Journal of Molecular Sciences, 24(5), 4920. https://doi.org/10.3390/ijms24054920
- Wilson, G.D. et al. (2021) 'Dacomitinib and gedatolisib in combination with fractionated radiation in head and neck cancer', Clinical and Translational Radiation Oncology, 26, pp. 15–23. Available at: https://doi.org/10.1016/J.CTRO.2020.11.003.
- Winter, M. et al. (2023) 'Mitochondrial adaptation decreases drug sensitivity of persistent triple negative breast cancer cells surviving combinatory and sequential chemotherapy', Neoplasia (United States), 46. Available at: https://doi.org/10.1016/j.neo.2023.100949.
- Wishart, D.et al., (2007) 'HMDB: the Human Metabolome Database'. Nucleic acids research, 35(Database issue), D521–D526. https://doi.org/10.1093/nar/gkl923
- Wolfe, A.R. et al. (2015) 'Simvastatin prevents triple-negative breast cancer metastasis in pre-clinical models through regulation of FOXO3a', Breast Cancer Research and Treatment, 154(3), pp. 495–508. Available at: https://doi.org/10.1007/S10549-015-3645-3/FIGURES/5.
- Won, K.A. and Spruck, C. (2020) 'Triple-negative breast cancer therapy: Current and future perspectives', International Journal of Oncology, 57(6), pp. 1245–1261. Available at: https://doi.org/10.3892/ijo.2020.5135.
- Wu, J. et al. (2024) 'The Tricarboxylic Acid Cycle Metabolites for Cancer: Friend or Enemy', Research, 7, p. 0351. Available at: https://doi.org/10.34133/RESEARCH.0351.
- World Health Organization. (2022, February 3). Cancer. World Health Organization. https://www.who.int/news-room/fact-sheets/detail/cancer

- Wu, Y. et al. (2023) 'Molecular mechanisms of tumour resistance to radiotherapy', Molecular Cancer 2023 22:1, 22(1), pp. 1–21. Available at: https://doi.org/10.1186/S12943-023-01801-2.
- Wylaź, M. et al. (2023) 'Exploring the role of PI3K/AKT/mTOR inhibitors in hormone-related cancers: A focus on breast and prostate cancer', Biomedicine & Pharmacotherapy, 168, p. 115676. Available at: https://doi.org/10.1016/J.BIOPHA.2023.115676.
- Xia, W. et al. (2023) 'Wild pink bayberry free phenolic extract induces mitochondriadependent apoptosis and G0/G1 cell cycle arrest through p38/MAPK and PI3K/Akt pathway in MDA-MB-231 cancer cells', Food Science and Human Wellness, 12(5), pp. 1510–1518. Available at: https://doi.org/10.1016/J.FSHW.2023.02.014.
- Xiao, Y. et al. (2022) 'Comprehensive metabolomics expands precision medicine for triplenegative breast cancer', Cell Research, 32(5), pp. 477–490. Available at: https://doi.org/10.1038/s41422-022-00614-0.
- Xing, J.L. and Stea, B. (2024) 'Molecular mechanisms of sensitivity and resistance to radiotherapy', Clinical and Experimental Metastasis, 41(4), pp. 517–524. Available at: https://doi.org/10.1007/S10585-023-10260-4/FIGURES/3.
- Xie W. et al (2019). β blockers inhibit the viability of breast cancer cells by regulating the ERK/COX 2 signalling pathway and the drug response is affected by ADRB2 single nucleotide polymorphisms. Oncol Rep, 41(1):341–50.
- Xiong, X. et al. (2025) 'Breast cancer: pathogenesis and treatments', Signal Transduction and Targeted Therapy 2025 10:1, 10(1), pp. 1–33. Available at: https://doi.org/10.1038/s41392-024-02108-4.
- Xu, L. et al. (2025) 'Advancements in clinical research and emerging therapies for triplenegative breast cancer treatment', European Journal of Pharmacology, 988, p. 177202. Available at: https://doi.org/10.1016/J.EJPHAR.2024.177202.
- Xu, M. et al. (2018) 'FGFR4 Links Glucose Metabolism and Chemotherapy Resistance in Breast Cancer', Cellular Physiology and Biochemistry, 47(1), pp. 151–160. Available at: https://doi.org/10.1159/000489759.
- Xu, Z. et al. (2020) 'Targeting PI3K/AKT/mTOR-mediated autophagy for tumour therapy', Applied Microbiology and Biotechnology, 104(2), pp. 575–587. Available at: https://doi.org/10.1007/S00253-019-10257-8/METRICS.
- Xue, D., Zhou, X. and Qiu, J. (2020) 'Emerging role of NRF2 in ROS-mediated tumour chemoresistance', Biomedicine and Pharmacotherapy, 131, p. 110676. Available at: https://doi.org/10.1016/j.biopha.2020.110676.
- Yadav, B et al. (2024). HYPofractionated Adjuvant RadioTherapy in 1 versus 2 weeks in highrisk patients with breast cancer (HYPART): a non-inferiority, open-label, phase III randomised trial. Trials, 25(1), p.21. https://doi.org/10.1186/s13063-023-07851-7
- Yadav, P. (2023). Simvastatin prevents BMP-2 driven cell migration and invasion by suppressing oncogenic DNMT1 expression in breast cancer cells. Gene, 882, p.147636. Available at: https://doi.org/10.1016/j.gene.2023.147636

- Yadav, S. et al. (2018) 'Impact of BRCA Mutation Status on Survival of Women with Triplenegative Breast Cancer', Clinical Breast Cancer, 18(5), pp. e1229–e1235. Available at: https://doi.org/10.1016/j.clbc.2017.12.014.
- Yang, F. (2024) 'The integration of radiotherapy with systemic therapy in advanced triplenegative breast cancer', Critical Reviews in Oncology/Hematology, 204, p. 104546. Available at: https://doi.org/10.1016/J.CRITREVONC.2024.104546.
- Yao, N. et al. (2023) 'Choline metabolism and its implications in cancer', Frontiers in Oncology, 13, p. 1234887. Available at: https://doi.org/10.3389/FONC.2023.1234887.
- Yoo, Y.A. et al. (2024) 'Asparagine Dependency is a Targetable Metabolic Vulnerability in TP53-Altered Castration-Resistant Prostate Cancer', Cancer research, 84(18), p. 3004. Available at: https://doi.org/10.1158/0008-5472.CAN-23-2910.
- Yu, L., Wei, J. and Liu, P. (2021) 'Attacking the PI3K/Akt/mTOR signalling pathway for targeted therapeutic treatment in human cancer', Seminars in Cancer Biology [Preprint], (April). Available at: https://doi.org/10.1016/j.semcancer.2021.06.019.
- Yu, Y. et al. (2023) 'Novel insight into metabolic reprogrammming in cancer radioresistance: A promising therapeutic target in radiotherapy', International Journal of Biological Sciences, 19(3), pp. 811–828. Available at: https://doi.org/10.7150/IJBS.79928.
- Zhang, B. et al. (2025) 'Targeting PI3K signalling in Lung Cancer: advances, challenges and therapeutic opportunities.', Journal of translational medicine, 23(1), p. 184. Available at: https://doi.org/10.1186/S12967-025-06144-8.
- Zhang, H. et al. (2021) 'The role of EMT-related IncRNA in the process of triple-negative breast cancer metastasis', Bioscience reports, 41(2). Available at: https://doi.org/10.1042/BSR20203121.
- Zhang, H.P. et al. (2024) 'PI3K/AKT/mTOR signalling pathway: an important driver and therapeutic target in triple-negative breast cancer', Breast Cancer, 31(4), pp. 539–551. Available at: https://doi.org/10.1007/S12282-024-01567-5/TABLES/1.
- Zhang, J. yuan et al. (2021) 'The metabolite α-KG induces GSDMC-dependent pyroptosis through death receptor 6-activated caspase-8', Cell Research, 31(9), p. 980. Available at: https://doi.org/10.1038/S41422-021-00506-9.
- Zhang, R. et al. (2016) 'Investigations on the cell metabolomics basis of multidrug resistance from tumour cells by ultra-performance liquid chromatography-mass spectrometry'.

 Analytical and bioanalytical chemistry, 408(21), 5843–5854. https://doi.org/10.1007/s00216-016-9696-4
- Zhang, S. et al. (2022) 'Radix Tetrastigma Extracts Enhance the Chemosensitivity in Triple-Negative Breast Cancer Via Inhibiting PI3K/Akt/mTOR-Mediated Autophagy', Clinical Breast Cancer, 22(2), pp. 89–97. Available at: https://doi.org/10.1016/J.CLBC.2021.07.015.
- Zhang, X. (2023) 'Molecular Classification of Breast Cancer: Relevance and Challenges', Archives of Pathology & Laboratory Medicine, 147(1), pp. 46–51. Available at: https://doi.org/10.5858/ARPA.2022-0070-RA.

- Zheng, W. et al. (2019). 'Anticancer activity of 1,25-(OH)2D3 against human breast cancer cell lines by targeting Ras/MEK/ERK pathway'. OncoTargets and therapy, 12, 721–732. https://doi.org/10.2147/OTT.S190432
- Zheng, X. et al. (2022) 'Energy metabolism pathways in breast cancer progression: The reprogramming, crosstalk, and potential therapeutic targets'. Translational oncology, 26, 101534. https://doi.org/10.1016/j.tranon.2022.101534
- Zhou, M. et al. (2021) 'Improving anti-PD-L1 therapy in triple negative breast cancer by polymer-enhanced immunogenic cell death and CXCR4 blockade', Journal of Controlled Release, 334(April), pp. 248–262. Available at: https://doi.org/10.1016/j.jconrel.2021.04.029.
- Zhou, Y. et al. (2019). Aspirin treatment effect and association with PIK3CA mutation in breast cancer: a biomarker analysis. Clinical Breast Cancer, 19(5), pp.354–362.e7. Available at: https://doi.org/10.1016/j.clbc.2019.05.004.
- Zhou, Z.-R. (2020) 'Building radiation-resistant model in triple-negative breast cancer to screen radioresistance-related molecular markers', Annals of Translational Medicine, 8(4), p. 108. doi: 10.21037/atm.2019.12.114.
- Zhu, K. et al. (2024) 'HER2-targeted therapies in cancer: a systematic review', Biomarker Research 2024 12:1, 12(1), pp. 1–17. Available at: https://doi.org/10.1186/S40364-024-00565-1.
- Zhu, S. et al. (2023) 'Recent advances in targeted strategies for triple-negative breast cancer', Journal of Hematology & Oncology 2023 16:1, 16(1), pp. 1–36. Available at: https://doi.org/10.1186/S13045-023-01497-3.

8 Appendix

A	В	С	D	E	F	G	Н	1	J	K	L	M	N
	RAD Dose (GY	Colony Cour	Plating Efficiency (9	%) cell counted/cells seeded	d Survival fraction	Colony Count	ating Efficiency	cell counted/cells seed	ed Survival fractio	Colony Count	Plating Efficiency (%	ell counted/cells see	deSurvival fractic
ľ	1	180	36	0.36	0.752	210	42	0.42	0.792	246	49	0.49	0.871
231	2	108	22	0.22	0.451	156	31	0.31	0.590	151	30	0.30	0.536
1B-	4	44	9	0.09	0.182	77	15	0.15	0.290	54	11	0.11	0.192
WT-MDA-MB-	6	35	7	0.07	0.147	28	6	0.06	0.107	25	5	0.05	0.087
DA	8	8	2	0.02	0.032	10	2	0.02	0.039	8	2	0.02	0.028
Σ	10	2	0.4	0.00	0.008	2	0.5	0.00	0.007	3	1	0.01	0.009
5	Control	240	48	0.48	1	265	53	0.53	1	282	56	0.56	1
	RAD Dose (GY) Colony Cour	n Plating Efficiency (§	%) cell counted/cells seeded	d Survival fraction	Colony Count	ating Efficiency	(cell counted/cells seed	ed Survival fractio	Colony Count	1Plating Efficiency (%] ell counted/cells see	edeŝurvival fractic
231	1	322	64	0.64	0.962	281	56	0.56	0.952	312	62	0.62	0.992
-23	2	262	52	0.52	0.781	177	35	0.35	0.6	275	55	0.55	0.872
AB	4	191	38	0.38	0.570	139	28	0.28	0.47	118	24	0.24	0.375
A-C	6	87	17	0.17	0.261	96	19	0.19	0.327	69	14	0.14	0.218
d l	8	41	8	0.08	0.055	35	7	0.07	0.117	57	11	0.11	0.182
RR-MDA-MB-	10	1 4	3	0.03	0.042	19	4	0.04	0.063	23	5	0.05	0.072
~	Control	335	67	0.67	1	295	59	0.59	1	315	63	0.63	1

Table 8.1 Raw data of survival fraction calculation for the wild type and radioresistant MDA-MB-231 cell lines following exposure to increasing doses of ionizing radiation.

Tukey's multiple comparisons test	P (*)	Significance	Adjusted P Value
Control vs. 0.05 GED	ns	No	>0.9999
Control vs. 0.1 GED	*	Yes	0.0358
Control vs. 0.5 Gy	ns	No	>0.9999
Control vs. 1 Gy	*	Yes	0.0119
Control vs. 2 Gy	***	Yes	0.0006
Control vs. 0.5 Gy + 0.05 GED	**	Yes	0.0119
Control vs. 0.5 Gy + 0.1 GED	**	Yes	0.0046
Control vs. 1 Gy + 0.05 GED	***	Yes	0.0005
Control vs. 1 Gy + 0.1 GED	***	Yes	0.0001
Control vs. 2 Gy + 0.05 GED	****	Yes	<0.0001
Control vs. 2 Gy + 0.1 GED	****	Yes	<0.0001
0.05 GED vs. 0.5 Gy + 0.05 GED	*	Yes	0.0226
0.1 GED vs. 0.5 Gy + 0.1 GED	ns	No	>0.9999
0.5 Gy vs. 0.5 Gy + 0.05 GED	ns	No	>0.9999
0.5 Gy vs. 0.5 Gy + 0.1 GED	ns	No	>0.9999
0.05 GED vs. 1 Gy + 0.05 GED	**	Yes	0.0015
0.1 GED vs. 1 Gy + 0.1 GED	**	Yes	0.004
1 Gy vs. 1 Gy + 0.05 GED	ns	No	>0.9999
1 Gy vs. 1 Gy + 0.1 GED	****	Yes	<0.0001
0.05 GED vs. 2 Gy + 0.05 GED	****	Yes	<0.0001
0.1 GED vs. 2 Gy + 0.1 GED	****	Yes	<0.0001
2 Gy vs. 2 Gy + 0.05 GED	ns	No	>0.9999
2 Gy vs. 2 Gy + 0.1 GED	***	Yes	0.0001

Appendix-Chapter 3- Figure 8-1 Survival fraction of MDA-MB-231 cells exposed to combination of gedatolisib and radiation.

B: Tukey's multiple comparisons test to determine significance, which was undertaken using GraphPad Prism 10.3.1 and the difference considered significant when P value < 0.05 where na= non-significant, *P < 0.05, **P < 0.01, ***P < 0.001 and ****P < 0.0001

Tukey's multiple comparisons test		Significant	Adjusted P Value
Control vs. DOX (0.1µM)	**	Yes	0.004
Control vs. GED (0.1µM)	*	Yes	0.0308
Control vs. DOX (0.05μM) +GED (0.05μM)	*	Yes	0.016
Control vs. DOX (0.005μM) +GED (0.1μM)	***	Yes	0.0002
Control vs. DOX (0.1µM) + GED (0.05µM)	***	Yes	0.0007
Control vs. DOX (0.1µM) + GED (0.1µM)	****	Yes	<0.0001
GED (0.05μM) vs. DOX (0.1μM) + GED (0.1μM)	****	Yes	<0.0001
GED (0.1μM) vs. DOX (0.1μM) + GED (0.1μM)	***	Yes	0.0002
DOX (0.005μM) vs. DOX (0.005μM) +GED (0.1μM)	***	Yes	0.0008
DOX (0.005μM) vs. DOX (0.1μM) + GED (0.1μM)	****	Yes	<0.0001
DOX (0.1μM) vs. DOX (0.1μM) + GED (0.1μM)	***	Yes	0.0002
Other comparisons	NS	No	> 0.05

Appendix-Chapter 3- Figure 8-2 Survival fraction of MDA-MB-231 cells exposed to combination of gedatolisib and doxorubicin.

B: Tukey's multiple comparisons test to determine significance, which was undertaken using GraphPad Prism 10.3.1 and the difference considered significant when P value < 0.05 where na= non-significant, *P < 0.05, **P < 0.01, ***P < 0.001 and ****P < 0.0001

Tukey's multiple comparisons test	P (*)	Significance	Adjusted P Value
Control vs. 0.05 GED	ns	No	>0.9999
Control vs. 0.1 GED	*	Yes	0.0358
Control vs. 0.5 Gy	ns	No	>0.9999
Control vs. 1 Gy	*	Yes	0.0119
Control vs. 2 Gy	***	Yes	0.0006
Control vs. 0.5 Gy + 0.05 GED	**	Yes	0.0119
Control vs. 0.5 Gy + 0.1 GED	**	Yes	0.0046
Control vs. 1 Gy + 0.05 GED	***	Yes	0.0005
Control vs. 1 Gy + 0.1 GED	***	Yes	0.0001
Control vs. 2 Gy + 0.05 GED	****	Yes	<0.0001
Control vs. 2 Gy + 0.1 GED	****	Yes	<0.0001
0.05 GED vs. 0.5 Gy + 0.05 GED	*	Yes	0.0226
0.1 GED vs. 0.5 Gy + 0.1 GED	ns	No	>0.9999
0.5 Gy vs. 0.5 Gy + 0.05 GED	ns	No	>0.9999
0.5 Gy vs. 0.5 Gy + 0.1 GED	ns	No	>0.9999
0.05 GED vs. 1 Gy + 0.05 GED	**	Yes	0.0015
0.1 GED vs. 1 Gy + 0.1 GED	**	Yes	0.004
1 Gy vs. 1 Gy + 0.05 GED	ns	No	>0.9999
1 Gy vs. 1 Gy + 0.1 GED	****	Yes	<0.0001
0.05 GED vs. 2 Gy + 0.05 GED	****	Yes	<0.0001
0.1 GED vs. 2 Gy + 0.1 GED	****	Yes	<0.0001
2 Gy vs. 2 Gy + 0.05 GED	ns	No	>0.9999
2 Gy vs. 2 Gy + 0.1 GED	***	Yes	0.0001

Appendix-Chapter 3- Figure 8-3 The growth curve for MDA-MB-231 spheroid exposed to a simultaneous combination of gedatolisib and radiation B: Tukey's multiple comparisons test, and the difference was considered significant

when P value < 0.05 where *P < 0.05, **P < 0.01, ***P < 0.001 and ****P < 0.0001

Tukey's multiple comparisons test		Significance	Adjusted P Value
Control vs. 0.05 µM GED	ns	No	>0.9999
Control vs. 0.1 μM GED	ns	No	0.1995
Control vs. 0.005 μM DOX	ns	No	>0.9999
Control vs. 0.01 µM DOX	ns	No	0.062
Control vs. 0.05 μM GED + 0.01 μM DOX	**	Yes	0.0021
Control vs. 0.1 µM GED + 0.005 µM DOX	****	Yes	<0.0001
Control vs. 0.1 µM GED + 0.01 µM DOX	****	Yes	<0.0001
0.05 μM GED vs. 0.1 μM GED + 0.005 μM DOX	**	Yes	0.0021
0.05 μM GED vs. 0.1 μM GED + 0.01 μM DOX	****	Yes	<0.0001
0.005 μM DOX vs. 0.05 μM GED + 0.01 μM DOX	**	Yes	0.0035
0.005 μM DOX vs. 0.1 μM GED + 0.01 μM DOX	****	Yes	<0.0001
0.005 μM DOX vs. 0.05 μM GED + 0.01 μM DOX	**	Yes	0.0035
0.1 μM GED vs. 0.1 μM GED + 0.01 μM DOX	****	Yes	<0.0001
0.01 μM DOX vs. 0.1 μM GED + 0.01 μM DOX	****	Yes	<0.0001
0.05 μM GED + 0.005 μM DOX vs. 0.1 μM GED + 0.005 μM DOX	**	Yes	0.0021
0.05 μM GED + 0.005 μM vs. 0.1 μM GED + 0.01 μM DOX	****	Yes	<0.0001
0.05 μM GED + 0.01 μM DOX vs. 0.1 μM GED + 0.01 μM	***	Yes	0.0001
0.1 μM GED + 0.005 μM DOX vs. 0.1 μM GED + 0.01 μM	**	Yes	0.003

Appendix-Chapter 3- Figure 8-4 Growth curve for MDA-MB-231 tumour spheroid exposed to a combination therapy of gedatolisib and doxorubicin

B: Tukey's multiple comparisons test, and the difference was considered significant when P value < 0.05 where *P < 0.05, **P < 0.01, ***P < 0.001 and ****P < 0.0001

Tukey's multiple comparison test	P (*)	Below threshold?	P-value
Control vs. GED (0.1 µM)	*	Yes	0.0155
Control vs. RAD (2 Gy)	*	Yes	0.0215
Control vs. RAD 0.5Gy+0.1 µM GED	*	Yes	0.0155
Control vs. RAD 1Gy+0.05 µM GED	**	Yes	0.002
Control vs. RAD 1Gy+0.1 µM GED	****	Yes	<0.0001
Control vs. RAD 2 Gy+0.05 µM GED	****	Yes	<0.0001
Control vs. RAD 2 Gy+0.1 µM GED	****	Yes	<0.0001
GED (0.05 μM) vs. RAD 1Gy+0.1 μM GED	**	Yes	0.0045
GED (0.05 μM) vs. RAD 2 Gy+0.05 μM GED	***	Yes	0.0009
GED (0.05 μM) vs. RAD 2 Gy+0.1 μM GED	****	Yes	<0.0001
GED (0.1 μM) vs. RAD 2 Gy+0.1 μM GED	**	Yes	0.0021
RAD (0.5 Gy) vs. RAD 1Gy+0.05 μM GED	*	Yes	0.033
RAD (0.5 Gy) vs. RAD 1Gy+0.1 µM GED	**	Yes	0.0017
RAD (0.5 Gy) vs. RAD 2 Gy+0.05 µM GED	***	Yes	0.0003
RAD (0.5 Gy) vs. RAD 2 Gy+0.1 µM GED	****	Yes	<0.0001
RAD (1 Gy) vs. RAD 1Gy+0.1 μM GED	*	Yes	0.0206
RAD (1 Gy) vs. RAD 2 Gy+0.05 μM GED	**	Yes	0.0043
RAD (1 Gy) vs. RAD 2 Gy+0.1 µM GED	****	Yes	<0.0001
RAD (2 Gy) vs. RAD 2 Gy+0.1 µM GED	**	Yes	0.0015
All other comparisons	NS	No	>0.05

Appendix-Chapter 4- Figure 8-5 Survival of RR-MDA-MB-231 cells following combination treatment with gedatolisib and radiation.

B: Tukey's multiple comparisons test to determine significance, which was undertaken using GraphPad Prism 10.3.1 and the difference considered significant when P value < 0.05 where *P < 0.05, **P < 0.01, ***P < 0.001 and ****P < 0.0001

Tukey's multiple comparison test	P (*)	Below threshold?	P-value
Control vs. 0.1µM GED	***	Yes	0.0005
Control vs. 0.01µM DOX	***	Yes	0.0003
Control vs. 0.05µM GED+0.005µM DOX	**	Yes	0.0068
Control vs. 0.05µM GED+0.01µM DOX	****	Yes	<0.0001
Control vs. 0.1µM GED+0.005µM DOX	****	Yes	<0.0001
Control vs. 0.1µM GED+0.01µM DOX	****	Yes	<0.0001
0.05μM GED vs. 0.01μM DOX	*	Yes	0.0462
0.05μM GED vs. 0.05μM GED+0.01μM DOX	****	Yes	<0.0001
0.05μM GED vs. 0.1μM GED+0.005μM DOX	****	Yes	<0.0001
0.05μM GED vs. 0.1μM GED+0.01μM DOX	****	Yes	<0.0001
0.1μM GED vs. 0.05μM GED+0.01μM DOX	**	Yes	0.0014
0.1μM GED vs. 0.1μM GED+0.01μM DOX	****	Yes	<0.0001
0.005μM DOX vs. 0.05μM GED+0.01μM DOX	****	Yes	<0.0001
0.005μM DOX vs. 0.1μM GED+0.005μM DOX	****	Yes	<0.0001
0.005μM DOX vs. 0.1μM GED+0.01μM DOX	****	Yes	<0.0001
0.01μM DOX vs. 0.05μM GED+0.01μM DOX	**	Yes	0.0022
0.01μM DOX vs. 0.1μM GED+0.01μM DOX	****	Yes	<0.0001
Other comparisons	NS	No	> 0.05

Appendix-Chapter 4- Figure 8-6 Survival of RR-MDA-MB-231 cells following combination treatment with gedatolisib and doxorubicin.

B: Tukey's multiple comparisons test to determine significance, which was undertaken using GraphPad Prism 10.3.1 and the difference considered significant when P value < 0.05 where *P < 0.05, **P < 0.01, ***P < 0.001 and ****P < 0.0001

Tukey's multiple comparison test	P (*)	Below threshold?	P-value
Control vs. GED (0.05 µM)	ns	No	0.9979
Control vs. GED (0.1 µM)	**	Yes	0.0029
Control vs. RAD (1 Gy)	ns	No	0.3013
Control vs. RAD (2 Gy)	****	Yes	<0.0001
Control vs. RAD 1Gy+0.05 μM GED	****	Yes	<0.0001
Control vs. RAD 1Gy+0.1 µM GED	****	Yes	<0.0001
Control vs. RAD 2 Gy+0.05 µM GED	****	Yes	<0.0001
Control vs. RAD 2 Gy+0.1 µM GED	****	Yes	<0.0001
GED (0.05 μM) vs. GED (0.1 μM)	*	Yes	0.0385
GED (0.05 μM) vs. RAD 1Gy+0.05 μM GED	***	Yes	0.0009
GED (0.05 μM) vs. RAD 1Gy+0.1 μM GED	****	Yes	<0.0001
GED (0.05 μM) vs. RAD 2 Gy+0.05 μM GED	****	Yes	<0.0001
GED (0.05 μM) vs. RAD 2 Gy+0.1 μM GED	****	Yes	<0.0001
GED (0.1 μM) vs. RAD (1 Gy)	ns	No	0.8077
GED (0.1 μM) vs. RAD (2 Gy)	ns	No	0.9849
GED (0.1 μM) vs. RAD 1Gy+0.05 μM GED	ns	No	0.9787
GED (0.1 μM) vs. RAD 1Gy+0.1 μM GED	ns	No	0.0771
GED (0.1 μM) vs. RAD 2 Gy+0.05 μM GED	**	Yes	0.0024
GED (0.1 μM) vs. RAD 2 Gy+0.1 μM GED	****	Yes	<0.0001
RAD (1 Gy) vs. RAD (2 Gy)	ns	No	0.1906
RAD (1 Gy) vs. RAD 1Gy+0.05 μM GED	ns	No	0.1683
RAD (1 Gy) vs. RAD 1Gy+0.1 μM GED	***	Yes	0.0003
RAD (1 Gy) vs. RAD 2 Gy+0.05 μM GED	****	Yes	<0.0001
RAD (1 Gy) vs. RAD 2 Gy+0.1 μM GED	****	Yes	<0.0001
RAD (2 Gy) vs. RAD 1Gy+0.05 μM GED	ns	No	>0.9999
RAD (2 Gy) vs. RAD 1Gy+0.1 μM GED	ns	No	0.5704
RAD (2 Gy) vs. RAD 2 Gy+0.05 μM GED	ns	No	0.0692
RAD (2 Gy) vs. RAD 2 Gy+0.1 μM GED	****	Yes	<0.0001
RAD 1Gy+0.05 μM GED vs. RAD 1Gy+0.1 μM GED	ns	No	0.6092
RAD 1Gy+0.05 μM GED vs. RAD 2 Gy+0.05 μM GED	ns	No	0.0804
RAD 1Gy+0.05 μM GED vs. RAD 2 Gy+0.1 μM GED	****	Yes	<0.0001
RAD 1Gy+0.1 μM GED vs. RAD 2 Gy+0.05 μM GED	ns	No	0.9806
RAD 1Gy+0.1 μM GED vs. RAD 2 Gy+0.1 μM GED	**	Yes	0.0013
RAD 2 Gy+0.05 μM GED vs. RAD 2 Gy+0.1 μM GED	*	Yes	0.0413

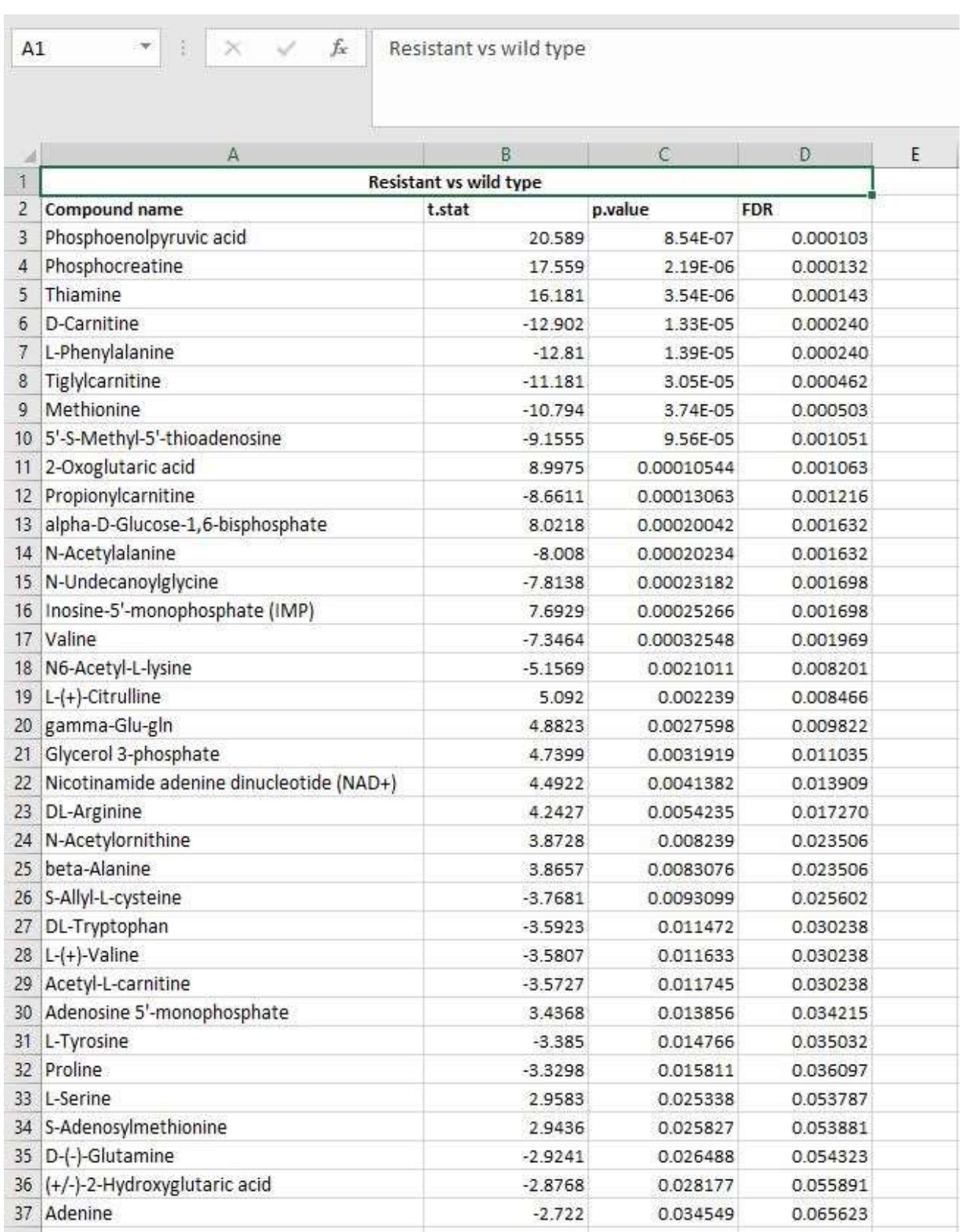
Appendix-Chapter 4- Figure 8-7 The growth curve of RR-MDA-MB-231 spheroids following exposure to a combination of gedatolisib and radiation

B: Tukey's multiple comparisons test, and the difference was considered significant when P value < 0.05 where *P < 0.05, **P < 0.01, ***P < 0.001 and ****P < 0.0001

Tukey's multiple comparison test	Below threshold?	P (*)	P-value
Control vs. 0.05 µM GED	No	ns	>0.9999
Control vs. 0.1 µM GED	Yes	****	<0.0001
Control vs. 0.005 μM DOX	No	ns	0.1736
Control vs. 0.01 µM DOX	Yes	****	<0.0001
Control vs. 0.05 µM GED + 0.005 µM DOX	Yes	****	<0.0001
Control vs. 0.05 µM GED + 0.01 µM DOX	Yes	****	<0.0001
Control vs. 0.1 µM GED + 0.005 µM DOX	Yes	****	<0.0001
Control vs. 0.1 µM GED + 0.01 µM DOX	Yes	****	<0.0001
0.05 μM GED vs. 0.05 μM GED + 0.005 μM DOX	Yes	****	<0.0001
0.05 μM GED vs. 0.05 μM GED + 0.01 μM DOX	Yes	****	<0.0001
0.05 μM GED vs. 0.1 μM GED + 0.005 μM DOX	Yes	****	<0.0001
0.05 μM GED vs. 0.1 μM GED + 0.01 μM DOX	Yes	****	<0.0001
0.1 μM GED vs. 0.005 μM DOX	No	ns	0.2478
0.1 μM GED vs. 0.01 μM DOX	No	ns	0.7166
0.1 μM GED vs. 0.05 μM GED + 0.005 μM DOX	No	ns	>0.9999
0.1 μM GED vs. 0.05 μM GED + 0.01 μM DOX	Yes	**	0.001
0.1 μM GED vs. 0.1 μM GED + 0.005 μM DOX	Yes	***	0.0002
0.1 μM GED vs. 0.1 μM GED + 0.01 μM DOX	Yes	****	<0.0001
0.005 μM DOX vs. 0.01 μM DOX	Yes	**	0.0011
0.005 μM DOX vs. 0.05 μM GED + 0.005 μM DOX	No	ns	0.1942
0.005 μM DOX vs. 0.05 μM GED + 0.01 μM DOX	Yes	****	<0.0001
0.005 μM DOX vs. 0.1 μM GED + 0.005 μM DOX	Yes	****	<0.0001
0.005 μM DOX vs. 0.1 μM GED + 0.01 μM DOX	Yes	****	<0.0001
0.01 μM DOX vs. 0.05 μM GED + 0.005 μM DOX	No	ns	0.787
0.01 μM DOX vs. 0.05 μM GED + 0.01 μM DOX	No	ns	0.2425
0.01 μM DOX vs. 0.1 μM GED + 0.005 μM DOX	No	ns	0.1056
0.01 μM DOX vs. 0.1 μM GED + 0.01 μM DOX	Yes	****	<0.0001
0.05 μM GED + 0.005 μM DOX vs. 0.05 μM GED + 0.01 μM DOX	Yes	**	0.0017
0.05 μM GED + 0.005 μM DOX vs. 0.1 μM GED + 0.005 μM DOX	Yes	***	0.0004
0.05 μM GED + 0.005 μM DOX vs. 0.1 μM GED + 0.01 μM DOX	Yes	****	<0.0001
0.05 μM GED + 0.01 μM DOX vs. 0.1 μM GED + 0.005 μM DOX	No	ns	>0.9999
0.05 μM GED + 0.01 μM DOX vs. 0.1 μM GED + 0.01 μM DOX	Yes	****	<0.0001
0.1 μM GED + 0.005 μM DOX vs. 0.1 μM GED + 0.01 μM DOX	Yes	****	<0.0001

Appendix-Chapter 4- Figure 8-8 The growth curve of RR-MDA-MB-231 spheroids treated with single and combination of gedatolisib and doxorubicin

B: Tukey's multiple comparisons test, and the difference was considered significant when P value < 0.05 where *P < 0.05, **P < 0.01, ***P < 0.001 and ****P < 0.0001



Appendix-Chapter 5- Raw data of t-test analysis of resistant vs wild type cell lines at 1 hr following exposure to radiation.